1971

Electrosorption Effects Of Organic Additives On The Cathode-overpotential Of Copper Electrodeposition

Raouf Loutfy

ELECTROSORPTION EFFECTS OF ORGANIC ADDITIVES ON THE CATHODE-OVERPOTENTIAL OF COPPER ELECTRODEPOSITION

by

Raouf Omar Loutfy
Department of Chemistry

Submitted in partial fulfillment
of the requirements for the degree of
Doctor of Philosophy

/

Faculty of Graduate Studies
The University of Western Ontario
London, Canada
February 1971

ABSTRACT

A study of the mechanism of copper deposition from aqueous $CuSO_4$ electrolyte showed that for acidified solutions the deposition is charge-transfer controlled, but for neutral solutions at low current density, the process is surface-diffusion controlled.

Thirty-five organic additives were studied in relation to their effects on the cathode overpotential and kinetics of copper deposition. These compounds were divided into four groups on the basis of their functional group and structural differences.

The compounds of Group I included the normal monocarboxylic and dicarboxylic acids of low molecular weight. They gave rise to an increase in cathode overpotential, but with no change in the kinetics of copper deposition.

The fractional surface coverage due to adsorption of these compounds on the cathode surface was calculated from the overpotential increment data by application of the simple blocking theory. As a first approximation, the Langmuir isotherm was used to calculate the standard free energy of adsorption, which was found to vary with coverage. This coverage dependence of the free energy was attributed to a spontaneous lateral interaction between the adsorbed molecules and approximate theoretical calculations showed that the lateral interaction is due mainly to dipole-dipole effects.

An adsorption isotherm was derived for these additives in which the effect of the lateral interaction was considered.

Group II compounds included low molecular weight thioacids, mercaptoacids, and thiols. Thioacids and mercaptoacetic acid, in acidified $CuSO_4$ electrolyte, caused a depolarization or decrease in cathode overpotential, and also changed the kinetics of copper deposition. This was attributed to the formation of additive-Cu(I) complexes. In the beginning of electrolysis, an initial maximum overpotential was always obtained with the depolarizing additives, and this was attributed to the sulfurization of the copper surface with formation of a copper sulfide film.

The thioacids and mercaptoacetic acid in neutral solution, and mercaptopropionic and mercaptobutyric acids and the thiols in neutral or acidified solution, caused an increase in the cathode overpotential. The fractional surface coverage and standard free energy of adsorption were calculated in the same manner as for the additives in Group I.

Group III addition agents included the normal diols up to hexanediol. These caused an increase in the cathode overpotential. An expression was developed to relate the initial slope of the overpotential increment-concentration curves to the standard free energy of adsorption at zero coverage. Accordingly, ΔG_a^o was calculated for the additives of this group.

The compounds of Group IV included benzoic, phthalic, and isophthalic acids, phenol, cyclohexanol, cyclohexanecarboxylic acid and 1,2 cyclohexanedicarboxylic acid. These compounds also caused an increase in the cathode overpotential. Just as for the additives in Croup III, the free energy of adsorption was calculated from the initial slope of the $\Delta\eta$ vs. C curves.

Calculated values of the standard free energy of adsorption of monofunctional compounds (monocarboxylic acids, thioacids and thiols) showed that the addition of each methylene group to the hydrocarbon chain caused the same increase in the free energy of adsorption, namely, -760 cal/mole. This was attributed to the applicability of Traube's rule to these homologous systems.

The free energy contributions of the functional groups were determined and it was found that their effectiveness in contributing to adsorptivity increases in the order $OH < COOH \ll SH < COSH$.

The overall effect of the hydrocarbon part of the organic additive was also examined and it was found that, generally, the adsorptivity increases in the order: saturated cyclic compounds < saturated aliphatic compounds < aromatic compounds.

For the difunctional compounds (dicarboxylic acids, diols and mercaptoacids), an alternation was observed in the effect on cathode overpotential with increasing number

of carbon atoms, corresponding to alternation in the structural configuration of these additives. Additives with an odd number of carbon atoms are more effective than additives with an even number of carbon atoms. An empirical equation for the standard free energy of adsorption was developed for the dicarboxylic acids, in which the structural difference between the even and the odd molecules was considered.

The results obtained suggest that the additives studied are physically adsorbed on the copper surface and that the free energy of adsorption can be calculated from the contribution of each part of the additive molecule. This generalization is particularly applicable in the case of monofunctional compounds. For difunctional compounds, total contribution from the whole molecule can only be expected if the molecule adsorbs with both functional groups.

ACKNOWLEDGEMENT

The author wishes to express sincere thanks and deep gratitude to Dr. A. J. Sukava, whose constant encouragement, useful discussions, and helpful advice made the completion of this work possible.

Thanks and profound gratitude are also extended to Dr. R. K. Chan of the Chemistry Department for his useful discussions.

Thanks are also due to other faculty members and graduate students of the Chemistry Department for their helpful suggestions.

The financial support of the National Research Council and the Department of Chemistry is gratefully acknowledged.

TABLE OF CONTENTS

LIST OF TABLES

LIST OF FIGURES

LIST OF SYMBOLS

a	intercept of the Tafel equation
b	slope of Tafel equation (i.e. Tafel slope)
C	bulk concentration
C_O	concentration of oxidized species at the electrode
C_R	concentration of reduced species at the electrode
C_r	reduced concentration of additive
C_s	saturation concentration of additive
C_o, $C_{o,add.}$	concentration of adions at equilibrium
C_{dl}	double layer capacity
$C_{\eta,t}$	concentration of adions at time t & overpotential η .
e	electron charge
E_o	electrode potential at zero current density
E	electrode potential at current density i
F	Faraday
ΔG^*	free energy of activation of charge transfer
ΔG_+^*	free energy of activation of the forward electrochemical reaction
ΔG_-^*	free energy of activation of the backward electrochemical reaction
ΔG_a^o	net standard free energy of adsorption
$\Delta G_{a\ \theta=0}^o$	standard free energy of adsorption at zero coverage
$\Delta G_{CH_2}^o$	standard free energy of adsorption due to the methylene group
ΔG_p^o	standard free energy of adsorption due to the functional group

$\Delta G^{o}_{elec.}$ electrostatic contribution of the non-adsorbing functional group to the standard free energy of adsorption

ΔG^{o}_{s} free energy contribution due to the solvation of the non-adsorbing functional group

$g(\theta)$ lateral interaction free energy of adsorption

ΔG^{o}_{Ph} standard free energy of adsorption due to the aryl group

ΔG^{o}_{CH} standard free energy of adsorption due to the methyline group

i current density

i_o exchange current density

K_+ rate constant of the forward electrochemical reaction

K_- rate constant of the backward electrochemical reaction

K adsorption equilibrium constant (i.e. adsorbability)

M molarity

n number of water molecules

N Avogadro's constant

R universal gas constant

T temperature

t time

ν rate of the overall electrochemical reaction

ν_+ rate of the forward electrochemical reaction

ν_- rate of the backward electrochemical reaction

V_o surface diffusion flux

V coverage surface diffusion flux

Z number of electrons taking part in the electrochemical reaction

α transfer coefficient

η overpotential

η' overpotential in the presence of additive

η_A activation overpotential

η_c concentration overpotential

η_{IR} ohmic overpotential

$\eta_{crys.}$ crystallization overpotential

η_t charge-transfer overpotential

$\Delta\eta$ overpotential increment

η_{total} total overpotential

θ fractional surface coverage

τ_{max} time required to reach initial maximum overpotential

μ_D dipole moment

μ chemical potential

ϵ dielectric constant

U_{dipole} dipole-dipole interaction

CHAPTER I

INTRODUCTION

General Theory of Overpotential

The development of an electrochemical potential difference between two phases requires the transport of electrically charged particles, ions or electrons, in either direction. Immersing a metal electrode M in a solution of its ions M^{Z+} involves the reaction

$$M \rightleftharpoons M^{Z+} + Ze \qquad \text{-------(1)}$$

and an electrochemical potential difference between the two phases takes place. When the electrochemical reaction reaches equilibrium, with the forward reaction rate compensated by a reverse reaction of identical rate, an equilibrium potential E_o is established across the metal-solution interface. When net current flows, the electrode potential E assumes a value different from that in the absence of current E_o. The deviation of the electrode potential E from the equilibrium value E_o is called the overpotential η, i.e.,

$$\eta = E - E_o \qquad \text{-------(2)}$$

The overpotential η is a function of the current density i. The difference between the equilibrium potential E_o, which is also called the reversible electrode potential, and the potential E, the irreversible electrode potential, is due to an inherent slowness of one or more of the kinetic steps in the electrode reaction. In electrode kinetics, as in ordinary reaction kinetics, the slowest partial reaction is rate-determining for the total reaction. The magnitude and type of overpotential η is therefore governed by the slowest partial reaction. If several of the reactions have low reaction rates of similar orders of magnitude, the corresponding overpotentials are superimposed to form the total overpotential. Generally, there are three different types of overpotentials, and accordingly η total can be represented by

$$\eta_{total} = \eta_{IR} + \eta_C + \eta_A \qquad \text{-------(3)}$$

where η_A is the activation overpotential, which arises from the hindrance of one or more of the kinetic steps necessary to transform a hydrated ion in solution to its final position in the lattice forming the solid electrode, η_C is the concentration overpotential, which is the overpotential due to concentration changes at the electrode surface (or more rigorously, immediately adjacent to the double layer), and η_{IR} is the ohmic overpotential, said

to arise from electrical resistance (i.e. IR potential drop) to the passage of ions to the surface of the electrode.

Vetter (1,2) has pointed out that the activation overpotential η_A is actually the sum of a charge-transfer overpotential η_t and crystallization overpotential $\eta_{crys.}$. The crystallization overpotential arises when the process by which atoms are incorporated into or removed from the crystal lattice is hindered. Accordingly:

$$\eta_{total} = \eta_{IR} + \eta_C + \eta_t + \eta_{crys.}$$

In the system and method of measurement employed here, η_{IR} was eliminated and concentration overpotential was kept to a fixed value which is in fact negligibly small (3) in comparison to the value of activation overpotential. Therefore, the overpotential measured in the presence of organic additives can be considered to indicate contribution only to the activation overpotential. The activation overpotential η_A, $(\eta_t + \eta_{crys.})$, is actually concerned with the reaction occurring during electrolytic deposition of ions, i.e., the sequence of events that each ion follows from the moment it arrives in the double layer until it becomes incorporated into the crystal lattice.

Charge-Transfer Overpotential at Metal/Ion Electrodes

The hindrance of the charge-transfer reaction causes the formation of charge-transfer overpotential

η_t. In metal/ion electrodes the charge carriers are metal ions M^{Z+} carrying Z elementary charges and the process can be represented by equation (1). The methods of electrochemical kinetics may be applied to the general charge-transfer reaction

$$O + Ze \underset{K-}{\overset{K+}{\rightleftharpoons}} R \qquad \text{-------(4)}$$

where O and R represent the oxidized and reduced species respectively, as

$$\upsilon_+ = K_+ C_O \qquad \text{-------(5)}$$

$$\upsilon_- = K_- C_R \qquad \text{-------(6)}$$

where υ_+ and υ_- are the rates in moles sec^{-1} cm^{-2} and C_O and C_R are the surface concentrations of the respective species at the interface. The rate constants K_+ and K_- of reaction (4) must be proportional to the Boltzman factor $\exp(-\Delta G^*_{\pm}/RT)$, which allows for the activation energy, as follows:

$$K_+ = \bar{K}^*_+ \exp(-\Delta G^*_+/RT) \qquad \text{-------(7)}$$

$$K_- = \bar{K}^*_- \exp(-\Delta G^*_-/RT) \qquad \text{-------(8)}$$

where ΔG^* is the free energy of activation, and $\bar{K}^*$ is the proportionality constant which depends on the activities, nature of the metal, and the temperature.

If the overall reaction involves the passage of ZF Coulombs $mole^{-1}$ of products cm^{-2}, the electrochemical rate υ in terms of current density i is

$$i = \upsilon ZF \qquad \text{-------(9)}$$

At equilibrium the rate of forward and backward reactions, determined by the free energy of activation, can be written as:

$$i_+ = C_0 ZF\bar{K}_+^* \exp(-\Delta G_+^*/RT) = K_+^* \exp(-\Delta G_+^*/RT) \qquad \text{-------(10)}$$

and

$$i_- = C_R ZF\bar{K}_-^* \exp(-\Delta G_-^*/RT) = K_-^* \exp(-\Delta G_-^*/RT) \qquad \text{-------(11)}$$

where K^* is equal to $CZF\bar{K}^*$.

As the electrode potential departs from the equilibrium value by an amount η, change in the reaction rates will take place. If the change from E_0 to E is such that the rate of discharge is faster than the rate of ionization, a net cathodic current will be produced. The free energy of activation for the discharge process will decrease from ΔG_+^* to $\Delta G_+^* - \alpha_c Z \eta F$ and it will increase for the ionization process from ΔG_-^* to $\Delta G_-^* + \alpha_a Z \eta F$ (4), where α_c and α_a are the transfer coefficients† for the cathodic and anodic processes respectively. The net electrochemical rate in terms of current density can be written as:

$$i = i_+ - i_-$$

---

†Appendix A

i.e.,

$$i = K_+^* \exp\left[(-\Delta G_+^* + \alpha_c \eta ZF)/RT\right] - K_-^* \exp\left[(-\Delta G_-^* - \alpha_a \eta ZF)/RT\right] \qquad \text{-------(12)}$$

Equation (12) can be written in terms of the exchange current density i_o, as

$$i_o = K_+^* \exp(-\Delta G_+^*/RT) = K_-^* \exp(-\Delta G_-^*/RT) \qquad \text{-------(13)}$$

i_o being the current which corresponds to the identical anodic and cathodic current densities that compensate each other at the equilibrium potential E_o, i.e. at $\eta = 0$. Therefore, equations (12) and (13) can be reduced to

$$i = i_o \left[\exp(\alpha_c \eta ZF/RT) - \exp(-\alpha_a \eta ZF/RT)\right] \qquad \text{-------(14)}$$

The validity of equation (14) is based on the assumption that C_0 and C_R are independent of current density and potential, and consequently, only pure charge-transfer overpotential is involved.

At low overpotential, i.e. $\eta < \frac{RT}{ZF}$, equation (14) can be reduced to a simpler form by employing a linear expansion of the exponential terms, giving

$$i = \frac{i_o Z \eta F}{RT} \qquad \text{-------(15)}$$

Equation (15) indicates that cathodic current density is linearly related to the overpotential at small η .

At low overpotentials, provided that charge-transfer is still the rate-determining step, this equation is found to be a good approximation. However, this is not always true in the case of metal deposition (5,6).

It can readily be seen that for larger charge-transfer overpotentials, $\eta \gg RT/Z\alpha F$, the second term in equation (14) can be neglected and the following expression is obtained

$$i = i_o \exp(\alpha \eta ZF/RT) \quad \text{-------(16)}$$

By a simple transformation of equation (16), the overpotential can be expressed in terms of current density by

$$\eta = \frac{-RT}{\alpha ZF} \ln i_o + \frac{RT}{\alpha ZF} \ln i \quad \text{-------(17)}$$

Equation (17) is similar to the empirical equation described by Tafel (7) for hydrogen overpotential

$$\eta = a + b \ln i \quad \text{-------(18)}$$

The Tafel slope b is, therefore, given by

$$b = \frac{RT}{\alpha ZF} \quad \text{-------(19)}$$

which permits its theoretical calculation.

Equation (17) indicates that the Tafel equation is obtained for the charge-transfer overpotential at metal/ion electrodes. When η is plotted vs. ln i, a straight line is obtained if charge transfer is rate determining. Extending the line to ln i = 0 to find the intercept for equation (17) allows calculation of the exchange-current density i_o.

The Mechanism of Metal Deposition

The main purpose in any investigation of a metal deposition-dissolution system is to obtain the mechanism of the process

$$(\text{metal ion})_{\text{solution}} + (Z \text{ electrons})_{\text{crystal}} \longrightarrow (\text{metal atom})_{\text{crystal}}$$

The sequence of events that each metal ion follows, from the bulk of the solution to incorporation into the crystal lattice, can be summarized according to the usually accepted mechanism of metal deposition as follows (8) (see figure 1a):

(1) The transfer of an ion from its hydration sheath in solution to some position on the metal surface, most likely a surface plane of the metal, where the ion is still partly hydrated.

(2) Charge-transfer process takes place, forming adions*. Whether water of hydration remains attached to a particle after the charge-transfer stage depends upon whether some ionic character is retained by the particle. Bockris & Conway (9) showed that the number of hydrating water molecules retained decreases as the depositing particle replaces these molecules in its coordinating sphere by other metal atoms on the surface. This model is shown in Figure 1b.

(3) The final step is the incorporation in the lattice at a kink or growth site. Accordingly, the following

*If the adsorbed particles retain part of their charge, they are called adsorbed ions or adions.

Figure 1

(1a) Consecutive ionic transfer, surface-diffusion of adsorbed ions during the building of the metal lattice in electrolytic metal deposition.
Diagram taken from the original reference (11).

(1b) Diagrammatic representation of possible modes of hydration of transferred adions at various sites upon the metal surface.
Figure (1b) was taken from the original reference (9).

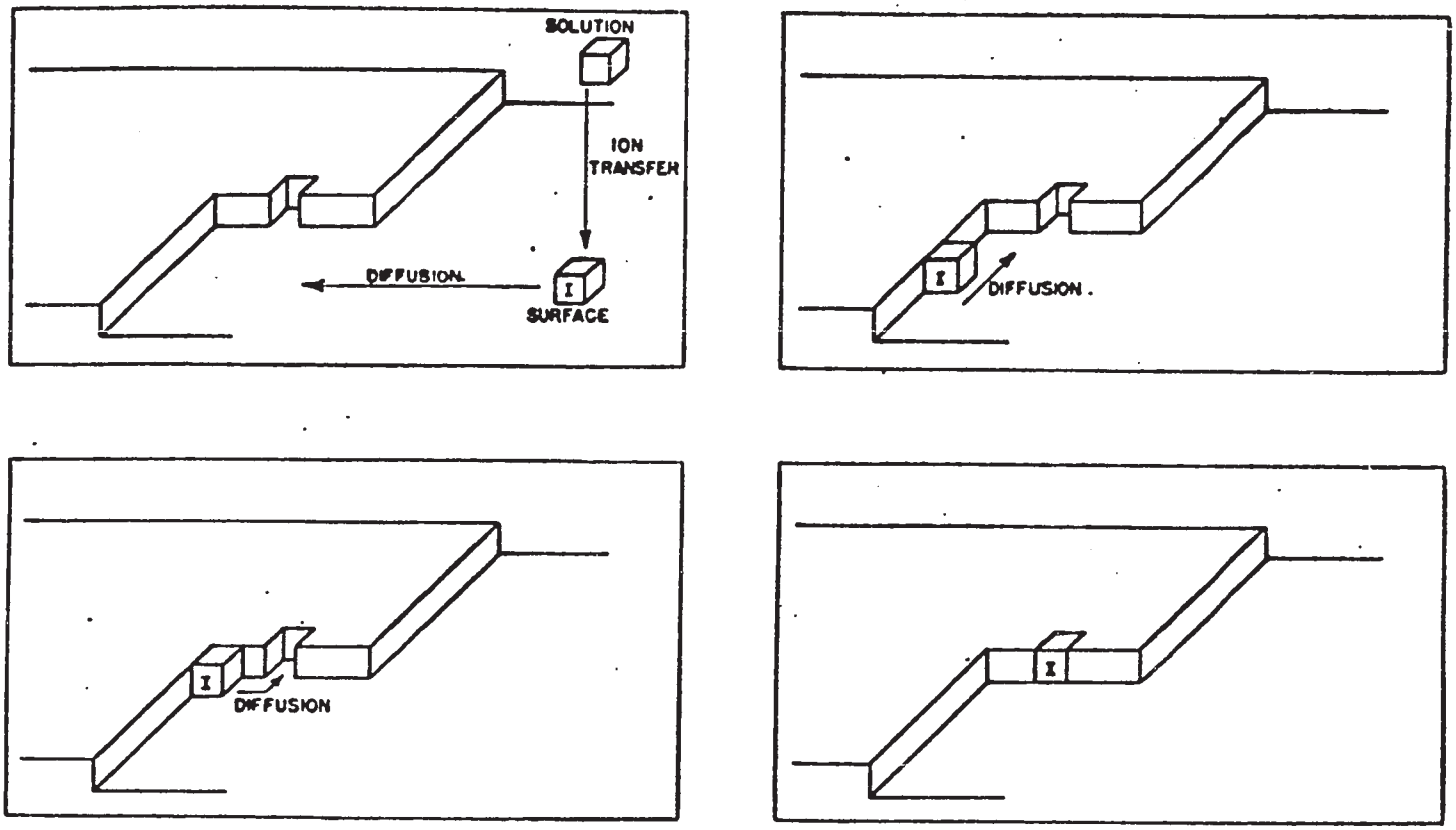

Figure (1a)

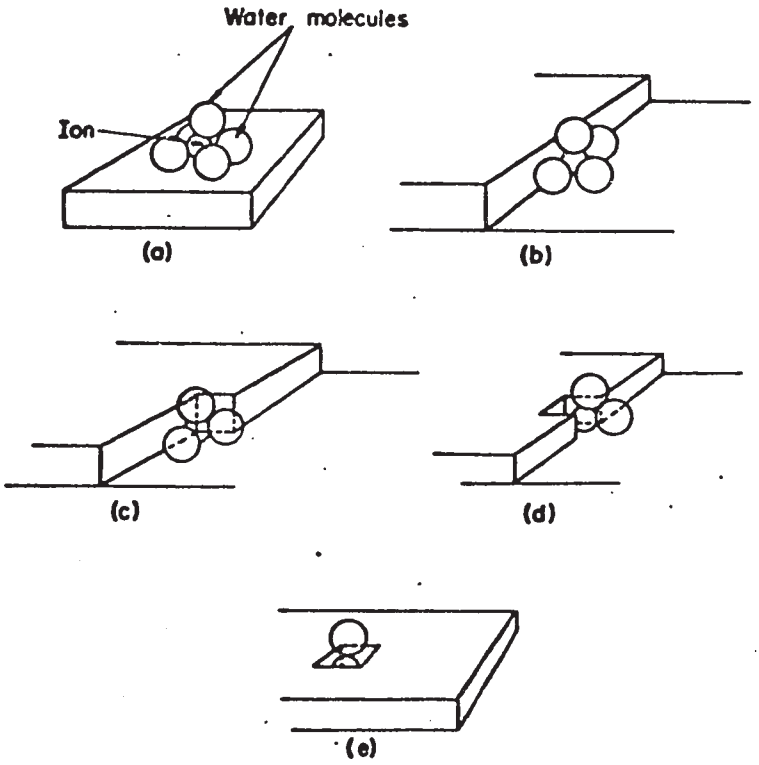

Figure (1b)

equation can be written;

$$\begin{pmatrix}\text{Ion in}\\ \text{double}\\ \text{layer}\end{pmatrix} \xrightarrow[\text{at planar site}]{\text{charge transfer}} \begin{pmatrix}\text{Adion in}\\ \text{planar}\\ \text{site}\end{pmatrix} \xrightarrow[\text{surface}]{\text{Diffusion across}} \begin{pmatrix}\text{Adion}\\ \text{at}\\ \text{kink}\end{pmatrix}$$

Therefore, the rate-determining step will depend on the rate of the kinetic process, either the charge-transfer or surface diffusion. The accepted mechanism for copper deposition (1,10) when the potential is relatively negative is a two-step charge-transfer reaction,

$$Cu^{2+} + e \xrightarrow{\text{slow}} Cu^{+}$$

$$Cu^{+} + e \xrightarrow{\text{fast}} Cu$$

Under these conditions, the overpotential for copper deposition may be attributed primarily to the charge-transfer reaction, the kinetic treatment of which has already been described. At low overpotentials, the rate-determining step is believed to be the surface diffusion of adions from their point of deposition to their final lattice position (8,10,12,13). However, there are conditions under which surface-diffusion can be rate-determining at other than low overpotentials (12,14,15).

Surface-Diffusion Overpotential

If the diffusion coefficient for an adion on the metal surface is sufficiently small, the surface diffusion process will be important in determining the rate of the overall reaction. The surface concentration of adions during polarization, i.e., during current flow, will be greater than the surface concentration corres-

equation can be written;

$$\begin{pmatrix}\text{Ion in}\\ \text{double}\\ \text{layer}\end{pmatrix} \xrightarrow[\text{at planar site}]{\text{charge transfer}} \begin{pmatrix}\text{Adion in}\\ \text{planar}\\ \text{site}\end{pmatrix} \xrightarrow[\text{surface}]{\text{Diffusion across}} \begin{pmatrix}\text{Adion}\\ \text{at}\\ \text{kink}\end{pmatrix}$$

Therefore, the rate-determining step will depend on the rate of the kinetic process, either the charge-transfer or surface diffusion. The accepted mechanism for copper deposition (1,10) when the potential is relatively negative is a two-step charge-transfer reaction,

$$Cu^{2+} + e \xrightarrow{\text{slow}} Cu^{+}$$

$$Cu^{+} + e \xrightarrow{\text{fast}} Cu$$

Under these conditions, the overpotential for copper deposition may be attributed primarily to the charge-transfer reaction, the kinetic treatment of which has already been described. At low overpotentials, the rate-determining step is believed to be the surface diffusion of adions from their point of deposition to their final lattice position (8,10,12,13). However, there are conditions under which surface-diffusion can be rate-determining at other than low overpotentials (12,14,15).

Surface-Diffusion Overpotential

If the diffusion coefficient for an adion on the metal surface is sufficiently small, the surface diffusion process will be important in determining the rate of the overall reaction. The surface concentration of adions during polarization, i.e., during current flow, will be greater than the surface concentration corres-

ponding to equilibrium. Accordingly equation (14), which is based on the assumption that the concentration of the ions in the vicinity of the metal surface is independent of current density and potential, will be invalid and the overpotential-current relation must then be modified accordingly. Bockris and Mehl (6) developed the following equation to represent this situation:

$$i = i_o \left[\exp(\alpha_c \eta ZF/RT) - \frac{C_\eta (t)}{C_0} \exp(-\alpha_a \eta ZF/RT) \right] \quad \text{-------(20)}$$

where C_o is the concentration of adions at equilibrium and $(C_{\eta (t)})$ is the concentration of adions at time t when the overpotential has reached a value η. For $\eta < (RT/\alpha ZF)$, and neglecting second-order terms, rearrangement of (20) gives

$$\eta_{(t)} = (RT/ZF) \ (i/i_o) + (RT/ZF) \ (\Delta C_{\eta,t}/C_o) \quad \text{-------(21)}$$

where

$$\Delta C_{\eta,t} = C_{\eta,t} - C_o$$

Hence η depends in this case on i_o for the charge-transfer reaction and on the concentration overpotential due to surface diffusion.

The rate of change of adion concentration at any point on a surface is given by the difference between the rate at which the adions arrive by deposition and the rate at which they diffuse away (6) as given in equation (22).

$$dc_{\eta,t}/dt = \frac{i}{ZF} - V \quad \text{-------(22)}$$

where V is the average surface diffusion flux of the adions during their passage from the point at which they are transferred to the metal surface and at which they meet a crystal building site. By assuming that the surface diffusion flux is proportional to the surface concentration, $(C_{\eta,t}/C_o - 1)$, we get

$$V = V_o (C_{\eta,t}/C_o - 1) \text{-------(23)}$$

Assuming further that the adion concentration near the kinks remains at an equilibrium value, then substitution of (23) in (22) followed by integration yields

$$\Delta C/C_o = \frac{i}{ZFV_o} (1 - e^{-(V_o/C_o)t}) \text{-------(24)}$$

Thus the steady-state value of the increased concentration of adions over that expected for pure transfer control is given for $t = \infty$ by:

$$\Delta C/C_o = i/ZFV_o \text{-------(25)}$$

Substituting (24) in (21) gives the overpotential as a function of surface diffusion and transfer of ions across the double layer as

$$\eta(t) = \frac{RT}{ZF} \left[\frac{i}{i_o} + \frac{i}{ZFV_o} (1-e^{-(V_o/C_o)t}) \right] \text{-------(26)}$$

Therefore for surface-diffusion to be rate-determining

$$ZFV_o < i_o \text{-------(27)}$$

Equation (27) has been derived with the assumption that

V_o is independent of overpotential, however, this assumption has been found to be incorrect (6,16). Bockris & Mehl (6) suggested the following empirical equation to show this overpotential dependence.

$$V_o\ (\eta) = V_o\ e^{-\eta ZF/RT} \qquad \text{-------(28)}$$

Substituting Equation (28) in (27) yields

$$ZFV_o\ (\eta) < i_o\ e^{\eta ZF/RT} \qquad \text{-------(29)}$$

From (26)

$$\eta_{(t)} - \eta_{(\infty)} = \frac{RT}{ZF}\ \frac{i}{ZFV_o}\left[e^{-(V_o/C_o)t}\right] \qquad \text{-------(30)}$$

and at t = 0

$$\eta_{t=0} = \frac{RTi}{ZFi_o} \qquad \text{-------(31)}$$

From Equation (30), plotting the natural logarithm of $(\eta_{(t)} - \eta_{(\infty)})$ vs. t should give a straight line with slope equal to $-V_o/C_o$, and from the extrapolation to t=0, the value of V_o can be obtained.

At $t = \infty$

$$\eta_{(\infty)} = \frac{RT}{ZF}\left(\frac{i}{i_o} + \frac{i}{ZFV_o}\right) \qquad \text{-------(32)}$$

This equation is valid at a time greater than the rise time of the transfer reaction, i.e., at the steady-state condition. From Equation (32) V_o can be calculated as a function of current density. This equation will be

employed in part of this work. Bockris and Mattson (10) concluded that if the Tafel slope observed in the deposition of divalent cation is less than, or equal to, .o295V. at 25°C, the rate-determining step cannot be a transfer process. Therefore, if this condition prevails, surface-diffusion should be applied according to the above equations. Evidence has been given (10) which makes it appear likely that ions transfer to surface planes and diffuse along the surface to the growth sites; that if the overpotential and the density of growth sites are sufficiently small, surface diffusion controls the rate; and finally, that rate-controlling surface diffusion turns into rate-controlling charge-transfer at higher overpotentials. It was also assumed (14,15) that relatively high concentration of cuprous ion, in copper deposition, might cause surface-diffusion to be controlling. Therefore, in the case of electrodeposition of copper under conditions where surface-diffusion is likely to be rate-controlling, the following mechanism may be expected (14)

$$Cu^{++} + e \longrightarrow Cu^{+}$$

$$Cu^{+} + e \xrightarrow{\text{fast}} Cu_{(\text{Adion})}$$

$$Cu_{(\text{Adion})} \longrightarrow Cu_{(\text{lattice})}$$

The last equation will be relatively slow, and will consequently determine the overall reaction rate.

The Effect of Organic Additives on Overpotential During Copper Deposition

During the development of modern electroplating practice, it was found that the inclusion of small amounts of the proper addition or brightening agent in the plating bath results in marked changes in the nature of the deposit obtained from the bath. In most cases addition agents are used to obtain smooth bright deposits although they may also be used in some cases to improve other physical properties. In the case of additives that result in a large increase in cathode overpotential, it is generally believed that the increase in overpotential is mainly caused by the adsorption of the additive on the cathode surface (17,18,19,20).

In metal deposition, it is generally believed that an overpotential increment, due to the adsorption of additives, arises from a partial blocking of the electrode, resulting in an increased current density on the uncovered fraction, hence, a corresponding increase in overpotential (21). Therefore, if a fraction θ of the cathode surface is covered by adsorbed additive, and if electrodeposition proceeds on the uncovered surface only, the true current density acting on the uncovered portion will be increased from i to $i/(1 - \theta)$. The true current density with additive, i', is therefore related to the true current density without additives, i, by

$$i' = \frac{i}{(1 - \theta)} \qquad \text{-------(33)}$$

If the charge-transfer reaction remains rate-determining, the relation between the overpotential in the presence of additive η' and the corresponding true current density i' can be described by the Tafel equation:

$$\eta' = a + b \ln i'$$

or

$$\eta' = a + b \ln \frac{i}{(1-\theta)} \qquad \text{-------(34)}$$

Since, in the absence of additive, the overpotential is related to the true current density i by equation (18), an expression relating $\Delta\eta$, the overpotential increment, to the fractional surface coverage θ can be obtained by subtracting equations (18) from (34), to give

$$\Delta\eta = b \ln \frac{1}{(1-\theta)} \qquad \text{-------(35)}$$

This equation, based on the simple blocking theory, has been used for investigating the hydrogen overpotential at solid electrodes (19,22). It is also presently accepted in interpreting overpotential increments caused by additives (25). Generally, equation (35) is expected to be valid for additives which adsorb randomly on the electrolytically active sites and behave primarily as an inert blanket on the electrode.

Electrosorption of Organic Additives from Solution

An understanding of adsorption at the electrolyte-electrode interface is necessary for understanding the

behavior of surface-active additives during electrodeposition of metals. Additives in the form of neutral molecules or ions are adsorbed either physically or chemically at the electrode. The reason that surface-active additives adsorb at an interface is because of a decrease in their free energy resulting either from increased bonding energy at the interface or because they otherwise find a lower free-energy environment at the interface than in solution. Numerous studies of adsorption of organic additives on mercury electrodes have been reported (23,24,25,26,27,28,29), where the extent of adsorption can be normally determined from electrocapillary measurements. Recently, radiotracer methods have been widely used in studying the electrosorption of organic additives at solid electrodes (30,31). These electrosorption measurements were conducted in a potential region which allows no charge transfer or other reaction at the electrode. The only difference between electrosorption and solution-phase adsorption is that the former is potential dependent. Accordingly, a great deal of information can be obtained from solution-phase adsorption studies (32) particularly concerning the adsorbability of additive and the type of bonding between additive and surface. For adsorption from solution, the extent of adsorption depends on the solubility of the additives (33). Generally, the lower the solubility, the higher

the adsorbability (34).

Adsorption from solution is influenced by interactions between the metal, the organic compounds, and the solvent, both on the surface and in the bulk solution. Competition between solvent and additives for the electrode will therefore occur. The equilibrium between adsorbed additives on an electrode surface and additives in the bulk solution can be described in the customary way by an adsorption isotherm. A great deal of information can be obtained from gas-phase adsorption studies (35,36) if it is borne in mind that the major difference between gas-phase and liquid-phase adsorption is merely that the substrate surface is bare in the former and solvated in the latter. It follows that isotherms originally derived for gas-phase adsorption can be applied to liquid-phase adsorption. In this study as a first approximation, the Langmuir-type isotherm has been applied and found useful. The Langmuir-type isotherm for adsorption from liquid phase has been developed by Bockris (34,37) and used by several other authors (30,33,34). It has the following form:

$$\frac{\theta}{(1-\theta)^n}\ \frac{[\theta + n(1-\theta)]^{n-1}}{n^n} = KC = \frac{C}{55.5}\, e^{-\Delta G^{o}_{a}/RT} \qquad \text{-------(36)}$$

where θ is the fractional surface coverage, K the adsorbability or equilibrium constant, C the bulk concentration of additive, ΔG^{o}_{a} the apparent standard free energy of

adsorption, and n the number of water molecules displaced per molecule of adsorbed additive. When n is unity, equation (36) reduces to the usual Langmuir isotherm

$$\frac{\theta}{(1-\theta)} = KC = \frac{C}{55.5} e^{-\Delta G_a^o / RT} \qquad \text{-------(37)}$$

CHAPTER II

EXPERIMENTAL

Electrolytic Cell & Overpotential Measurements

Cathodic overpotential measurements were made with an H-type electrolytic cell shown schematically in Fig. 2. In constructing this cell, two essential features were considered. First, it was necessary to avoid any possible IR drop between the non-working reference electrode and the cathode. Secondly, it was necessary to prevent shielding of the surface of the working electrode from access of polarizing current by the Luggin probe. Accordingly, the cell was designed as a specially constructed glass H-cell connected to a reference electrode as shown. The reference attachment consisted of a copper electrode and standard solution connected to the cathode compartment by means of a Luggin capillary. The Luggin tip was designed to give a ratio of outside to inside diameter of about 2.0 (38). The cathode was fitted snugly into the reference attachment and was brought close to the Luggin probe at a distance of about 2mm and at about 0.5 cm of the bottom of the cathode as shown in Fig. 2. The counter electrode was arranged to achieve a cylindrically symmetrical field at the cathode, by having it at a distance from the

Figure 2

Electrolytic Cell

1	Cathode
2	Luggin probe
3	Teflon sleeve
4	Reference electrode
5	Anode
6	Teflon cap

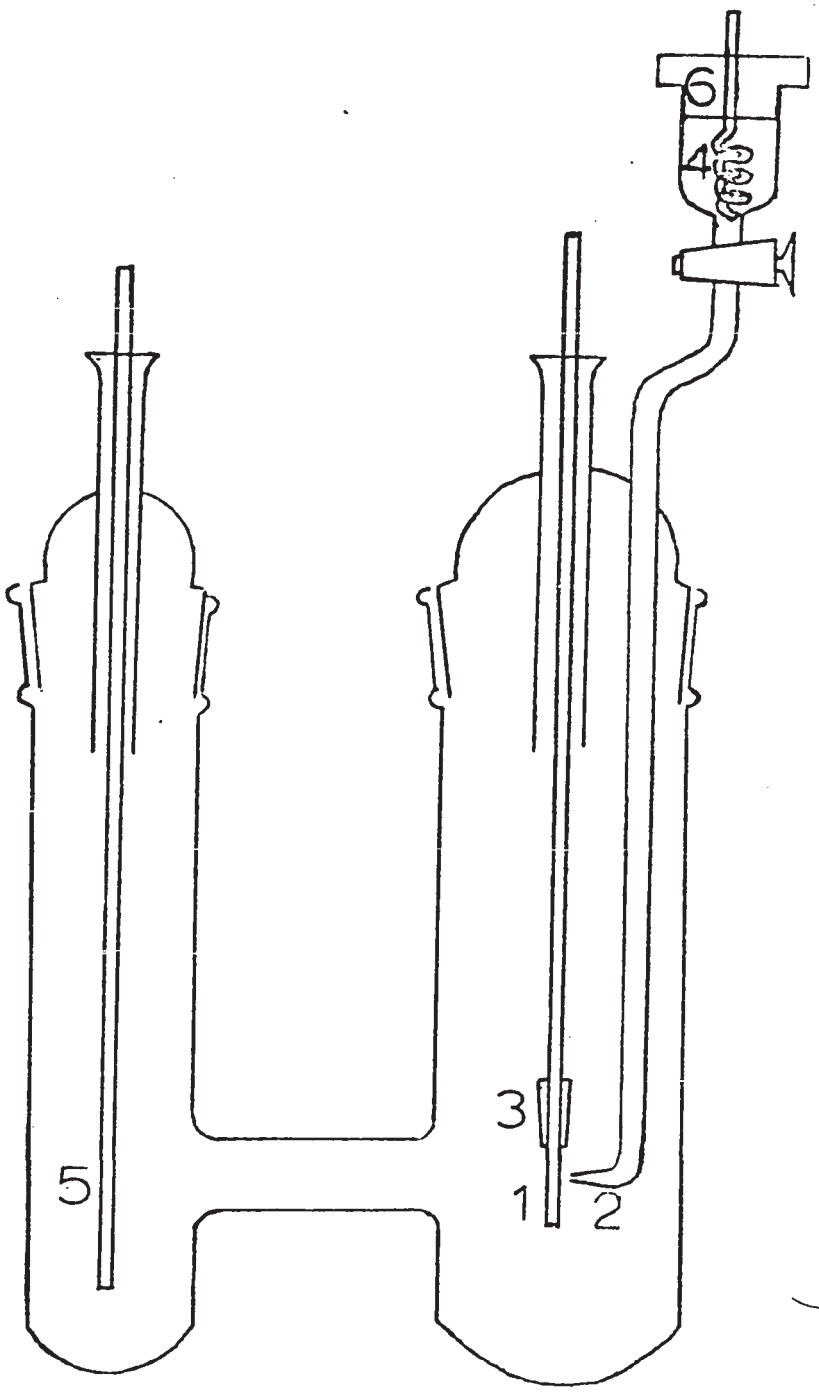

Fig. 2

cathode appreciably greater than the diameter of the cathode (38).

According to this arrangement, the essential factors that determine the IR drop between cathode surface and Luggin tip are the radius of the cathode and the resistance of the solution. A thin copper rod of 2mm diameter, and high conductivity solution (1 mole/1 H_2SO_4) were used, making the IR drop negligibly small.

The IR drop was measured experimentally from the transient build-up of the overpotential for all the additive-containing solutions as well as the standard solution; the values were found to be in the order of $3\pm$ 2mV in all cases.

The electrical arrangement for overpotential measurement is shown in Fig. 3. Current for electrolysis was supplied by a Harrison Regulated Power Supply Model 6201A. The current was measured with a three-range Weston Model 931 milliammeter accurate to one percent.

Three types of overpotential measurement were made in this work. The first measurement, at the beginning of electrolysis, was to follow the build-up transient of the overpotential from which the IR drop and the capacity of the double layer were obtained. A cathode ray oscilloscope, Tektronix type 535A with D plug-in unit, and a specially designed high speed switch, using Northern Electric Relay type NE275B, with a rise time of about 1μsec.

(10) see Fig. 3, were used for this measurement. Secondly, a Sargent Model SR Recorder was used to measure the overpotential as a function of time until a steady-state value was attained. Generally, the time required for attaining a steady-state overpotential was less than an hour (30-45 minutes) in all the experiments except for those where depolarization took place. In the latter, the steady-state overpotential was attained more slowly, usually in about 1½ hours. After a steady-state was attained, the overpotential was measured with a Leeds & Northrup type K-2 potentiometer in conjunction with a Weston standard cell, 1.01925 Volts, and a G.M. Laboratories galvanometer.

At zero current, the cathode overpotential relative to the reference electrode was zero. During current flow between the cathode and anode, the cathode potential becomes more negative, whereas the potential of the non-working reference electrode remains unchanged as no current passes through it. Thus, the cathode potential measured relative to the reference represents the cathode overpotential during current flow. In investigating the effect due to the additive, the H-cell shown in Fig. 2 was filled with standard solution containing additive, whereas the reference cell contained the same solution with no additive. Under these circumstances, since the potential of the reference electrode remains unchanged, any increase in overpotential of the cathode will be due primarily to

Figure 3

Circuit Diagram

S_1	Single-pole single-throw manual switch.
S_2	Double-pole double-throw manual switch.
S_3	Microswitch.
R_1	½ watt, 500 ohms variable resistance.
R_2	½ watt, 250 ohms variable resistance.
R_3	½ watt, 5k ohms variable resistance.
C	1 μ Farad capacity.
B	90 volts battery.
NE-275B	Northern Electric mercury relay type NE-275B.
PS.	Power supply, Harrison model 6201A.
A	Weston three-range milliammeter.
C.R.O.	Cathode Ray Oscilloscope, type 535A.
Pot.	Potentiometer, Leeds & Northrup type K-2.
Rec.	Recorder, Sargent Model SR.
1	Anode.
2	Reference electrode.
3	Cathode.

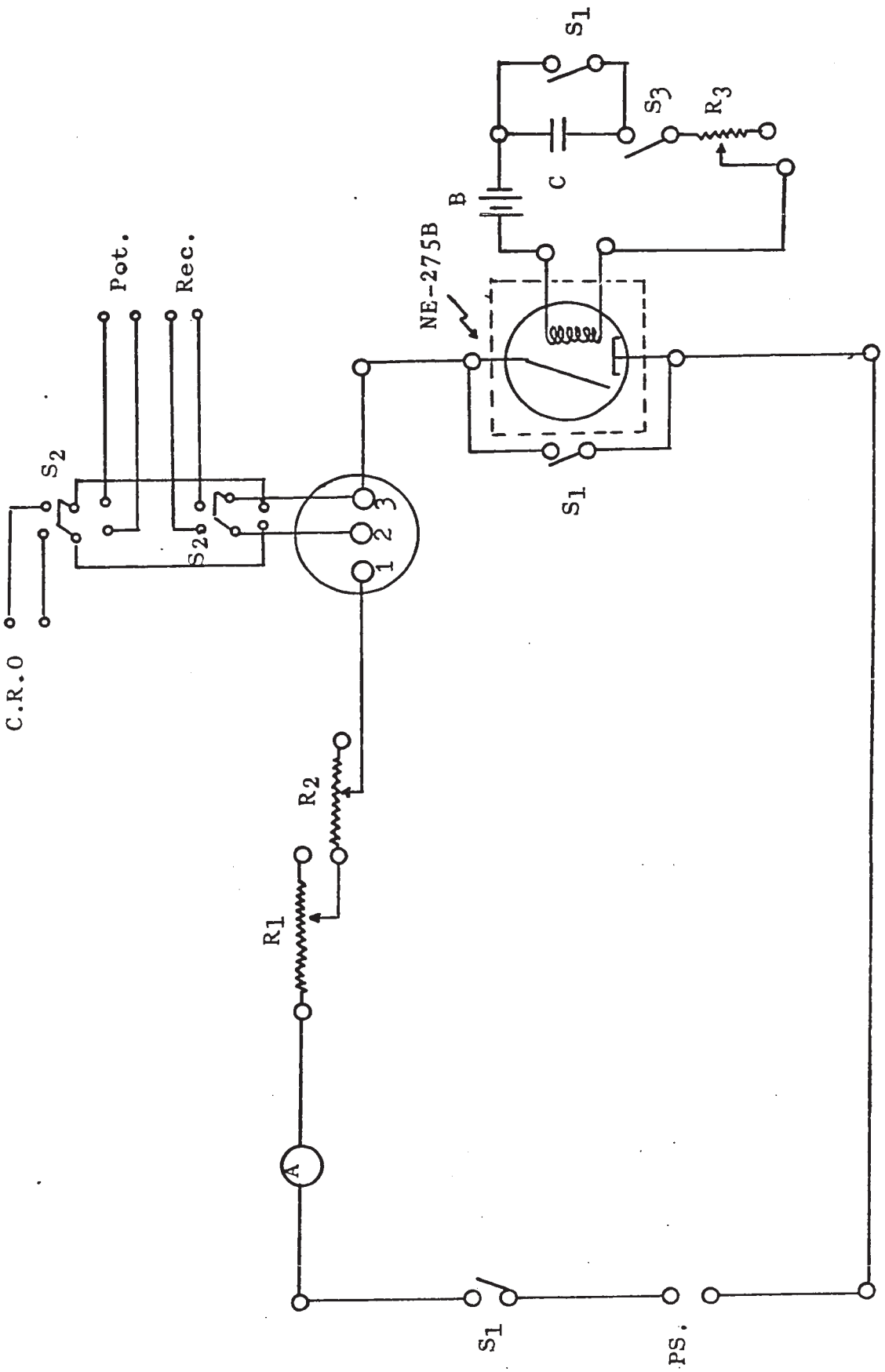

Fig. 3

the influence of the additive.

Overpotential measurements at different current densities were obtained, after the steady-state overpotential was first attained at 20 mA/cm^2, by reducing the current in two-milliampere steps from 20 mA/cm^2 to 2 mA/cm^2. The time required for steady-state at each new current density ranged from two to five minutes.

After the measurements were completed, the solution was discarded and the cell was first rinsed with $KMnO_4$ and conc. H_2SO_4 followed by a thorough rinsing with distilled water. The second rinse was with a solution of HNO_3 and H_2O_2 and then again a rinse with distilled water. The final rinse was done with double distilled water and then followed with triple distilled water until no change in conductivity of the rinse water was observed. The cell was finally dried at 120^o in an oven for at least 4 hours.

Preparation of the Solution

Electrolyte containing 0.5M $CuSO_4$ and various conc. of H_2SO_4 was used as standard solution. The copper sulfate pentahydrate was Fisher Scientific Co. Certified Reagent grade. Reagent grade sulfuric acid (Shawinigan Chem. Co.) was used. Triply distilled water was used for all solutions. The initial distillation of the centrally supplied water was done in a Corning Still, Model AG-2. To remove or destroy possible surface-active impurities, the distillate was redistilled from acidic sodium dichromate solution

directly to the distillation vessel from which the final distillation was done. The second and third distillations were done in all-glass apparatus. The triply distilled water obtained by this method normally gave conductivities of about 10^{-6} ohm^{-1}, which was considered to be of sufficient purity for present purposes.

To investigate the effect of organic additives on the cathode overpotential in copper deposition, the desired amount of additive was added to the standard solution. The final concentration of the solution was 0.5M $CuSO_4$, 1.0M H_2SO_4 and the required concentration of additive.

The additives were of reagent grade and most of them were subjected to further purification. Purification procedures were chosen in accordance with the type of organic compound and its condition. Only one of the additives, thiobutyric acid, was prepared in this laboratory. It was doubly distilled, and a fraction was collected to agree with the literature (39). With the exception of thioacids, mercapto acids and thiols, the addition agents were added directly to the standard solution immediately before use. Thioacids, mercaptoacids and thiols were added from a concentrated solution prepared from the additive and triply distilled water. This avoided the formation of gummy precipitation products when liquid additives were added to acid copper sulfate solution.

Preparation of Electrodes

The cathode and anode were copper rods of 2mm diameter. Both electrodes were mounted vertically by slipping through Pyrex glass tubes (7.5mm O.D. with 12/2 ball and socket joint) which formed part of the male joints as shown in Fig. 2. The reference electrode was a copper rod 2mm in diameter and coiled in a spiral to allow a maximum area to be in contact with the solution. The vertical part of the reference electrode was mounted in a piece of Teflon, which in turn was fitted snugly into the reference compartment (see Fig. 2). The required surface area of the cathode for electrodeposition was fixed by enclosing a part of the cathode in a tightly fitting Teflon sleeve. The apparent geometrical area of the cathode was $1cm^2$ for all experiments.

Before each electrolysis the electrodes were cleaned with 1:1 nitric acid for 60 seconds and then washed thoroughly with triply distilled water. The freshly prepared electrode was immediately employed for electrolysis.

Temperature Regulation

Control of the temperature was achieved by immersing the electrolytic H-cell up to the solution level in a temperature-regulated water bath. A thermometer-type Sargent thermoregulator operating a 500 watt

heater element controlled the temperature. The bath was stirred by bubbling a stream of air through it. The temperature of the water bath was maintained at $25^{o} \pm 0.5^{o}C$. All the overpotential measurements were carried out at this temperature.

Organic Additives Used

The effects of thirty-five organic compounds on the copper electrodeposition were studied. These compounds can be divided into four groups, according to their functional group. Each group can be divided further into classes according to the following scheme.

Group One: - Monocarboxylic acids

Propanoic, Butanoic, Pentanoic, Hexanoic, Heptanoic and Octanoic acids.

- Dicarboxylic acids

Propanedioic, Butanedioic, Pentanedioic, Hexanedioic, Heptanedioic, Octanedioic, Nonanedioic acids

Group Two: - Thioacids

Thioacetic, Thiopropionic, Thiobutyric acids

- Mercaptoacids

Mercaptoacetic, Mercaptopropionic, Mercaptobutyric acids

- Thiols

1-Ethanethiol, 1-Propanethiol, 1-Butanethiol

Group Three: - Diols

1,2 Ethanediol, 1,3 Propanediol, 1,4 Butanediol, 1,5 Pentanediol, 1,3 Butanediol, 1,6 Hexanediol.

Group Four: - Cyclohexane derivatives

Cyclohexanecarboxylic acid, 1,2 cyclohexanedicarboxylic acid, and cyclohexanol.

- Benzene derivatives

Phenol, Benzoic, Phthalic, Isophthalic acids.

CHAPTER III

RESULTS & DISCUSSION

The organic compounds used will be divided into four groups, as indicated previously, and the results and discussion of each group will be dealt with separately. All overpotentials reported in this work are steady state total values unless otherwise stated.

PART I

Behavior of the Standard Solution

1) Results:

Generally, the term standard solution denotes acidified or non-acidified $CuSO_4$ solution without additives. In Groups One, Three and Four, the standard solution was 0.5M $CuSO_4$ and 1.0M H_2SO_4. In the case of Group Two additives the standard solution had the same amount of $CuSO_4$, but the sulfuric acid concentration varied between zero and 1.0M H_2SO_4.

The total cathode overpotential for the standard solution (0.5M $CuSO_4$, 1.0M H_2SO_4) at 25$\pm$.1°C and 20 mA cm^{-2} was 100$\pm$ 5 millivolts which satisfactorily agrees with values obtained elsewhere (17,18,40,41). Typical overpotential-time relations for the standard solution (0.5M

$CuSO_4$, 1.0M H_2SO_4) are shown in Fig. 4.

Relation Between Overpotential & Current Density for Standard Solutions

The relation between activation overpotential η_A and current density is given, for the rate-determining charge-transfer reaction, by Equation (14), i.e.,

$$i = i_o \left[\exp(\alpha_c \eta_A ZF/RT) - \exp(-\alpha_a \eta_A ZF/RT) \right] \quad (14)$$

where α_c is the cathodic transfer coefficient and α_a is the anodic transfer coefficient. For $|\eta| > 40$ mV (10), for divalent ions, Equation (14) can be simplified to the Tafel equation (18),

$$\eta = a + b \ln i \quad (18)$$

The experimental steady-state overpotential was plotted against ln i, for 0.5M $CuSO_4$ and 1.0M H_2SO_4, for both cathodic and anodic overpotentials as shown in Fig. 5. The numerical values are given in Table 1a. The η - ln i diagram showed a good linear Tafel relation, both for cathodic and anodic curves. The i_o - values obtained by extrapolation of the Tafel line to $\eta = 0$ were the same for dissolution and deposition. The transfer coefficients were calculated according to Equation (16). The results of α_c, α_a, i_o, b_c, and b_a are given in Table 1b. These results obtained are in agreement with those calculated theoretically for charge-transfer as a rate-determining step (10,12,13).

Figure 4

Overpotential-time relation (η vs. t) for copper deposition from 0.5M $CuSO_4$ & 1.0M H_2SO_4

a standard solution (Run 1)

b standard solution (Run 2)

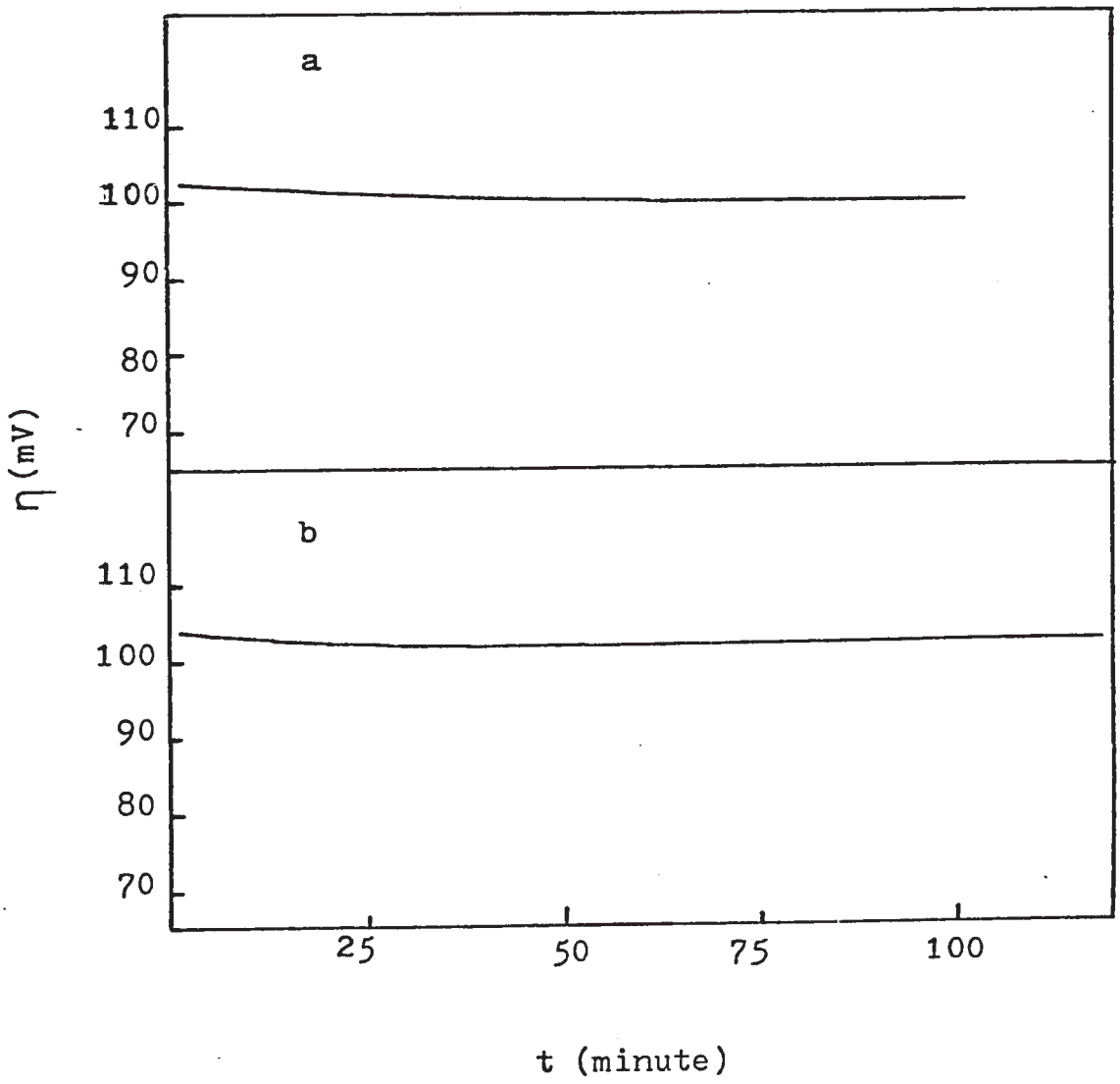

Fig. 4

Figure 5

Overpotential-current density relation (η vs. ln i)

a	0.5M $CuSO_4$, 1.0M H_2SO_4	(cathodic)(Run 1)
b	0.5M $CuSO_4$, 1.0M H_2SO_4	" (Run 2)
1	0.5M $CuSO_4$, Nil H_2SO_4	"
2	0.5M $CuSO_4$, .1M H_2SO_4	"
3	0.5M $CuSO_4$, .25M H_2SO_4	"
4	0.5M $CuSO_4$, .5M H_2SO_4	"
5	0.5M $CuSO_4$, .75M H_2SO_4	"
6	0.5M $CuSO_4$, 1.0M H_2SO_4	"
O	0.5M $CuSO_4$, 1.0M H_2SO_4	"
□	0.5M $CuSO_4$, 1.0M H_2SO_4	(anodic)

Fig. 5

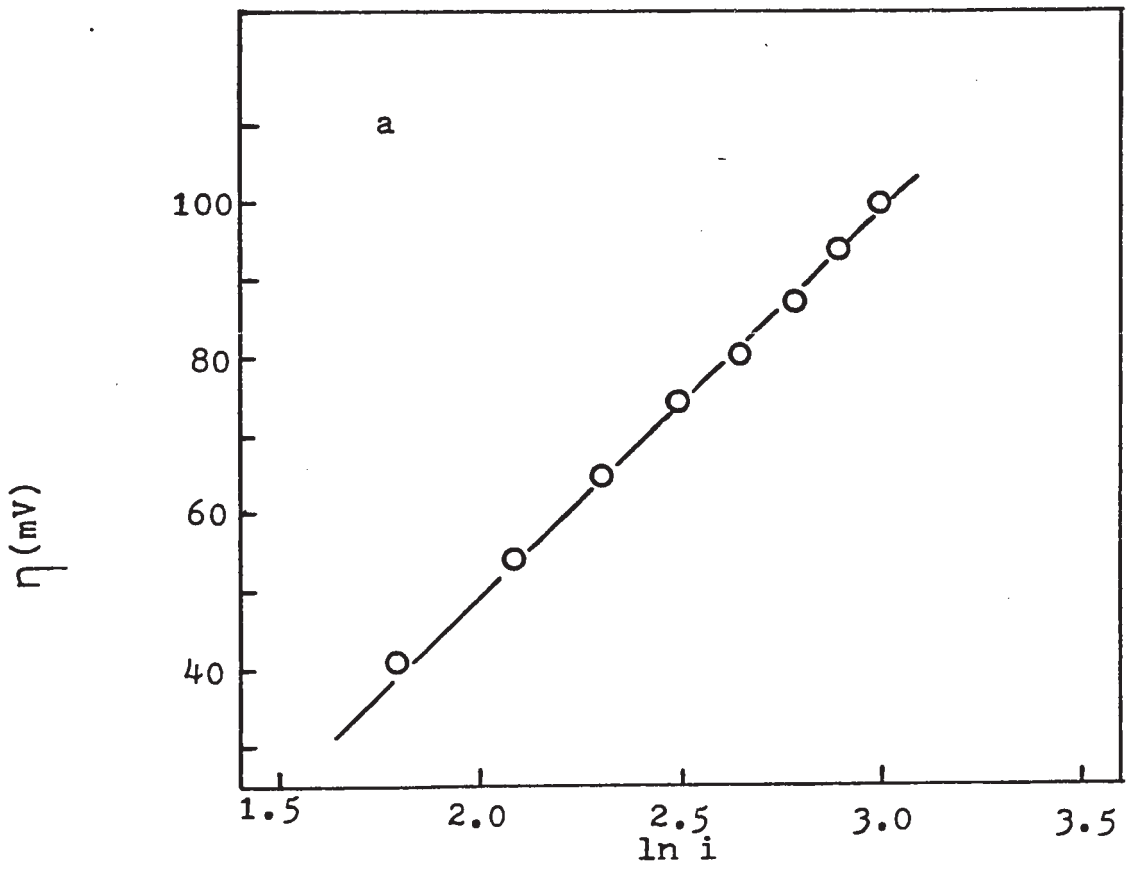
a
100
80
60
40
η (mV)
1.5
2.0
2.5
3.0
3.5
ln i

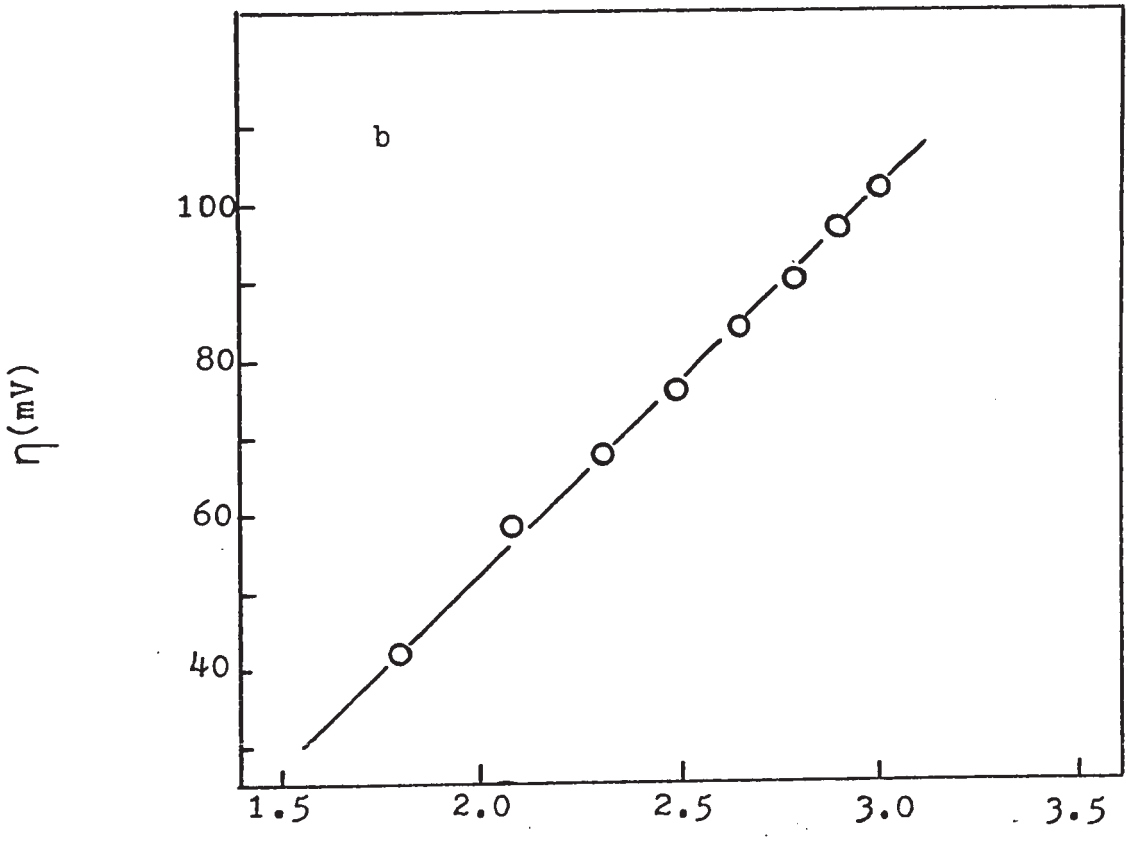
b
100
80
60
40
η (mV)
1.5
2.0
2.5
3.0
3.5
ln i

Fig. 5

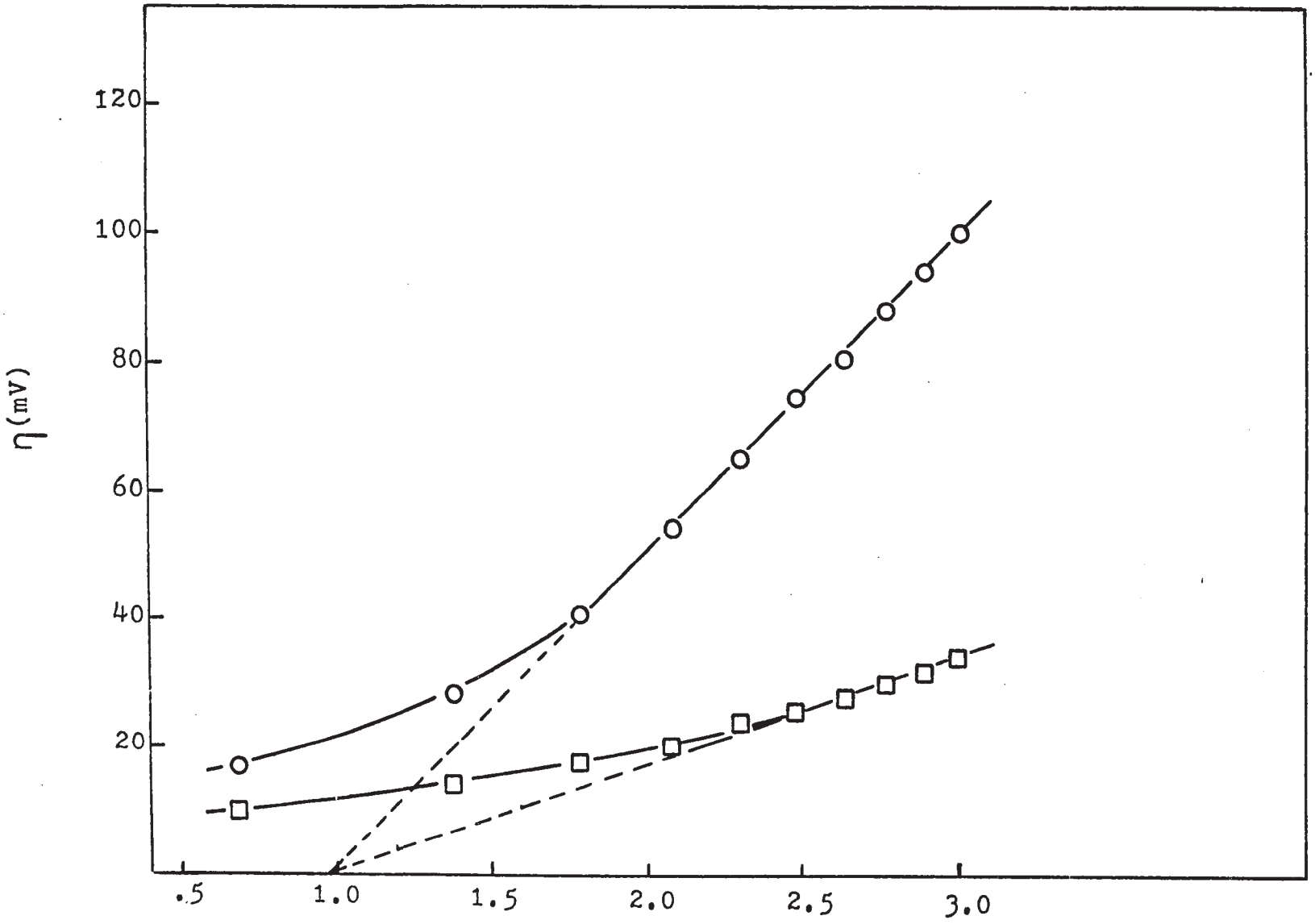

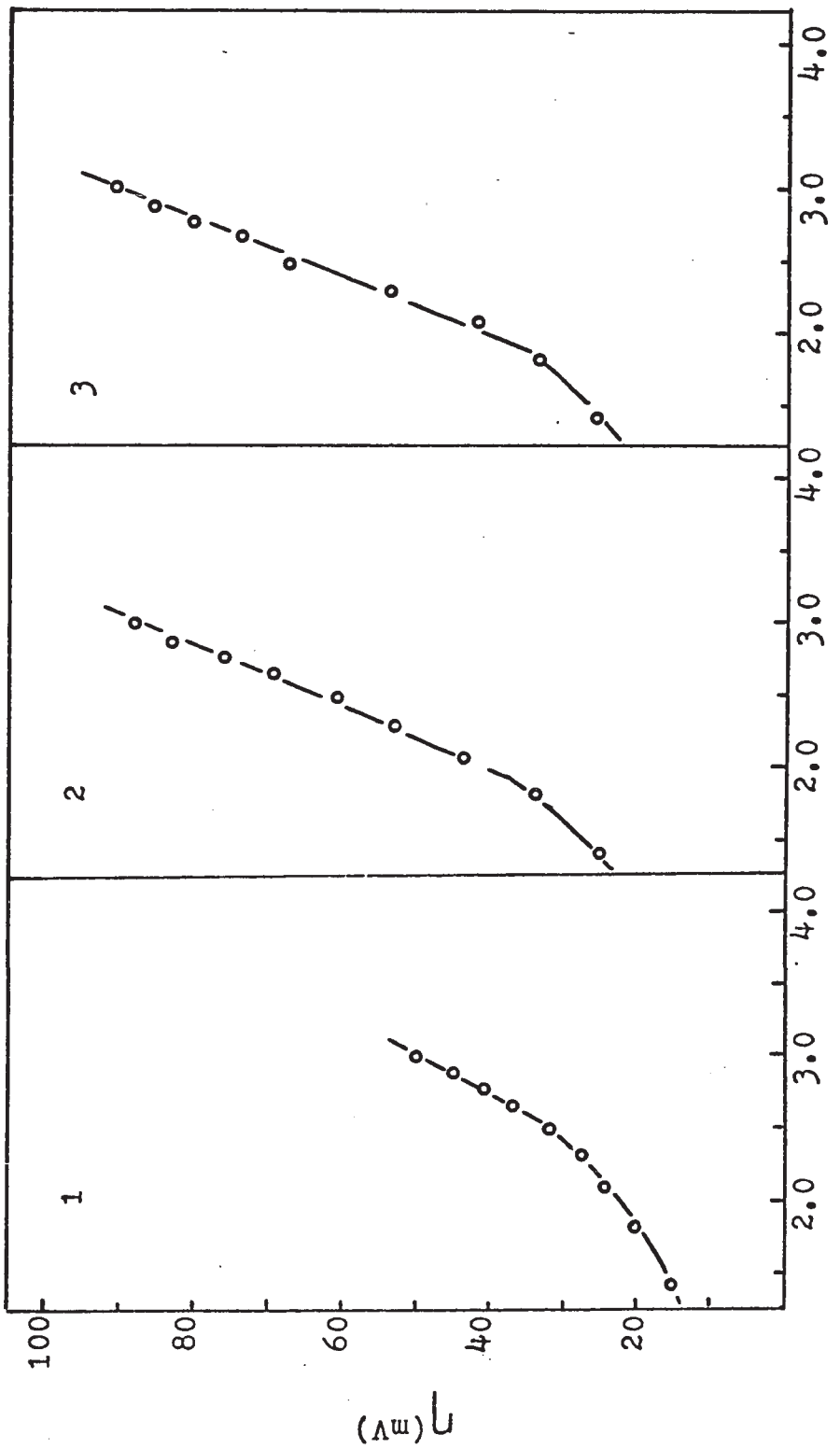

Fig.5

Fig. 5

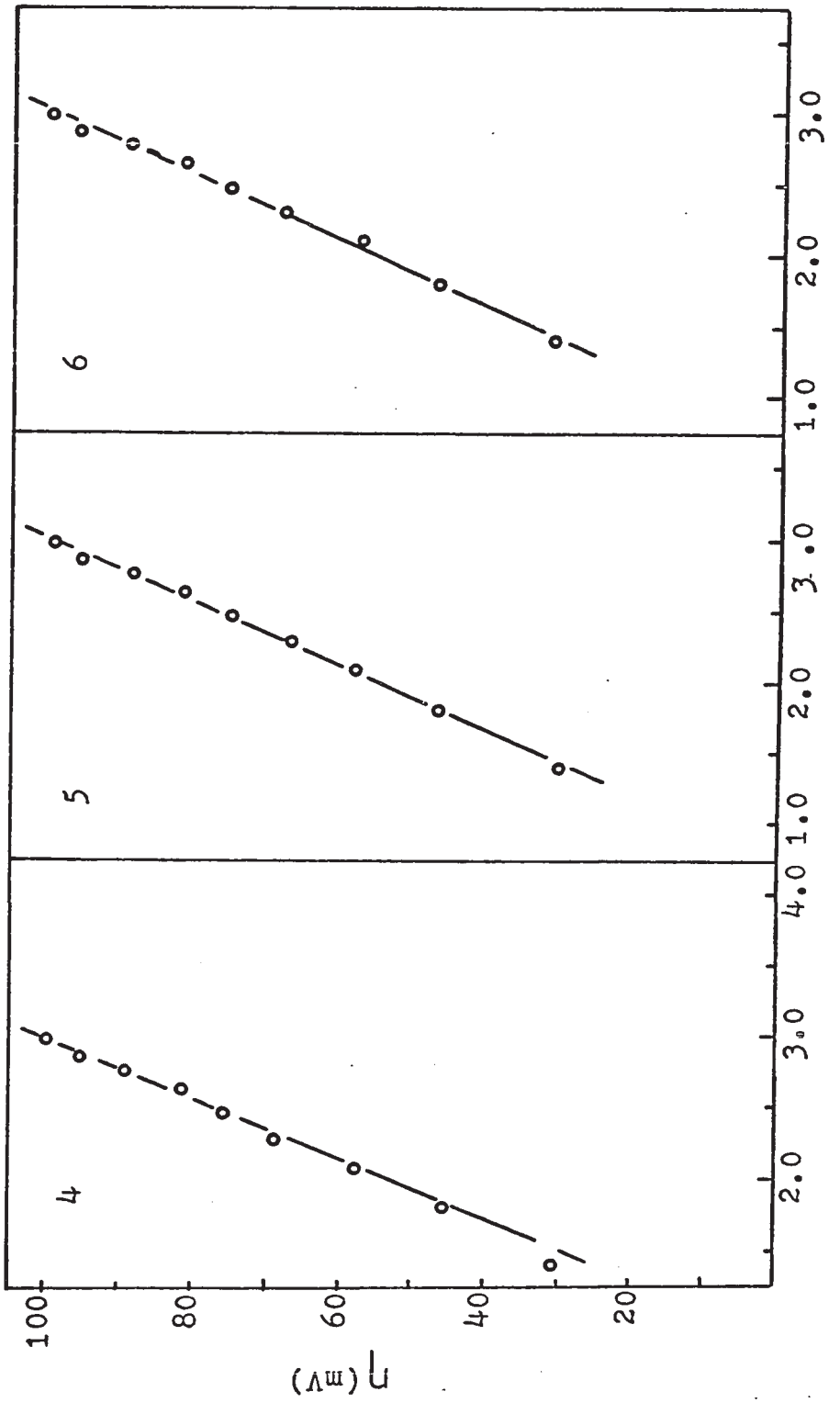

Table 1a

Overpotential-current density relation for copper deposition from standard solution 0.5M $CuSO_4$ + 1.0M H_2SO_4

T = 25°C

Current density (mA/cm^2)	Anodic Overpotential (mV)	Cathodic Overpotential (mV)	
		Run 1	Run 2
20	34	102	100.0
18	32	97	94.4
16	30	90	88.0
14	28	84	80.7
12	25.5	76	76.6
10	24	68	65.0
8	20	59	54.4
6	18	42	41.2
4	14	28	28.0
2	10	17	17.0

Table 1b

b_c	b_a	i_o cathodic & anodic	αc	αa	$\alpha c + \alpha a$
50	19	2.44	.58	1.52	2.10

The value $\alpha_a + \alpha_c$ corresponds to the number of electrons involved in the overall electrochemical process, which is equal to two in this work. The fact that the anodic and the cathodic transfer coefficients are different in this work suggests that the rate-determining step involves some other transfer process than two electron-transfer process (10,13). This will be dealt with further in the discussion section.

The overpotential-current density relation was also determined for standard solution with 0.5M $CuSO_4$ containing 0.0, 0.1, 0.25, 0.5, 0.75 and 1.0M sulfuric acid respectively. The results are shown in Fig. 5(1-6). It can be seen that the Tafel region increases with increasing sulfuric acid concentration. The steady-state overpotential, at 20 mA/cm^2, and the exchange current density of the above standard solutions are given in Table 2.

Double Layer Capacity Measurement with Standard Solution

A standard method of measuring double layer capacity follows the fact that the initial slope of the overpotential build-up curve is proportional to the inverse of the capacity.

$$i = C_{dl} \frac{d\eta_t}{dt} \qquad \text{-------(38)}$$

A time scale of 10 to 25 μsec and a vertical scale of 10 mV were employed for evaluating the initial tangent in the measurement of C_{dl}. Using the fast rise time switching

Table 2

The overpotential as a function of sulfuric acid concentration for copper deposition from 0.5M $CuSO_4$

$T = 25^{o}C$

Current density = 20 mA/cm^2

Sulfuric acid concentration (mole/l)	Overpotential (mV)	Tafel Slope b (mV)	$i_o (mA/cm^2)$
0.0	50	39.13	4.75
0.1	88	52.85	3.16
0.25	91	48.94	3.32
0.5	98	49.00	2.35
0.75	100	49.92	2.30
1.0	100	49.92	2.29
2.0	104	52.00	-

circuit, the conditions for accurate estimation of C_{dl} were achieved. The values of C_{dl} obtained for standard solution (0.5M $CuSO_4$, 1.0M H_2SO_4) were in the order of 72 ± 8 $\mu F/cm^2$. These are in satisfactory agreement with the results obtained from overpotential build-up measurements by Bockris & Conway (10,12).

2) Discussion

Mechanism of Copper Deposition from Standard Solution - (0.5M $CuSO_4$, 1.0M H_2SO_4)

The mechanism of copper deposition from standard solution without additives has been studied previously (10,12). In this work the proposed mechanism was examined and confirmed to be as follows

Cathodic

$$Cu^{2+} + e \xrightarrow{\text{slow}} Cu^{+}$$

$$Cu^{+} + e \xrightarrow{\text{fast}} Cu^{o}$$

Anodic

$$Cu \xrightarrow{\text{fast}} Cu^{+} + e$$

$$Cu^{+} \xrightarrow{\text{slow}} Cu^{++} + e$$

As shown in the preceding results the experimentally-found Tafel lines appear consistent only with a charge-transfer step. Because of the equality of i_o as obtained from anodic and cathodic Tafel-lines, it may be concluded that the same rate-determining process is effective for deposition and dissolution. Because the Cu^{2+} ion would be more difficult to discharge than the Cu^{+}, due to the greater heat

of hydration of Cu^{2+}, and also, because of the experimentally calculated values of α_c and α_a, two-electron charge-transfer may be ruled out as a possible rate-determining step.

$$Cu^{++} + 2e \rightleftharpoons Cu^{o}$$

A comparison of theory (10,42) and experiment, assuming charge-transfer is rate-determining, is shown in Table 3.

Table 3

Comparison of theoretical and experimental transfer coefficients according to model of rate-determining reaction: $Cu^{2+} + e \rightleftharpoons Cu^{+}$

	Values calculated theoretically	Experimental values
α_c (cathodic)	0.50	0.512
α_a (anodic)	1.50	1.510
$\alpha_c + \alpha_a$	2.00	2.022

Therefore, at a current density higher than 6 mA/cm^2 i.e., where the Tafel-relation is applicable, see Fig. 5, the rate-determining step of copper electrodeposition is the charge-transfer reaction described by equation (14), and the mechanism of the copper deposition can be represented by the equations on page 37.

The Effect of Sulfuric Acid Concentration on Copper Deposition from 0.5M $CuSO_4$

As shown by the results in Table 2 for solution containing 0.5M $CuSO_4$ and no added acid, the steady-state

overpotential was comparatively small, and the deposit was coarsely crystalline, Fig. 30. Addition of acid caused an appreciable increase in overpotential, but a change from 0.25 to 2.0M H_2SO_4 caused only a relatively small further increase and the deposits formed were finely crystalline. While all the acidified $CuSO_4$ solutions gave almost the same Tafel slope, 0.5M $CuSO_4$ with no acid gave a relatively small Tafel slope. Furthermore, the Tafel-region was much more restricted to high current densities.

It has been argued that if the Tafel slope observed in the deposition of a divalent cation is less than or equal to 0.0293V at 25°C, the rate-determining step cannot be a charge-transfer process (10). Accordingly, for 0.5M $CuSO_4$ with no acid, and at low current density, where the Tafel slope is $<.0293$V, the mechanism and the rate-determining step cannot be entirely charge-transfer. However, it is most likely a mixed step in which surface diffusion will contribute to the total overall process. Therefore, the total overpotential for 0.5M $CuSO_4$, 0.0M H_2SO_4 can be written as

$$\eta_{total} = \eta_{transfer} + \eta_{surf.\ diff.} \qquad \text{-------(39)}$$

where

$$\eta_{transfer} = RTi/ZFi_o \quad \& \quad \eta_{surf.\ diff.} = RTi/Z^2F^2V_o$$

with V_o the surface diffusion flux (6).

Equation (39) is another form of expressing Equation (32), and it can also be rewritten as follows (13):

$$\frac{\eta_{total}}{\eta_{transfer}} = 1 + \frac{i_o}{ZFV_o} \qquad \text{-------(40)}$$

It can be seen that if $ZFV_o \gg i_o$, the charge-transfer process will prevail, and if $ZFV_o < i_o$, surface diffusion will dominate.

It should be noted that i_o as extrapolated for 0.5M $CuSO_4$ 0.0M H_2SO_4 is considerably greater than that obtained for acidified solution. This fact together with the low overpotential, the low value of the Tafel slope, and the large region of inapplicability of the Tafel relation, is consistent with a mixed overpotential (13), i.e., mixed rate-determining step for copper deposition from neutral 0.5M $CuSO_4$ solution. The reasons for this behavior might possibly be the following: In non-acidified solution the copper ion concentration appears to be sufficient to permit it to diffuse rapidly into the cathode film and thereby prevent excessive overpotential (43). Since there are no other positively charged ions to compete with the copper ions in occupying the cathode film, sufficient supply of the copper ions will be maintained. This will lead to an increase in the adion concentration C_{ad}, consequently, the rate of removal of adions from the surface will be important, and the surface-diffusion will be an important factor in controlling

the electrodeposition and lower overpotential will be expected.

In the case of acidified $CuSO_4$ solution, the increase in the overpotential is due not only to a decrease in the activity of the copper ion in the cathode film, but also to a considerable increase in the concentration of more electropositive hydronium ions. It is also possible that the added hydronium ions in some way inhibit the deposition, consequently increase the overpotential, but it is doubtful whether this inhibition could arise purely as a result of physical blocking in view of the small size and high mobility of these ions. On the other hand, it is possible that unhydrated hyrogen ions could be chemisorbed on the metal surface. The bond strength Cu-H has been estimated to in the order of 60Kcal/mole (44).

At high concentration of copper ions in the cathode film and at low overpotential, parallel crystal growth will be expected (43). This was observed for 0.5M $CuSO_4$, 0.0M H_2SO_4.

In the case of acidified $CuSO_4$, reduction in the grain size was observed, due undoubtedly to the inhibition effect of the hydronium ions and the decrease in the activity of the copper ions in the cathode film, leading to enhanced nucleation.

Surface Diffusion Flux as a Function of Current Density for Copper Deposition from 0.5M $CuSO_4$, 0.0M H_2SO_4

Values of V_o, the surface diffusion flux were found

to be a function of current density, according to equation (32).

$$\eta = \frac{RT}{ZF}\left[\frac{i}{i_o} + \frac{i}{ZFV_o}\right] \qquad (32)$$

The surface diffusion flux was calculated from the above equation at different current densities. The numerical values are given in Table 4.

The value of the exchange current density i_o extrapolated from the Tafel line for 0.5M $CuSO_4$, 0.0M H_2SO_4 is 0.00475 A/cm^2 (see Table 2). In comparing i_o and ZFV_o, and by applying equation (40), the reaction mechanism as a function of current density for copper deposition from 0.5M $CuSO_4$ can be summarized as shown in Table 5.

It should also be mentioned that the fraction of growth sites, which are active, increases with the current density. Therefore, the effective average path length through which an adion has to move decreases, i.e., the rate of surface diffusion for a given adion concentration increases and, hence, the tendency to rate control by surface diffusion decreases (8,23).

Table 4

Surface diffusion flux as a function of current density for 0.5M $CuSO_4$

i (A/cm^2)	ZFV_o (A/cm^2)	Log i	Log ZFV_o
.020	-	- 1.698	-
.018	-	- 1.744	-
.016	-	- 1.795	-
.014	.1324	- 1.853	- .8781
.012	.0628	- 1.920	- 1.202
.010	.0266	- 2.00	- 1.575
.008	.0155	- 2.095	- 1.809
.006	.00883	- 2.221	- 2.054
.004	.00523	- 2.397	- 2.281
.002	.00259	- 2.693	- 2.586

Table 5

The reaction mechanism as a function of current density for 0.5M $CuSO_4$, 0.0M H_2SO_4

Current density mA/cm^2	Mechanism
$2 < i < 4$	Surface diffusion predominates
$4 < i < 14$	Transfer & surface diffusion
$i > 14$	Charge-transfer predominates

PART II

Results & Discussion, Group I Addition Agents

1) Results:

A series of straight-chain monocarboxylic and dicarboxylic acids were studied to determine their relative effectiveness in increasing the cathode overpotential. The purpose was to examine the effect of the number of functional groups present in the additive molecule, and the effect of the size of the hydrocarbon portion of the molecules. Due to the fact that there is an alternation in the behavior of the dicarboxylic acids with increasing number of methylene groups, the effect of variation in the structural relation between the two carboxyl groups was also considered.

Variation of Overpotential with Time & the Overpotential-Current Density Relation

Typical cathodic overpotential-time relations for some of the additives of Group I are shown in Fig. 6. Typical overpotential-current density relations are shown in Fig. 7. The values of the Tafel slopes as determined from these plots are given in Table 6. These are seen to be nearly the same, 52$\pm$ 1mV, whether or not additives were present. Therefore, in the current density region where charge transfer is rate-determining, mono- and dicarboxylic acids appear to have no significant effect on the kinetics of copper deposition. It was found that in some cases the experimental Tafel slope

Figure 6

Variation of overpotential with time (η vs. t)

Curve 1	7.49×10^{-3}M octanedioic acid
Curve 2	1.0×10^{-2}M heptanedioic acid
Curve 3	2.5×10^{-3}M heptanoic acid

Fig. 6

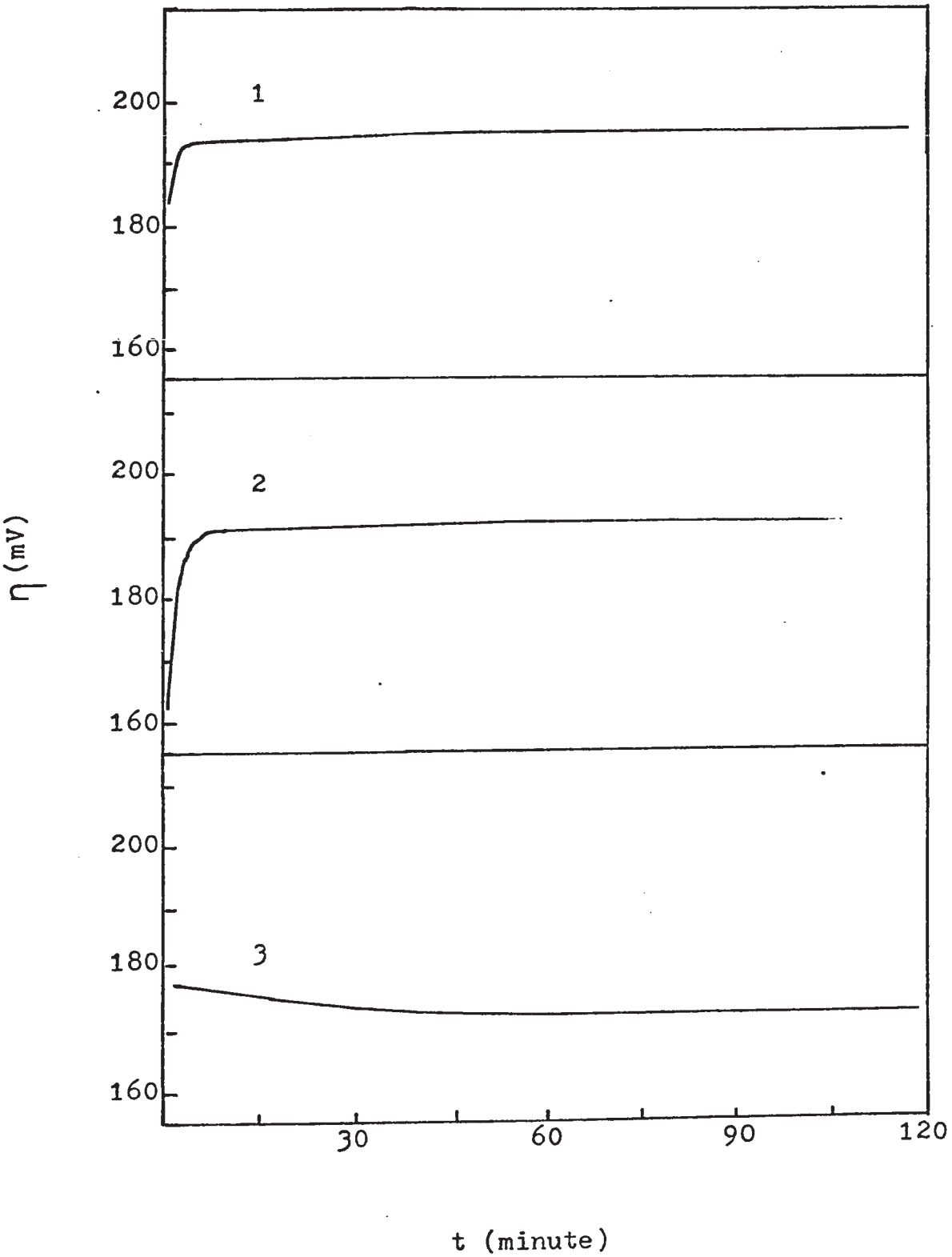

Figure 7

Overpotential-current density relation (η vs. ln i)

Curve 1 — 2.5×10^{-3}M heptanoic acid

Curve 2 — 1.0×10^{-2}M heptanedioic acid

Curve 3 — 7.49×10^{-3}M octanedioic acid

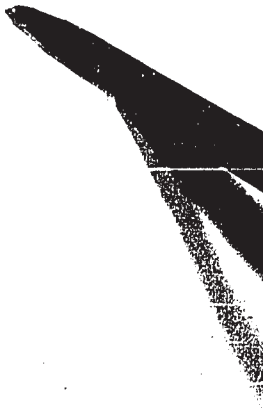

Fig. 7

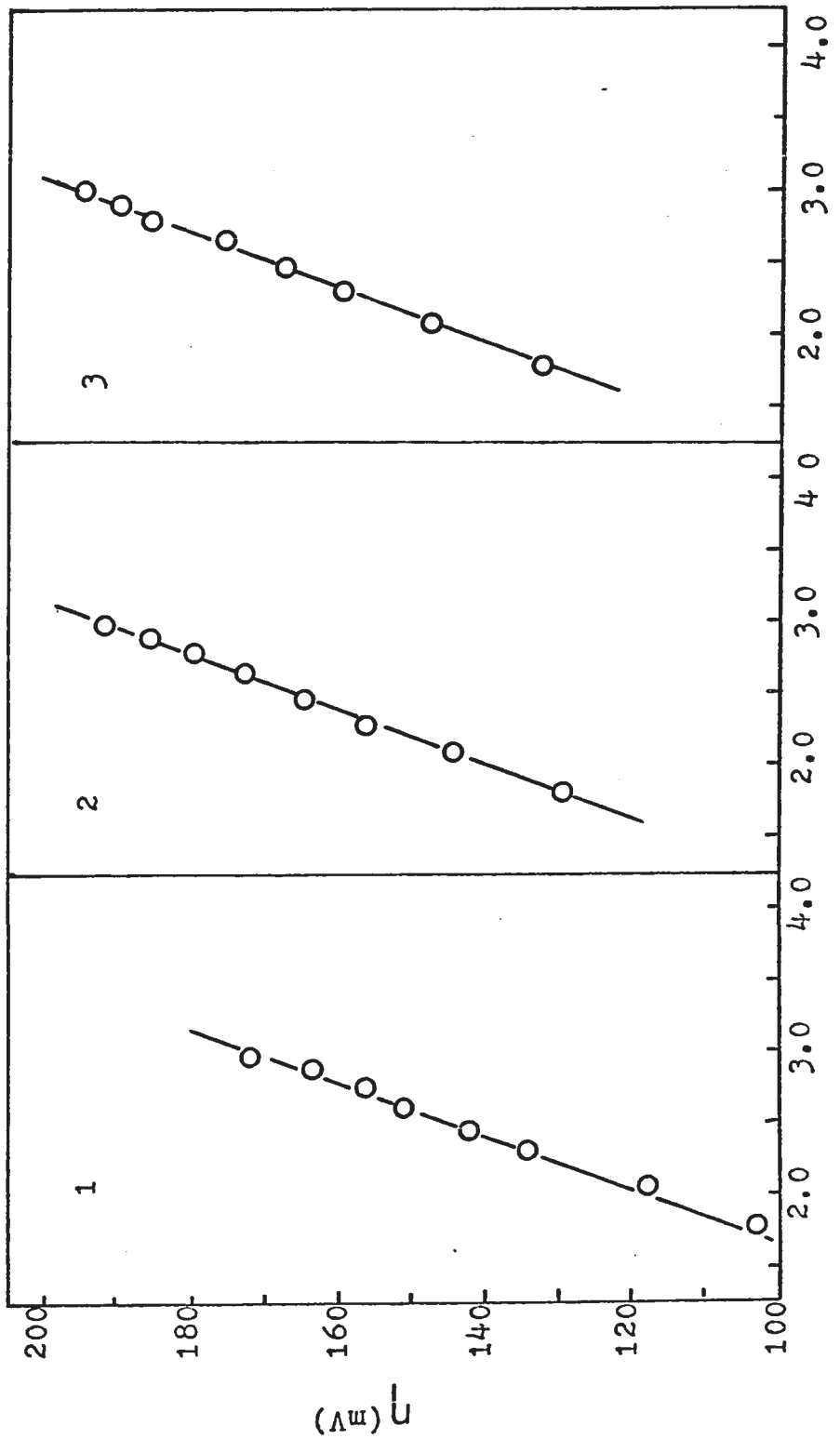

Table 6

Overpotential-current density relation for copper depostion from standard solution with additive

$T = 25^{o}C$

Current density (mA/cm^2)	Overpotential (mV)		
	$2.5x10^{-3}M/l$ Heptanoic	$1.0x10^{-2}M/l$ Heptanedioic	$7.49x10^{-3}M/l$ Octanedioic
20	172.5	192.0	195
18	164.0	186.4	190
16	156.8	180.8	186.0
14	151.0	173.0	176.0
12	142.0	165.4	168.0
10	134.5	157.4	160.0
8	118.5	145.0	148.0
6	103.5	130.0	133.0
4	81.0	108.0	111.0
2	46.0	68.0	71.0
Tafel Slope	52.0	52.5	52.5

differed from that given previously. However, correction for the IR drop brought these values within the theoretical 50± 1mV value. The overpotential increment, $\Delta\eta$, was obtained by subtracting the overpotential with standard solution from the overpotential with solution containing additives.

Overpotential Increment as a Function of Additive Concentration

The overpotential increment, $\Delta\eta$, is shown as a function of additive concentration for straight-chain monocarboxylic acids in Fig. 8. Numerical values are given in Table 7. A discrepancy of about ± 10% was observed between the cathodic overpotentials obtained for the standard solution containing propanoic, pentanoic and heptanoic acids and results obtained previously (40). However, this discrepancy can be attributed to the different technique and mainly to the different type of cell and electrodes used (8).

Another factor that might contribute to this discrepancy is the time at which the steady-state was assumed to be reached. While it was considered as attained in 45 minutes in this work, it was assumed to be attained in several hours in the work done previously (40).

The overpotential increments for dicarboxylic acids with an odd number of carbon atoms (ONCA) (propanedioic, pentanedioic, heptanedioic and nonanedioic acids) and an even number of carbon atoms (ENCA) (butanedioic, hexanedioic, and octanedioic) are shown as a

Figure 8

Overpotential increment as a function of additive concentration

monocarboxylic acids

○ Propanoic acid

⬡ Butanoic acid

□ Pentanoic acid

● Hexanoic acid

⬢ Heptanoic acid

■ Octanoic acid

1 Propanoic acid (smoothed)

2 Butanoic acid "

3 Pentanoic acid "

4 Hexanoic acid "

5 Heptanoic acid "

6 Octanoic acid "

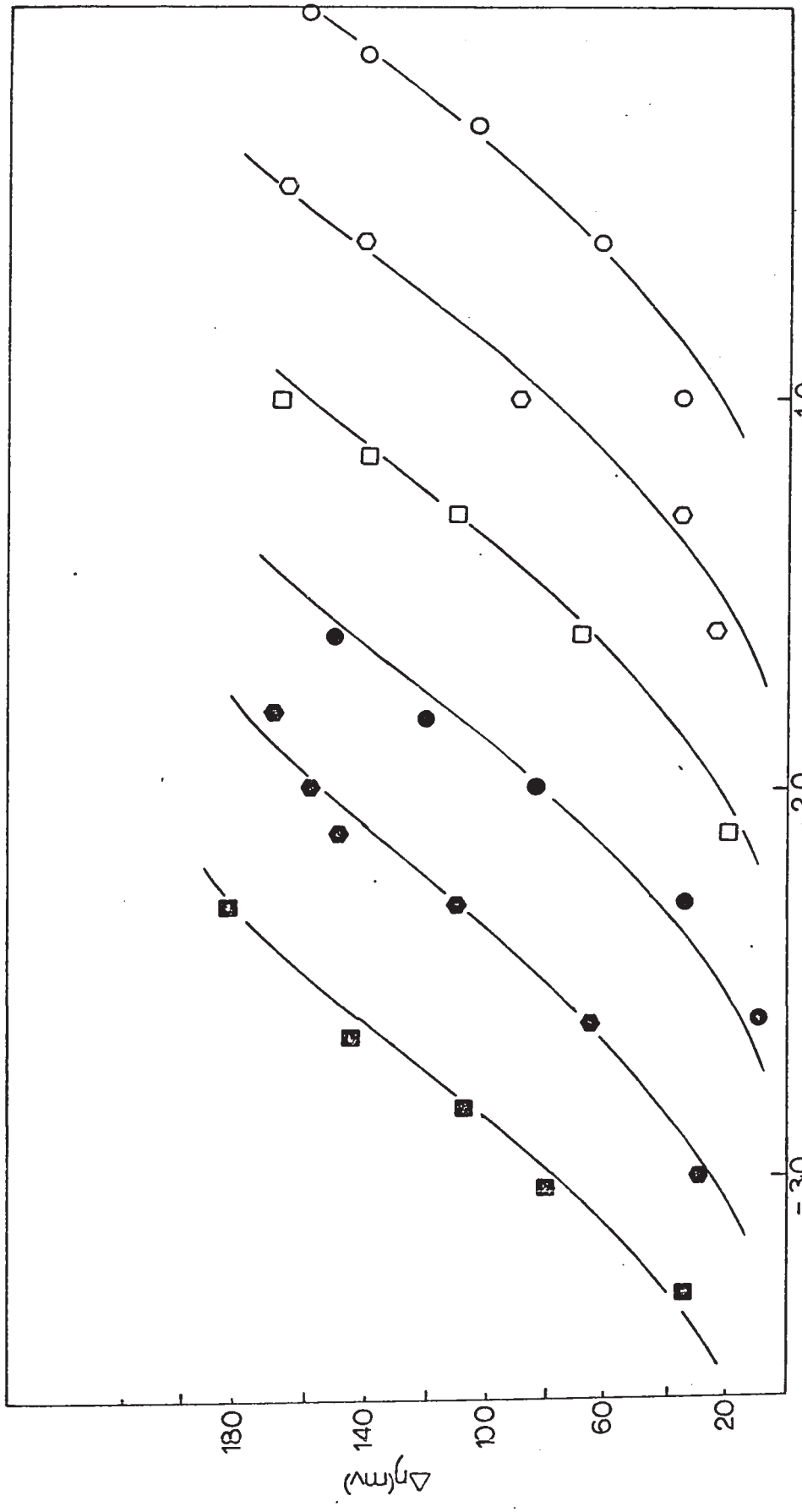

Fig. 8

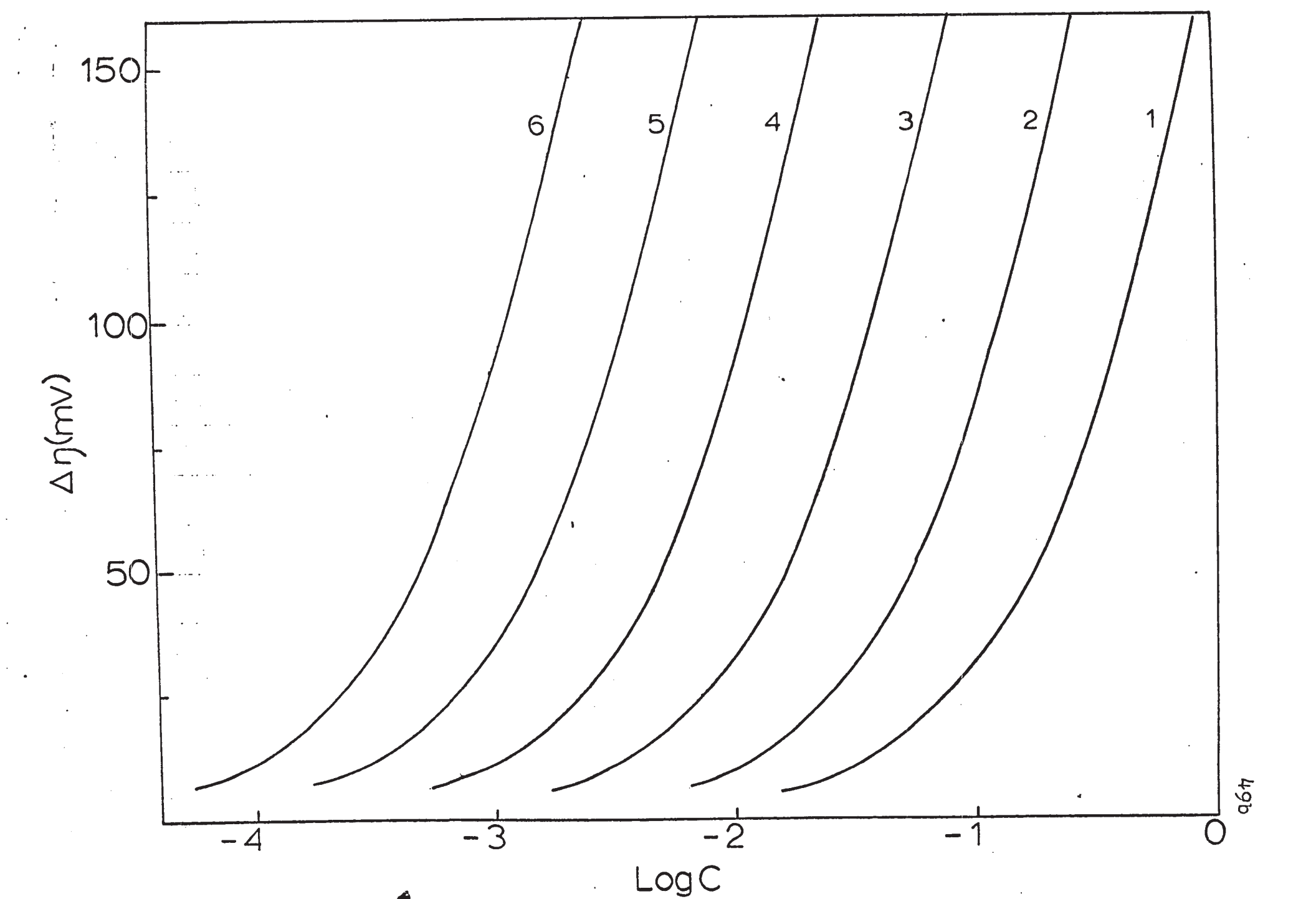
150
100
50
Δη(mV)
6
5
4
3
2
1
-4
-3
-2
-1
0
Log C
4976

Table 7

Overpotential as a function of additive concentration

monocarboxylic acids

Current density = 20 mA/cm^2

$T = 25^oC$

(a) Propanoic acid

Additive concentration (mole/l)	Overpotential Increment (mV)
$1.0x10^{-1}$	36
$2.5x10^{-1}$	62
$5.0x10^{-1}$	102
$7.5x10^{-1}$	140
1.0	164

(b) Butanoic acid

Additive concentration (mole/l)	Overpotential Increment (mV)
$2.5x10^{-2}$	24
$5.0x10^{-2}$	38
$1.0x10^{-1}$	88
$2.5x10^{-1}$	140
$3.5x10^{-1}$	168

(c) Pentanoic acid

Additive concentration (mole/l)	Overpotential Increment (mV)
$7.5x10^{-3}$	20
$2.5x10^{-2}$	68
$5.0x10^{-2}$	110
$7.2x10^{-2}$	140
$1.0x10^{-1}$	168

Table 7 (continued)

(d) Hexanoic acid

Additive concentration (mole/l)	Overpotential Increment (mV)
2.5×10^{-3}	22
5.0×10^{-3}	43
1.0×10^{-2}	84
1.5×10^{-2}	120
2.5×10^{-2}	150

(e) Heptanoic acid

Additive concentration (mole/l)	Overpotential Increment (mV)
1.0×10^{-3}	32
2.5×10^{-3}	72
5.0×10^{-3}	110
7.5×10^{-3}	150
1.0×10^{-3}	160
1.6×10^{-2}	170

(f) Octanoic acid

Additive concentration (mole/l)	Overpotential Increment (mV)
5.0×10^{-4}	37
8.5×10^{-4}	82
1.5×10^{-3}	110
2.3×10^{-3}	146
4.9×10^{-3}	184

function of additive concentration in Fig. 9. Numerical values are given in Table 8.

Figure 8 indicates that the overpotential increment increases with increasing concentration of the additive. At a given concentration, the overpotential increment increases with the length of hydrocarbon chain of the additive molecule.

In the case of Fig. 9, the overpotential in general increases with increasing concentration of normal dicarboxylic acid. However, the overpotential effect of increasing the hydrocarbon chain length is seen to alternate. This alternation can be seen most clearly in the first four members of this homologous series. The dicarboxylic acids with an odd number of carbon atoms (ONCA) (propanedioic, pentanedioic), caused a greater overpotential increment than their next higher homologues with an even number of carbon atoms (ENCA), butanedioic, hexanedioic. The alternation effect is less pronounced in the higher homologues of this series.

From Fig. 8 & 9 the overpotential increment of the first four acids of the dicarboxylic series can be compared to the corresponding acids of the monocarboxylic series. The effectiveness on increasing the cathodic overpotential of copper deposition is as follows: dicarboxylic acids with (ENCA) $<$ monocarboxylic acids $<$ dicarboxylic acids with (ONCA).

Figure 9

Overpotential increment as a function of additive concentration

dicarboxylic acids

Butanedioic acid

Hexanedioic acid

Octanedioic acid

Propanedioic acid

Pentanedioic acid

Heptanedioic acid

Nonanedioic acid

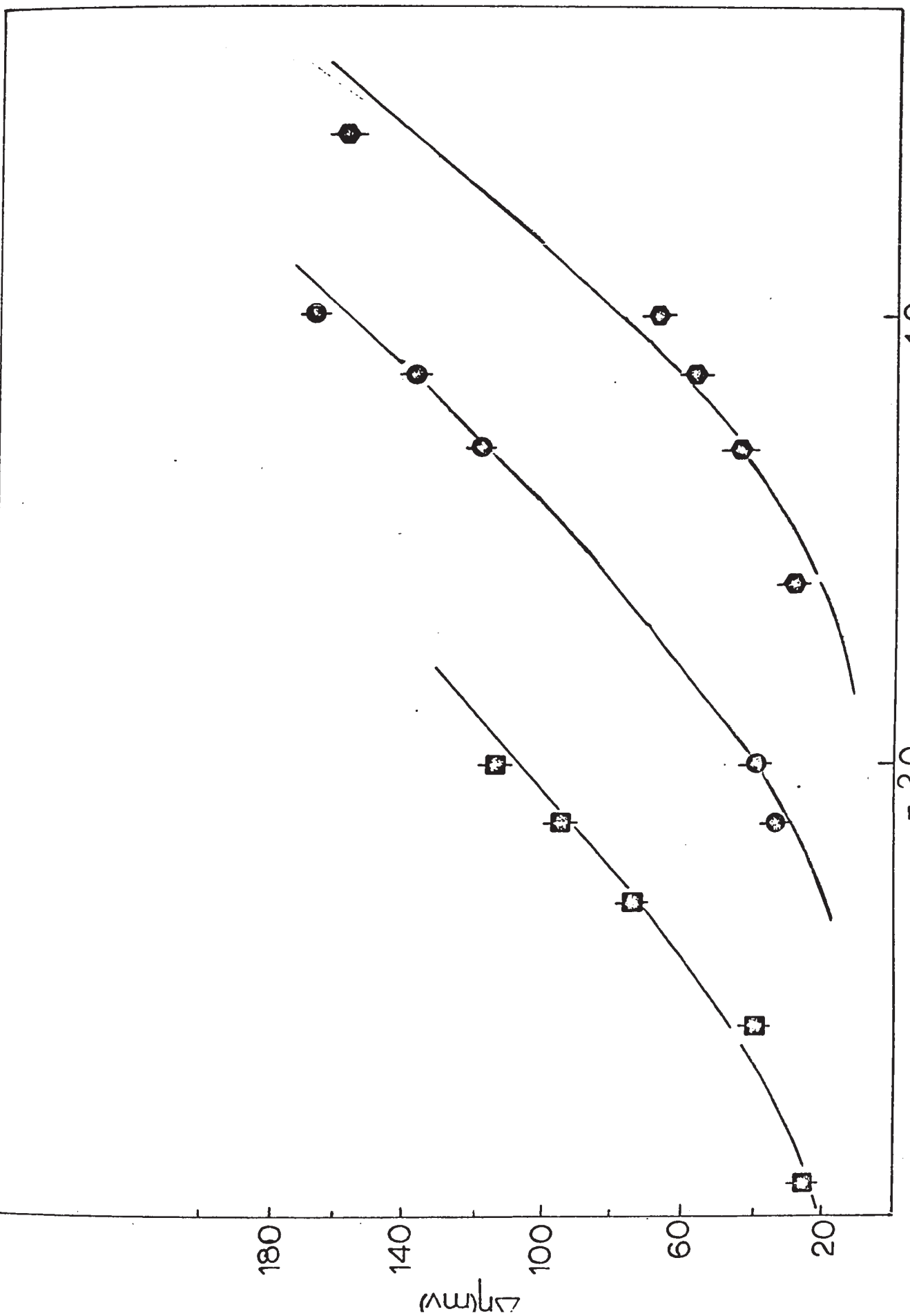
180
140
100
60
20
-1.0
-2.0
Log C

Fig. 9

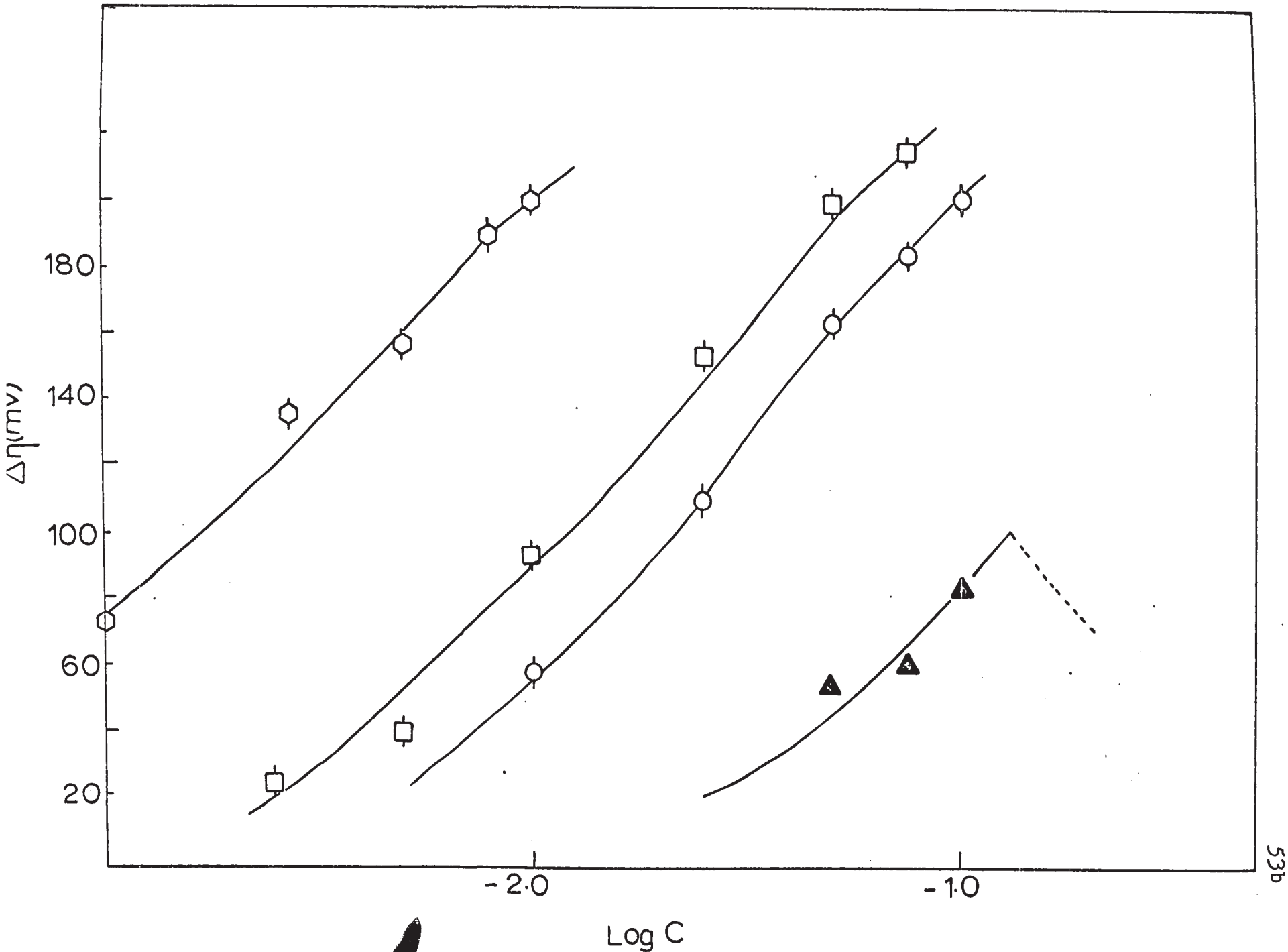

Table 8

Overpotential as a function of additive concentration

dicarboxylic acids

$T = 25^{o}C$

Current density = 20 mA/cm^2

(a) Propanedioic acid

Additive concentration (mole/l)	Overpotential Increment (mV)
$5.0x10^{-2}$	56
$7.5x10^{-2}$	60
$1.0x10^{-1}$	85
$5.0x10^{-1}$	25
$7.5x10^{-1}$	23

(b) Pentanedioic acid

Additive concentration (mole/l)	Overpotential Increment (mV)
$1.0x10^{-2}$	58
$2.5x10^{-2}$	110
$5.0x10^{-2}$	164
$7.5x10^{-2}$	186
$1.0x10^{-1}$	200

(c) Heptanedioic acid

Additive concentration (mole/l)	Overpotential Increment (mV)
$2.5x10^{-3}$	24
$5.0x10^{-3}$	40
$1.0x10^{-2}$	92
$2.5x10^{-2}$	154
$5.0x10^{-2}$	200
$7.5x10^{-2}$	214

Table 8 (continued)

(d) Nonanedioic acid

Additive concentration (mole/l)	Overpotential Increment (mV)
1.0×10^{-3}	75
2.7×10^{-3}	137
5.0×10^{-3}	156
8.0×10^{-3}	190
1.0×10^{-2}	200

(e) Butanedioic acid

Additive concentration (mole/l)	Overpotential Increment (mV)
2.5×10^{-2}	28
5.0×10^{-2}	44
7.5×10^{-2}	56
1.0×10^{-1}	70
2.5×10^{-1}	159

(f) Hexanedioic acid

Additive concentration (mole/l)	Overpotential Increment (mV)
7.5×10^{-3}	34
1.0×10^{-2}	40
5.0×10^{-2}	120
7.5×10^{-2}	138
1.0×10^{-1}	168

Table 8 (continued)

(g) Octanedioic acid

Additive concentration (mole/l)	Overpotential Increment (mV)
1.13×10^{-3}	26
2.6×10^{-2}	40
5.0×10^{-3}	74
7.49×10^{-3}	95
1.0×10^{-2}	114

2) Discussion:

The regular increase in adsorption of aliphatic monobasic acids at a given concentration on ascending the homologous series has long been known, both in regards to adsorption at solution-air (45) and solution-solid (32,46) interfaces. For dicarboxylic acids the behavior of adsorption on ascending the homologous series is different than that of the monoacids because of the well-known alternation in the properties which depend on whether the chain contains an even or an odd number of carbon atoms (32,47,48) (see Fig. 10). The relative position of the two carboxyl groups in the dibasic acids are trans-configuration with an even number of carbon atoms and cis-configuration for acids with an odd number of carbon atoms (as shown in Fig. 11).

Since the adsorbability depends to a large extent on the additive solubility, the amount of adsorption increases as the solubility of the adsorbate decreases (49), and since there is alternation in the solubility of the dibasic acids, therefore, alternation in the adsorbability can be expected. Dibasic acids with an even number of carbon atoms (ENCA) are less soluble than dibasic acids with an odd number of carbon atoms (ONCA). Accordingly, the former would be expected to have a higher adsorbability compared to the latter compounds, which is the opposite of that found experimentally.

Figure 10

The change in maximum adsorption of dicarboxylic acids with the number of carbons in the chain on charcoal

This figure was taken from the original reference(47).

Fig. 10

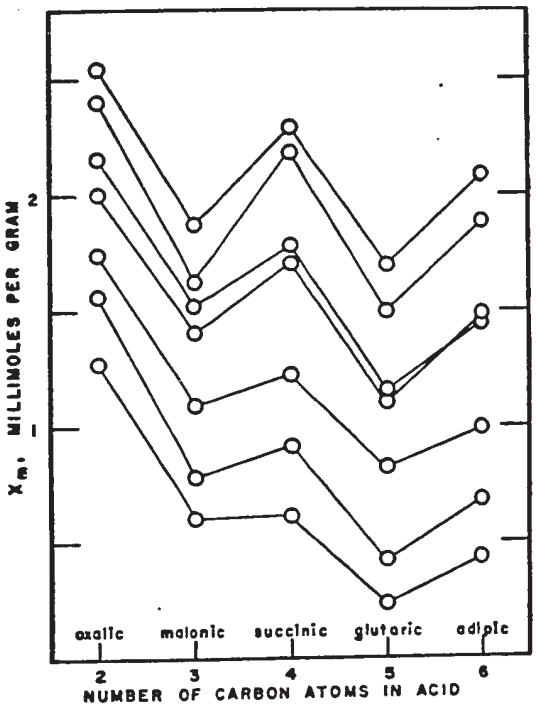
X_m, MILLIMOLES PER GRAM
2
1
oxalic
malonic
succinic
glutaric
adipic
2
3
4
5
6
NUMBER OF CARBON ATOMS IN ACID

Figure 11

Cis & Trans-configuration of the dicarboxylic acids

Fig. 11

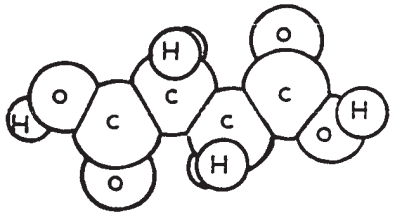

trans-configuration

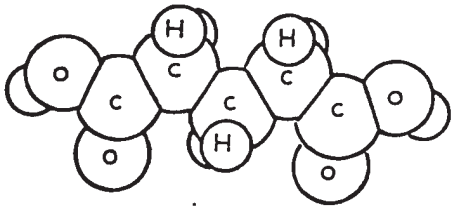

cis-configuration

Monocarboxylic and dicarboxylic acids apparently adsorb with the carboxyl group toward the metal surface. This assumption has been supported experimentally by observing the formation of oleophilic film which is not wet by the solution (32,50,51). It has been attributed to the orientation of the adsorbed molecules with the hydrocarbon chain directed away from the solid surface, therefore forming a hydrophobic film on the metal surface. In support to this argument are the results obtained by Morrison & Miller (47) for the adsorption of mono & dicarboxylic acids on charcoal (see Fig. 10). It was observed (47) that the adsorption of monocarboxylic acids was appreciably greater than dicarboxylic acids and that the adsorbability of dicarboxylic acids was higher for those with (ENCA) than for those with (ONCA), which is the opposite to that observed in this study. Accordingly, it can be concluded that for adsorption of the above compounds on copper, the carboxyl group is most likely directed toward the metal. Furthermore, the hydrophobic repulsion between water and the hydrocarbon portion of the molecule will assist the preferential orientation in which the functional group is directed toward the metal surface.

With the support of this argument, the experimental results with the dicarboxylic acids can be explained as follows: dibasic acids with (ENCA) have the terminal carboxyl groups in trans-configuration, so that their adsorption can only take place by one carboxyl group, while the dibasic acids with (ONCA) have their terminal

carboxyl groups in cis-configuration, and therefore, adsorption can take place by two-point attachment. This places the (ENCA) and (ONCA) of the dicarboxylic acids in two different categories. Within each category the previously mentioned observation that the adsorbability increases as the solubility of the adsorbate decreases, holds true.

Steady-State Overpotentials with Mono- & Dicarboxylic Acids

The steady-state overpotentials are correlated best with the adsorbability by plotting the overpotential increment against the reduced concentration C_r which accounts for the effect due to solubility. The reduced concentration has been defined as (46,51).

$$C_r = \frac{C}{C_s} \qquad \text{-------(41)}$$

where, C & C_s are the concentrations of bulk and saturated solution respectively. A generalized behavior for moncarboxylic acids is obtained as shown in Fig. 12, which indicates that the overpotential increment for a given reduced concentration is approximately the same for all the monocarboxylic acids regardless of the chain length. These results may be compared with those obtained for the adsorption of carboxylic acids on graphite (45). It is known generally that the solubility of a hydrocarbon compound is carbon-chain dependent, thus the longer the carbon chain, the higher the adsorbability and the lower the solubility.

Regarding dicarboxylic acids, a plot of the over-

Figure 12

Overpotential increment as a function of reduced concentration for monocarboxylic acids

$(\Delta\eta$ vs. $C_r)$

$$C_r = \frac{C}{C_s^*}$$

- ○ Propanoic acid
- △ Butanoic acid
- ⬡ Pentanoic acid
- □ Hexanoic acid
- ⬢ Heptanoic acid
- ● Octanoic acid

C_s^*: The values of C_s were taken from the solubility data at 20°C (52, 53). C_s for propanoic and butanoic acids were obtained by extrapolation of C_s vs. number of carbon atoms in the monocarboxylic acids plot.

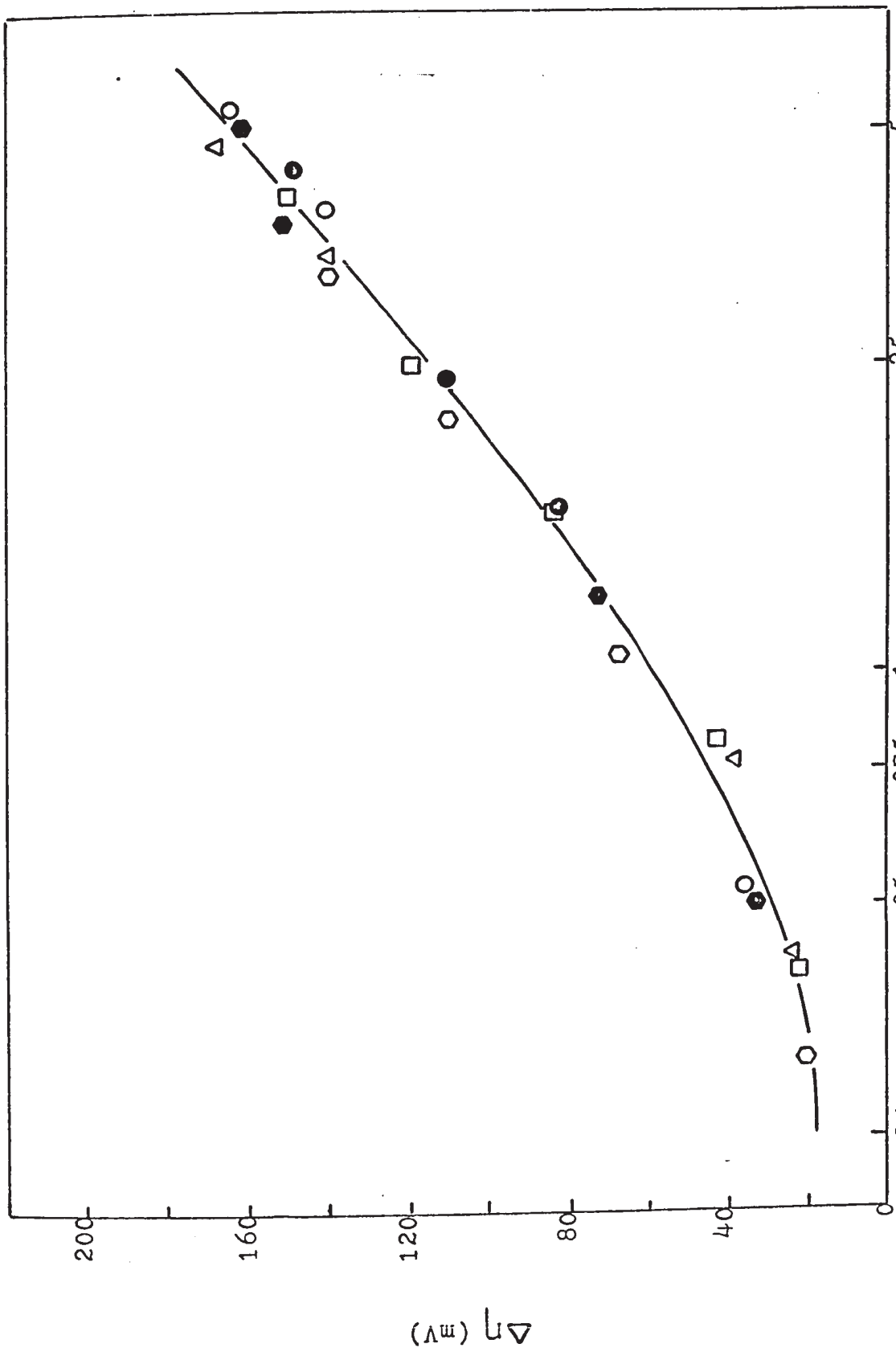

Fig. 12

potential increment against reduced concentration is shown in Fig. 13. For dicarboxylic acids with (ENCA) a generalized behavior was obtained, while for dicarboxylic acids with (ONCA), it was observed that at a given reduced concentration, the overpotential increment decreases with increasing the hydrocarbon chain length. Thus, for dibasic acids with (ENCA), the contribution of the carbon-chain length to the overpotential increment is likely due to its effect on the adsorbability, i.e., the solubility. For dibasic acids with (ONCA), there must be another factor affecting the overpotential increment besides the solubility. This will be discussed later. When comparing Fig. 12 & 13, it will be noted that, at a given concentration, the ability of carboxylic acids to increase the overpotential decreases in the following order: dicarboxylic acids with (ONCA) > monocarboxylic acids > dicarboxylic acids with (ENCA). These results can be understood in terms of the following mechanism and factors affecting the adsorption of the additives.

It may be assumed, for monocarboxylic acids, that the polar-group has a higher affinity for the metal than it does for the solvent, as previously mentioned, and that the hydrophobic carbon-chain is effectively rejected by the solvent. Due to this solvent rejection and the affinity of the polar-group for the metal, the additive will transfer spontaneously from the bulk of the solution to the pre-electrode layer, thus making interaction

Figure 13

Overpotential increment as a function of reduced concentration for dicarboxylic acids

($\Delta\eta$ vs. C_r)

Butanedioic acid

Hexanedioic acid

Octanedioic acid

Pentanedioic acid

Heptanedioic acid

Nonanedioic acid

Fig. 13

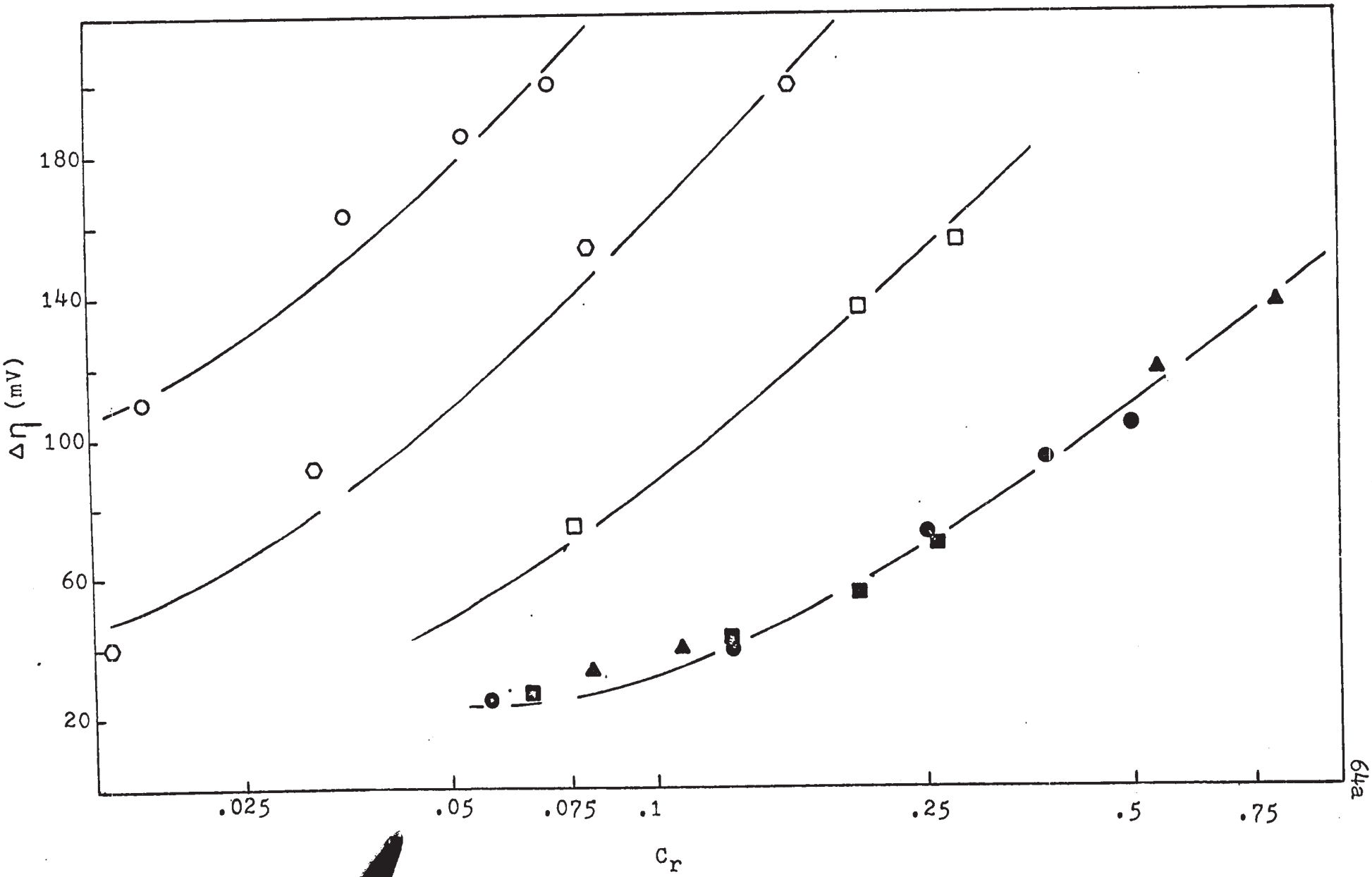

with the electrode surface possible.

In the case of dicarboxylic acids with (ENCA) with the two carboxyl groups in trans-configuration, only one of the carboxyl groups will be able to interact with the electrode surface. Consequently, the second carboxyl group will be directed toward the solution, and will in effect be attracted by the solvent and possibly solvated as well. Accordingly, a decrease in the adsorption power of the dicarboxylic acids with (ENCA) will occur. It may therefore be expected that their reactivity will be less than the corresponding monobasic acids. A factor that might contribute in increasing the interaction between dicarboxylic acids and the metal surface is the electron-withdrawing character of the non-adsorbing carboxyl group. This will decrease the electron density on the adsorbing carboxyl group, therefore leading to possible increase in the adsorbability (29).

In the case of the dicarboxylic acids with (ONCA) with the two carboxyl groups in cis-configuration, a higher overpotential increment is found at a given reduced concentration than that observed with the corresponding monocarboxylic acids. This can be expected if we consider the possibility of two-point attachments. The lack of generalization in the plot of the overpotential increment vs. reduced concentration for dicarboxylic acids with (ONCA) can be attributed to the internuclear distances between the two carboxyl groups. For propane-

dioic acid the internuclear distance between the two carboxyl groups is 2.49 Å, calculated from the geometrical model, and for pentanedioic acid, 4.98 Å. The internuclear distances for heptanedioic and nonanedioic acids are 7.47 Å and 10.96 Å respectively. Comparing these values with the three shortest internuclear distances in the copper lattice, 2.55, 3.6 and 5.1 Å, it can be seen that propanedioic acid is more apt to form strain-free two-point attachments with the copper surface. Pentanedioic acid follows as another likely possibility in forming such attachments without strain. Therefore, it might be concluded that having the two carboxyl groups further apart will decrease the probability of two-point attachments. If this assumption can be made, then the decreasing value of the overpotential increment at a given concentration of the dicarboxylic acids with (ONCA) can be expected.

The Influence of Additives of Group One on the Mechanism of Copper Deposition

The Tafel slope values obtained for copper deposition from standard solution containing mono- or dicarboxylic acids were found to be of the order of 52 mV, see Fig. 7 (33). These Tafel slope values do not differ from the values obtained for standard solution, where charge transfer is rate-determining, or from the values calculated theoretically from equation (19)

$$b = \frac{RT}{\alpha ZF} \qquad (19)$$

From these results, it may be concluded that the additives of Group I do not significantly alter the kinetics of copper deposition, and therefore, the charge-transfer reaction remains rate-determining. The charge-transfer overpotential remains, however, a function of true current density. This means that the additive must affect the current; i.e. the current density increases as a result of adsorbed additive, hence charge-transfer overpotential increases in accordance with the Tafel relation (38).

It is suggested that the blocking of deposit growth sites by additives results only in an increase in the overpotential due to increased true current density in the uncovered portion of the metal surface. This will speed up the rate of deposition to compensate for this inhibition due to the adsorbed additives.

Fractional Surface Coverage

The fractional surface coverage θ, caused by the adsorbed material was calculated from Equation (35), which is based on the simple blocking theory. Equation (35) can be written as

$$\theta = 1 - \exp(-\Delta\eta/b) \quad \text{-------(42)}$$

For the calculation of the surface coverage θ, the Tafel slope b was taken as the experimental 52 mV.

Free Energy of Adsorption and the Nature of the Isotherm

As a first approximation, the modified Langmuir-type isotherm (33,34) was employed from which the standard free energy of adsorption can be written as

$$\Delta G_a^o = - RT \ln \frac{55.5}{C_{org}} \frac{\theta}{(1-\theta)^n} \frac{[\theta + n(1-\theta)]^{n-1}}{n^n}$$

-------(43)

where n is the number of water molecules replaced by one molecule of the organic additive and is assumed to be independent of coverage or charge on the electrode. The standard free energy in the above equation refers to unit mole fraction of additive or water in solution and on the surface. Equation (43) corresponds to the isotherm given in Equation (36).

Taking the theoretical value of n as 2 (34,40) and using Equation (43), the apparent standard free energy of adsorption was calculated. A family of parallel ΔG_a^o vs. θ curves shown in Fig. 14 & 15 results for each type of carboxylic acid. It is obvious that ΔG_a^o is markedly dependent on the coverage θ. This behavior is much the same as that observed by Bockris & Swinkels (34) for the adsorption of n- decylamine on copper. The increasingly negative ΔG_a^o with increasing θ in Fig. 14 & 15 is presumably attributable to a spontaneous and increasing lateral interaction in the adsorbed phase (34). Therefore, in stressing the above point, the effect of the lateral interaction should be calculated.

Lateral Interaction Free Energy

Equation (36), which is a general modification of the Langmuir isotherm for adsorption from solution involving solvent displacement, depends for its basic

Figure 14

Free energy of adsorption as a function of coverage for monocarboxylic acids

1	Propanoic acid
2	Butanoic acid
3	Pentanoic acid
4	Hexanoic acid
5	Heptanoic acid
6	Octanoic acid

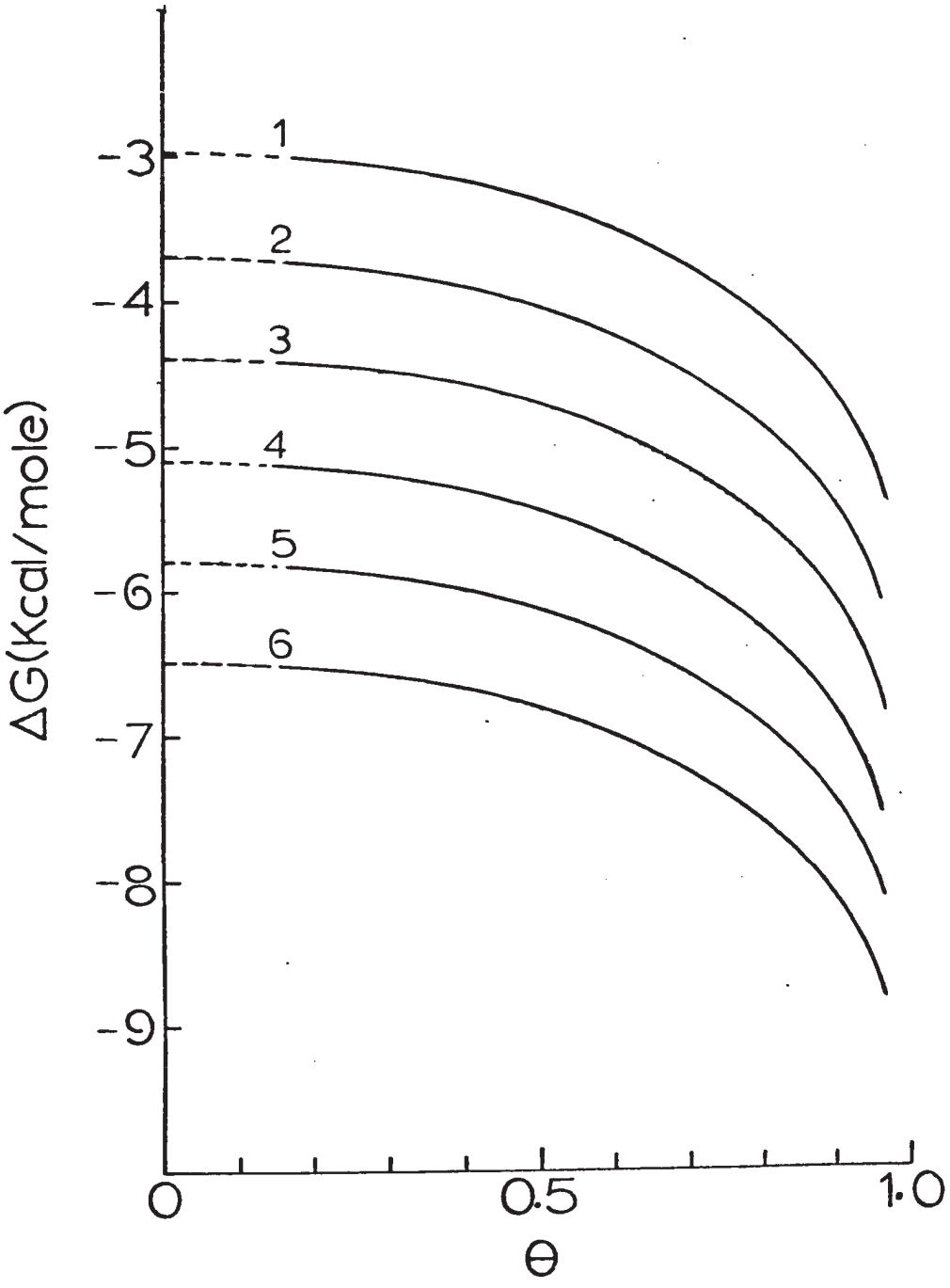

Fig. 14

Figure 15

Free energy of adsorption as a function of coverage for dicarboxylic acids

1	Propanedioic acid
2	Pentanedioic acid
3	Heptanedioic acid
4	Nonanedioic acid
5	Butanedioic acid
6	Hexanedioic acid
7	Octanedioic acid

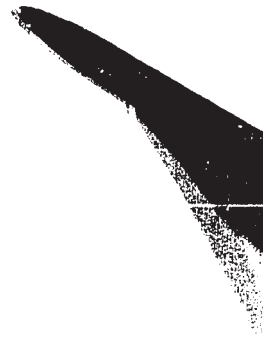

Fig. 15

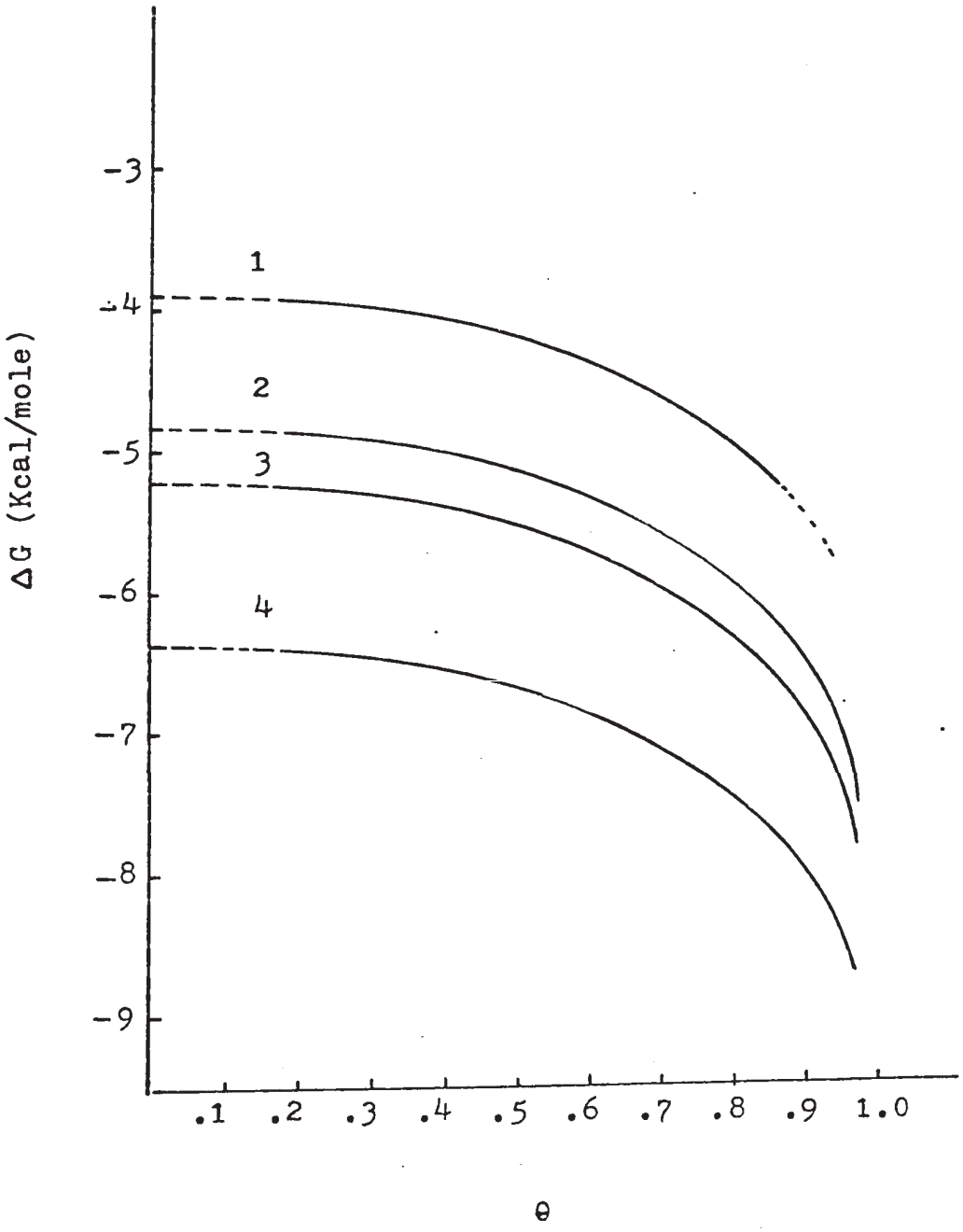

Fig. 15

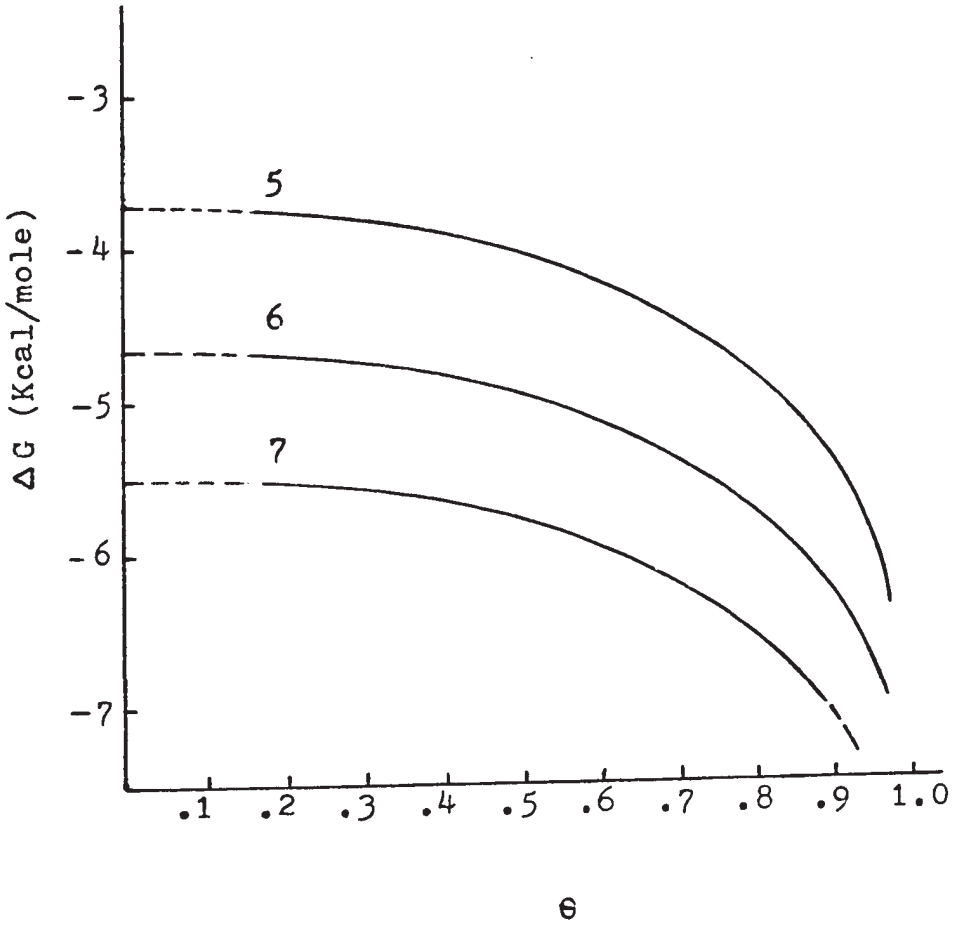

derivation on the assumption that no lateral interaction occurs in the adsorbed phase (25,34,54). In this equation the adsorption free energy ΔG_a^o should therefore be regarded, strictly, as independent of coverage θ. However, the use of this equation in calculating ΔG_a^o as a function of coverage for Fig. 14 assumes the applicability of a modified isotherm similar to that discussed by Conway & Barradas (25) and Bockris & Blomgren (55).

In the case of monocarboxylic acids, the data in Fig. 14 show that the addition of each methylene group results in the same increase in the adsorption free energy regardless of coverage. It is seen that the hydrocarbon portion of a monocarboxylic acid makes no significant net contribution to the lateral interaction in the adsorbed phase. This behavior, which is consistent with the applicability of Traube's rule (56) to the adsorption of compounds in a homologous series (40,57), means that the standard free energy of adsorption of a given monocarboxylic acid on copper can be written as

$$\Delta G_a^o = x \Delta G_{CH_2}^o + \Delta G_p^o + g(\theta) \text{-------} (44)$$

where x is the number of methylene groups present (including the terminal methyl), $\Delta G_{CH_2}^o$ is the adsorption free-energy contribution of each methylene group, ΔG_p^o is the contribution of the polar carboxyl group, and $g(\theta)$ is the coverage-dependent lateral interaction free energy, which is the same for all the monocarboxylic acids

at the same coverage. Obviously, $g(\theta)$ approaches zero as θ approaches zero.

An appropriate isotherm for the adsorption from solution of a normal monocarboxylic acid on copper can be written by substituting Equation (44) for ΔG_a^o in Equation (36) and rearranging to give

$$f(\theta)\exp(g(\theta)/RT) = \frac{C}{55.5}\exp\left(\frac{-x\Delta G^o_{CH_2} - \Delta G^o_p}{RT}\right) \qquad \text{-------(45)}$$

where $f(\theta)$ is the left-hand side of (36). It will be noted that the θ-dependent exponential factor on the left of (45) is a Frumkin-like correction for lateral interaction (28) except that $g(\theta)$ does not vary linearly with θ at other than very low coverages. While values of $\Delta G^o_{CH_2}$ and ΔG^o_p can be estimated by extrapolating the curves in Fig. 14 & 15 to zero coverage, it will be useful to consider methods by which these quantities can be obtained more accurately by calculation from the cathode overpotential and additive concentration data. This will be discussed later.

The Lateral Interaction Free Energy Calculation

The data in Fig. 14 & 15, for both monocarboxylic and dicarboxylic acids, indicate that the hydrocarbon part of the molecule makes no significant net contribution to the lateral interaction. Therefore, the dispersion interaction force, which mainly concerns the hydrocarbon-chain, can be neglected, and this assumption was confirmed

by calculating $U_{disp.}$, which was found to be about 10 to 50 times smaller than the dipole-dipole interaction. Similar conclusions have been reached by Pospisil & Kuta (58) for the adsorption of succinic acid on mercury. Accordingly, the main contribution to the lateral interaction free energy will in all probability be from the polar group through dipole-dipole interaction. This interaction, U_{dipole}, can be calculated by using the equation (34)

$$U_{dipole} = \frac{\mu_D^2}{\epsilon r^3} \qquad \text{-------(46)}$$

where μ_D is the dipole moment of the pure organic compound, 1.3 Debye for monocarboxylic acids (59,60,61) and 2.3 Debye for dicarboxylic acids (61,62), r is the distance between the dipoles (about 4.0 Å as calculated from the dimensions of the carboxyl group), and ϵ is the dielectric constant of the medium, which varies with coverage. Therefore, for monocarboxylic acids

$$U_{dipole} = - \frac{(1.3)^2 \times 6.02 \times 10^{23} \times 10^{-46}}{\epsilon \times (4.0)^3 \times 4.18 \times 10^{-24}}$$

$$= - \frac{.380}{\epsilon} \text{ Kcal/mole}$$

The chemical potential μ for localized adsorption*, assuming parallel dipoles in hexagonal array (34) is given by

*If adsorption takes place on a surface where potential energy fluctuations are appreciable, the troughs will represent adsorption sites and the adsorption is said to be localized. If, however, the fluctuations are so small as effectively to vanish, adsorption is said to be non-localized.

$$\mu_{dipole} = 9.24\ \theta \qquad U_{dipole} = \frac{-3.511}{\epsilon}\ \theta$$

-------(47)

For non-localized adsorption* with parallel dipoles in hexagonal array (34), the chemical potential is given by

$$\mu_{dipole} = 11.5\ \theta^{3/2} \qquad U_{dipole} = \frac{-4.37}{\epsilon}\ \theta^{3/2} \text{Kcal/mole}$$

-------(48)

At a low coverage, the dipoles are separated by water molecules and therefore the dielectric constant is that of the water if it is assumed that the functional group is present only in the primary electrode layer, for which it has been estimated that $\epsilon = 6$ (63). At full coverage the dipoles are separated by organic molecules and ϵ will be approximately equal to the pure-additive value of 2.5 (64). Assuming a linear combination at intermediate coverages, we have

$$\epsilon = 6 - 3.5\ \theta \qquad \text{-------(49)}$$

therefore, for localized adsorption

$$\mu_{dipole} = \frac{-3.511}{(6-3.5\theta)}\ \theta$$

and for non-localized

$$\mu_{dipole} = -\frac{4.37}{(6-3.5\theta)}\ \theta^{3/2}$$

*See previous page.

Substituting $\mu_{dicarboxylic}$ in Equation (46), the dipole interaction of dicarboxylic acids can be calculated as

$$U_{dipole} = \frac{-(2.3)^2 \times 6.02 \times 10^{23} \times 10^{-46}}{\epsilon \times (4.0)^3 \times 4.18 \times 10^{-24}}$$

$$= - \frac{1.19}{\epsilon} \text{ Kcal/mole}$$

Therefore, the chemical potential for localized adsorption with parallel dipoles* is

$$\mu_{dipole} = - \frac{10.99}{\epsilon} \theta \text{ Kcal/mole}$$

and for antiparallel dipoles* (34) it is

$$\mu_{dipole} = 4.5 \theta \quad U_{dipole} = - \frac{5.35}{\epsilon} \theta$$

-------(50)

For non-localized adsorption with parallel dipoles, the chemical potential is given by

$$\mu_{dipole} = 11.5 \theta^{3/2} \quad U_{dipole} = - \frac{13.7}{\epsilon} \theta^{3/2}$$

and for antiparallel dipoles, by

$$\mu_{dipole} = 5.625 \theta^{3/2} \quad U_{dipole} = - \frac{6.7}{\epsilon} \theta^{3/2}$$

-------(51)

In the case of dicarboxylic acids with functional group at each end of the molecule, the dipole-dipole interaction will possibly be a combination of different models.

*In parallel dipoles, the molecules are oriented in the same fashion with respect to the metal surface, while for antiparallel dipoles, the molecules are orientated with their dipoles opposite to each other.

Since the length of the dicarboxylic acid molecule is greater than the thickness of the primary layer at the metal-solution interface, the dielectric constant ϵ in Equation (50) cannot be taken as 6, the dielectric constant of the primary layer, at zero coverage. Its value will probably be a combination of the dielectric constants of the water layers at the electrode-solution interface (62). In addition to this uncertainty about ϵ at zero coverage, there are no exact data available for the dielectric constant of the pure dicarboxylic acids. Accordingly, no calculation can be made with any assurance of accuracy. However, the dielectric constant at intermediate coverage for the adsorption of succinic acid at a mercury-solution interface has been given as 15-13θ by Pospisil & Kuta (58), who assume that the dielectric constant of pure succinic acid is 2. If this value can be assumed applicable to the dicarboxylic acids used in this work, μ_{dipole} for the above models can be estimated. The results are given in Table 9.

Components of the Free Energy of Adsorption

When the overpotential increment for monocarboxylic acids is plotted against the concentration of a given additive, it is found that the curve approaches linearity as the concentration approaches zero. Typical behavior is shown in Fig. 16. The initial slopes for the monocarboxylic acids, given in Table 10, show that the logarithm of the initial slope increases linearily with the

Table 9

Calculated lateral interaction free energy for monocarboxylic acids (Kcal/mole)

θ	Localized	non-localized
.1	- .062	- .025
.2	- .133	- .074
.3	- .213	- .146
.4	- .306	- .242
.5	- .413	- .365
.6	- .541	- .523
.7	-. 693	- .725
.8	-. 879	- .982
.9	-1.110	-1.316

Calculated lateral interaction free energy for dicarboxylic acids (Kcal/mole)

	Parallel dipoles		Antiparallel dipoles	
θ	Localized	non-localized	Localized	non-localized
.1	- .080	- .0316	- .038	- .015
.2	- .177	- .098	- .086	- .042
.3	- .297	- .202	- .144	- .098
.4	- .448	- .353	- .218	- .173
.5	- .646	- .569	- .314	- .278
.6	- .916	- .884	- .446	- .432
.7	-1.303	-1.259	- .634	- .660
.8	-1.911	-2.129	- .930	-1.041
.9	-2.997	-3.545	-1.459	-1.733

Figure 16

Overpotential increment as a function of additive concentration($\Delta\eta$ vs. C)

Propanoic acid

Butanoic acid

Pentanoic acid

Pentanedioic acid

Octanedioic acid

Figure 16

Overpotential increment as a function of additive concentration($\Delta\eta$ vs. C)

Propanoic acid

Butanoic acid

Pentanoic acid

Pentanedioic acid

Octanedioic acid

Fig. 16

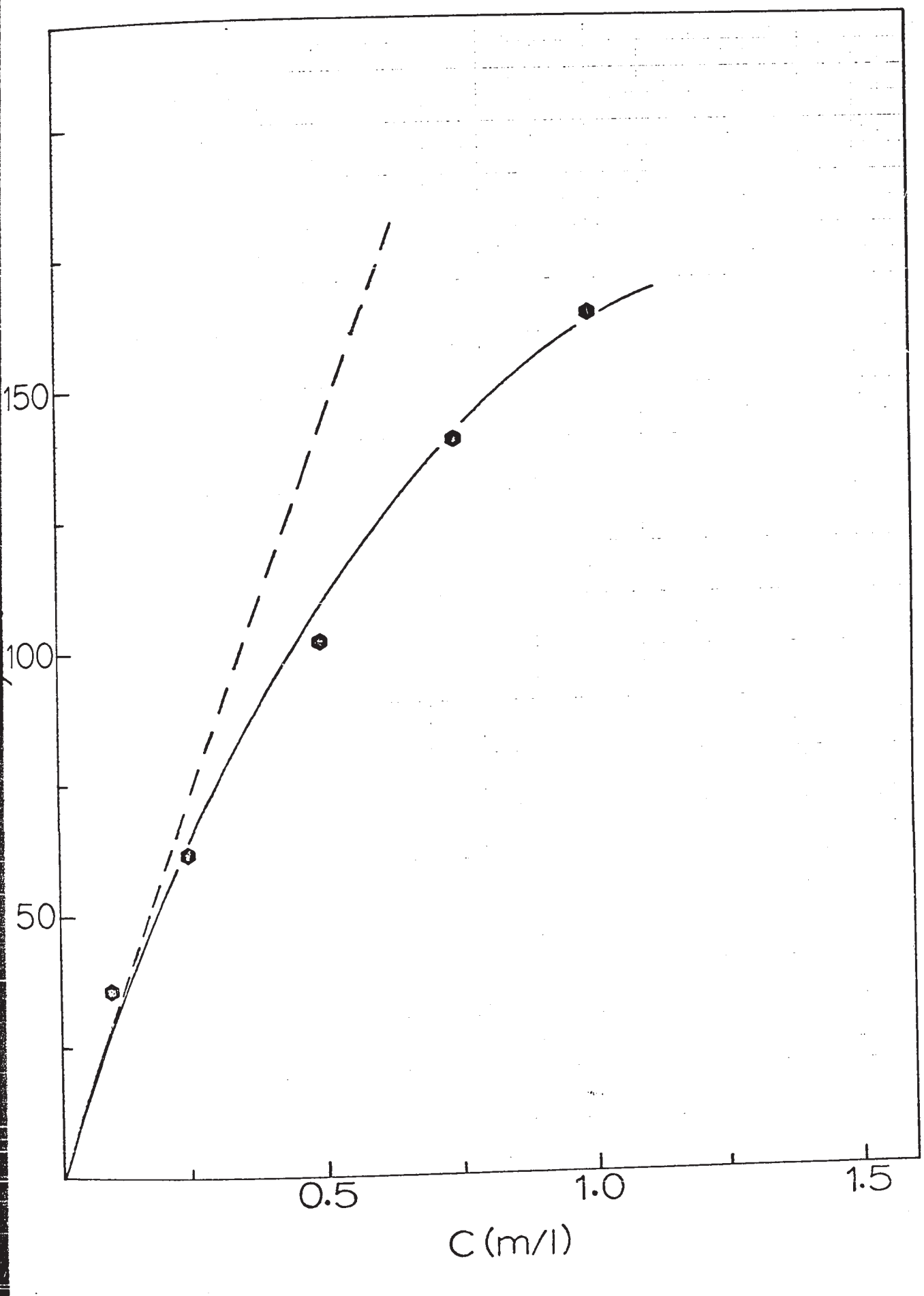

Fig. 16

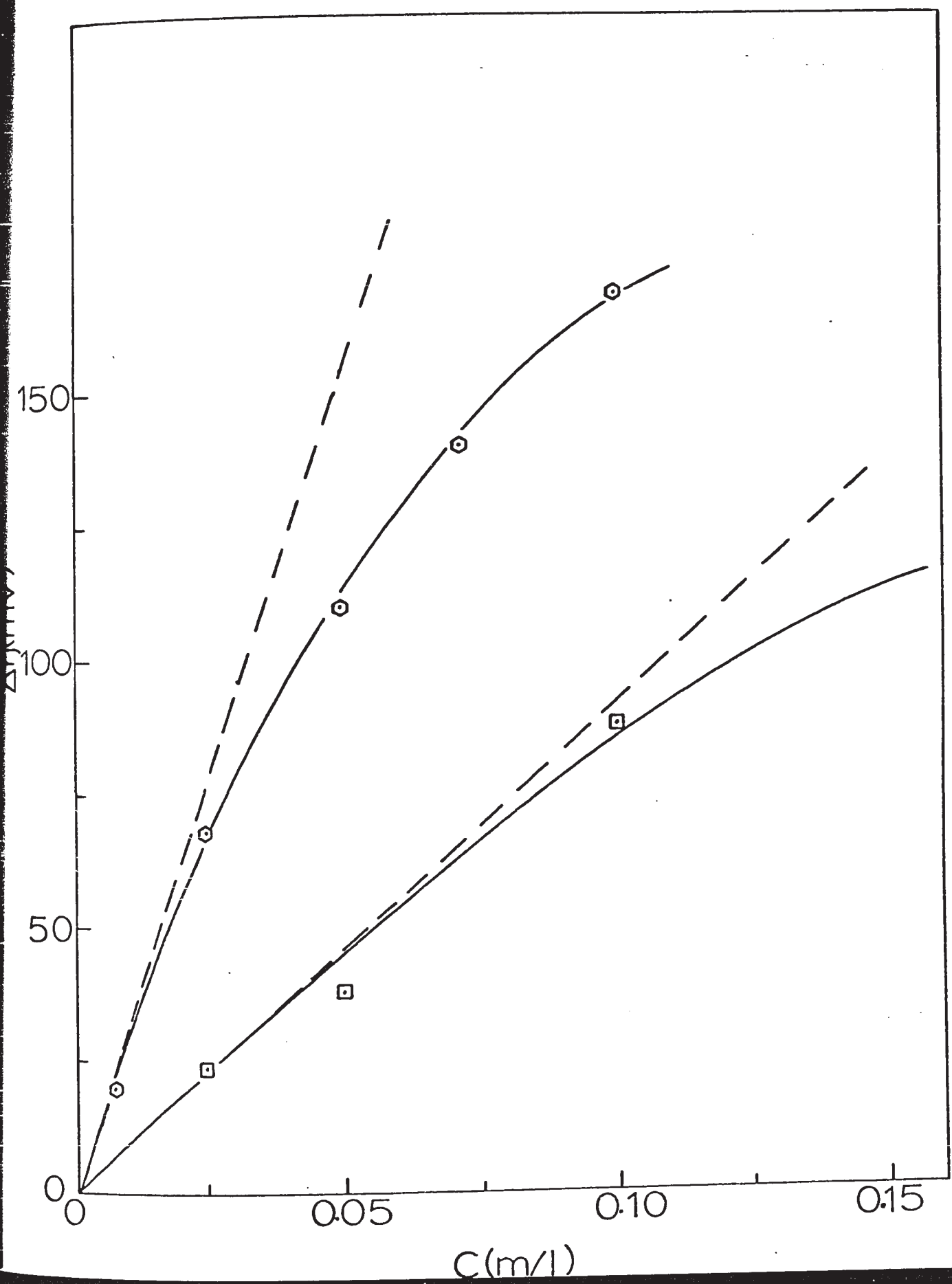

Fig. 16

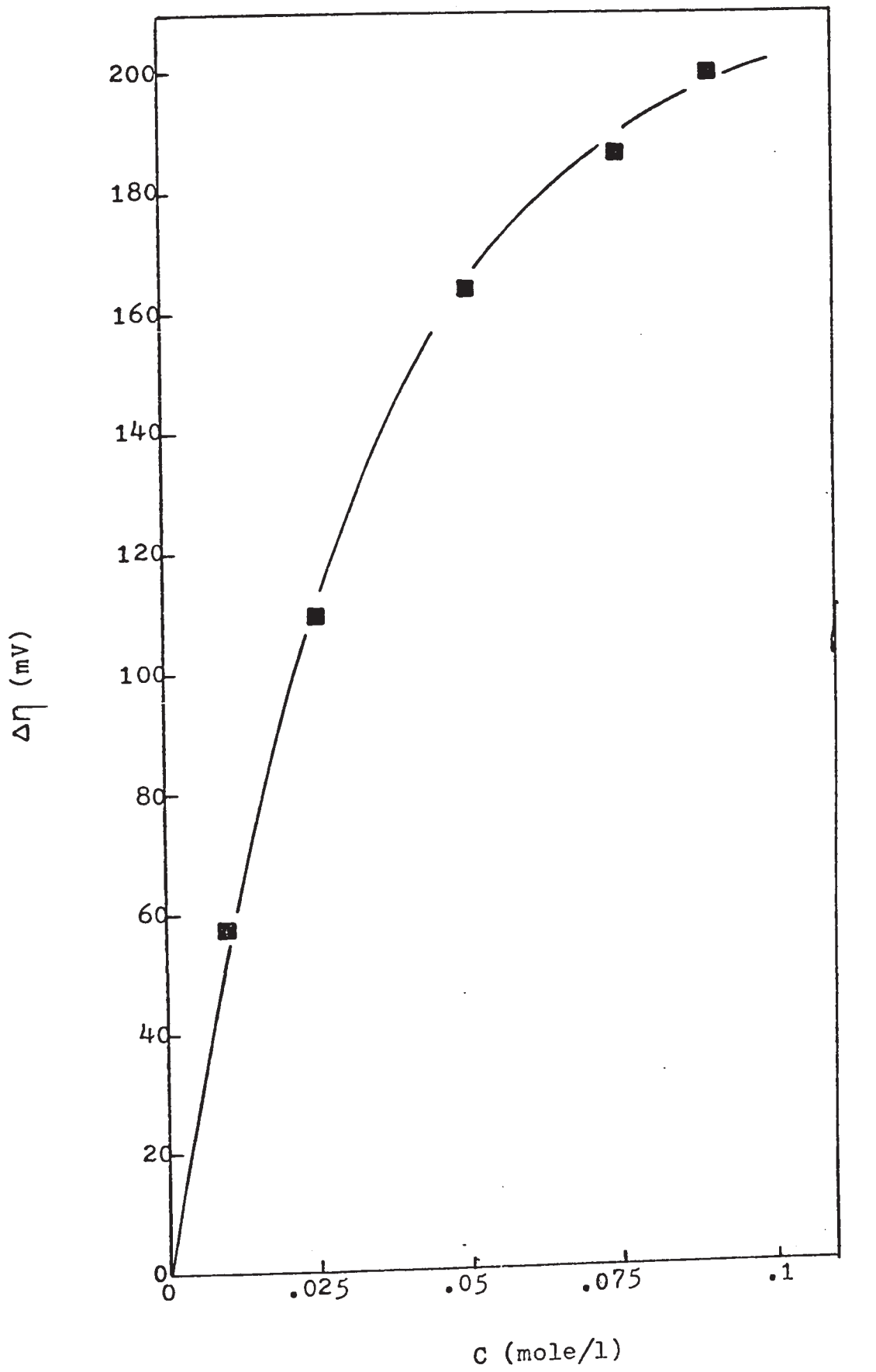

Fig. 16

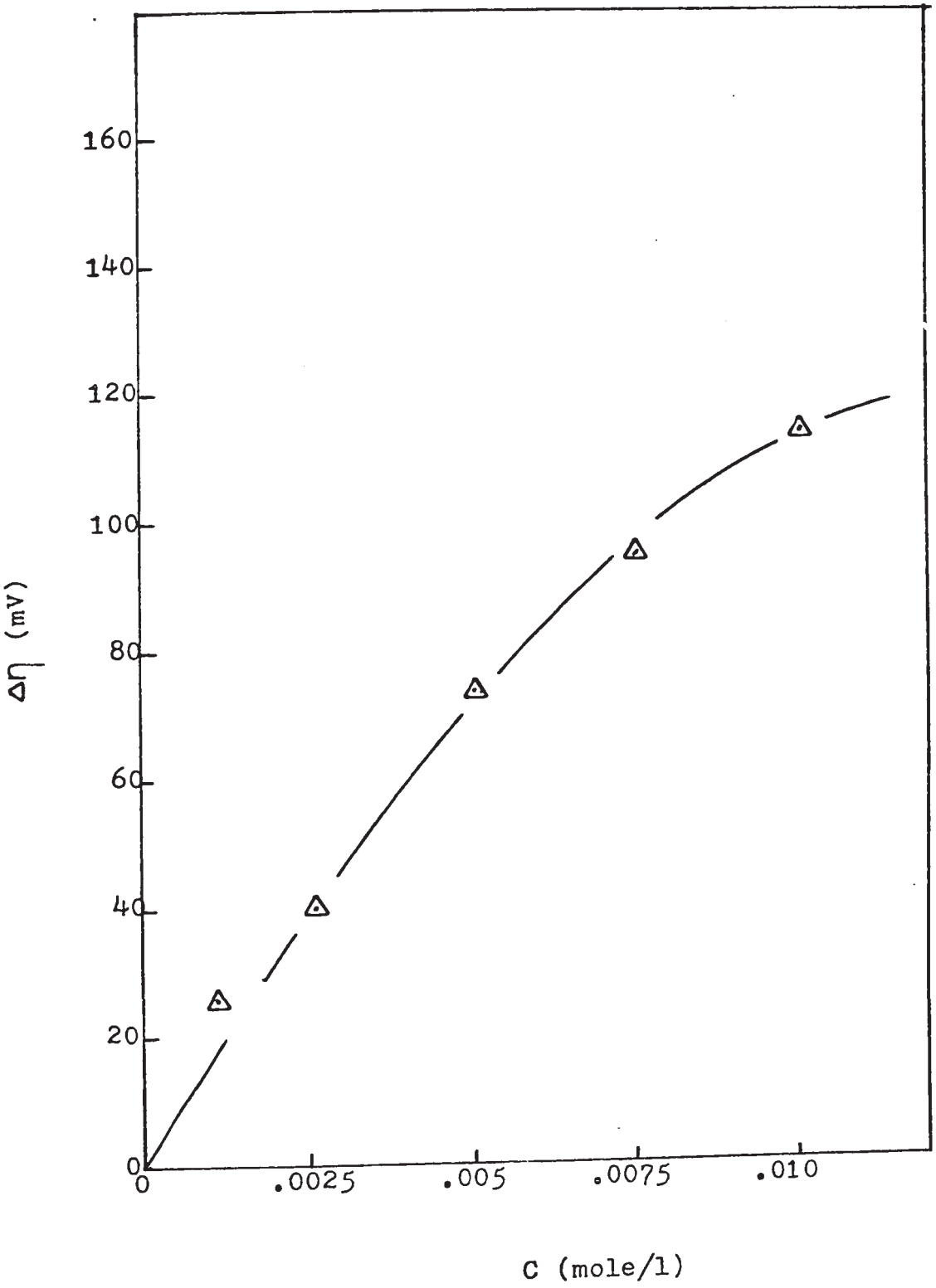

Table 10

The initial slope of $\Delta\eta$ vs. C curve as C→0

monocarboxylic acids

Additive	$(\Delta\eta/C)_{C\to 0}$	$(\Delta\eta/C)_{C\to 0}$ (smoothed)
Propanoic acid	2.83×10^{2}	2.86×10^{2}
Butanoic acid	9.10×10^{2}	9.40×10^{2}
Pentanoic acid	3.00×10^{3}	3.08×10^{3}
Hexanoic acid	9.75×10^{3}	1.01×10^{4}
Heptanoic acid	3.55×10^{4}	3.32×10^{4}
Octanoic acid	1.17×10^{5}	1.09×10^{5}

number of methylene groups in the additive molecule, counting the terminal methyl, as shown in Fig. 17.

Advantage was taken of this linearity, in the case of monocarboxylic acids, to obtain graphically-smoothed overpotential data for low concentration of these additives. For this purpose, smoothed values of the initial slopes, as obtained from Fig. 17 are given in the last column in Table 10. For dicarboxylic acids, no smoothed initial slopes were obtained due to the lack of linearity of $\log(\Delta\eta/C)_{C-0}$ vs. x.

For monocarboxylic acids, the linearity observed in Fig. 17 follows as a consequence of the applicability of Traube's rule to this homologous system, and corresponds in essence to the known behavior of these compounds in affecting the surface tension of aqueous solutions as described by Ward (57). A useful equation directly pertinent and applicable to Fig. 17 can be derived from Equation (45).

According to the behavior shown in Fig. 14, $g(\theta)$ becomes zero as θ approaches zero. Application of Equation (45) to the zero-coverage condition then gives for the homologous series of monocarboxylic acids

$$f(\theta) = C\left[\frac{e^{-\Delta G^{o}_{p}/RT}}{55.5}\right]\left[e^{-\Delta G^{o}_{CH_2}/RT}\right]^{x} = C\alpha\beta^{x} \qquad \text{-------(52)}$$

where α & β are constants at constant temperature as shown.

Figure 17

Logarithm of the initial slope, $(\Delta\eta/C)_{C\to 0}$ vs. number of methylene groups in the monocarboxylic acid molecule

Fig. 17

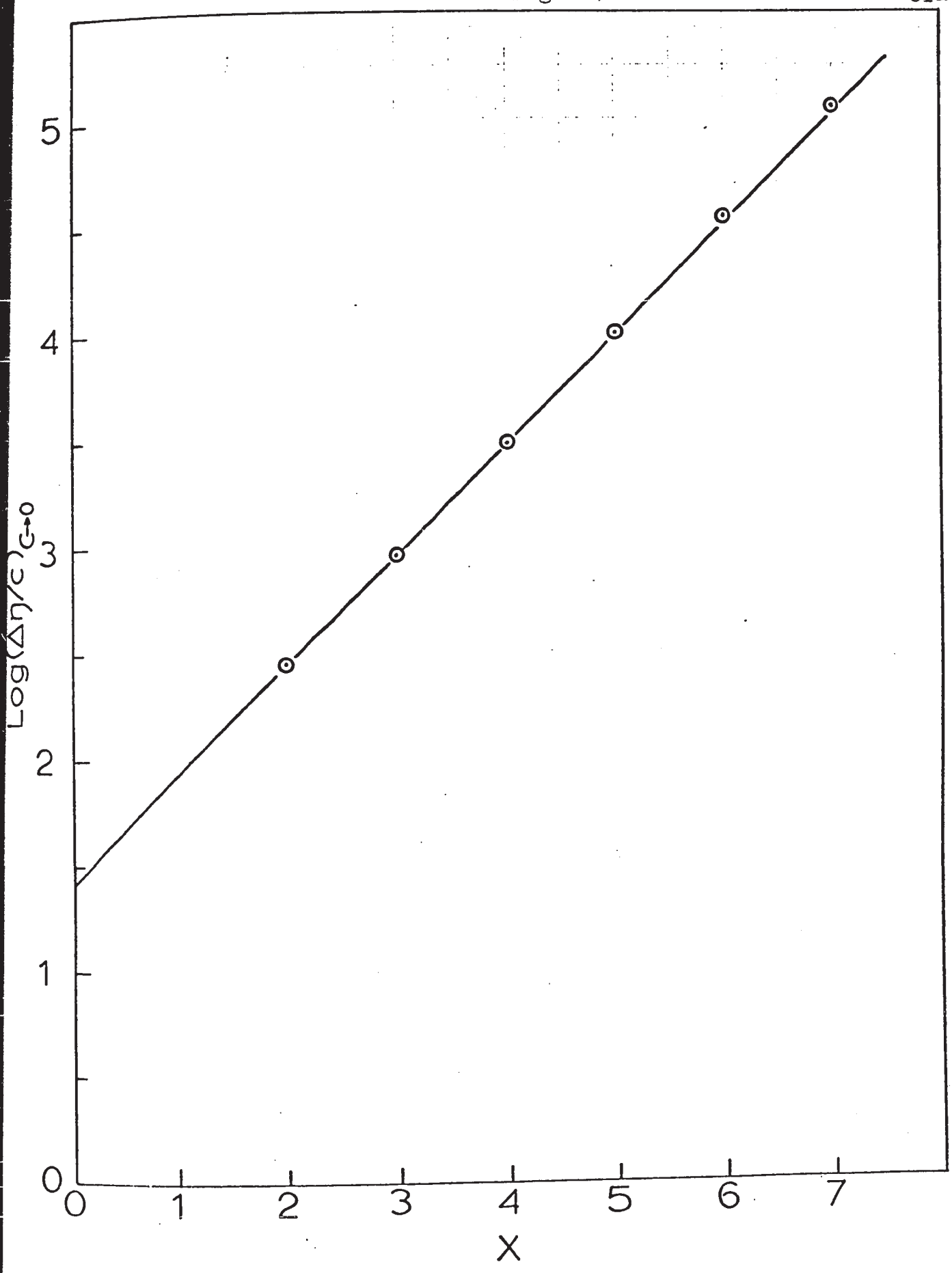

On substituting for θ in Equation (42), and taking n as 2, it is easily shown that f(θ), the left-hand side of Equation (52) can be written as

$$\tfrac{1}{4}(e^{2\Delta\eta/b} - 1)$$

With these subsitutions Equation (52) becomes

$$e^{2\Delta\eta/b} - 1 = 4C\alpha\beta^{x} \qquad \text{--------(53)}$$

which, on substituting the series expansion for $e^{2\Delta\eta/b}$ and dividing through by C, gives

$$\frac{2}{b}\frac{\Delta\eta}{C} + \left(\frac{2}{b}\cdot\frac{\Delta\eta}{C}\right)^{2}\cdot\frac{C}{2!} + \left(\frac{2}{b}\cdot\frac{\Delta\eta}{C}\right)^{3}\cdot\frac{C^{2}}{3!} + \text{---} = 4\alpha\beta^{x}$$

-------(54)

In the limit, as C approaches zero at zero coverage, this becomes

$$\left(\frac{\Delta\eta}{C}\right)_{C\to 0} = 2b\alpha\beta^{x} \qquad \text{-------(55)}$$

The logarithmic form gives the straight-line equation for Fig. 17 as

$$\log(\Delta\eta/C)_{C\to 0} = \log(2b\alpha) + x\log\beta$$

-------(56)

Clearly ΔG^{o}_{p} and $\Delta G^{o}_{CH_2}$ can be calculated from the experimental intercept and slope respectively in Fig. 17. In this work, because of some uncertainty in the values of $(\Delta\eta/C)_{C\to 0}$ in Table 10 and Fig. 17, it was decided to use a calculated slope, $\log\beta$ in (56), which was obtained by arranging Equation (45) to give

$$g(\theta) = RT\ \ln C - RT\ \ln f(\theta) - x\,\Delta G^{o}_{CH_2} - (\Delta G^{o}_{p} + RT\ \ln 55.5)$$

-------(57)

where the combination of terms

$$RT \ln C - RT \ln f(\theta) - x\Delta G^{o}_{CH_2} = f(C,\theta,x) \text{ -------(58)}$$

is the same for all the monocarboxylic acids since the same $g(\theta)$ vs. θ relation applies to all, Fig. 14. $\Delta G^{o}_{CH_2}$ can be calculated directly from the concentration data in Fig. 8 by subtracting Equation (58) for any two of the additives at a given overpotential increment, since the term $RT \ln f(\theta)$ cancels out in the subtraction. The value found is -704 calories per mole. Accordingly, the line in Fig. 17 has been drawn with the slope, 0.516, corresponding to this value of $\Delta G^{o}_{CH_2}$ in Equation (56), giving a value of 1.425 for the intercept, $\log(2b\alpha)$ in (56). Taking the Tafel slope as the experimental value, 52mV, ΔG^{o}_{p} is found to be -1570 calories per mole for the electrosorption of monocarboxylic acids on copper. This result is at least in theory the free energy of adsorption of methanoic acid (formic acid) at zero coverage, as is indicated by the extrapolation to $x = 0$ in Fig. 17, assuming that formic acid behaves as a regular member of this homologous series.

It should be noted that the value found for $\Delta G^{o}_{CH_2}$ in this study, -704 calories, is of the same order of magnitude as Ward's value of -760 calories (57) obtained from surface tension measurements for adsorption of monocarboxylic acids at the air-solution interface. This means, presumably, that no great specific interaction

occurs between the hydrocarbon part of the additive molecule and the copper surface and that this part of the adsorption must be primarily physical in nature (34). The average $\Delta G^{o}_{CH_2}$ for the adsorption of aliphatic alcohols (C_2-C_6) on mercury has been found to be -770 calories per mole, (65), and also for the adsorption of aliphatic alcohols (C_2-C_7) on a bismuth cathode (66) $\Delta G^{o}_{CH_2}$ was found to be -800 cal/mole. The results are in satisfactory agreement with the results obtained in this work for the adsorption of fatty acids on a copper cathode. The value of ΔG^{o}_{p} as extrapolated from results obtained by Ward (56) for the adsorption of monocarboxylic acids at the air-solution interface was found to be of the order of -900 cal/mole. This result, compared with the value of ΔG^{o}_{p} found in this work, -1570 cal/mole, supports the view that the carboxyl group is most likely adsorbed toward the metal with a metal-carboxyl interaction energy of about 700 cal/mole.

It should be noted that β in Equation (56) is the Traube coefficient for the homologous monocarboxylic acids. This coefficient is the factor by which the initial slope $(\Delta\eta/C)_{C\to 0}$ in Table 10 is multiplied on addition of each successive methylene group to the additive molecule. Its value based on the data obtained in this work is 3.28.

The free energies of adsorption at zero coverage, for monocarboxylic acids, calculated using Equation (44),

are given in Table 11. The standard energies of adsorption obtained by extrapolating the ΔG_a^o vs. θ curves to zero coverage are also given in Table 11 in the last column.

From the magnitude of the net standard free energy (ranging from -3.0 to -6.5 Kcal/mole), it would appear that physical forces are perhaps primarily involved in the adsorption process.

It should be noted that the free energy of adsorption of pentanoic and octanoic acids from aqueous perchloric acid solution on mercury have been found to be -4.37 and -7.16 Kcal/mole, respectively, as calculated from the experimental differential double layer capacity (66). These results are in reasonable agreement with the values obtained here for pentanoic and octanoic acids, -4.39 and -6.5 Kcal/mole respectively (see Table 11). The values of ΔG_a^o obtained for the adsorption of pentanoic acid from acidic HCl solution on mercury was obtained as -4.5 Kcal/mole from electrocapillary measurements by Blomgren, Bockris & Jesch (49). This too, is in satisfactory agreement with the result obtained here. The magnitude of ΔG_a^o and its relatively constant value for different metals suggest that only physical forces are involved in the adsorption process (34) and that no specific interaction occurs between the metal and the methylene groups.

Behavior of Dicarboxylic Acids

Equation (56) can be rewritten in view of (52) as follows:

Table 11

Standard free energy of adsorption of monocarboxylic acids at zero coverage

Additive	ΔG_a^o (Kcal/mole)	ΔG_a^o (Kcal/mole) extrapolated
Propanoic acid	-2.978	-3.0
Butanoic acid	-3.682	-3.7
Pentanoic acid	-4.398	-4.4
Hexanoic acid	-5.09	-5.1
Heptanoic acid	-5.794	-5.8
Octanoic acid	-6.498	-6.5

$$(\Delta\eta/C)_{C\to 0} = \frac{2b}{55.5}\, e^{-(\Delta G_a^o)_{\theta=0}/RT} \qquad \text{-------(59)}$$

where $(\Delta G_a^o)_{\theta=0}$ is the net free energy of adsorption at zero coverage. Accordingly, the initial slope of the overpotential increment vs. concentration can be used to calculate the net free energy of adsorption. The initial slopes $(\Delta\eta/C)_{C\to 0}$ and the calculated net free energies of adsorption for dicarboxylic acids are given in Table 12. The last column in Table 12 gives the net free energy of adsorption obtained by extrapolating ΔG_a^o to zero coverage from Fig. 15. It is seen that ΔG_a^o obtained from both methods are fairly close.

A plot of $\log(\Delta\eta/C)_{C\to 0}$ against the number of methylene groups in the dicarboxylic acid molecule is shown in Fig. 18. From this figure it is clear that alternation in behavior occurs, particularly with the first four members of the homologous series. This alternation behavior vanishes as the number of carbon atoms separating the two carboxyl groups increases. Similar alternation in the melting points of dicarboxylic acids has been reported by Fairweather (68) as shown in Fig. 19, and similarly too, the alternation becomes quite small for the high molecular weight homologues.

Fig. 18 indicates that there is a linear relation between $\log(\Delta\eta/C)_{C\to 0}$ and the number of methylene groups for the dicarboxylic acids with (ENCA). This result,

Table 12

Standard free energy of adsorption of dicarboxylic acids at zero coverage

Additive	$(\Delta\eta/C)_{C\to 0}$	ΔG_a°(Kcal/mole)	ΔG_a°(Kcal/mole) extrapolated
Propanedioic acid	1.3×10^3	-3.92	-3.90
Pentanedioic acid	6.1×10^3	-4.85	-4.85
Heptanedioic acid	11.6×10^3	-5.23	-5.22
Nonanedioic acid	7.0×10^4	-6.30	-6.36
Butanedioic acid	8.1×10^2	-3.64	-3.70
Hexanedioic acid	4.2×10^3	-4.64	-4.65
Octanedioic acid	16.0×10^3	-5.42	-5.50

Figure 18

Logarithm of the initial slope, $(\Delta\eta/C)_{C\to 0}$ vs. number of methylene groups in the dicarboxylic acid molecule

Fig. 18

Figure 19

Melting point as a function of the number of carbon atoms in the dicarboxylic acid molecules

The figure was taken from the original reference (68).

Fig. 19

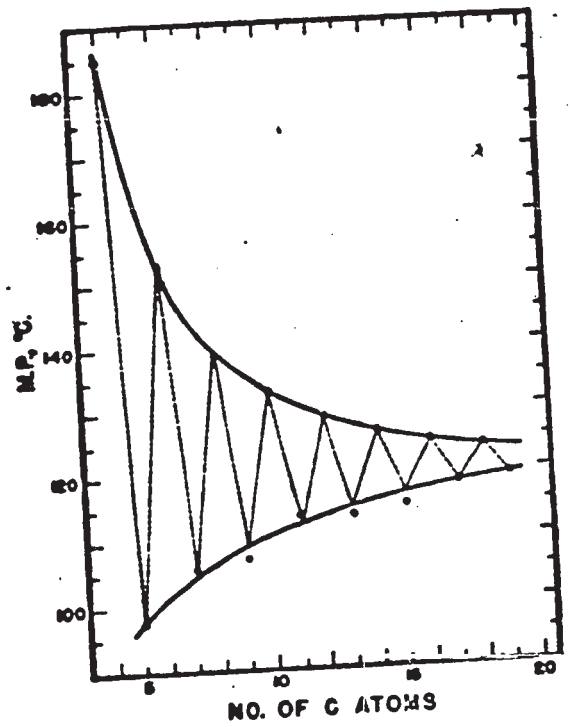

supported by the generalized behavior obtained for $\Delta\eta$ vs. C_r for the dicarboxylic acids with (ENCA) indicates that these acids most likely adsorb in the same fashion, i.e. with one carboxyl group toward the metal and the other non-adsorbing carboxyl group toward the solution. The slope for this linear behavior is .48 which is equivalent to -660 cal/mole corresponding to the free energy contribution of the methylene group, $\Delta G^{o}_{CH_2}$. This value is smaller than the value of $\Delta G^{o}_{CH_2}$ obtained for monocarboxylic acids, indicating that there is most likely some factor affecting the methylene group contribution and causing it to decrease. This is probably due to the presence of the non-adsorbing and possibly solvated carboxyl group oriented toward the solution.

In the case of dicarboxylic acids with (ONCA) there is no special trend in the $\log(\Delta\eta/C)_{C\to 0}$ vs. x relation except that increasing the number of methylene groups brings the adsorption pattern of these compounds into close similarity to that of the dicarboxylic acids with (ENCA). A more extended study of higher molecular weight dicarboxylic acids than the ones used here might be useful.

Using the mean value of ΔG^{o}_{p} and $\Delta G^{o}_{CH_2}$ found in the case of monocarboxylic acids, for the dicarboxylic acids, and taking into account the two functional groups, the calculated ΔG^{o}_{a} are given in Table 13.

From Table 13 it is possible to conclude that

Table 13

Experimental and calculated free energy of adsorption for dicarboxylic acids

Additive	ΔG_a^o Experimental	ΔG_a^o calculated*	ΔG_a^o calculated**
Propanedioic acid	-3.92	-3.84	-2.27
Pentanedioic acid	-4.85	-5.25	-3.68
Heptanedioic acid	-5.23	-6.66	-5.09
Nonanedioic acid	-6.30	-8.07	-6.50
Butanedioic acid	-3.64	-4.55	-2.98
Hexanedioic acid	-4.64	-5.96	-4.39
Octanedioic acid	-5.42	-7.36	-5.79

* Both carboxyl groups adsorbed.

** One carboxyl group adsorbed.

for dicarboxylic acids with (CNCA), the experimental and calculated* values of the free energy agree to a large extent for propanedioic and pentanedioic acids. This result suggests that since the internuclear distances between the two carboxyl groups are similar to the shortest internuclear distances of the copper lattice, therefore, a higher probability of strain-free two point attachments might be possible. However, for propanedioic acid the experimental result is slightly higher than as calculated*, therefore, another factor must contribute to this greater free energy of adsorption. This difference can be speculatively explained considering the electron-withdrawing power of the carboxyl group, since the two carboxyl groups are only one carbon apart. Accordingly, an increase in the adsorption is expected, due to the electron-withdrawing nature of each carboxyl group on the other. In the case of pentanedioic acid the experimental result is slightly less than the calculated*. This may be due in part to the fact that the internuclear distance between the two carboxyl groups, as mentioned before, is slightly different than the third shortest internuclear distance for the copper lattice, 4.98Å and 5.1Å respectively.

Comparing the experimental and the calculated** results for propanedioic and pentanedioic acids, it can be seen that adsorption with both carboxyl groups is most probable for these two acids. In the case of heptanedioic and nonanedioic acids, the experimental results are much

less than the calculated*, therefore, strain-free two-point attachments appear to be less likely. These results agree with the view that the internuclear distances for these two acids, 7.47Å and 10.96Å respectively, are probably not likely to allow two-point attachments since the nearest internuclear copper lattice distances are 7.65Å and 10.20Å. Therefore, one-point attachment is most likely to occur. However, the relative probability of adsorption of these acids is still higher than the corresponding monocarboxylic acids. Comparison of the experimental and calculated** values shows approximate agreement for heptanedioic and nonanedioic acids, but the greater magnitude of the calculated** value for nonanedioic acid compared to the experimental suggests a further contributing factor in the adsorbability of this compound. While the effect of each carboxyl group on the other is zero, possible solvation of one carboxyl group may be a factor causing a decrease in the adsorbability. In the case of heptanedioic acid the solvation power of the non-adsorbing carboxyl group and the two-point attachment probability might be of the same order of magnitude, with the effect that the net free energy of adsorption will be equivalent to the contributions of one carboxyl group and five methylene groups. Support for this assumption is found on comparing the nearly equal overpotential values for hexanoic and heptanedioic acids in Tables 7 & 8. For nonanedioic

acid, the probability of two-point attachment is expected to be even less than that of heptanedioic. The solvation of the non-adsorbing functional group might increase since the two carboxyl groups are much farther apart. Therefore, the net result is a lower free energy of adsorption. Accordingly, the free energy of adsorption will be even less than for one carboxyl group and seven methylene groups.

Considering the dicarboxylic acids with (ENCA), the calculated* free energy of adsorption is always higher than the experimental values (Table 13). This suggests that adsorption takes place with only one carboxyl group. Comparing experimental and calculated** values shows that the experimental result is much higher for butanedioic, slightly higher for hexanedioic, and lower for octanedioic. These results can be explained on the basis of two opposing factors: 1) the decrease of adsorption by the solvation of the non-adsorbing carboxyl group, and 2) the increase of adsorption by the electron-withdrawing nature of this group (29). The experimental free energy of adsorption of butanedioic acid is much greater than calculated on the basis of one carboxyl and two methylene groups but less than calculated if both carboxyl groups are involved. Therefore, the effect of the second carboxyl group cannot be due to complete adsorption. Since the two carboxyl groups are not far apart, the non-adsorbing group will increase the adsorption of the other by decreasing its

electron density; i.e. factor 2 will dominate. Hexanedioic acid shows experimental free energy of adsorption slightly higher than calculated**. Since the two carboxyl groups are further apart, the second factor decreases and a lowering of the relative free energy of adsorption is expected. With the two carboxyl groups still further apart, as in octanedioic acid, factor 2 will be small or zero and the solvation power of the non-adsorbing carboxyl group will increase, and further lowering in the relative free energy of adsorption is expected as compared with the calculated**. A similar behavior, considering one and two-point attachment, has been reported (18).

From Fig. 8 it can be seen that for octanoic and heptanoic acids at high concentration, the overpotential begins to level off. This behavior was not considered in the calculation of the lateral interaction, however, it seems that for high molecular weight acids at high concentration, possible repulsion between the hydrocarbon parts of the molecules might take place. Further work with higher molecular weight monocarboxylic acids should prove useful, and might reveal a behavior different than those considered here. In the case of propanedioic acid at higher concentration, the cathodic overpotential falls as seen in Fig. 9. No proper explanation can be given at present for this behavior.

Components of the Free Energy of Adsorption of Dicarboxylic Acids

From the preceding discussion concerning the factors affecting the free energy of adsorption of the dicarboxylic acids, the following empirical equation can be given to account for the components of the free energy at zero coverage:

For dicarboxylic acids with (ENCA),

$$\Delta G_a^o = \Delta G_p^o + x\,\Delta G_{CH_2}^o + \left(\frac{6-x}{4}\right)\Delta G_{elec.}^o + \left(\frac{x-2}{4}\right)\Delta G_s^o \qquad \text{-------(60)}$$

where $\Delta G_{elec.}^o$ is the electrostatic contribution of the non-adsorbing carboxyl group to the free energy of adsorption, and ΔG_s^o is the free energy contribution due to the solvation of the non-adsorbing carboxyl group (desorbing energy). It should be indicated that the coefficients in Equation (60) are merely empirical and were chosen to account for the free energy for the particular acids studied in this work.

ΔG_s^o can be obtained by subtracting ΔG_a^o for heptanoic acid from ΔG_a^o for octanedioic acid. Since the two functional groups of octanedioic acid are sufficiently far apart, $\Delta G_{elec.}^o$ can be assumed to approximate zero. In this way, ΔG_s^o is found to be .30 Kcal/mole (the positive value should be noted). Assuming that ΔG_s^o is sufficiently small to be neglected for butanedioic acid, $\Delta G_{elec.}^o$ can be calculated. Accordingly,

$\Delta G^{o}_{elec.}$ was found to be -.65 Kcal/mole. Using these values of $\Delta G^{o}_{elec.}$ and ΔG^{o}_{s}, the free energy of adsorption of hexanedioic acid, where both the electrostatic and the desorbing energies of the non-adsorbing carboxyl group are present, is found by calculation from Equation (60) to be -4.56 Kcal/mole, which is in reasonable agreement with the experimental -4.64 Kcal/mole, and which might be taken to indicate that this equation is at least approximately correct.

For dicarboxylic acids with (ONCA) ΔG^{o}_{a} can be given as

$$\Delta G^{o}_{a} = \Delta G^{o}_{p} + \frac{(7-x)}{8}\Delta G^{o}_{p} + \frac{(7-x)}{6}\Delta G^{o}_{elec.} + x\Delta G^{o}_{CH_2} + \frac{(x-1)}{6}\Delta G^{o}_{s} \qquad \text{-------(61)}$$

Here again, the coefficients are internally empirical to account for the free energy of the dicarboxylic acids with (ONCA) done in this work. The second term accounts for the effect of the cis-structural configuration of the two carboxyl groups. For higher homologues, e.g. nonanedioic acid, the second and third terms of Equation (61) will be nearly zero and accordingly, ΔG^{o}_{s} can be obtained. It was found to be .30 Kcal/mole, in agreement with the value obtained for dicarboxylic acids with (ENCA). $\Delta G^{o}_{elec.}$ was obtained from ΔG^{o}_{a} for pentanedioic acid instead of propanedioic acid, since the results for the latter were uncertain. It was found to be -.35 Kcal/mole. Accordingly, ΔG^{o}_{a} was calculated for dicarboxylic acids with (ONCA),

using Equation (61). The experimental and the calculated results are given in Table 14.

Table 14

Free energy of adsorption for dicarboxylic acids with (ONCA)

Additive	ΔG_a^o experimental	ΔG_a^o calculated
Propanedioic acid	- 3.9	- 3.82
Pentanedioic acid	- 4.85	- 4.60
Heptanedioic acid	- 5.23	- 5.39
Nonanedioic acid	- 6.20	- 6.20

The satisfactory agreement between experimental and calculated free energies in Table 14 indicates empirical validity of Equation (61).

The Experimental and Calculated Lateral Interaction Free Energy

For monocarboxylic acids, as mentioned previously, the lateral interaction free energy, $g(\theta)$, is the same for all these additives at the same coverage; therefore, this $g(\theta)$ can be obtained from the overpotential increment and the additive concentration of any member of the series. Pentanoic acid was chosen for this purpose, and $g(\theta)$ was calculated using Equation (57). The results are given in Table 15.

A plot of $g(\theta)$ vs. θ is given for both the experimental (Table 15) and the calculated (Table 9) values in

Table 15

The experimental lateral interaction free energy-fractional coverage relation for monocarboxylic acids

θ	$g(\theta)$ cal/mole
.1425	- 59
.1749	- 79
.2505	- 135
.3191	- 191
.4382	- 311
.5362	- 444
.6175	- 570
.6844	- 700
.7396	- 846
.7851	- 985
.8227	-1134
.8537	-1285
.9004	-1584
.9322	-1885

Fig. 20. It can be seen from this figure that while the non-localized adsorption model appears to give the better agreement with experimental results, there is no distinct difference between the two models, particularly at low coverage. Accordingly, no definite conclusion can be drawn except that dipole-dipole interaction is most likely the main contribution to the lateral interaction free energy. Considering also the rough approximation used to develop the above models, the distinction between particular models will be uncertain. Adjustment of the parameters can be made to improve agreement with experiment, but the data are not sufficiently reliable to justify this procedure.

In the case of dicarboxylic acids, the experimental lateral interaction free energy was obtained by subtracting ΔG_a^o at zero coverage, which was obtained by Equation (59), (see Table 12) from the free energy of adsorption at various coverages as obtained from Equation (36). Average values are given in Table 16.

The experimental and calculated lateral interactions for dicarboxylic acids are shown in Fig. 20. Comparing Tables 9 & 16, and also comparing the results in Fig. 20 for dicarboxylic acids, it can be seen that the non-localized model, antiparallel dipoles, agree best with the experimental results, particularly at high coverage. However, as mentioned in the case of monocarboxylic acids, and also because there is more uncertainty in the calculation of μ_{dipole} for dicarboxylic acids than for monocarboxylic

Figure 20

Lateral interaction free energy vs. coverage

O experimental curves & calculated values for:

△ Localized adsorption (monocarboxylic acids)

○ Non-localized adsorption (monocarbcxylic acids)

□ Localized adsorption (dicarboxylic acids), ε = 15-13 θ

. Non-localized adsorption (dicarboxylic acids), ε = 15-13 θ

× Localized adsorption (dicarboxylic acids), ε = 32-29.5 θ

■ Non-localized adsorption (dicarboxylic acids), ε = 32-29.5 θ

Fig. 20

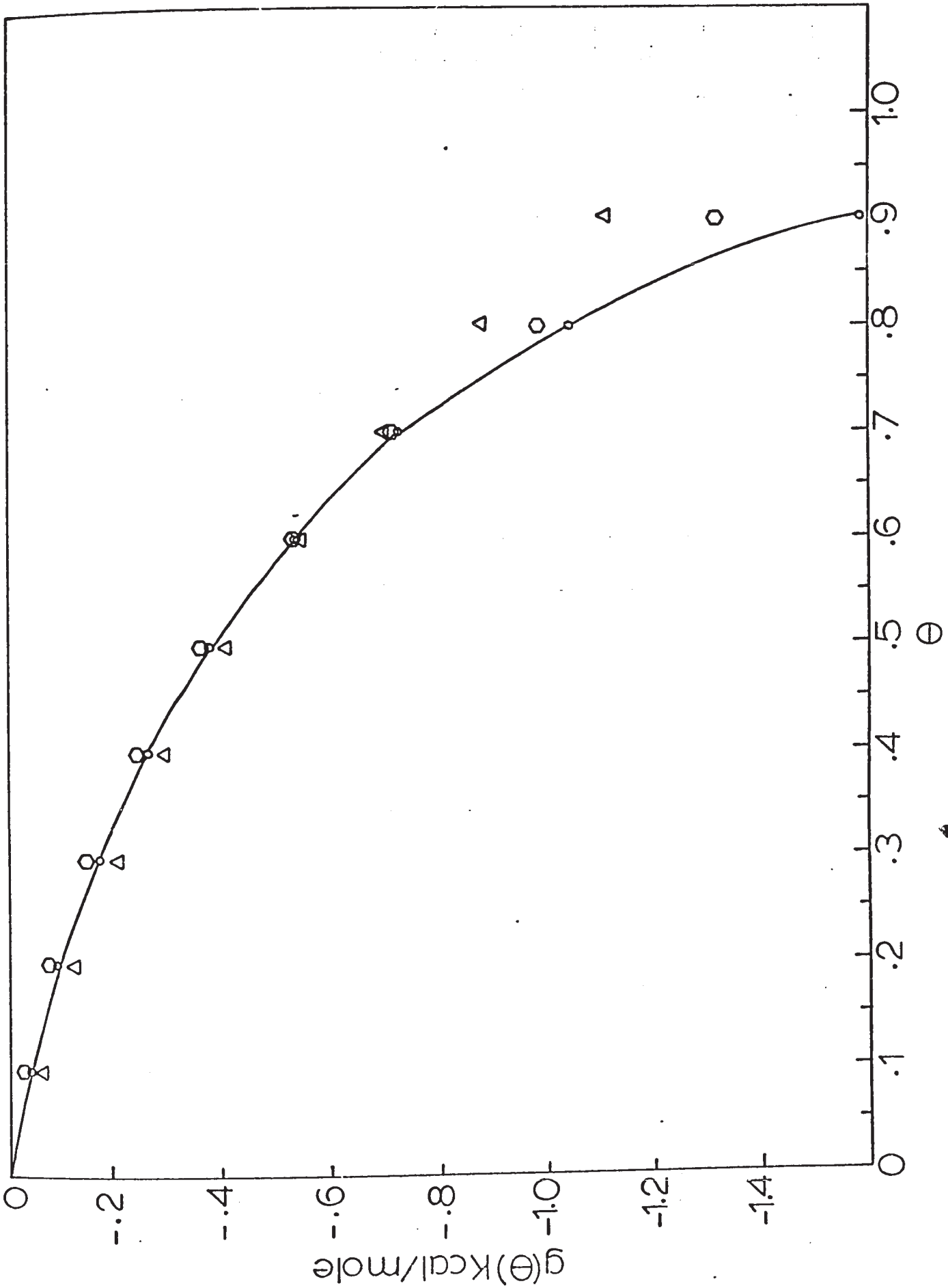

Fig. 20

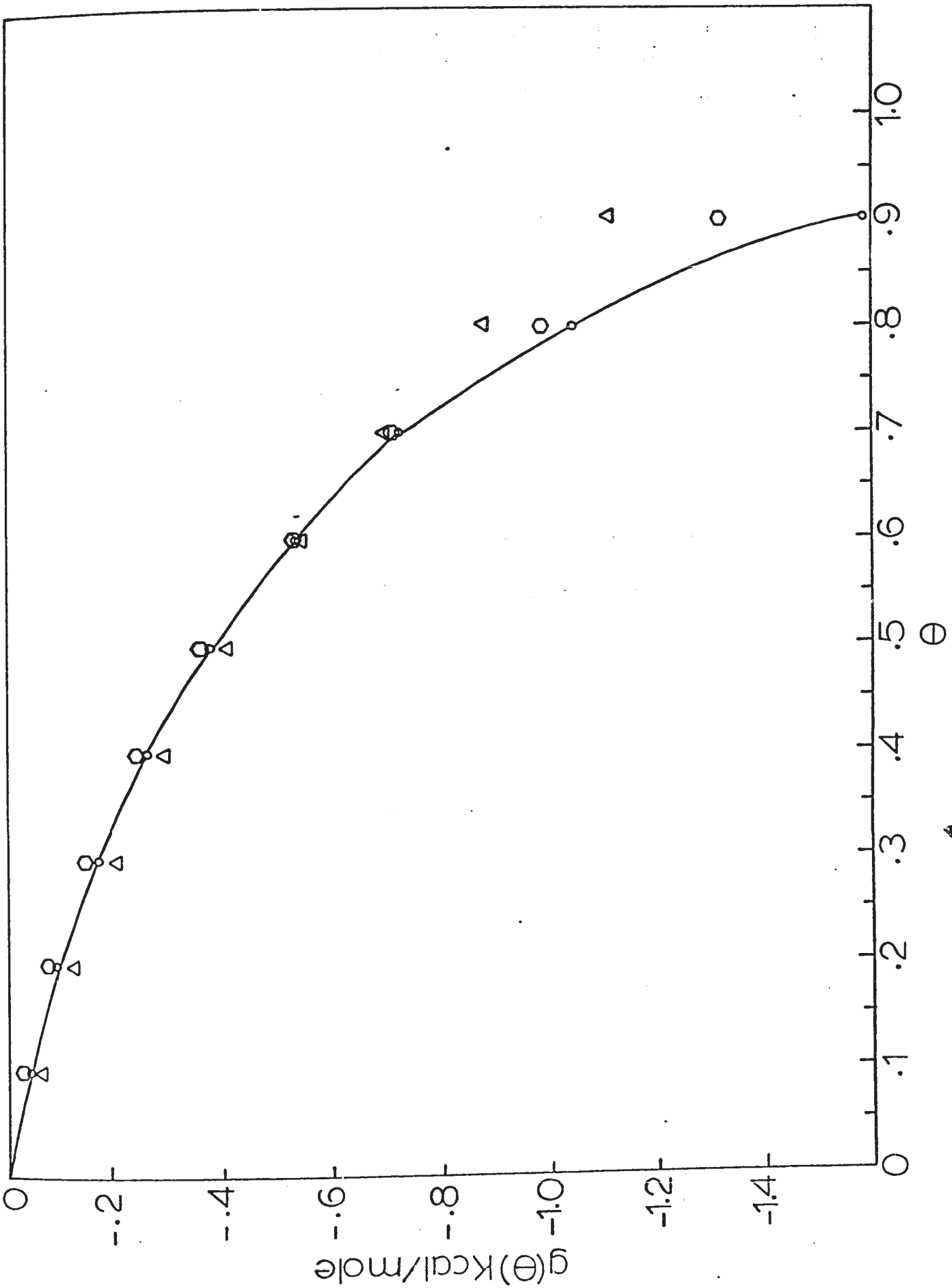

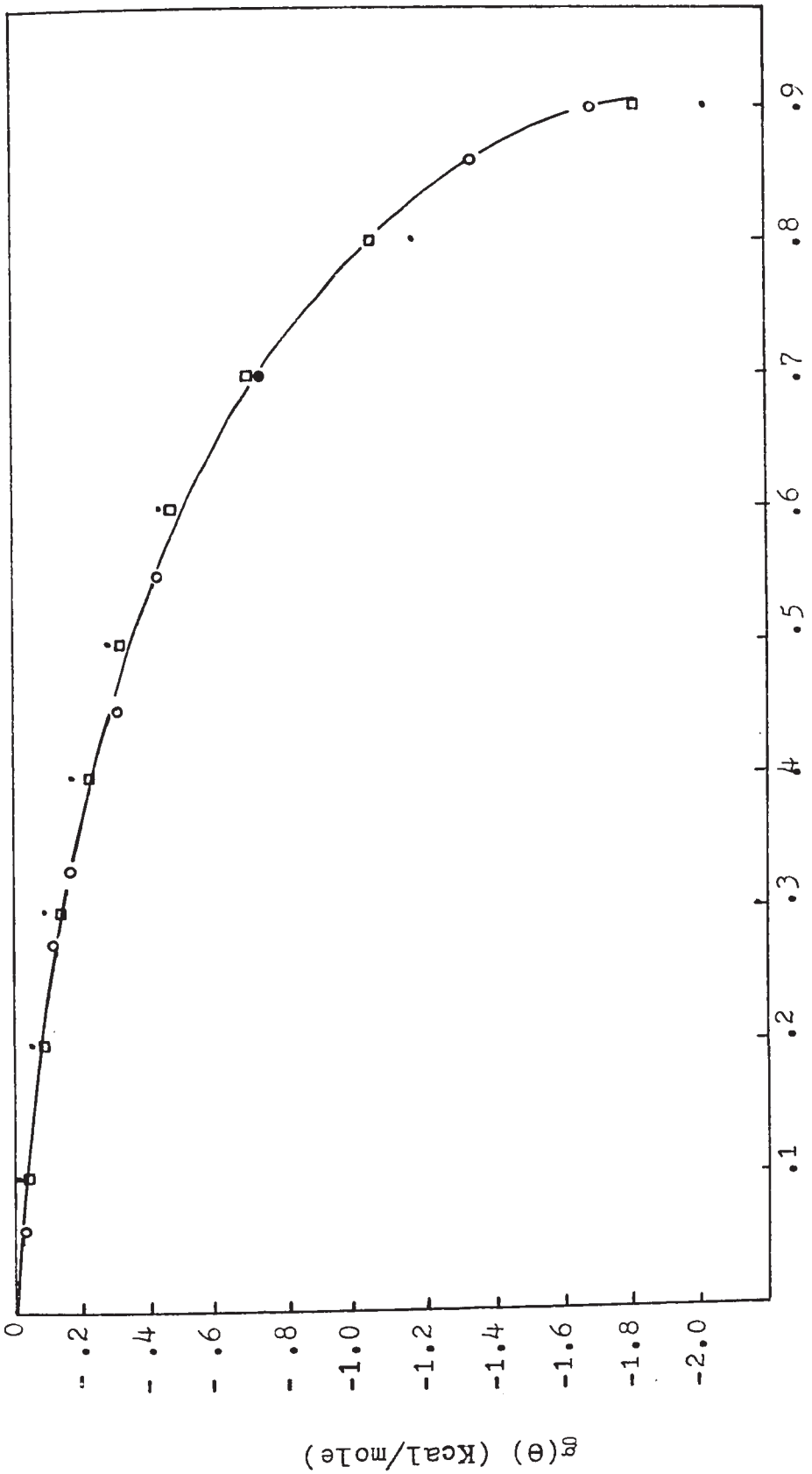

Fig. 20

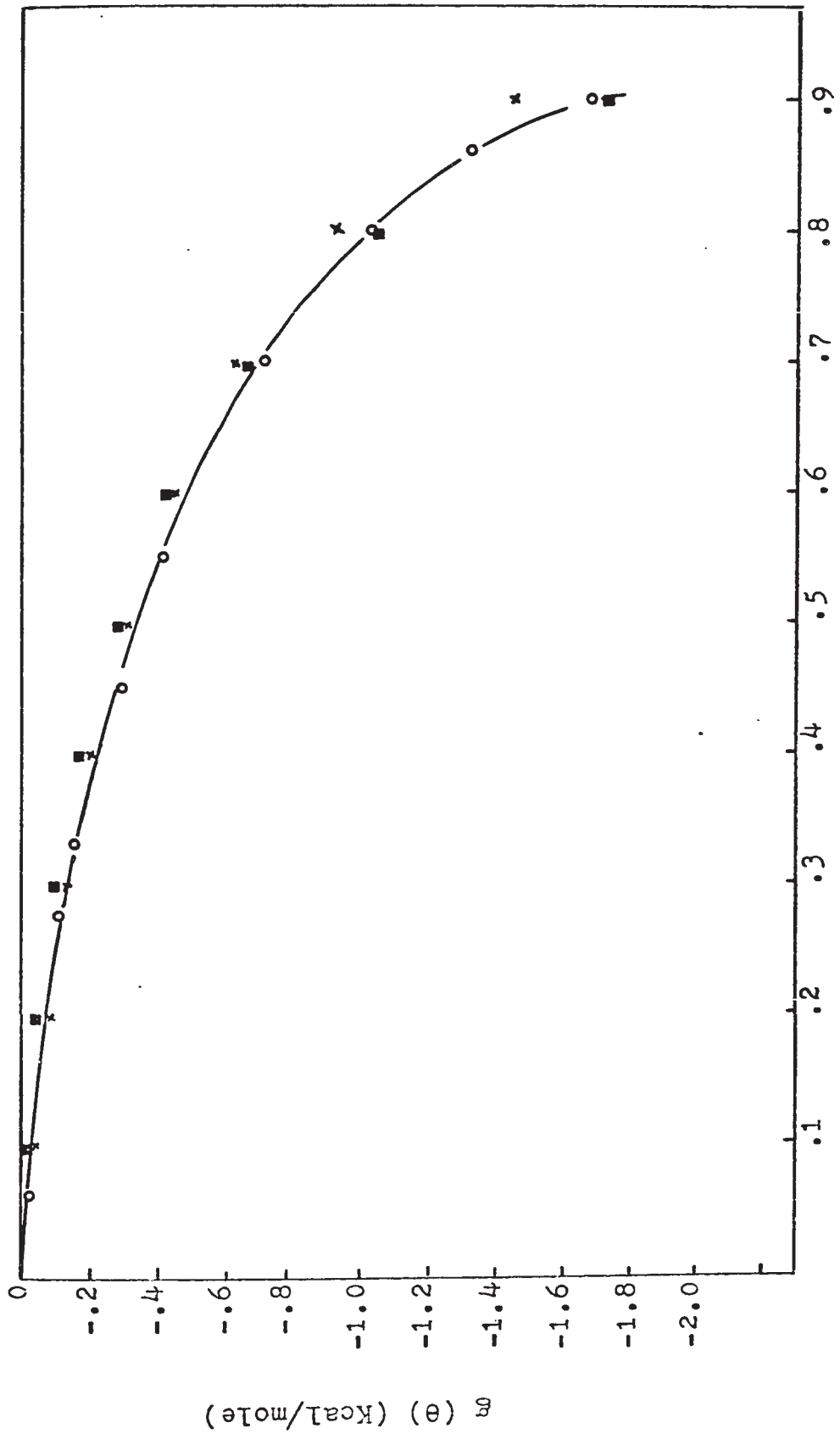

Fig. 20

Table 16

The experimental lateral interaction free energy-fractional coverage relation for dicarboxylic acids

θ	$g(\theta)$ cal/mole)
.060	- 24
.274	- 112
.330	- 166
.450	- 304
.550	- 421
.700	- 715
.800	-1029
.860	-1324
.900	-1681

acids, no particular model can be considered to represent the experimental results completely with any real certainty. Using different values ϵ , the dielectric constant, could change the models entirely. For example, if ϵ is taken as the dielectric constant of the second water layer at the electrode-solution interface (63), then the dielectric constant at intermediate coverages can be given as

$$\epsilon = (32-29.5\ \theta) \qquad \text{-------(62)}$$

Using this value and calculating μ_{dipole} as a function of coverage and comparing it to the experimental results reveals that the calculation for localized parallel dipoles agrees with experiment more satisfactorily (see Fig. 20).

Accordingly, the only conclusion that can be drawn is that dipole-dipole interaction is the main contribution to the lateral interaction free energy for the dicarboxylic acids. It should also be mentioned that the dielectric constant used for the pure dicarboxylic acids, about 2.5, is probably invalid since dimethyl succinate has a value of 5.2 at 20°C, which is most probably close to ϵ of the free acid. It should be noted, in addition, that the dipole moment has been treated in this calculation as a constant, while it might in all probability vary with coverage.

PART III

Results & Discussion of Group II Addition Agents

1) Results:

This group includes the thioacids, mercaptoacids, and thiols. The thioacids and mercaptoacetic acid of the mercaptoacids series exhibited a distinctly different phenomenon from most organic additives used in metal deposition, in that they caused a depolarization, i.e. a decrease in the cathode overpotential during electrodeposition of copper. S. C. Barnes (69) has reported that thio-compounds act as polarizers in neutral solution. Accordingly, the effect of the thioacids and mercaptoacids on the cathode overpotential were studied in standard solution with various concentrations of sulfuric acid. Thiols did not exhibit any depolarization effect; they caused high overpotential increments in every case. Therefore, these compounds were studied only in acidified standard solution, i.e., 0.5M $CuSO_4$ and 1.0M H_2SO_4.

In order to compare the results of additives in standard solution with various concentrations of H_2SO_4, the overpotential of the corresponding solution without additives was also measured. The results are given in Part I, (see page 36).

The Steady-State Overpotential Effect of Thioacids in Neutral 0.5M $CuSO_4$

In agreement with the results obtained by Barnes (69), thioacids caused an increase in cathode overpotential

in 0.5M $CuSO_4$ and 0.0M H_2SO_4 solution. Fig. 21 shows the overpotential increment as a function of additive concentration. In a manner similar to Group I additives, increasing the concentration of a thioacid increases the overpotential increment, and at a given concentration, increasing the hydrocarbon chain length of the molecule increases the overpotential increment. Numerical values are given in Table 17.

Steady-State Overpotential Effects of Mercaptoacids

In the case of mercaptoacids only mercaptoacetic acid showed depolarization behavior in the acidified solution. Mercaptopropionic and mercaptobutyric acids caused overpotential increments for all solutions, acidified or non-acidified. The overpotential at a given concentration of mercaptopropionic or mercaptobutyric acids was higher the greater the concentration of sulfuric acid, but the overpotential increment due to the additive was the same regardless of concentration of sulfuric acid. Numerical results are given in Table 18. Fig. 22 shows a plot of the overpotential increment as a function of additive concentration for mercaptoacetic acid in 0.5M $CuSO_4$ and 0.0M H_2SO_4, and also the average $\Delta\eta$ values for mercaptopropionic and mercaptobutyric acids. The numerical results for mercaptoacetic acid in 0.5M $CuSO_4$ are shown in Table 19. Here again, alternation behavior can be observed between the mercaptopropionic and mercaptobutyric acids, see Fig. 22. It may be noted that this agrees very

Figure 21

Overpotential increment as a function of additive concentration for copper deposition from .5M $CuSO_4$ & thioacids

($\Delta\eta$ vs. log c)

⊙ Thioacetic acid

⊡ Thiopropionic acid

⬡ Thiobutyric acid

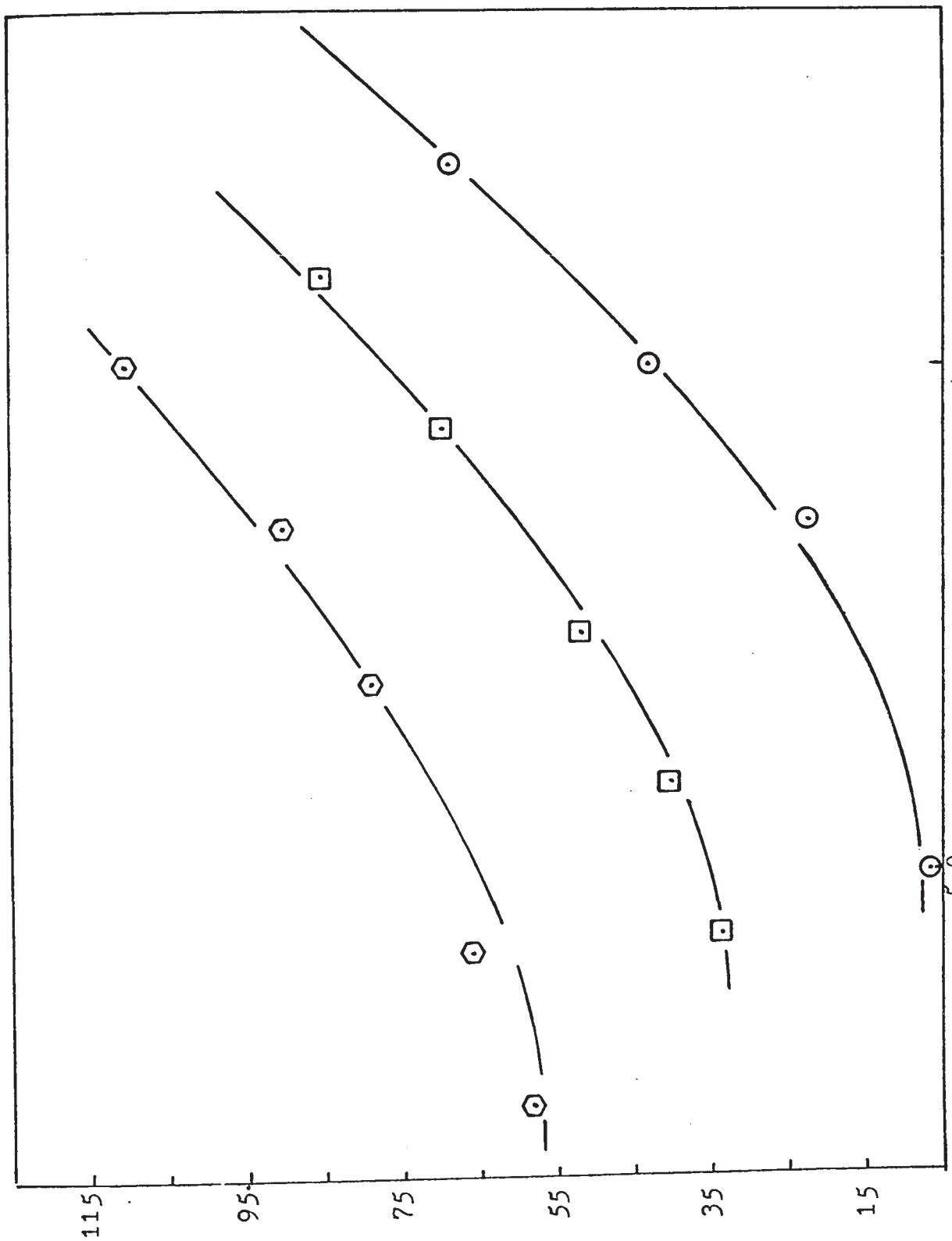

Fig. 21

Table 17

Overpotential as a function of additive concentration for copper deposition from 0.5M $CuSO_4$ standard solution

current density = 20 mA/cm^2

$T = 25^{\circ}$

(a) Thioacetic acid

Additive concentration (mole/l)	Overpotential (mV)	Overpotential Increment (mV)
$1x10^{-5}$	56	6
$5x10^{-5}$	72	22
$1x10^{-4}$	93	43
$2.5x10^{-4}$	119	69

(b) Thiopropionic acid

Additive concentration (mole/l)	Overpotential (mV)	Overpotential Increment (mV)
$7.5x10^{-6}$	84	34
$1.5x10^{-5}$	90	40
$3.0x10^{-5}$	100	50
$7.5x10^{-5}$	120	70
$1.5x10^{-4}$	134	84

(c) Thiobutyric acid

Additive concentration (mole/l)	Overpotential (mV)	Overpotential Increment (mV)
$3.5x10^{-6}$	108	58
$7.0x10^{-6}$	117	67
$2.4x10^{-5}$	129	79
$4.7x10^{-5}$	140	90
$1.0x10^{-4}$	160	110

Figure 22

Overpotential increment as a function of additive concentration for mercapto acids ($\Delta\eta$ vs. log c)

⊙ Mercaptoacetic acid

⊡ 3 - Mercaptopropionic acid

Δ 4 - Mercaptobutyric acid

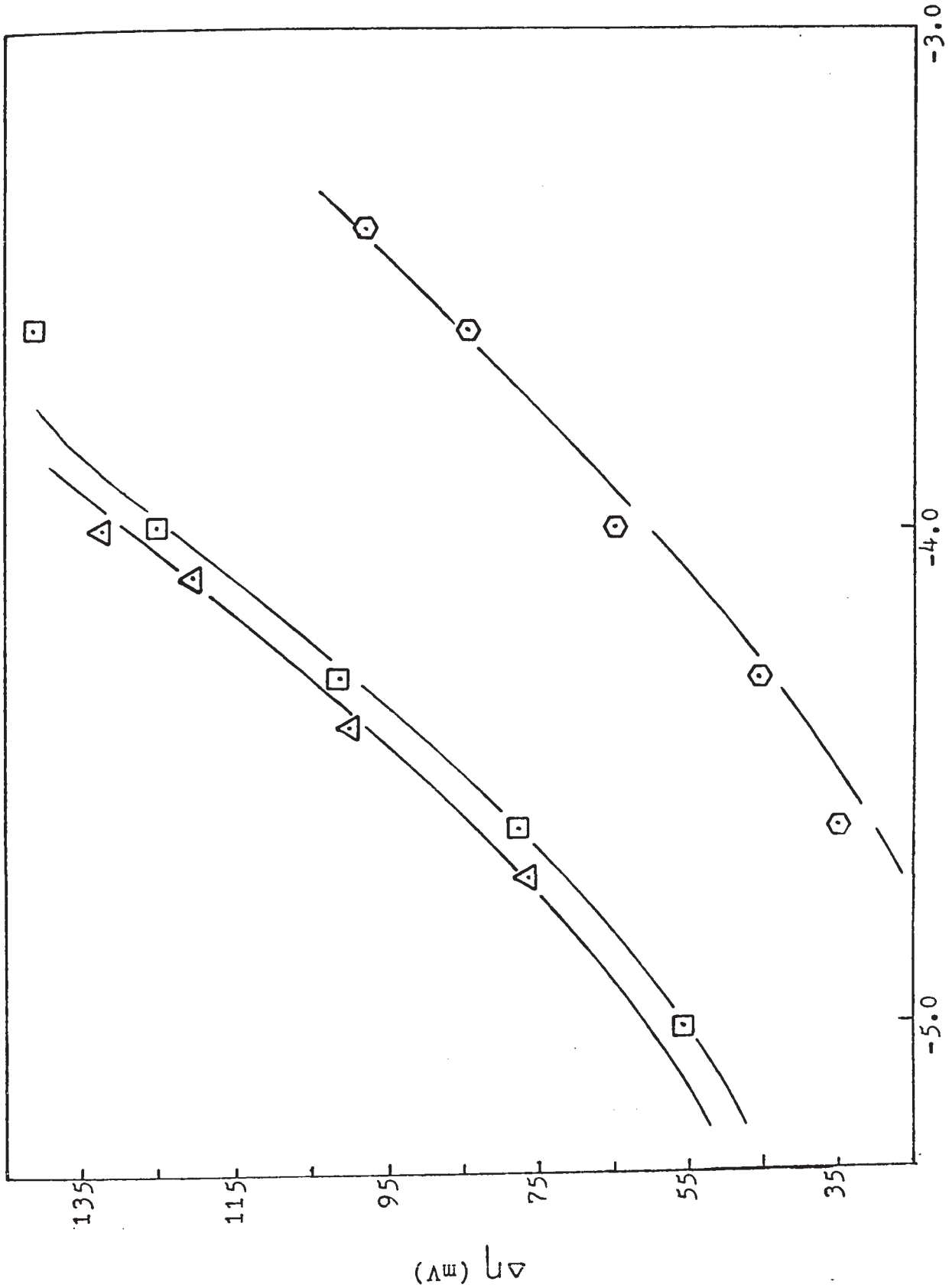

Fig. 22

Table 18

Overpotential as a function of additive concentration for copper deposition from 0.5M $CuSO_4$ and various concentrations of sulfuric acid

Current density = 20 mA/cm^2

(a) Mercaptopropionic acid

Additive concentration (mole/l)	Sulfuric acid concentration (mole/l)	Overpotential (mV)	Overpotential Increment (mV)	Average (mV)
$1x10^{-4}$	0.0	175	125	126.5
	0.1	215	127	
	0.5	220	124	
	1.0	230	130	
$8x10^{-5}$	0.0	157	107	114.5
	0.1	200	112	
	0.5	220	124	
	1.0	215	115	
$4x10^{-5}$	0.0	145	95	100.0
	1.0	206	106	
$2x10^{-5}$	1.0	180	80	80.0
$1x10^{-5}$	1.0	155	55	55.0

Table 18 (continued)

(b) 4 - Mercaptobutyric acid

Additive concentration (mole/l)	Sulfuric acid concentration (mole/l)	Overpotential (mV)	Overpotential Increment (mV)	Average (mV)
2.5×10^{-5}	0.0	128	78	79
	1.0	180.5	80.5	
5.0×10^{-5}	0.0	152	102	102
	1.0	202	102	
7.5×10^{-5}	0.0	154	104	112
	1.0	219	119	
1.0×10^{-4}	0.0	173	123	125
	1.0	227.5	127.5	
2.5×10^{-4}	0.0	192	142	142
	1.0	242	142	
5.0×10^{-4}	0.0	217	167	164
	1.0	262	162	

Table 19

Overpotential as a function of additive concentration for copper deposition from neutral 0.5M $CuSO_4$

Current density = 20 mA/cm^2

Mercaptoacetic acid

Additive concentration (mole/l)	Overpotential (mV)	Overpotential Increment (mV)
$2.5x20^{-5}$	85	35
$5.0x10^{-5}$	97	47
$1.0x10^{-4}$	116	66
$2.5x10^{-4}$	134	84
$4.0x10^{-4}$	148	98

well with the behavior of the dicarboxylic acids, where mercaptopropionic can be considered to correspond to propanedioic acid and mercaptobutyric to butanedioic acid.

A comparison of Fig. 21 & 22 shows that mercaptopropionic acid gave much higher overpotential increments than the corresponding thiopropionic acid, while mercaptobutyric acid gave values similar to the corresponding thiobutyric acid. A generalized order of effectiveness may be given - with some reservation - as follows: mercaptoacids with (ENCA) $\leq$ thioacids $<$ mercaptoacids with (ONCA). This agrees well with the results obtained previously for the mono- and dicarboxylic acids.

In general, for a given mercaptoacid the overpotential increases with increasing concentration, but a much smaller concentration was required to give the same overpotential increment compared to monocarboxylic and dicarboxylic acids.

Overpotential Effects of the Thiols

As mentioned previously, thiol compounds caused only increases in cathode overpotential. Accordingly, these compounds were studied only in 0.5M $CuSO_4$ and 1.0N H_2SO_4 standard solution. An important experimental point that should be mentioned is that choosing high concentrations of sulfuric acid is most appropriate because in high conductivity solution the IR drop between the Luggin probe and cathode can be neglected. In all

the previous measurements where the standard solution was free from sulfuric acid, some difficulty was encountered in determining the true cathode overpotential. In these cases oscillographic measurement was made to determine the value of the IR drop which was found to be in the range of 5-15 mV. The total steady-state overpotential was corrected by subtracting the corresponding IR drop. In the case of standard solution containing thiols as additive the measured value of the IR drop was small enough to be neglected. Therefore, the values reported are the total steady-state overpotentials. Another necessary precaution was the use of an anode with large surface area to avoid any possible oxidation of the thiol compounds. This was achieved by using a copper rod coiled in a spiral. Fig. 23 shows the overpotential increment as a function of thiol concentration. As shown in this figure, increasing the thiol concentration or increasing the hydrocarbon chain length of a thiol increases the overpotential increment. This follows the same pattern as found previously for carboxylic acids. The numerical values are given in Table 20.

The Depolarization Effect of Thioacids

In the case of thioacetic, thiopropionic, and thiobutyric acids in standard solution with various concentrations of sulfuric acid, a lower overpotential was obtained than in the absence of the additive. The steady-state overpotentials are shown as a function of additive

Figure 23

Overpotential increment as a function of additive concentration for thiols ($\Delta\eta$ vs. log C)

● Ethanethiol

⬢ Propanethiol

■ Butanethiol

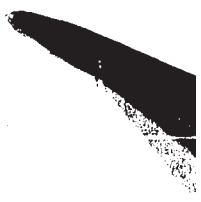

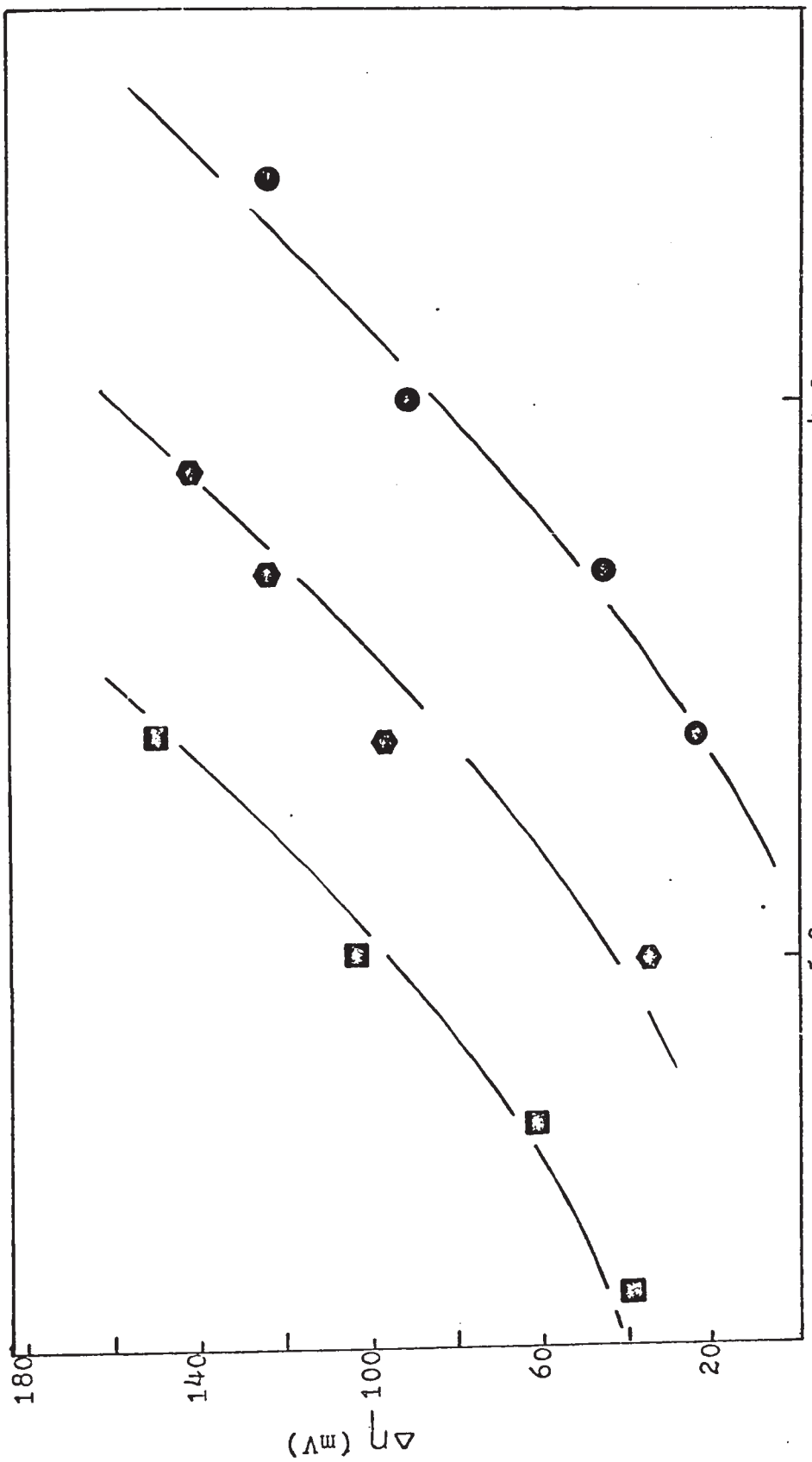

Fig. 23

Table 20

Overpotential as a function of additive concentration for thiols

Current density = 20 mA/cm^2

(a) Ethanethiol

Additive concentration (mole/l)	Overpotential Increment (mV)
2.5×10^{-5}	24
5.0×10^{-5}	47
1.0×10^{-4}	92
2.5×10^{-4}	124

(b) Propanethiol

Additive concentration (mole/l)	Overpotential Increment (mV)
1.0×10^{-5}	36
2.5×10^{-5}	98
5.0×10^{-5}	124
7.6×10^{-5}	144

(c) Butanethiol

Additive concentration (mole/l)	Overpotential Increment (mV)
2.5×10^{-6}	40
5.0×10^{-6}	64
1.0×10^{-5}	104
2.5×10^{-5}	150

concentration at a given sulfuric acid concentration in Table 21. From these data, the following observations can be made: 1) at a given concentration of sulfuric acid, an increase in the additive concentration increases the depolarization effect, and 2) at a given additive and sulfuric acid concentration, increasing the size of the hydrocarbon chain of the thioacid molecule increases the depolarization slightly.

The Overpotential-Current Density Relation for Thioacids

The steady-state overpotential of thioacids was measured as a function of current density. Typical plots are shown in Fig. 24. The numerical values are tabulated in Table 22, including the calculated values of the Tafel slope. Clearly, the Tafel slope decreases on increasing the concentration of sulfuric acid, or on increasing the concentration of the additives. The Tafel slopes are much less than the 50 mV theoretical value for the charge-transfer rate-controlling step. Therefore, it can be assumed that these additives cause a change in the kinetics of the copper deposition mechanism.

Initial Overpotential with Thioacids

A peculiar phenomenon was observed at the beginning of each electrolysis and before attaining the steady-state overpotential value. When the current was first switched on, a maximum overpotential was initially obtained during the first 15 to 30 seconds, following which the overpotential gradually decreased to the steady-

Table 21

Steady-state overpotential as a function of additive concentration for copper deposition from 0.5M $CuSO_4$ and various sulfuric acid concentrations

Current density = 20 mA/cm^2

(a) Thioacetic acid

Additive concentration (mole/l)	Sulfuric acid concentration (mole/l) 0.1 η(mV)	0.25 η(mV)	0.5 η(mV)	0.75 η(mV)	1.0 η(mV)
$2.5x10^{-4}$	69	49	45	40	37
$1.0x10^{-4}$	73	52	51	47	46
$5.0x10^{-5}$	75	55	53	48	47
$1.0x10^{-5}$	79	59	55	51	48

(b) Thiopropionic acid

Additive concentration (mole/l)	Sulfuric acid concentration (mole/l) 0.1 η(mV)	0.25 η(mV)	0.5 η(mV)	0.75 η(mV)	1.0 η(mV)
$1.5x10^{-4}$	69	46	34	38	38
$7.5x10^{-5}$	71	48	44	42	40
$3.0x10^{-5}$	76	54	50	45	43
$1.5x10^{-5}$	78	57	50	47	45
$7.5x10^{-6}$	80	65	57	52	49

Table 21 (continued)

(c) Thiobutyric acid

Additive concentration (mole/l)	Sulfuric acid concentration (mole/l) 0.1 η(mV)	0.5 η(mV)	1.0 η(mV)
5.0×10^{-5}	69	39	37
2.5×10^{-5}	70	48	40
1.0×10^{-5}	72	50	45
7.5×10^{-6}	73	51	47
2.5×10^{-6}	74	53	49

Figure 24

Overpotential-current density relation (η vs. ln i) for thioacids

1 1.0×10^{-5}M thioacetic acid, 0.1M H_2SO_4

2 " , 0.25M H_2SO_4

3 " , 0.5M H_2SO_4

4 " , 0.75M H_2SO_4

5 " , 1.0M H_2SO_4

6 1.0×10^{-5}M thiopropionic acid, 0.1M H_2SO_4

7 " , 0.75M H_2SO_4

8 " , 0.5M H_2SO_4

9 " , 0.75M H_2SO_4

10 " , 1.0M H_2SO_4

11 5.0×10^{-5}M thiobutyric acid, 0.1M H_2SO_4

12 " , 0.5M H_2SO_4

13 " , 1.0M H_2SO_4

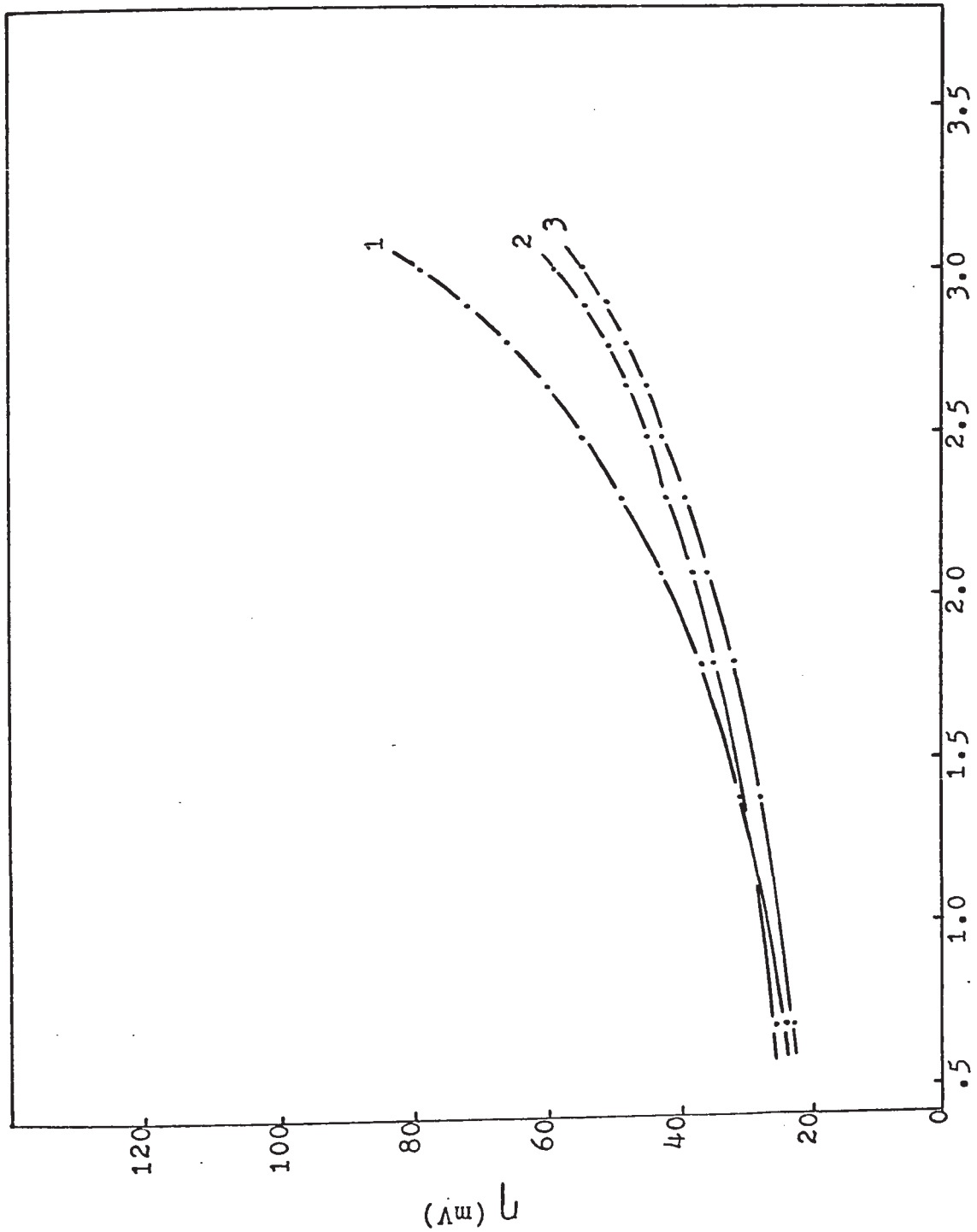

Fig. 24

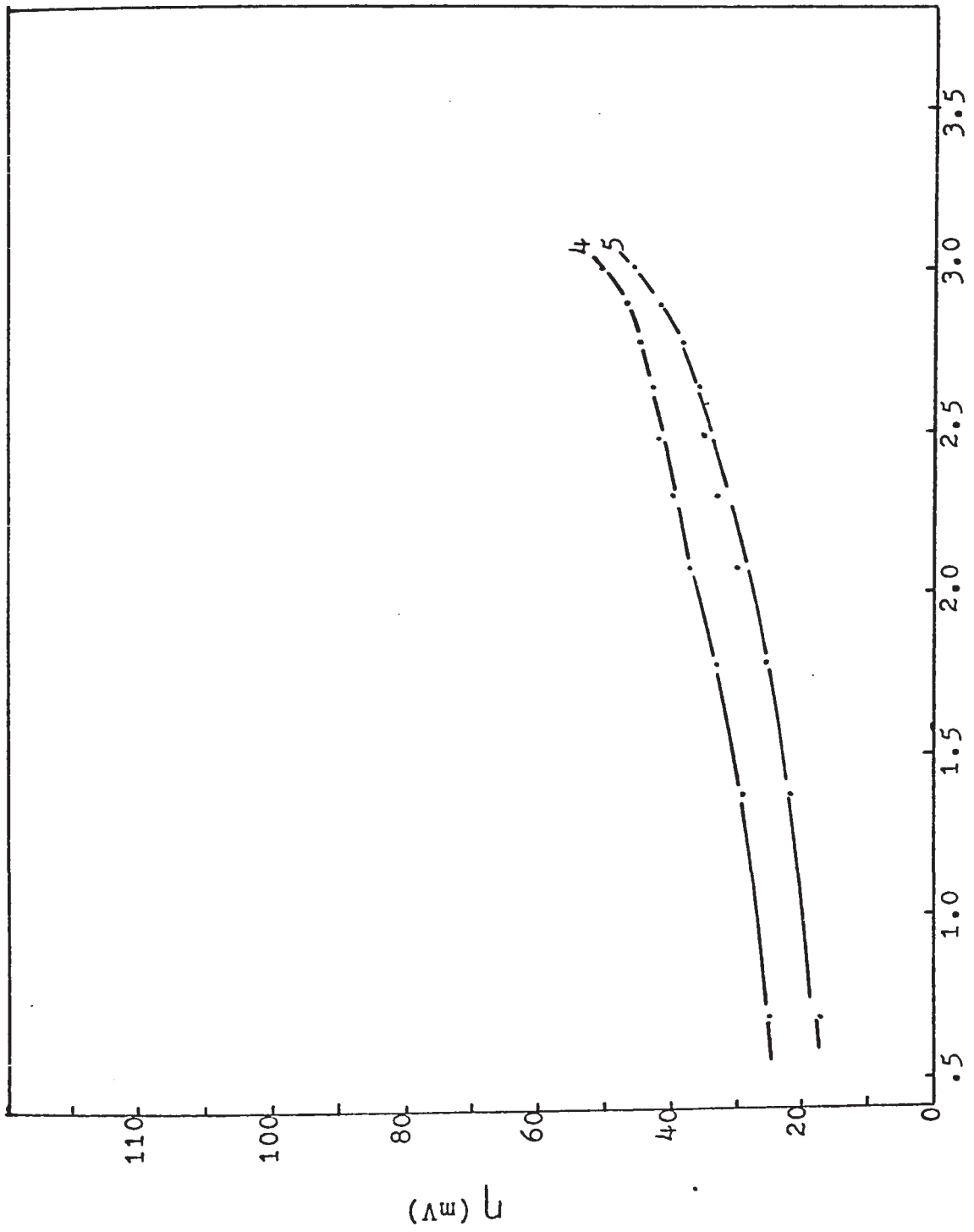

Fig. 24

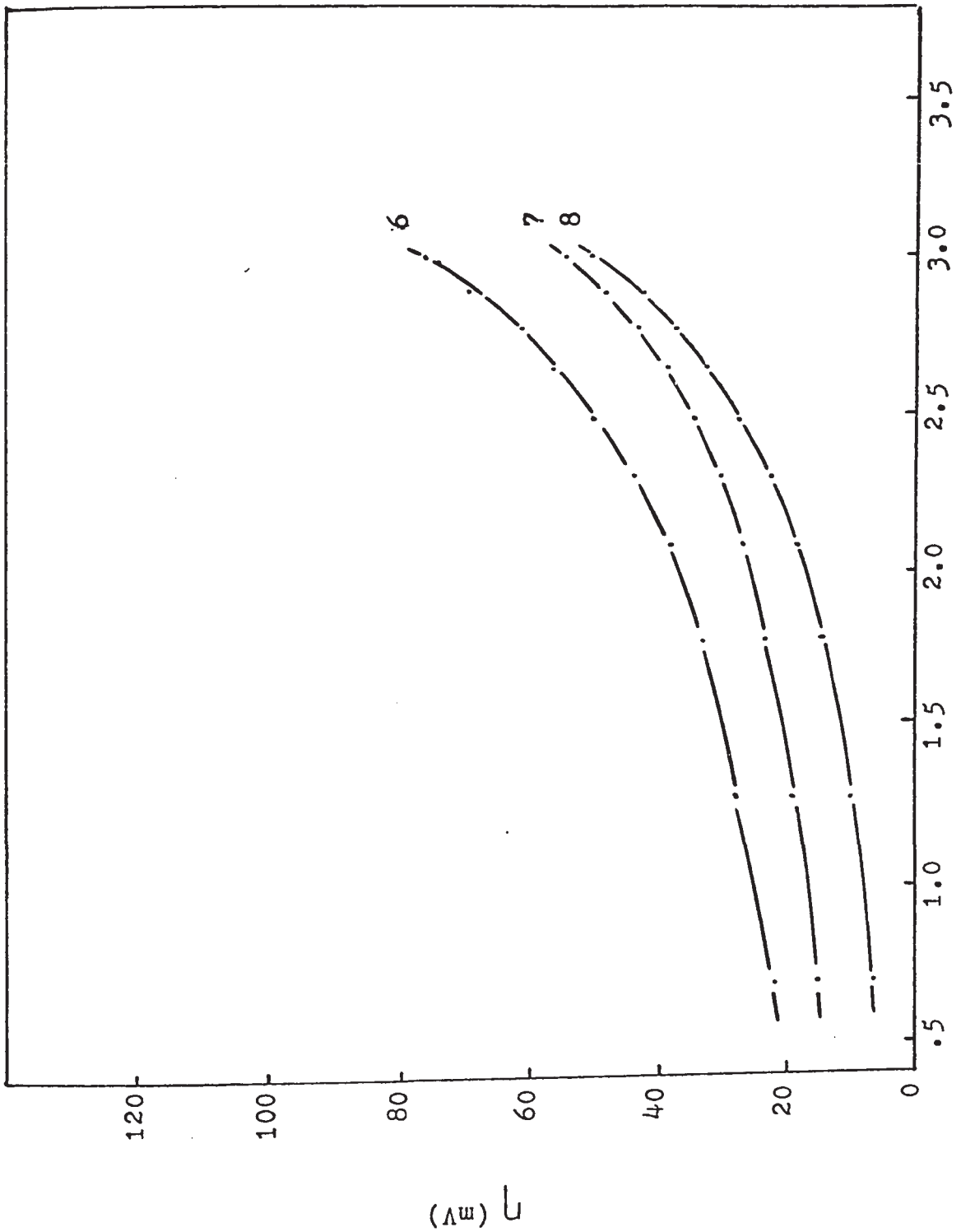

Fig. 24

Fig. 24

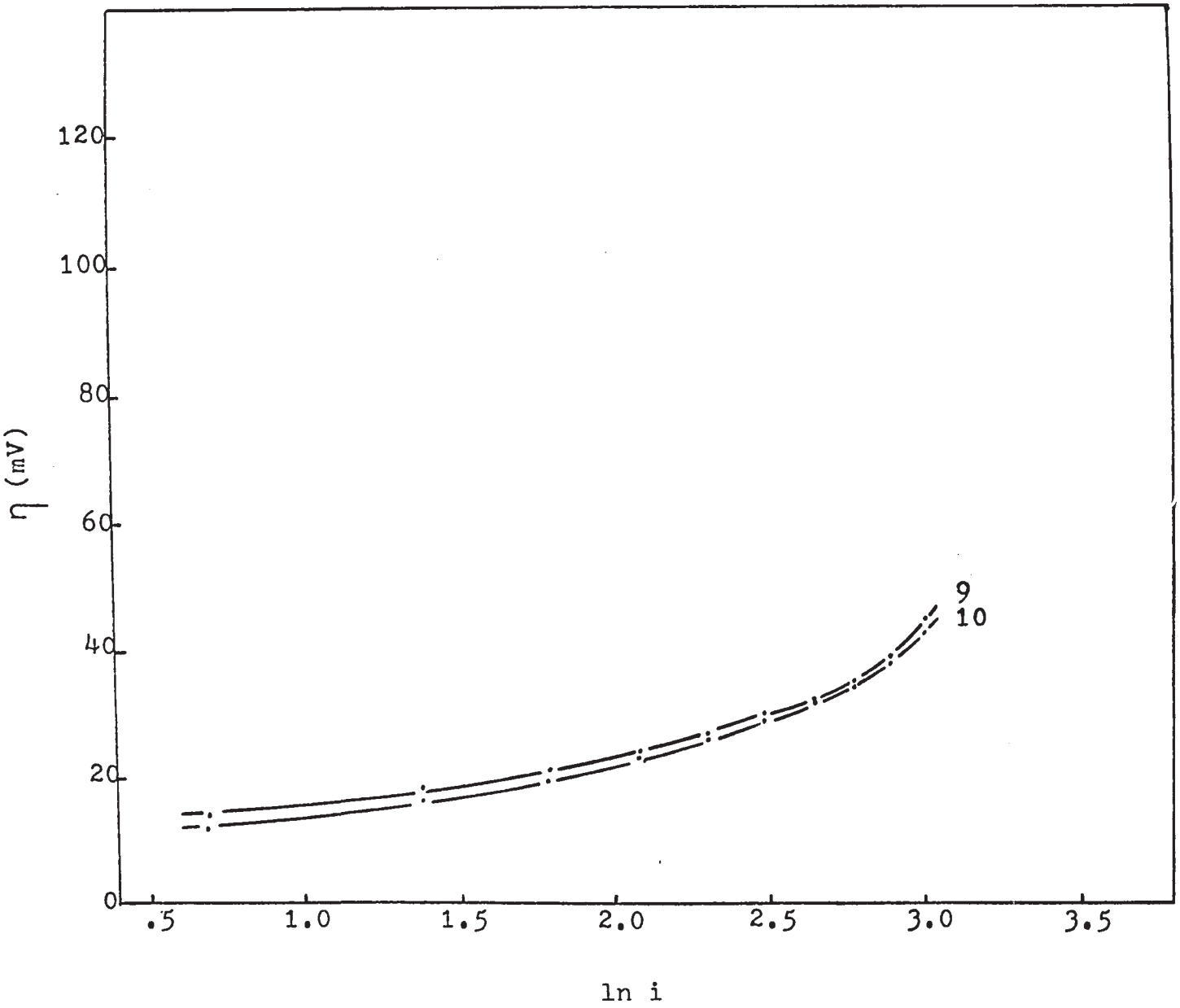

Fig. 24

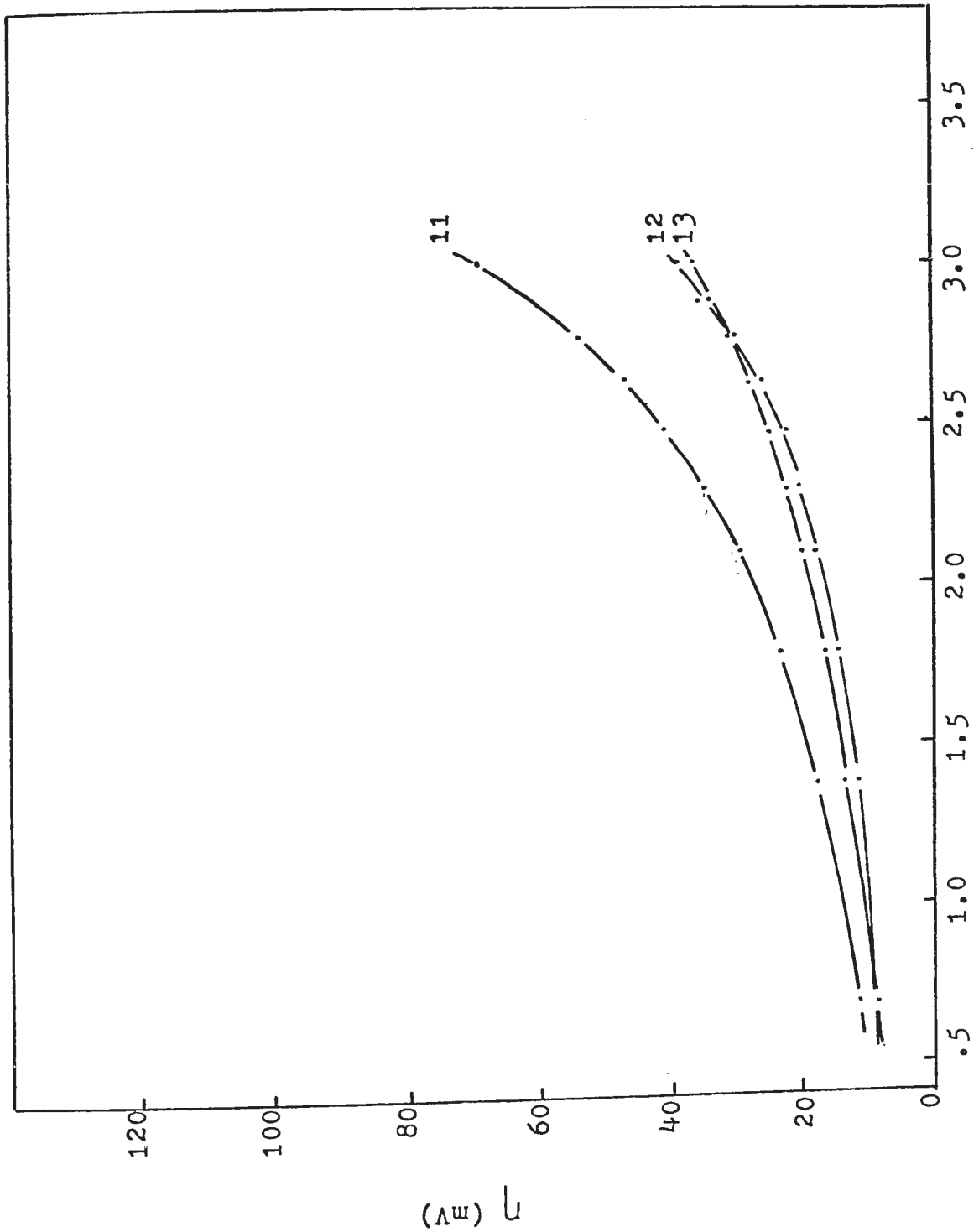

Table 22

Overpotential as a function of current density for copper deposition from 0.5M $CuSO_4$ and various sulfuric acid concentrations

(a) Thioacetic acid

Additive concentration (mole/l)	H_2SO_4 (mole/l)	Current density mA/cm^2 20	18	16	14	12	10	8	6	4	2	Tafel Slope (mV)	i_o(mA)
$2.5x10^{-4}$	.25	49	45.5	39	35	31	27	24	21	17	13	44	6.55
	.50	45	41	35	31	25	24	21	17	14	11	39	7.02
	.75	40	35	31	27	24	21	17	14	11	7	37	7.39
	1.0	37	32	28	24	21	16	13	10	6	2	32	7.69
$1.0x10^{-4}$	.1	73	65	59	52	46	40	35	29	23	17	52	6.55
	.25	52	46	42	38	34	30	26	22	18	14	46	6.55
	.5	51	47	41	36	32	29	25	20	15	10	42	6.82
	1.0	46	44	40	38	36.5	35	33	31	29	27	15	-
$5.0x10^{-5}$	.1	75	60	53	46	42	36	31	25	20	14	51	6.05
	.25	55	50	44	39	35	31	27	24	19.5	14.5	48	6.36
	.5	53	50	44	39	35	31	27	23	19	14	48	6.55
	.75	48	42.5	39.5	37	34.5	32	28	25	21	17	42	6.55
	1.0	47	42	39	36	34	31	28	24	20	15	41	6.68

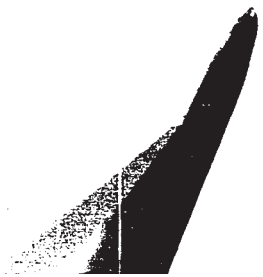

Table 22 (continued)

(a) Thioacetic acid

Additive concentration (mole/l)	H_2SO_4 (mole/l)	Current density mA/cm^2 20	18	16	14	12	10	8	6	4	2	Tafel Slope (mV)	i_o(mA)
$1.0x10^{-5}$	.1	79	72	66	60	55	49	43	37	31	24	56	5.47
	.25	59	54	51	48	45	42	38	35	31	26	43	5.69
	.5	55	51	48	45	43	39	36	32	28	23	39	5.87
	.75	51	47	45	43	42	40	37	33	29	25	35	5.93
	1.0	48	42	38	36	35	33	30	25	22	17	35	6.29

(b) Thiopropionic acid

$1.5x10^{-4}$	.1	69	62	55	49	43	37	32	27	21	15	54	4.95
	.25	46	39	37	34	31	28	25	22	19	15	41	6.42
	.5	34	30	28	26	24	22	20	18.5	17	16	32	7.10
	.75	38	35	32	28	25	23	20	18	15	13	28	-
	1.0	38	36	32	28	25	23	20	18	14	12	28	-
$7.5x10^{-5}$	.1	71	64	57	50	44	38	33	27	22	15	57	5.69
	.25	48	44	39	34	30	27	24	20	17	14	35	5.93
	.5	44	40	36	33	30	28	26	24	20	19	36	6.05
	.75	42	37	33	29	25	22	20	17	14	10	35	6.29
	1.0	40	36	30	26	22	19	16	13	10	7	31	6.68

Table 22 (continued)

(b) Thiopropionic acid

Additive concentration (mole/l)	H_2SO_4 (mole/l)	Current density mA/cm^2 20	18	16	14	12	10	8	6	4	2	Tafel Slope (mV)	i_o(mA)
3.0×10^{-5}	.1	76	69	62	56	50	44	38	33	28	22	54	4.95
	.25	54	48	43	38	34	30	26.5	23	19	15	41	5.93
	.5	50	42	37	32	27	22	18	14	10	6	41	6.68
	.75	45	39	35	32	30	27	24	21	18.5	14	40	7.10
	1.0	43	38	34	32	29	26	23	19	16	12	37	9.02
1.5×10^{-5}	.1	78	71	64	58	52	48	42	38	32	28	54	4.76
	.25	57	51	46	52	38	35	31	28	23	20	41	5.47
	.5	50	45	42	38	36	33	30	26	22	20	37	5.47
	.75	47	44	40	36	33	30	26	22	19	14	35	5.58
	1.0	45	42	40	37	34	31	28	26	22	18	33	5.93
7.5×10^{-6}	.1	80	74	67	60	54	48	42	37	31	25	54	4.71
	.25	65	58	52	48	43	39	35	30	26	20	49	5.15
	.5	57	52	47	44	40	37	34	31	27	23	42	5.31
	.75	52	47	43	40	37	34	30	27	23	18	40	5.47
	1.0	49	45	43	40	38	35	32	29	25	21	37.3	5.69

Table 22 (continued)

(c) Thiobutyric acid

Additive concentration (mole/l)	H_2SO_4 (mole/l)	Current density mA/cm^2 20	18	16	14	12	10	8	6	4	2	Tafel Slope (mV)	i_o (mA
5.0×10^{-5}	.1	69	61	54	47	41	35	29	23	17	11	54	5.69
	.5	39	36	30	26	22	20	17	14	11	8	39	7.31
	1.0	37	34	31	28	25	22	20	16	13	8	27	7.31
2.5×10^{-5}	.1	70	63	56	51	45	40	34	28	22	16	51	5.31
	.5	48	43	39	34	31	27	22	19	14	9	38	5.93
	1.0	40	36	33	30	28	25	21	18	15	10	33	6.42
7.5×10^{-6}	.1	73	64	57	51	45	39	33	27	21	15	54	5.15
	.5	51	46	40	36	32	28	25	21	17	12	44	6.29
	1.0	47	42	35	30	26	23	20	14	11	7	41	7.10
2.5×10^{-6}	.1	74	68	62	56	49	42	35	28	21	13	49	4.34
	.5	53	46	41	37	34	30	26	23	18	13	43	5.93
	1.0	49	42	38	35	32	28	25	22	18	13	38	6.29

state value. A similar behavior has been reported by Bockris (10) for the case of surface-diffusion as the rate-controlling step in copper electrodeposition. Bockris called this initial maximum overpotential a super-polarization. A similar initial maximum has been reported by others (69,70,71) for depolarizing additives. Typical initial overpotential maxima are shown in Fig. 25, and numerical data are given in Table 23. It is seen that at a given sulfuric acid concentration, an increase in the additive concentration increases the overpotential maximum. Similarly, at a given additive concentration, increasing the sulfuric acid concentration increases the initial maximum slightly. The time at which the overpotential maximum was attained is shown as τ_{max}. This value was between 20-30 seconds at 20 mA/cm^2 current density.

Initial Overpotential-Current Density Relation

The initial overpotential was determined as a function of current density. A special procedure was employed in all these experiments in that the cathode was first immersed for 5 minutes before electrolysis was started. For each current density from 20 mA/cm^2 to 4 mA/cm^2, a new cathode was used. The results are shown in Table 23. This indicates that the value of $\tau_{max.}$ increases with decreasing current density, while the initial overpotential decreases with decreasing current density. A plot of the initial over-

Figure 25

Initial maximum overpotential

Overpotential-time relation (η vs. t) for thioacids

1 5.0×10^{-5} M thioacetic acid, .75M H_2SO_4

2 5.0×10^{-5} M thioacetic acid, .25M H_2SO_4

3 7.5×10^{-6} M thiopropionic acid, .75M H_2SO_4

4 7.5×10^{-6} M thiopropionic acid, .25M H_2SO_4

5 2.5×10^{-5} M thiobutyric acid, 1.0M H_2SO_4

6 2.5×10^{-5} M thiobutyric acid, .5M H_2SO_4

Fig. 25

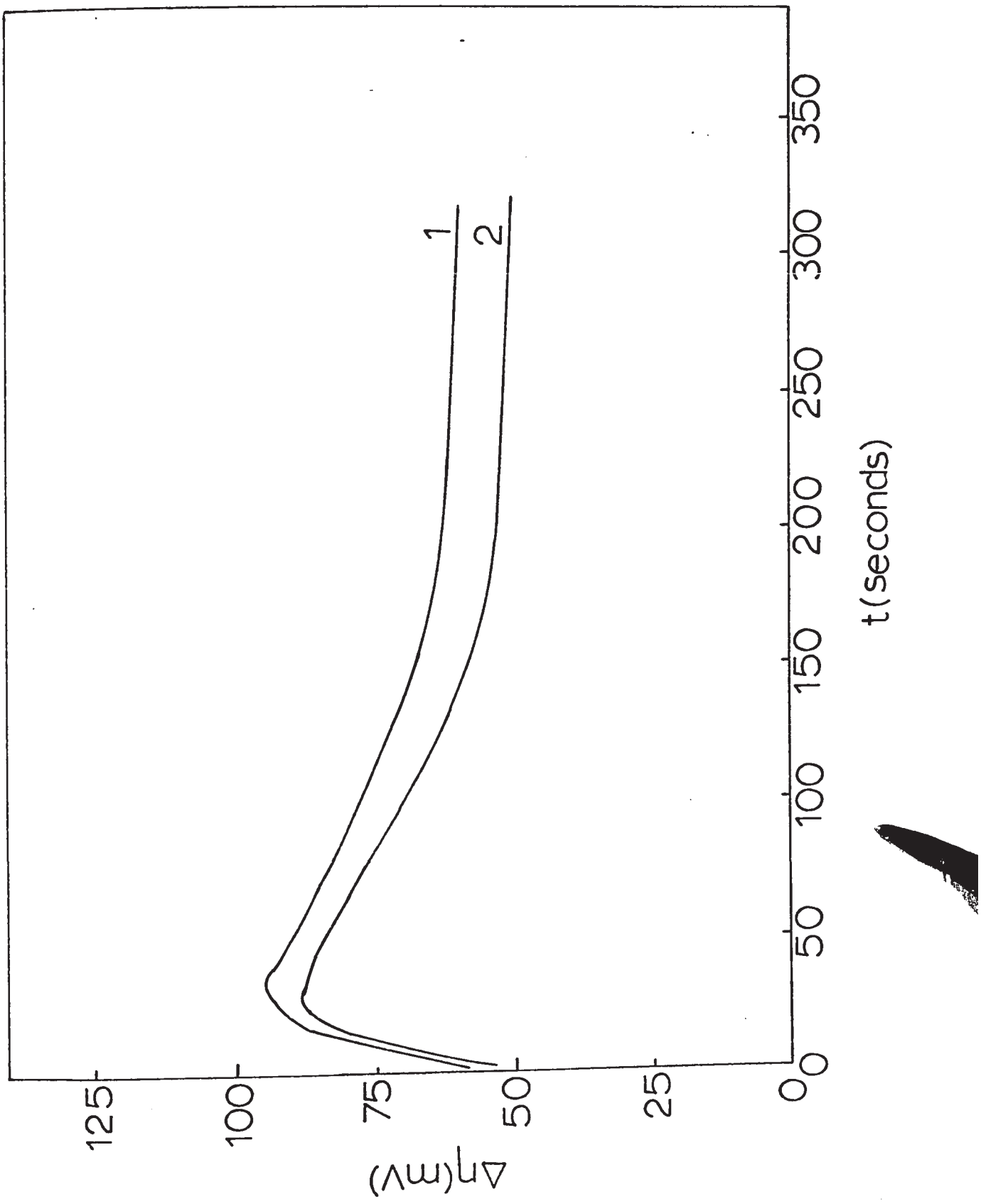

Fig. 25

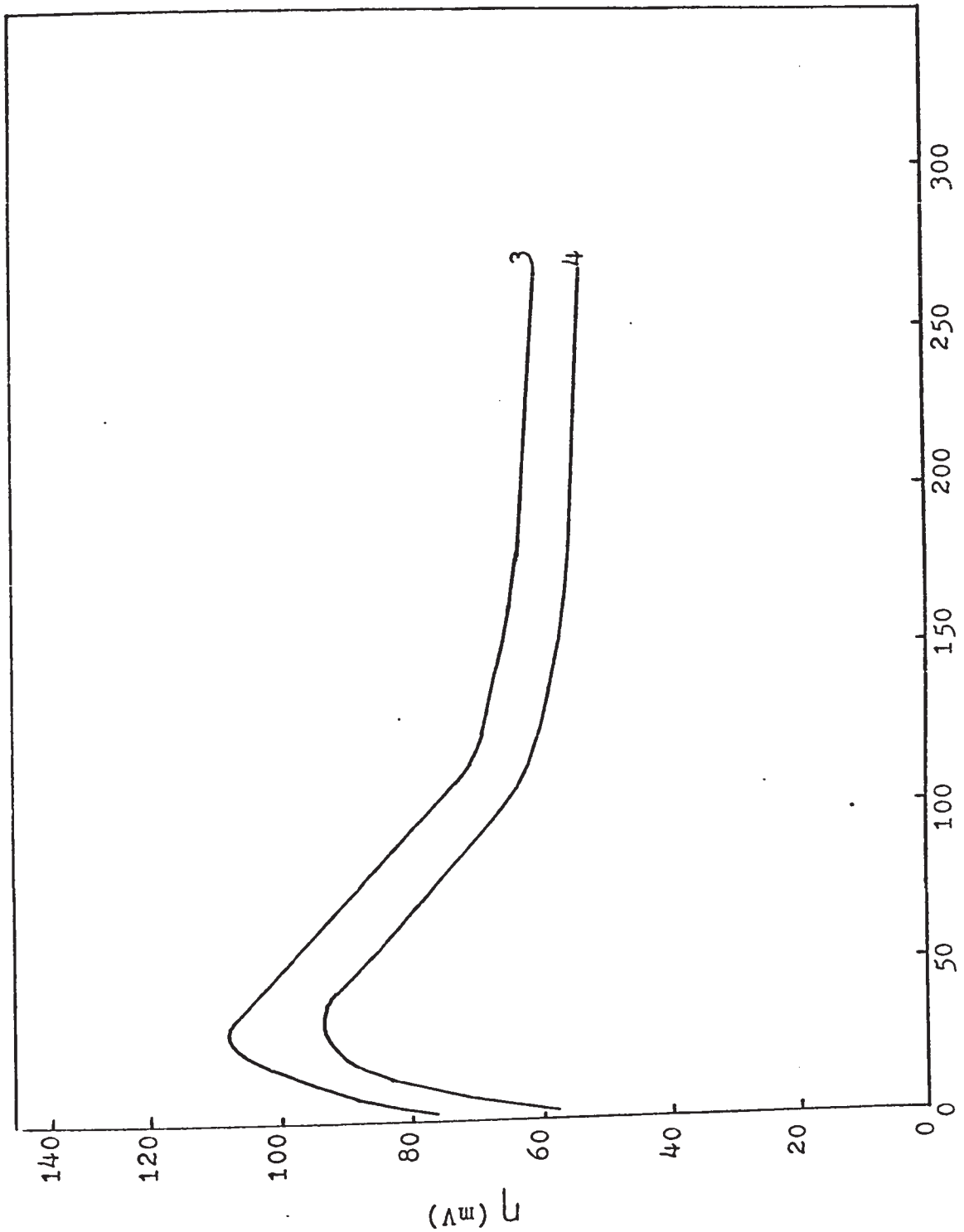

Fig. 25

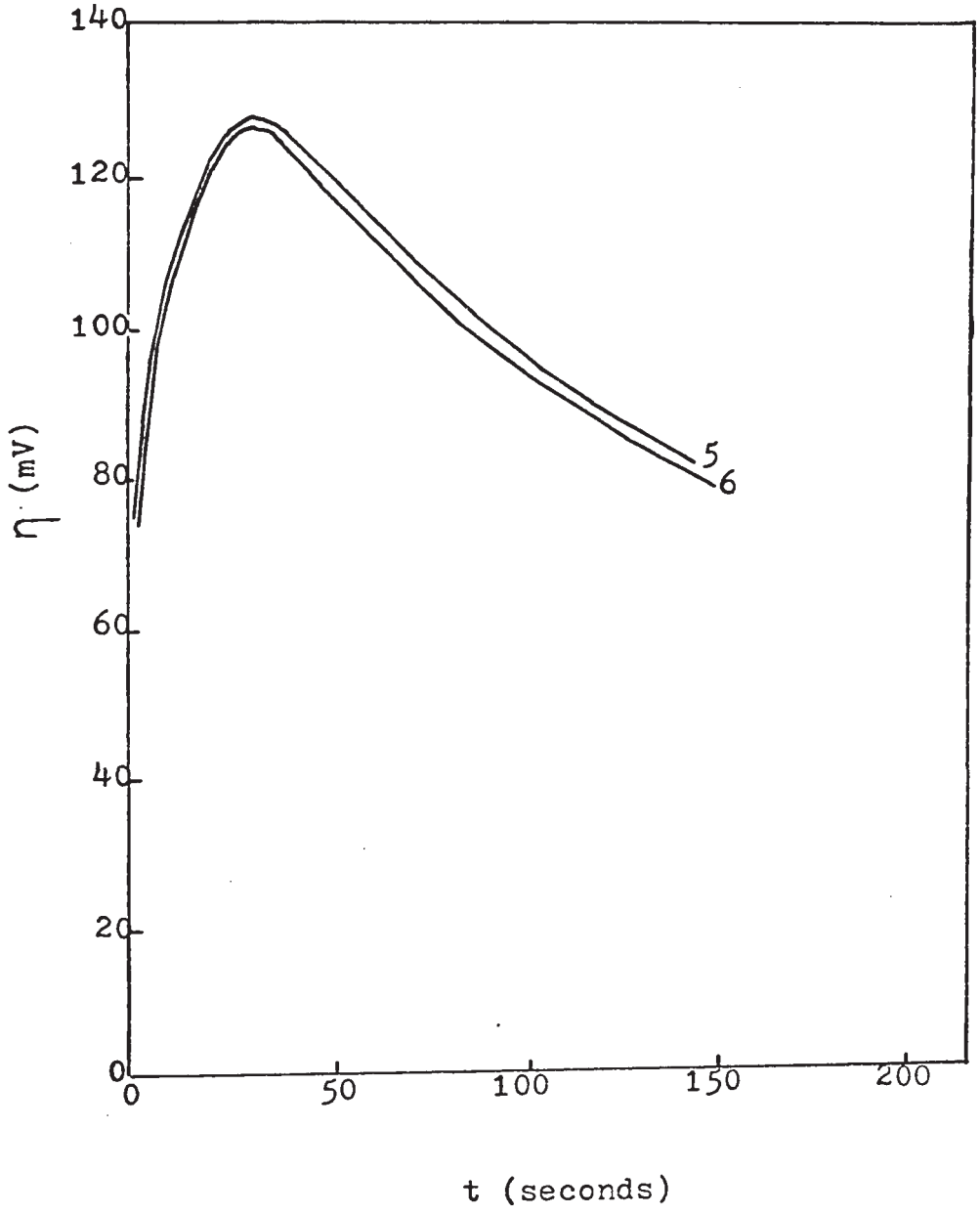

Table 23

Initial overpotential-current density relation for copper deposition from standard solution containing thioacids as additives

(a) 0.5M $CuSO_4$, 0.5M H_2SO_4, 2.5×10^{-5}M thiobutyric acid

Current density (mA/cm^2)	Initial max. Overpotential (mV)	$\tau_{max.}$ (sec.)
20	125	27
14	95	32
10	58	45
6	47	84

(b) 0.5M $CuSO_4$, 1.0M H_2SO_4, 2.5×10^{-5}M thiobutyric acid

20	127	30
14	81	33
10	62	46
6	45	92

(c) 0.5M $CuSO_4$, 1.0M H_2SO_4, 7.5×10^{-6}M thiobutyric acid

20	105	30
16	100	37.5
12	95	42
8	59	67.5
6	51	94
4	41	140

(d) 0.5M $CuSO_4$, 0.5M H_2SO_4, 7.5×10^{-6}M thiobutyric acid

20	100	27
16	99	32
12	75	39
8	64.5	48
6	48.5	94
4	28.5	129

potential as a function of current density is shown in Fig. 26. The Tafel slope was found to be about 54 mV.

Initial Overpotential-Immersion Time Relation

The cathode was immersed for 5 minutes before starting the electrolysis for all the experiments with Group II compounds. Here, the cathode was immersed for different periods of time from 5 to 45 minutes before electrolysis to determine the initial overpotential as a function of the immersion time. This relation is shown in Fig. 27. The numerical values are given in Table 24. Clearly, increasing the time of immersion prior to electrolysis increases the initial overpotential and also increases slightly the value of $\tau_{max.}$. A few experiments were made in which the cathode was immersed for 18 hours and the initial overpotential was much higher than that for which the electrode was immersed for only 5 minutes. Numerical values are given in Table 25.

Depolarization Effect of Mercaptoacetic Acid

The depolarization effect of mercaptoacetic acid (thioglycolic acid), has been reported previously (69,71). In agreement with these results, mercaptoacetic acid caused a depolarization in acidified standard solution. The amount of depolarization increases with the additive and sulfuric acid concentrations. The relation between these variables follows the same pattern as for the thioacids. Numerical values are given in Table 26. It should be noted that the depolarizing ability of mercaptoacetic acid is considerably

Figure 26

Initial maximum overpotential-current density relation for thiobutyric acid

1 7.5×10^{-6} thiobutyric acid, 1.0M H_2

2 7.5×10^{-6} thiobutyric acid, 0.5M H_2SO_4

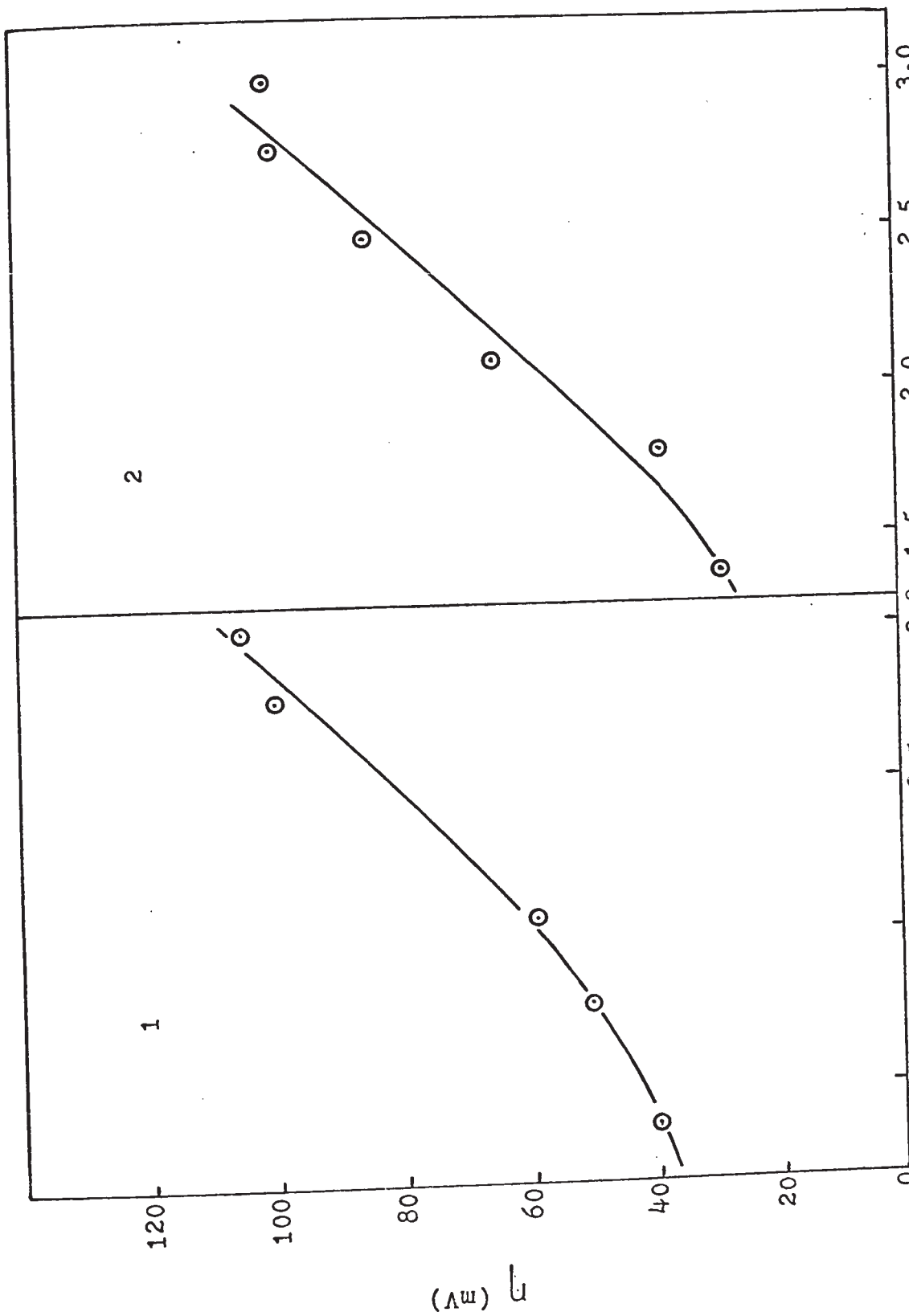

Fig. 26

Figure 27

Initial maximum overpotential as a function of immersion time (η vs. $t^{\frac{1}{2}}$) for thiobutyric acid

1 2.5×10^{-6} thiobutyric acid, 1.0M H_2SO_4

2 2.5×10^{-6} thiobutyric acid, 0.5M H_2SO_4

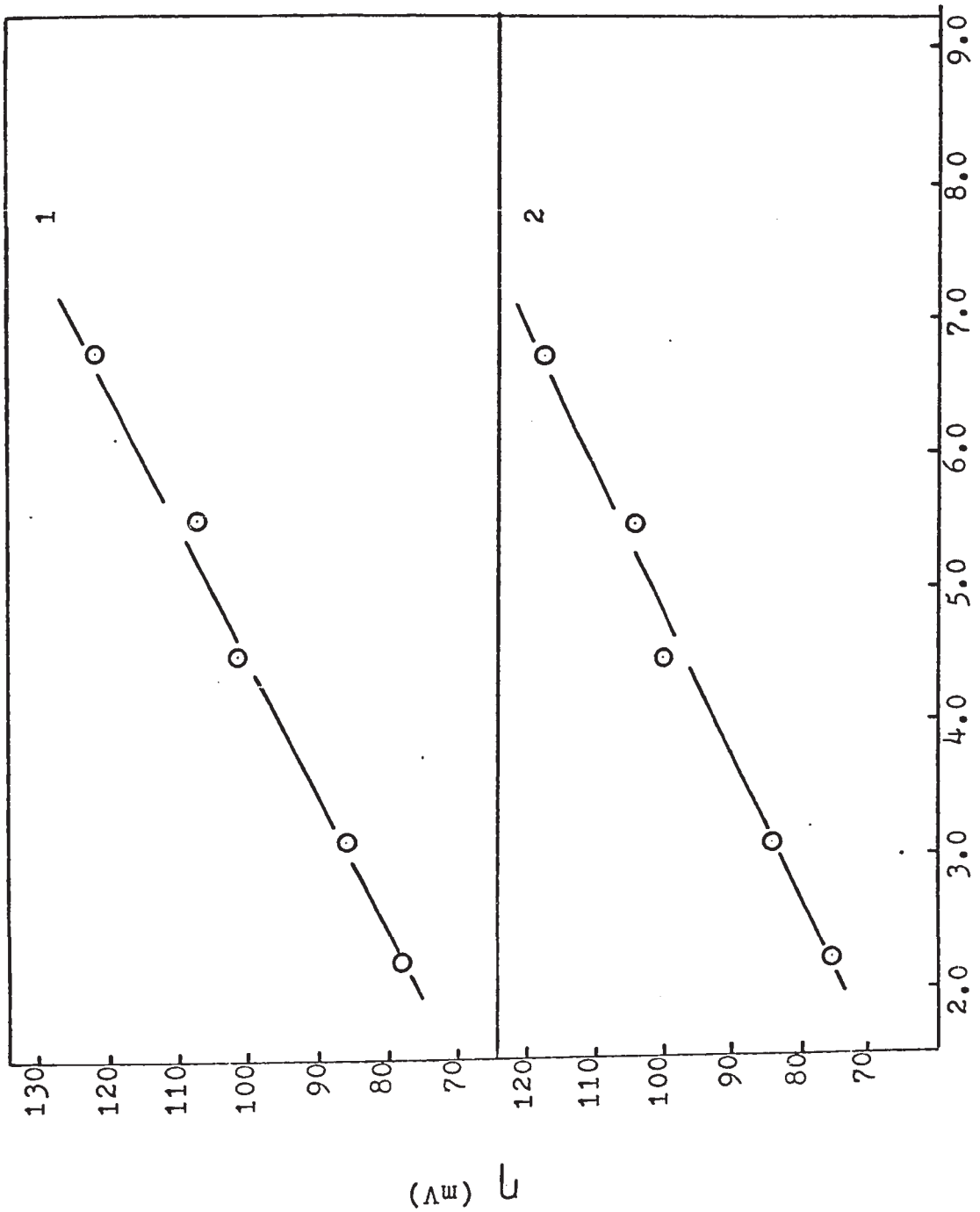

Fig. 27

Table 24

Initial overpotential as a function of immersion time for copper deposition from standard solution containing thioacids as additives

Current density = 20 mA/cm^2

(a) 0.5M $CuSO_4$, 0.5M H_2SO_4, 7.5×10^{-6}M thiobutyric acid

Time of immersion (minutes)	Initial max. overpotential (mV)	$\tau_{max.}$ (sec.)
10	89	40
20	99	42
30	109	30
45	110	42

(b) 0.5M $CuSO_4$, 1.0M H_2SO_4, 7.5×10^{-6}M thiobutyric acid

10	97	49
20	102	49
30	103	45
45	105	42

(c) 0.5M $CuSO_4$, 0.5M H_2SO_4, 2.5×10^{-6}M thiobutyric acid

5	75	30
10	84	42
20	101	45
30	103	36
45	47	45

(d) 0.5M $CuSO_4$, 1.0M H_2SO_4, 2.5×10^{-6}M thiobutyric acid

5	78	30
10	86	45
20	102	45
30	108	52
45	123	45

Table 25

Initial overpotential-immersion time relation for copper deposition

Current density = 20 mA/cm^2

0.5M $CuSO_4$, 0.1N H_2SO_4, 2.5×10^{-6}M thiobutyric acid

Time of immersion (min.)	Initial max. polarization (mV)	$\tau_{max.}$ (sec.)	η_{steady} (mV)
5	85	33	80
1080	205	30	76

Table 26

Steady-state overpotential as a function of additive concentration for copper deposition from .5M $CuSO_4$ and various sulfuric acid concentrations

Current density = 20 mA/cm^2

Mercaptoacetic acid

Additive concentration (mole/l)	Sulfuric acid concentration (mole/l) 0.1 η(mV)	0.5 η(mV)	1.0 η(mV)
$5.0x10^{-4}$	63	49	43
$2.5x10^{-4}$	76	48	46
$1.0x10^{-4}$	73	50	49
$5.0x10^{-5}$	79	55	53
$2.5x10^{-5}$	81	58	53

less than that of the corresponding thioacetic acid. Compare Tables 21 & 26.

Steady-State Overpotential-Current Density Relation, Mercaptoacetic Acid

Figure 28 shows some typical steady-state overpotentials with mercaptoacetic acid as a function of current densities. Tafel slopes were calculated from these curves. Just as with thioacids, the Tafel slope decreases the greater the depolarization. Numerical values are given in Table 27.

Initial Overpotential with Mercaptoacetic Acid

Again as with the thioacids, mercaptoacetic acid exhibited an initial maximum overpotential immediately on closing the electrolysis circuit. However, there is a distinct difference in the $\tau_{max.}$ behavior with thioacid and with mercaptoacetic acid. With the former, $\tau_{max.}$ could be recorded with the Sargent SR recorder operating at medium chart speed, 0.5 inch per minute, while with the latter $\tau_{max.}$ was relatively very small, requiring use of an oscilloscope and camera. $\tau_{max.}$ for mercaptoacetic acid was found to be in the range of 10 to 20 msec. Typical results are shown in Fig. 29. On the other hand, the effect of additive concentration and sulfuric acid concentration on the initial overpotential follows the same pattern as with thioacids. Numerical values are given in Table 28.

The Effect of Deoxygenation of the Solution on the Initial Overpotential

Acidified standard solutions containing additives

Figure 28

Overpotential-current density relation (η vs. ln i)
for mercaptoacetic acid

a	1	5.0×10^{-4} mercaptoacetic acid, .1M H_2SO_4
	2	5.0×10^{-4} mercaptoacetic acid, .5M H_2SO_4
	3	5.0×10^{-4} mercaptoacetic acid, 1.0M H_2SO_4
b	1	2.5×10^{-4} mercaptoacetic acid, .1M H_2SO_4
	2	2.5×10^{-4} mercaptoacetic acid, .5M H_2SO_4
	3	2.5×10^{-4} mercaptoacetic acid, 1.0M H_2SO_4

Fig. 28

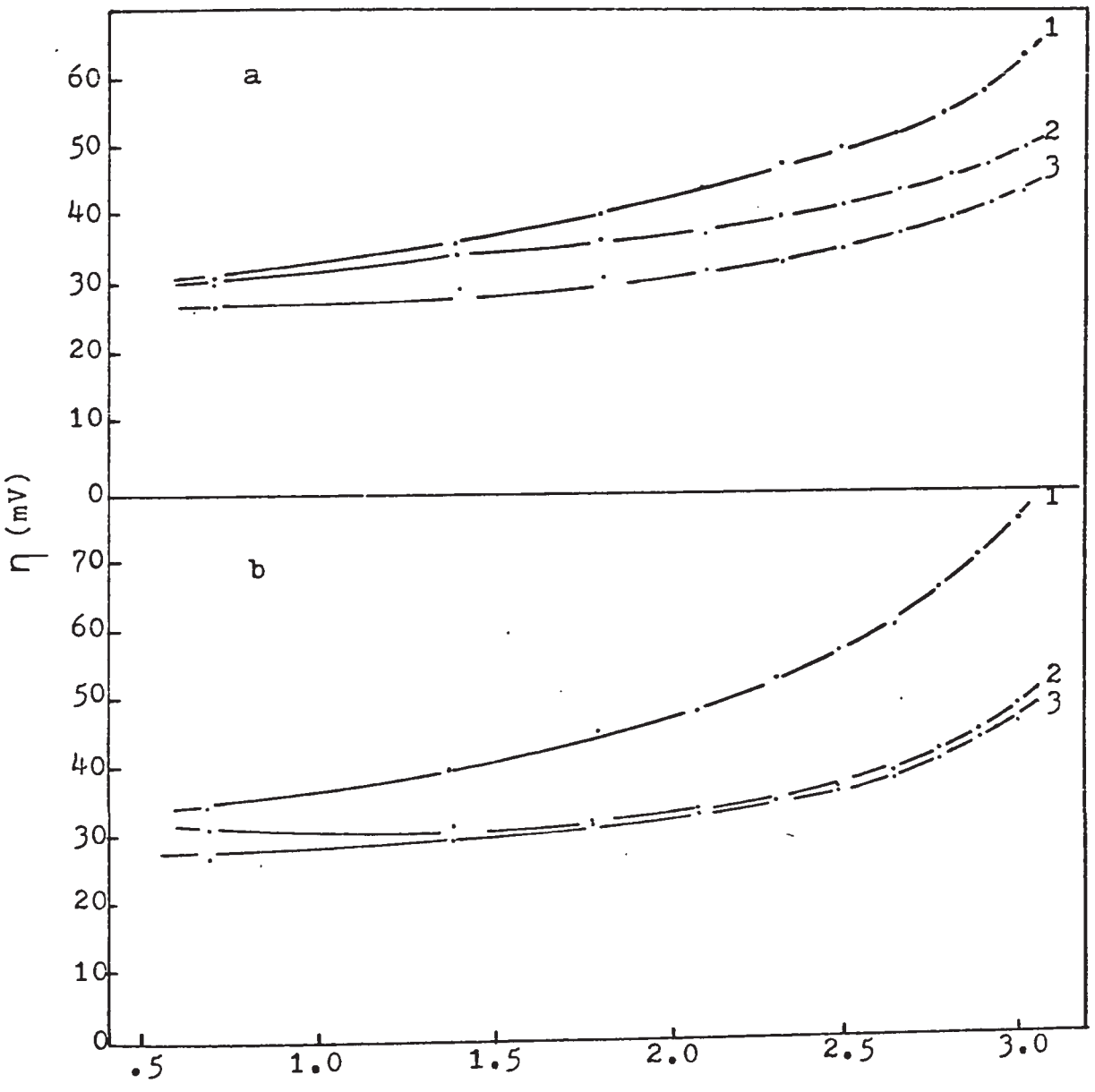

Table 27

Overpotential as a function of current density for copper deposition from 0.5M $CuSO_4$ and various sulfuric acid concentrations

Mercaptoacetic acid

Additive concentration (mole/l)	H_2SO_4 (mole/l)	Current density (mA/cm^2) 20	18	16	14	12	10	8	6	4	2	Tafel Slope (mV)	i_o(mA)
$5.0x10^{-4}$	.1	63	58	55	52	50	47	44	40	36	30	40	4.26
	.5	49	47	45	43	41	41	37	36	34	31	16	-
	1.0	43	41	39	37	35	33	32	31	29	27	15	-
$2.5x10^{-4}$	.1	76	71	66	60	57	53	48	45	40	34	43	3.53
	.5	48	45	42	39	37	35	34	32	31	31	29	3.82
	1.0	46	44	41	38	36	35	33	32	29.5	27	24	3.98
$1.0x10^{-4}$	.1	73	66	60	54	49	44	40	36	32	27	46	3.98
	.5	50	46	42	38	35	33	30	28	27	25	33	4.39
	1.0	49	44	40	37	34	31	28	27	26	24	33	4.62
$5.0x10^{-5}$	.1	79	71	64	57	50	45	40	38	28	22	54	4.62
	.5	55	50	47	43	39	36	33	31	27	25	34	3.86
	1.0	53	47	43	39	34	31	27	24	22	20	34	4.18
$2.5x10^{-5}$	.1	81	71	64	58	51	46	41	35	30	24	49	4.13
	.5	58	52	48	44	41	38	35	32	29	25	34	3.53
	1.0	53	48	43	39	36	32	28	26	22	19	32	3.82

Figure 29

Overpotential-time relation (η vs. t) for solution containing .5M $CuSO_4$, 1.0×10^{-4}M mercaptoacetic acid & various sulfuric acid concentration

1	0.1M sulfuric acid
2	0.5M sulfuric acid
3	1.0M sulfuric acid
Vertical full scale	300 mV.
Horizontal full scale	500 msec.

Fig. 29

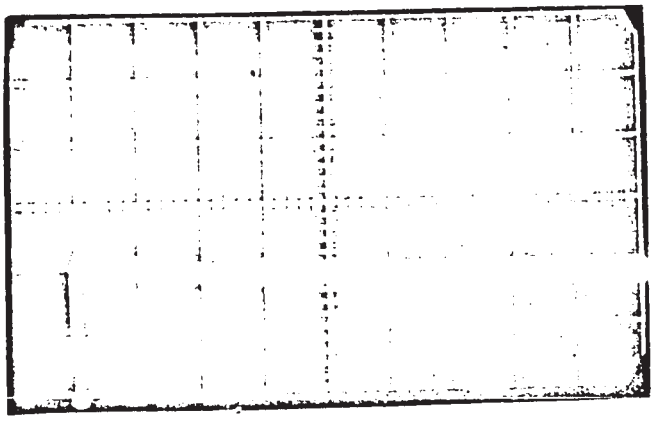

1

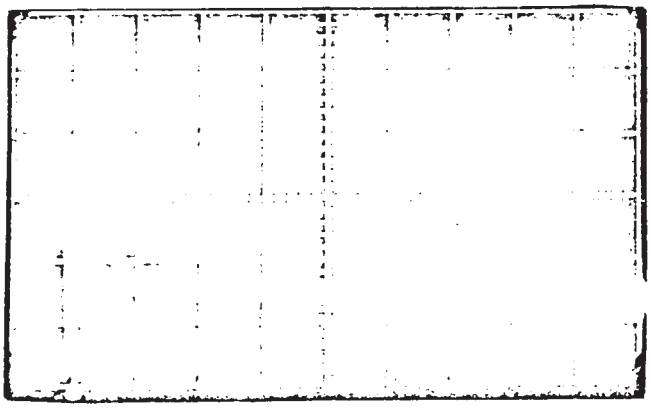

2

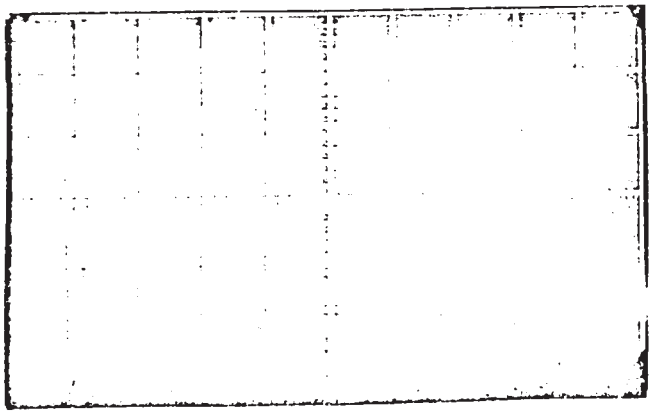

3

Table 28

Initial overpotential-H_2SO_4 and additive concentration relation for copper deposition for mercaptoacetic acid

Current density = 20 mA/cm^2

Additive concentration (mole/l)	H_2SO_4 (mole/l)	Initial max. overpotential (mV)	$\tau_{max.}$ (msec.)
5.0×10^{-4}	0.5	155	10
	1.0	180	10
1.0×10^{-4}	0.1	105	15
	0.5	120	10
	1.0	145	10
5.0×10^{-5}	0.1	90	15
	0.5	100	10
	1.0	130	10
2.5×10^{-5}	0.1	75	12
	0.5	78	12
	1.0	124	12

Table 28

Initial overpotential-H_2SO_4 and additive concentration relation for copper deposition for mercaptoacetic acid

Current density = 20 mA/cm^2

Additive concentration (mole/l)	H_2SO_4 (mole/l)	Initial max. overpotential (mV)	$\tau_{max.}$ (msec.)
5.0×10^{-4}	0.5	155	10
	1.0	180	10
1.0×10^{-4}	0.1	105	15
	0.5	120	10
	1.0	145	10
5.0×10^{-5}	0.1	90	15
	0.5	100	10
	1.0	130	10
2.5×10^{-5}	0.1	75	12
	0.5	78	12
	1.0	124	12

were deoxygenated by bubbling nitrogen for 5 to 20 minutes. A clean cathode was immediately immersed, after bubbling of N_2 was stopped, and kept in contact with this solution for 5 minutes before determining the initial overpotential. The results are shown in Table 29. Comparing these results with those obtained without deoxygenation show that there are no significant differences. Other experiments were done in which the cathode was immersed while bubbling the nitrogen. The results are shown in Table 29, showing an increase in the initial overpotential.

Sulfide Film Formation on the Cathode Surface

It was observed that in each case where the cathode was immersed in standard solution containing thioacids or mercaptoacetic acid, tarnishing of the surface took place. A brown-black deposit was formed immediately on the cathode surface. However, after electrolysis, this film disappeared completely. The darkness of this film depended on the kind of additive used and its concentration, also on the concentration of sulfuric acid. An experiment was made to examine the chemical structure of this film, in which copper rods were immersed in standard solution containing thiopropionic acid for about 2 days. The rods were washed thoroughly with water and then dried with tissue paper and scraped to remove the brownish-black deposit. An x-ray powder diffraction examination was made of the collected material. By matching the x-ray diffraction result with ASTM cards, good agreement was found to

Table 29

Initial overpotential-deoxygenation relation for copper deposition from 0.5M $CuSO_4$, 7.5×10^{-6}M thiobutyric acid and various sulfuric acid concentrations

Current density = 20 mA/cm^2

Time of bubbling N_2 (min.)	time (min.)	H_2SO_4 concentration (mole/l)	Initial max. overpotential (mV)	max. (sec.)
0	5	0.5	99	30
5	5	0.5	108	30
20	5	0.5	106	36
0	5	1.0	105	30
5	5	1.0	107	36
20	5	1.0	108	37
5*	5	1.0	118	36

*N_2 bubbling took place while the cathode was in solution.

indicate that the material was the non-stiochiometric copper sulfide $Cu_{1.96}S$ (see Table 30). It is therefore most likely that the formation of $Cu_{1.96}S$ is the cause of the initial overpotential. Another experiment was done to check this assumption. After attaining the steady-state overpotential, the current was turned off for about 30 seconds and then turned on again. No initial overpotential was observed. However, by turning the current off for about 15 minutes, then on again, an initial maximum overpotential was obtained.

The Effect of H_2S on the Copper Surface

To investigate the fact that the initial overpotential is due to copper sulfide formation on the metal surface, the following experiments were conducted: The cathode was pickled in 50% nitric acid, thoroughly washed with water, then immersed in distilled water previously saturated with H_2S. A black film of copper sulfide appeared instantaneously on the cathode surface. The electrode was removed from the solution, washed with distilled water, and then used for electrolysis. On electrolysis in 0.5M $CuSO_4$ and 0.0M H_2SO_4 but with no additive, a maximum overpotential of 110 mV was initially obtained after which the overpotential dropped slowly to about 56 mV at steady state.

A second experiment was done in which the electrode prepared as mentioned above was electrolyzed in

Table 30

X-ray diffraction results

Experimental		$Cu_{1.96}S$ (A.S.T.M.)	
Internuclear distances d	Approx. Intensity I/I_o	Internuclear distances d	Intensity I/I_o
1.824	100	1.824	100
2.14	60	2.135	60
3.01	30	3.011	30
2.47	10	2.472	30
2.069	10	2.07	10
2.047	5	2.057	30
2.107	5	2.104	30

0.5M $CuSO_4$, 1.0M H_2SO_4 solution, also with additive. An initial overpotential was also obtained and a maximum of 115 mV was reached in about 50 seconds, after which the overpotential fell slowly to a steady-state value of 104 mV.

Thioacids in 0.5 $CuSO_4$, Na_2SO_4 Solution

To investigate the probability that depolarization of copper deposition by thioacids may be due to the change in the ionic strength, from 0.0M H_2SO_4 to 1.0M H_2SO_4, or due to the change of hydrogen ion concentration, the following experiments were done.

Steady-state overpotentials with standard solutions containing 0.5M $CuSO_4$ & 0.0, 0.1, 0.5, 1.0 m/l Na_2SO_4 respectively were determined. The results are shown in Table 31. The steady-state overpotentials with the above solutions containing 7.5×10^{-5} m/l thiopropionic acid and 2.5×10^{-5} m/l thiobutyric acid respectively were measured and are also given in Table 31. A comparison between the steady-state overpotential of the standard solutions with and without additive indicates the following: a) for standard solution without additive the steady-state overpotential increases with increasing Na_2SO_4 concentration, b) a definite overpotential increment was obtained with standard solutions containing additives. However, this overpotential decreased with increasing the Na_2SO_4 concentration.

At high concentration of Na_2SO_4, i.e. 1.0 m/l, no significant additive effect was obtained. The possible reason for this behavior is the specific adsorbability of

Table 31

Overpotential for copper deposition from .5M $CuSO_4$ and sodium sulfate solution with and without additive

Current density = 20 mA/cm^2

(a) 0.5M $CuSO_4$ - without additive

Concentration of Na_2SO_4 (mole/l)	Overpotential (mV)	Overpotential Increment (mV)
0.0	50	-
0.1	65	-
0.5	82	-
1.0	84	-
(b) 0.5M $CuSO_4$ + 7.5×10^{-5}M thiopropionic acid		
0.0	115	65
0.1	107	42
0.5	90	8
1.0	83	-1
(c) 0.5M $CuSO_4$ + 2.5×10^{-5}M thiobutyric acid		
0.0	124	74
0.1	95	30
0.5	87	5
1.0	85	1

sodium ions with less mobility than the hydrogen ions. Therefore, the overpotential effect of the thioacids will decrease with increasing the Na_2SO_4 concentration.

Results of Qualitative Experiments

It was noticed that by adding mercaptoacetic acid to the standard solution containing 0.0, 0.1, 0.25, 0.5, 0.75 and 1.0 m/l sulfuric acid respectively, different colors were obtained for each solution. In the first solution with no H_2SO_4, a violet-blue color was obtained, while for the rest, a yellowish-blue color was observed in which the yellow color definitely increased with increasing the sulfuric acid concentration. Quantitative spectroscopic experiments were not successful because of the relatively high concentration of cupric ions which absorb strongly in the region required for investigation. The following qualitative results were obtained:

1) Mercaptoacetic acid + H_2SO_4 = no reaction (colorless solution)

2) Mercaptoacetic acid + copper sulfate solution = violet-blue color.

3) The violet-blue solution + sulfuric acid = yellowish-blue solution.

4) Mercaptoacetic acid solution + sodium sulfate solution + copper sulfate solution = violet-blue color.

5) Mercaptoacetic acid + H_2SO_4 solution + $CuSO_4$ solution = yellowish-blue solution, + H_2O_2 = violet-blue solution = blue solution of the $CuSO_4$.

6) The violet-blue solution + Na_2SO_3 = yellow solution.

7) The yellow solution + NaOH = violet-blue solution = brown ppt.

8) The violet-blue solution in the cathode compartment separated from the anode by fine sintered glass, cathodically reduced = yellowish-blue solution.

9) The violet solution in the anode compartment, separated from the cathode by fine sintered glass, anodically oxidized = no change.

These results can be summarized as follows:

a) Violet-blue solution $\underset{OH^-}{\overset{H^+}{\rightleftharpoons}}$ yellowish-blue(greenish solution)

b) Violet-blue solution $\underset{\text{Oxidation}}{\overset{\text{Reduction}}{\rightleftharpoons}}$ yellowish-blue (greenish solution).

A high concentration of the mercaptoacetic acid (0.05M) was added to 0.5M $CuSO_4$, 1.0M H_2SO_4, whereupon a fine yellow precipitate was found. The overpotential of this solution was measured and was found to be 51 mV. This yellow precipitate was filtered with extra fine sintered glass, and both the precipitate and the filtrate were collected. The filtrate was $CuSO_4$ blue, the overpotential of which was measured and found to be much higher than previously ($\sim$75mV). The precipitate was added to standard solution (0.5M $CuSO_4$ + 1.0M H_2SO_4) and the measured overpotential was 35 mV.

Polarographic Studies & Results

A Sargent Polarograph Model XV was used in this part of the study. Initially this work was done to test

the ability of RSH compounds, i.e. thioacids and mercapto-acids, to oxidize and reduce electrochemically, and also to see the effect of $CuSO_4$ solution on their behavior or vice versa. A 1.0×10^{-4}M thiobutyric acid solution was prepared in 0.0, 0.1, 0.5, 0.75 & 1.0 m/l sulfuric acid solution respectively in sodium sulfate supporting electrolyte. The results of potential sweep from +1.0 to -1.0 Volt for the above solutions are given in Table 32. Two waves were observed - one cathodic and the other anodic. The diffusion current of the anodic wave increases with increasing sulfuric acid concentration, also the oxidation process takes place at less positive potential with increasing sulfuric acid. With the cathodic wave, similarly, the diffusion current increased with increasing sulfuric acid concentration and the wave also shifts to more negative potential. Surprisingly, the shift in both cathodic and anodic waves, are the same, equivalent to -0.12 Volt.

A potential sweep from 0 to -0.5 Volt results in a very small cathodic wave. For additives with 0.0, 0.5, & 1.0 m/l H_2SO_4, the diffusion current of the cathodic wave was 0.0584, .054, and .056 μa respectively.

The diffusion currents obtained for the above solutions for a potential sweep from +1.0 to -1.0 Volt were 0.17, 0.25 and 0.33μa respectively. Another experiment was done in which the thiobutyric acid was oxidized chemically by iodine to RSSR before electrolysis. The result was

Table 32

Polarographic behavior of solution containing 1.0×10^{-4} thiobutyric acid as a function of H_2SO_4 concentration

concentration (mole/l)	cathodic wave $E_{\frac{1}{2}}$ (V)	I_d (μa)	Anodic wave $E_{\frac{1}{2}}$ (V)	I_d (μa)
0.0 H_2SO_4	-.18	.17	+.45	.46
0.1 H_2SO_4	-.18	.23	+.40	1.20
0.5 H_2SO_4	-.22	.25	+.42	1.60
0.75 H_2SO_4	-.26	.32	+.40	4.26
1.0 H_2SO_4	-.32	.33	+.34	5.45
0.25 H_2SO_4	-.22	.49	+.52	.29
1.0 H_2SO_4*	-.20	.48	-	-

*Treated with I_2.

an increase in the diffusion current of the cathodic wave and decrease in the anodic wave. Numerical values are given in Table 32. A possible reason for these results is that the anodic wave corresponds to anodic oxidation of the RSH to RSSR, and the cathodic wave is most probably due to the cathodic reduction of RSSR to RSH.

Polarographic runs were made for two sets of solutions. The first set was 0.01 m/l $CuSO_4$ in 0.0, 0.1, 0.5 and 1.0 m/l H_2SO_4 respectively, with sodium sulfate as supporting electrolyte. The second set was like the first except that each solution included 1.0×10^{-4} m/l thiobutyric acid. The results are given in Table 33.

Table 33 indicates that sulfuric acid concentration does not affect the cathodic wave(1) in the first set of experiments, which is most likely due to the reduction of copper II (72). However, in the presence of thiobutyric acid, a marked shift or most likely a new cathodic wave (2) was observed which increases with increasing sulfuric acid concentration.

Test for Cuprous Ion in Solution

The results obtained in the previous two sections indicate the presence of copper in the cuprous state in the solution of $CuSO_4$ and H_2SO_4 with thioacid or mercaptoacetic acid. Accordingly, a test of the presence of cuprous ions was done. The method used was that reported in (73). However, instead of using neocuproine, 1,10 phenanthraline was used, which formed a complex with curpous ions absorbing

Table 33

Polarographic behavior of solution containing 0.1M $CuSO_4$ as a function of sulfuric acid concentration

(a) 0.0 thiobutyric acid

Solution (mole/l)	cathodic wave(1) $E_{\frac{1}{2}}$ (V)	I_d (μa)	cathodic wave(2) $E_{\frac{1}{2}}$ (V)	I_d (μa)
0.0 H_2SO_4	-.050	27		
0.1 H_2SO_4	-.055	26		
0.5 H_2SO_4	-.055	27		
1.0 H_2SO_4	-.055	26		
(b) 1.0×10^{-4} thiobutyric acid				
0.0 H_2SO_4	-.05	16.5	-.12	6.5
0.5 H_2SO_4			-.10	12.0
0.5 H_2SO_4			-.12	10.0
1.0 H_2SO_4			-.10	14.0
1.0 H_2SO_4			-.11	12.9
1.0 H_2SO_4			-.10	17.0

at 325 mμ. The procedure was first employed on standard solution without thioacids, 0.5 $CuSO_4$, 1.0 m/l H_2SO_4. The result was negative, i.e., no cuprous ions were present. A yellow-coloured complex was obtained in the case of standard solution containing mercapotacetic acid. The mercaptoacetic acid concentration used was reasonably high to give sufficient product to be detected. This yellow complex absorbed at 325 mμ.

Microscopic Examination of the Electrodeposited Surface

It has been reported (41) that the depolarization effect of mercaptoacetic acid might be partially due to an increase in the surface area of the cathode, and consequently a decrease in the true current density. Therefore, a microscopic examination of the cathode surface was done for standard solution with and without depolarizer. All electrolyses were carried out for exactly 60 minutes. Solutions of 0.5M $CuSO_4$ and 0.0, 0.1, 0.5, and 1.0M H_2SO_4 respectively were used for electrolysis and the electrodeposited cathode surfaces were examined microscopically. Similarly, solutions of 0.5 $CuSO_4$, 2.5×10^{-5}M thiobutyric acid and 0.0, 0.1, 0.5, and 1.0M H_2SO_4 acid respectively were examined. The magnification used was about 4000 times the original surface. It was observed that for standard solutions, increasing the sulfuric acid caused the deposit to be finer and smaller, in agreement with results reported previously (73,74). For solutions containing additives there was no difference

between the cathodic surfaces obtained and the surfaces obtained from solutions containing no additives (see Fig. 30). Due to illumination problems, photographs of cathode electrolyzed from acidified 0.5 $CuSO_4$ were not obtained, because of the fine texture of the surface and low reflection of the light. However, it can be seen from Fig. 30 that there is no marked difference between the electrodeposited copper for solution with and without additives, i.e., change in the surface area cannot play an important role in depolarization.

2) Discussion:

The Effect of Thioacids (in 0.5M $CuSO_4$, 0.0M H_2SO_4)

The addition of thioacids to 0.5 $CuSO_4$, 0.0 H_2SO_4 caused an increase in the overpotential of copper electrodeposition (see Fig. 21). From the values of the overpotential and Tafel slopes obtained, charge transfer is expected to be rate-determining. Accordingly, the simple blocking theory can be applied to this system. The fractional surface coverage was calculated using Equation (42) from the overpotential increments for thioacetic, thiopropionic and thiobutyric acids. The overpotential increments were obtained by subtracting the 50 mV obtained with standard 0.5M $CuSO_4$, 0.0M H_2SO_4 solution from each measured steady-state overpotential value. The standard free energy of adsorption was calculated using Equation (40). The number of water molecules replaced by one organic molecule is expected to be 2, similar to the monocarboxylic acids, since the -COSH group has the same projected area as the -COOH group.

Figure 30

Microscopic pictures of the electrodeposited copper from 0.5M $CuSO_4$ solution

1 0.0M sulfuric acid without additive

2 0.0M sulfuric acid & 2.5×10^{-5} thiobutyric acid

Fig. 30

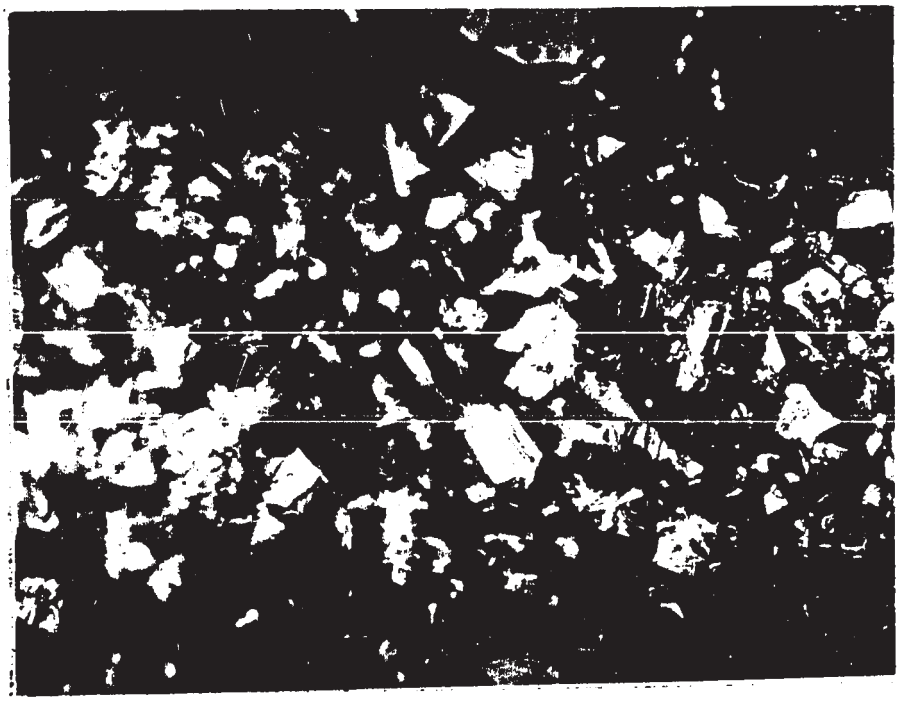

1

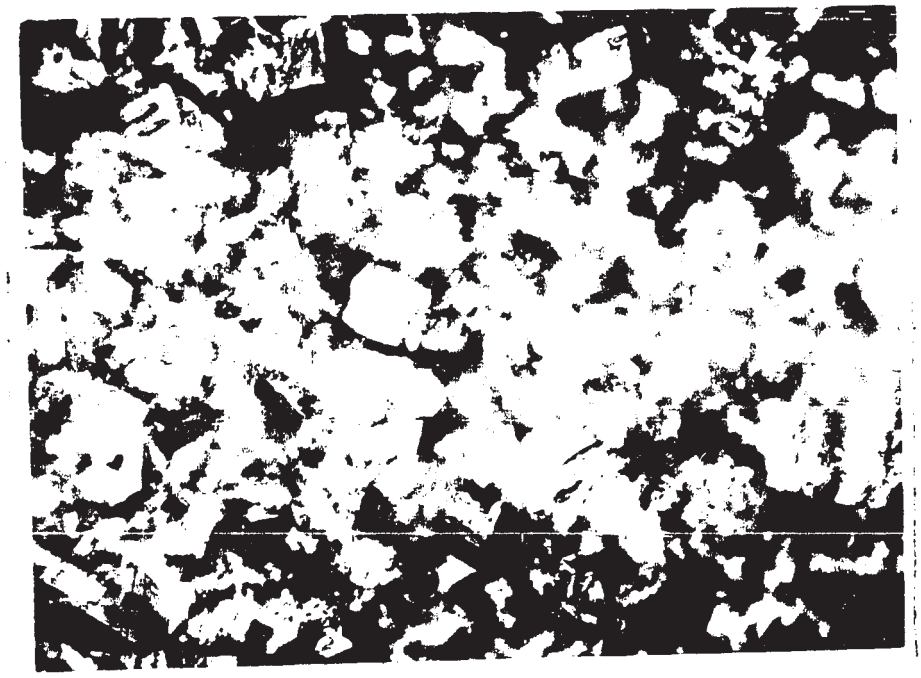

2

Fig. 30

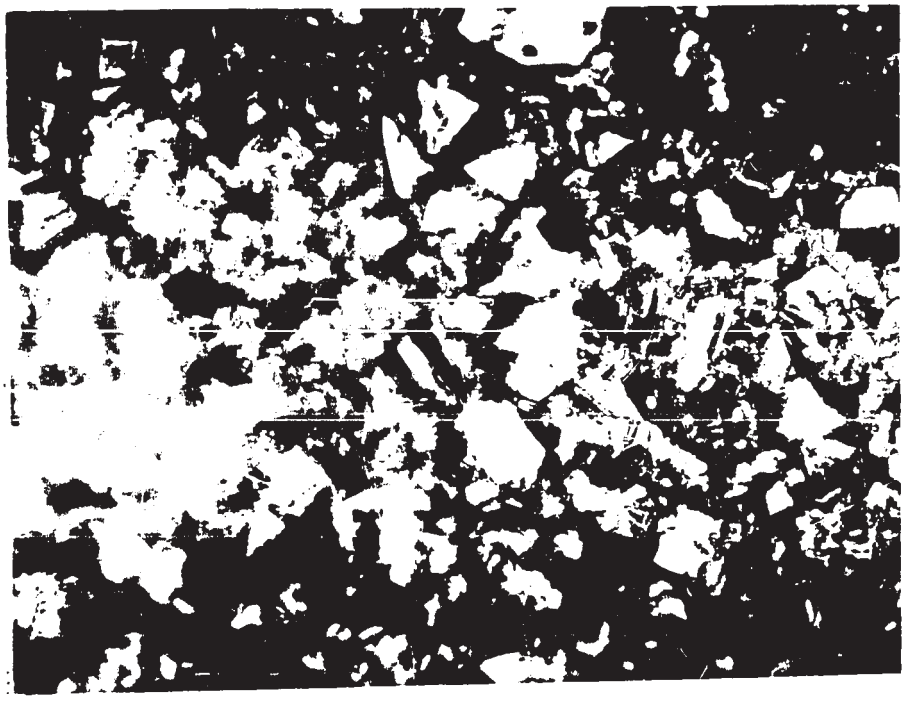

1

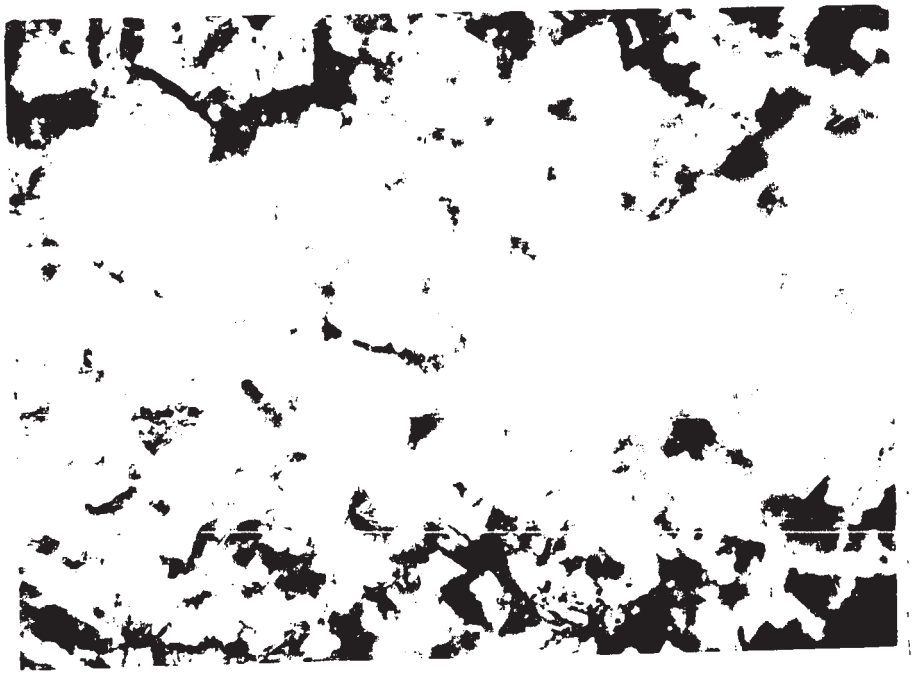

2

The apparent free energy of adsorption was found to be independent of the coverage. This result is expected, considering the low concentration of the additive used. Equation (36) can be rewritten as:

$$\frac{\theta^2 + 2\theta - 2\theta^2}{4(1-\theta)^2} = KC \qquad \text{-------(63)}$$

$$\frac{\theta(2-\theta)}{(1-\theta)^2} = 4KC$$

$$\frac{\theta(2-\theta)}{1-\theta(2-\theta)} = 4KC$$

$$\theta(2-\theta) + 4KC\ \theta(2-\theta) = 4KC$$

divide by $4K\ \theta(2-\theta)$

$$C/\theta(2-\theta) = \tfrac{1}{4}K^{-1} + C \qquad \text{-------(64)}$$

Plotting $C/\theta(2-\theta)$ vs. C gave a straight line with slope equal to unity and an intercept equal to $\frac{1}{4}K^{-1}$ for the thioacids. The value of K and the calculated free energies of adsorption of the thioacids are given in Table 34.

Table 34

Free energy of adsorption and adsorbability of thioacids at zero coverage

Additive	$-\Delta G_a^o$ (Kcal/mole)	K(1 mole^{-1})
Thioacetic acid	7.950	1.1×10^4
Thiopropionic acid	8.800	4.5×10^4
Thiobutyric acid	9.570	1.7×10^5

It can be seen from the above table that the free energies of adsorption of thioacids are much higher than for the corresponding monocarboxylic acids. However, their

magnitudes are within the range of physical forces in the adsorption process. In applying Equation (44), taking $g(\theta)$ as zero, ΔG^{o}_{COSH} and $\Delta G^{o}_{CH_2}$ were calculated, and found to be -7.150 Kcal/mole and -810 cal/mole respectively. The value of $\Delta G^{o}_{CH_2}$ is in the same order of magnitude as $\Delta G^{o}_{CH_2}$ obtained for the monccarboxylic acids. Based on the assumption that physical forces are the only forces involved in the adsorption of the additives, the contribution of the methylene groups to the adsorption free energy can be expected to be the same, even when using organic additives with different functional groups. This assumption will hold true as there is no chemical interaction between the organic molecule and the metal surface, and also, as long as the presence of the functional group does not affect the hydrocarbon part of the molecule to any great extent. The fact that $\Delta G^{o}_{CH_2}$ obtained in this work is close to that obtained for monocarboxylic acids, -704 cal/mole, and close to values obtained by other workers (57,62,66), i.e. -760, -770 and -800, (see page 84), indicates that physical forces must be the primary forces involved in the adsorption process. It can also be predicted that thioacids most likely adsorb with the functional group toward the metal.

Since there is a constant increase in the overpotential increment on addition of each methylene group, Traube's rule is expected to apply to this system. Traube's coefficient for thioacids was found to be 3.65.

The Effect of Thiols in Acidified Aqueous $CuSO_4$

Thiols did not show any depolarization effect in acidified $CuSO_4$ solution. On the contrary, high overpotential increments were obtained. It should be mentioned that for this group of organic compounds only low concentrations were used to avoid any precipitation of the copper salts of these organic additives. Just like for the thioacids, θ was calculated using Equation (42) and the standard free energies were calculated using Equation (36). The apparent free energy of adsorption was found to vary with coverage, similar to the mono- and dicarboxylic acids. The dipole moments of the thiols are in the range of 1.35-1.55 D. Accordingly, the magnitude of the lateral interaction will be very close to the lateral interaction free energy of the monocarboxylic acids. Therefore, the adsorption isotherm given in Equation (45) will also be applicable to this system. Considering the difficulty and uncertainty in the calculation of the lateral interaction encountered in the case of monocarboxylic and dicarboxylic acids, no attempt will be made to calculate the lateral interaction for thiols. However, since μ_D of the thiol is very close to that of the monocarboxylic acid, dipole-dipole interaction can be expected to be the main contribution in the lateral interaction.

Similar to the monocarboxylic acids, the overpotential increment was plotted against the concentration, from which the initial slope was obtained, (see Fig. 31). The logarithm of the initial slope is given in Fig. 32 as a

The Effect of Thiols in Acidified Aqueous $CuSO_4$

Thiols did not show any depolarization effect in acidified $CuSO_4$ solution. On the contrary, high overpotential increments were obtained. It should be mentioned that for this group of organic compounds only low concentrations were used to avoid any precipitation of the copper salts of these organic additives. Just like for the thioacids, θ was calculated using Equation (42) and the standard free energies were calculated using Equation (36). The apparent free energy of adsorption was found to vary with coverage, similar to the mono- and dicarboxylic acids. The dipole moments of the thiols are in the range of 1.35-1.55 D. Accordingly, the magnitude of the lateral interaction will be very close to the lateral interaction free energy of the monocarboxylic acids. Therefore, the adsorption isotherm given in Equation (45) will also be applicable to this system. Considering the difficulty and uncertainty in the calculation of the lateral interaction encountered in the case of monocarboxylic and dicarboxylic acids, no attempt will be made to calculate the lateral interaction for thiols. However, since μ_D of the thiol is very close to that of the monocarboxylic acid, dipole-dipole interaction can be expected to be the main contribution in the lateral interaction.

Similar to the monocarboxylic acids, the overpotential increment was plotted against the concentration, from which the initial slope was obtained, (see Fig. 31). The logarithm of the initial slope is given in Fig. 32 as a

Figure 31

Overpotential increment as a function of additive concentration for thiols

Ethanethiol

Propanethiol

Butanethiol

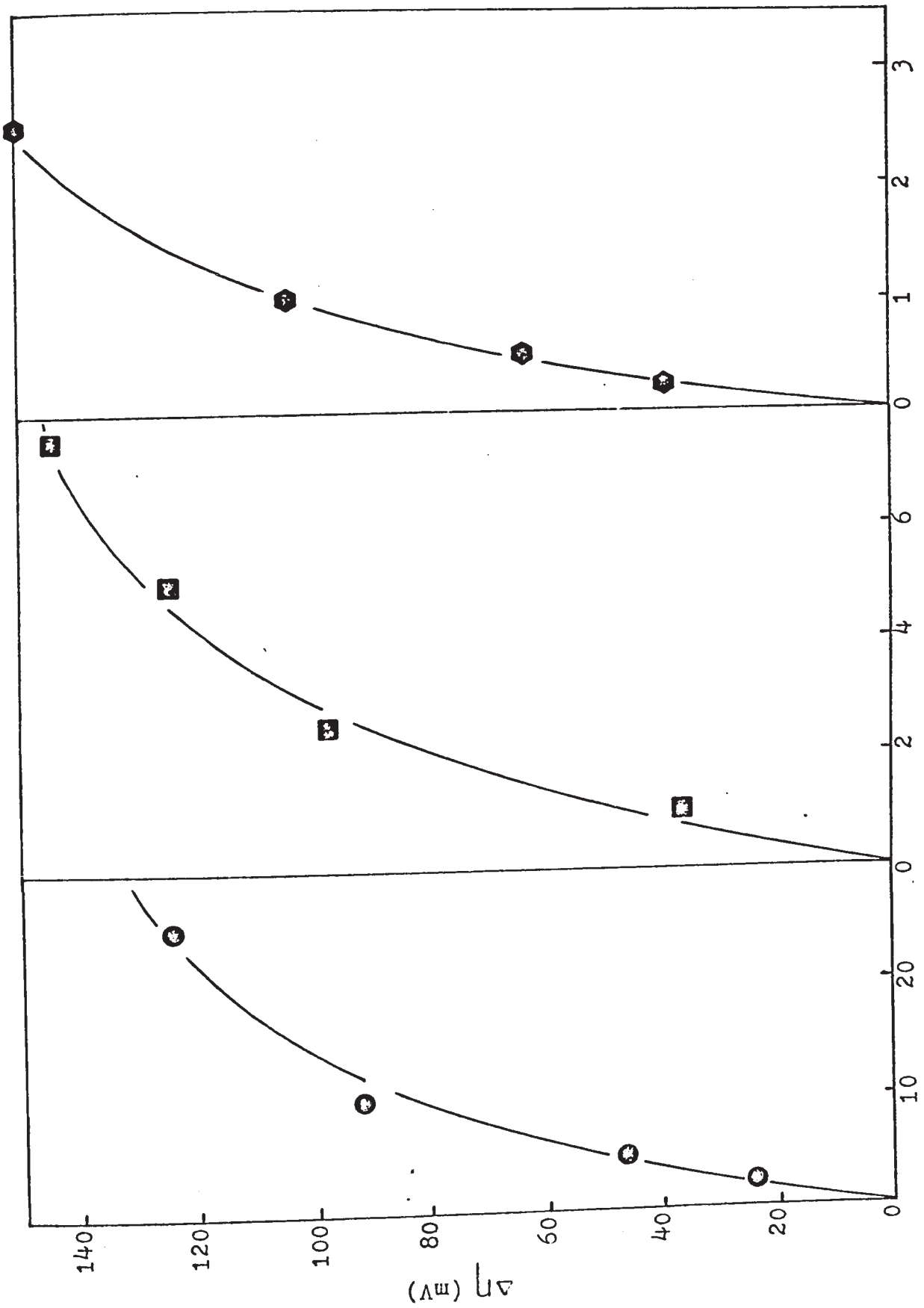

Fig. 31

Figure 32

Logarithm of the initial slope $(\Delta\eta/c)_{c\to 0}$ vs. number of methylene groups in the thiol molecule

Fig. 32

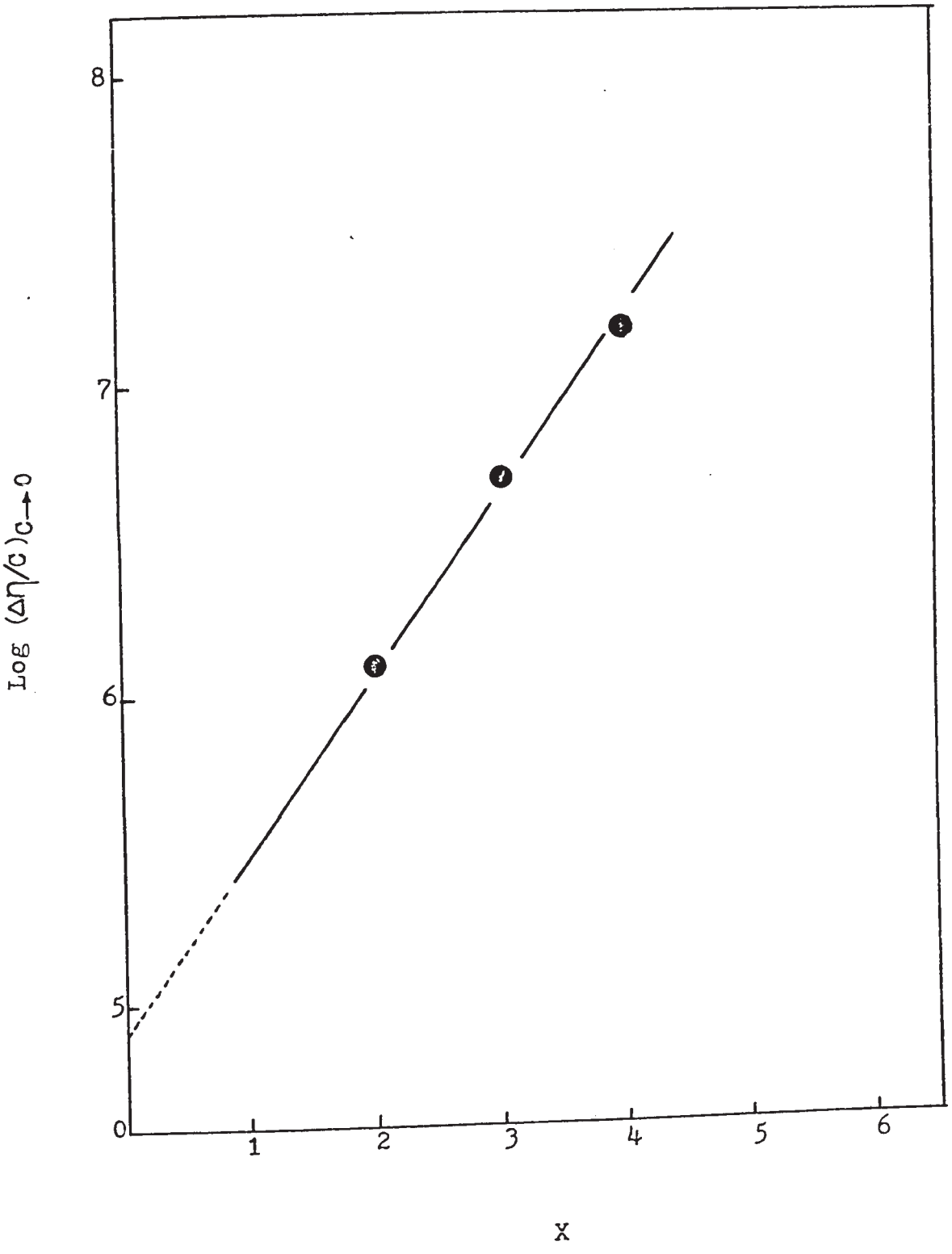

function of the number of methylene groups in the thiol molecule. From this figure, giving more weight to the first two points, the values of $\Delta G^{o}_{CH_2}$ and ΔG^{o}_{SH} were obtained from the slope and intercept respectively. They were found to be -769 cal/mole and -6375 cal/mole respectively. The value of $\Delta G^{o}_{CH_2}$ satisfactorily agrees with the values obtained for monocarboxylic acids and thioacids. Again, this supports the argument that considering physical adsorption, the contribution of the methylene group to the adsorption of an organic molecule should be the same for compounds with different functional groups. The standard free energies of adsorption at zero coverage for the thiols are given in Table 35.

Table 35

Standard free energy of adsorption of thiols

Additive	ΔG^{o}_{a} (Kcal/mole)
Ethanethiol	-7.9
Propanethiol	-8.7
Butanethiol	-9.5

The Effect of Mercaptoacids

Mercaptoacetic acid caused an increase in the overpotential of copper electrodeposition only in 0.5M $CuSO_4$, 0.0M H_2SO_4 solution. However, 3-mercaptopropionic acid and 4-mercaptobutyric acid, increased the overpotential, both in non-acidified as well as acidified aqueous $CuSO_4$ solution. It should be noted, therefore, that an additive with the -SH group far from an electron-with-

drawing group or with an -SH group alone (see the results of thiols) cannot cause depolarization in electrodeposition from acidified $CuSO_4$ electrolyte. This point will be discussed further in the next section.

From the overpotential increment with mercaptoacetic, 3-mercaptopropionic and 4-mercaptobutyric acids, the fractional surface coverage was calculated using Equation (42). The apparent standard free energies of adsorption were calculated using Equation (36), and were found to be independent of coverage. Accordingly, Equation (64) was applied and the adsorbability K and the corresponding free energy of adsorption were obtained. These values are given in Table 36. A plot of $C/\theta(2-\theta)$ vs. C is shown in Fig. 33.

Table 36

Standard free energy of adsorption & adsorbability for mercaptoacids

Additive	ΔG_a^o (Kcal/mole)	K(l/mole)
Mercaptoacetic acid	-8.35	2.5×10^4
3-Mercaptopropionic acid	-9.79	2.5×10^5
4-Mercaptobutyric acid	-9.67	1.92×10^5

It can be seen that the free energy of adsorption of mercaptobutyric acid is less than that of mercaptopropionic acid. Considering that the free energy of adsorption is the sum of the contributions of each part of the molecule, the free energy of adsorption of mercapto-

Figure 33

$C/\theta(2-\theta)$ function vs. additive concentration for mercapto acids

○ mercaptoacetic acid

△ mercaptopropionic acid

□ mercaptobutyric acid

Fig. 33

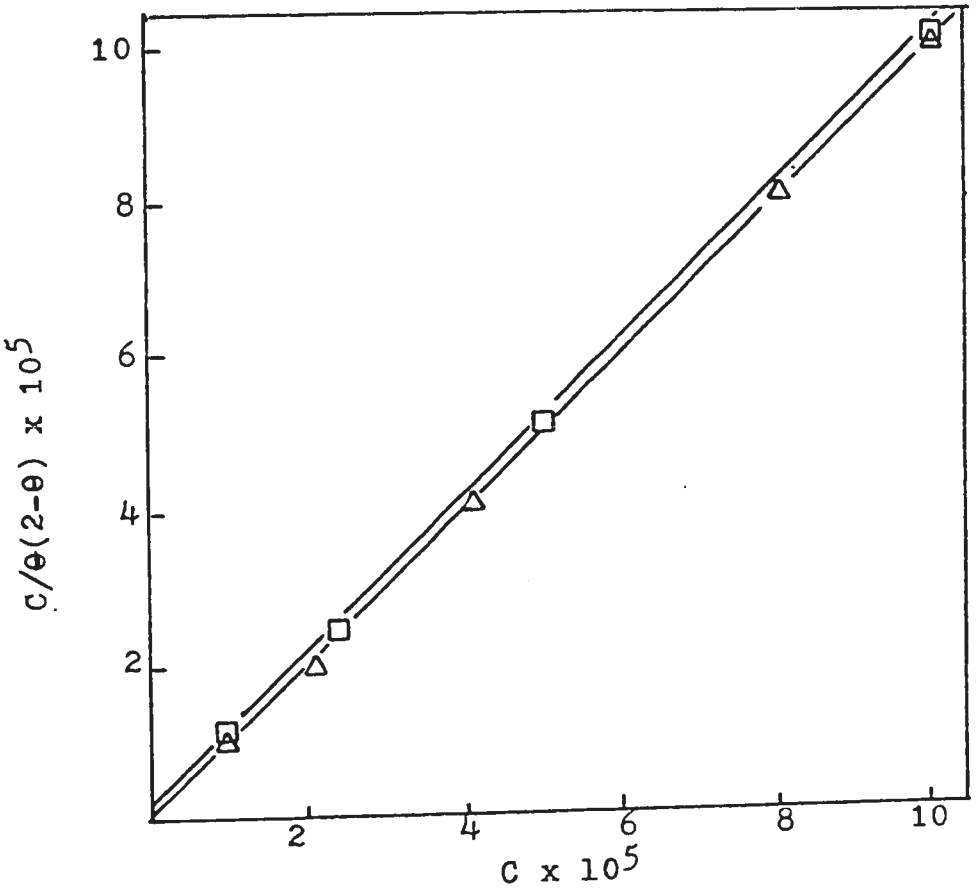

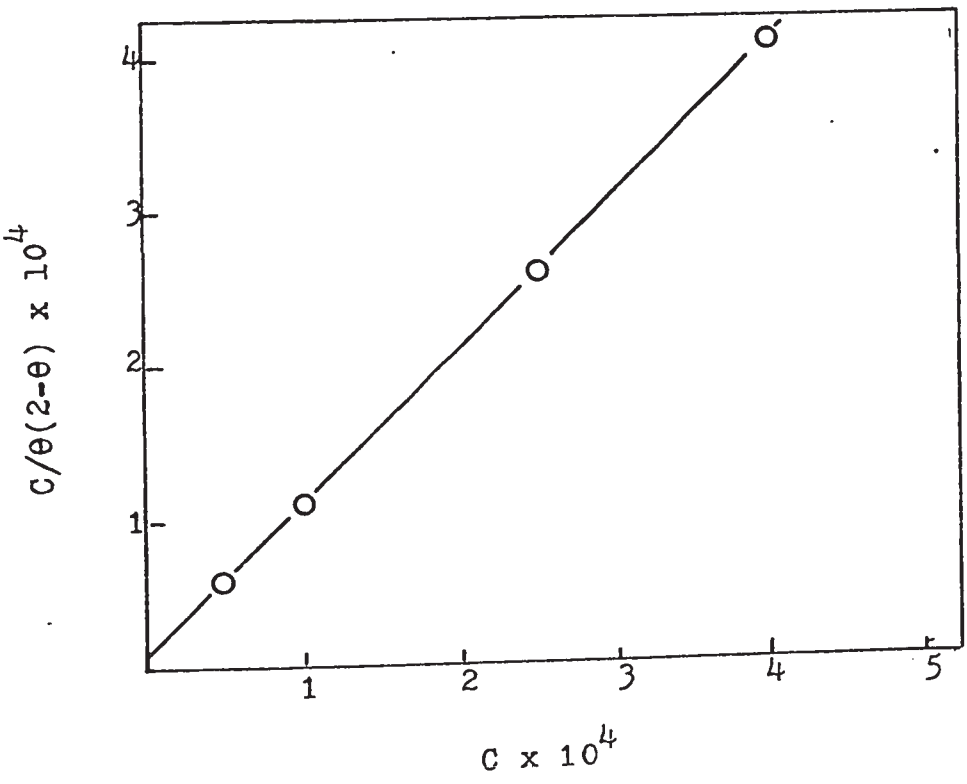

acid will consist of ΔG^{o}_{SH}, and ΔG^{o}_{COOH}. Since the free energy of adsorption of mercaptobutyric acid is less than that of mercaptopropionic, an alternation behavior similar to that of dicarboxylic acids can be expected. Accordingly, mercaptopropionic acid, which corresponds to propanedioic acid, is likely to adsorb with both functional groups toward the metal, and a full contribution from each part of the molecule will be possible. Applying the values of ΔG^{o}_{COOH} (-1570 cal/mole as obtained for monocarboxylic acids), $\Delta G^{o}_{CH_2}$ (-760 cal/mole, the average for monocarboxylic acids, thioacids and thiols), and ΔG^{o}_{SH} (-6375 cal/mole obtained for thiols), the standard free energy of adsorption of mercaptopropionic acid can be calculated. It is found to be -9.465 Kcal/mole. This result is in good agreement with but somewhat lower than the experimental value for mercaptopropionic acid given in Table 36. This is similar to the case of propanedioic acid, where the experimental free energy of adsorption is also slightly higher than that calculated from the contributions of each part of the molecule. This discrepancy might be attributed to a mutual effect between the carboxyl and thiol groups, an effect that can be expected to increase the adsorbability because of the electron-withdrawing nature of both groups. By using mean values of ΔG^{o}_{COOH}, $\Delta G^{o}_{CH_2}$ and ΔG^{o}_{SH} (from the thiols) for mercaptoacids, calculated ΔG^{o}_{a} values are found as in Table 37.

Table 37

Experimental & calculated free energy of adsorption for mercaptoacids (in Kcal/mole)

Additive	$-\Delta G_a^o$ experimental	$-\Delta G_a^o$ calculated*	$-\Delta G_a^o$ calculated**	$-\Delta G_a^o$ calculated***
Mercaptoacetic	8.35	8.70	7.13	2.33
Mercaptopropionic	9.79	9.56	7.89	3.09
Mercaptobutyric	9.67	10.32	8.65	3.85

*considering adsorption with both functional groups.

** " " " -SH group.

*** " " " -COOH group.

The following observations can be made:

1) For mercaptoacetic and mercaptobutyric acids, the experimental free energy of adsorption is lower than the calculated*. Accordingly, adsorption with only one functional group is most likely. Also, the experimental free energy of adsorption is higher than the calculated**, and much higher than the calculated***, therefore, adsorption with the -SH group is expected. It will also be noticed that the difference between the experimental results and calculated** decreases on passing from mercaptoacetic to mercaptobutyric. An explanation similar to that of the dicarboxylic acids with (ENCA) can be applied here. While the carboxyl group cannot fully contribute to the free energy of adsorption, it will partially do so by decreasing the electron density on the adsorbing functional group due to its electron-withdrawing behavior. Accordingly,

the effect of the -COOH will be higher for mercaptoacetic acid than for mercaptobutyric because of the increase in the chain-length.

2) For mercaptopropionic acid, comparing the experimental results with calculated* and calculated**, it is possible to conclude that two-point adsorption is most likely, as mentioned previously. Therefore, cis-configuration of the two functional groups is the most likely factor here. Mercaptoacetic, mercaptopropionic and mercaptobutyric acids correspond to ethanedioic (oxalic), propanedioic and butanedioic acids respectively.

Discussion of the Depolarization Phenomenon

The depolarization phenomenon with some additives, has been reported by several authors (41,43,69,75,76,77). Mercaptoacetic acid (MAA) in acidified $CuSO_4$ electrolyte was found to decrease the cathode overpotential throughout the course of electrolysis (41). This effect was attributed to a substitution of a more readily dischargeable MAA-Copper II complex for the aquo-copper complex. Turner & Johnson (76) found that thiourea in acid copper sulfate solution displaces the rest potential of a copper electrode in the positive direction. They suggested that the depolarization effect of relatively small amounts of thiourea might be due either to the reduction of thiourea at the cathode or to complexes with cuprous ions and suggested that the kinetics of copper deposition is limited by surface diffusion of adatoms. Mercaptosuccinic acid was found to be a

strong depolarizer, in acidified $CuSO_4$ solution, which was believed to be due to the formation of more readily dischargeable mercaptosuccinic-copper complex (77). The depolarization effect of sulfo-acids at low concentration has been studied by Lebedeva & Popercka (78); and the reduction in overall overpotential was attributed to secondary electrochemical conversion of the organic substances.

Shreir & Smith (43) studied the depolarization effect of sulfur-containing compounds, thiourea, sodium thiosulfate, hydrogen sulfide and carbon disulfide. Their explanation was that these compounds, or products derived from them, may form complexes with copper ions which are more readily adsorbed on the cathode than hydrogen ions, and cover most of the adsorption sites. In the adsorbed film the complex may accept electrons from the cathode, at the same time releasing the sulfur compound to form a complex with another copper ion which is immediately adsorbed. This was thought to explain why such a very small amount of additive suffices to produce the large effect on the discharge process. The effect of thio-compounds, sodium thiosulfate, thioglycolic acid, thiosemicarbazide, rubeanic acid, thioacetamide and sodium sulfite, on copper deposition was studied by Barnes (69). These experiments indicated that under certain conditions thio-compounds caused marked depolarization. They explained this phenomenon on the basis that divalent sulfur compounds prevent H^+ ion inhibition by forming a

barrier between the cathode surface and the electrolyte. On account of the high polarizability of the $-HS^-$ anions, which are preferentially adsorbed on the metal surface, the electrochemical discharge reaction will be stimulated.

In agreement with the above authors, thioacids and mercaptoacetic acid caused marked depolarization during electrodeposition of copper from acidified copper sulfate solution. The following discussion will be an attempt to explain the behavior of these additives on the basis of the results obtained in this work.

The Mechanism of Copper Deposition from Acidified $CuSO_4$ Containing Depolarizer

The overpotential-current density relation for copper deposition from acidified $CuSO_4$ solution containing thioacetic, thiopropionic, thiobutyric or mercaptoacetic acids (Fig. 25 & 29) does not follow the Tafel relation. The applicability of the Tafel-region is completely restricted to low additive concentration, low sulfuric acid concentration and high current density. The absence of a Tafel-region and the low steady-state overpotential obtained at a given current density could indicate a change in the rate-determining step. The definite increase in the exchange current density (Table 22,27) with increasing additive concentration at a given H_2SO_4 concentration, or with increasing H_2SO_4 concentration at a given additive concentration, could also indicate a shift in the rate-determining process (11). Therefore, the total overpoten-

tial might be expressed by Equation (32).

$$\eta = \frac{RT}{ZF}\left[\frac{i}{i_o} + \frac{i}{ZFV_o}\right] \qquad (32)$$

From this equation, the surface diffusion flux V_o was calculated at different current densities and i_o was obtained from the extrapolation of the overpotential-current density curve to $\eta = 0$ at high current density. The numerical values obtained for different additives at various concentrations are given in Table 38.

Bockris & co-workers (6) have indicated that for surface diffusion to be rate-determining, equation (29) should be satisfied (see page 13).

$$ZFV_o \; e^{-\eta ZF/RT} < i_o \qquad (29)$$

The values of $ZFV_o e^{-\eta ZF/RT}$ and the corresponding i_o are given in Table 38. It can be seen that for thioacetic, thiopropionic and thiobutyric acids, generally, at $i <$ 18 mA/cm^2, equation (29) is satisfied, i.e. surface-diffusion is rate-controlling. For mercaptoacetic acid, the same holds true but at $i <$10 mA/cm^2.

From Table 38, it can be seen that ZFV_o is a function of the following: 1) The current density: ZFV_o increases with increasing current density. At low current density, <10 mA/cm^2 for thioacids, ZFV_o is smaller than the corresponding i_o. For mercaptoacetic acid ZFV_o is smaller than the corresponding i_o at i <6 mA/cm^2. 2) Additive concentration: the higher the

Table 38

Surface diffusion flux as a function of current density for copper deposition from 0.5M $CuSO_4$, 1M H_2SO_4 and additives

(a) Thioacetic acid

Additive concentration (mole/l)	i_o (mA/cm^2)		Current density (mA/cm^2) 20	18	16	14	12	10	8	6	4	2
1.0×10^{-4}	7.0	ZFV_o	27	20	19	14	10	7	5	3	2	1
		$F(V_o)$*	.7	.7	.8	.7	.6	.5	.4	.3	.2	.1
3.0×10^{-5}	6.7	ZFV_o	-	31	25	19	14	11	8	6	4	2
		$F(V_o)$*	-	1.1	1.2	1.2	1.0	1.0	.9	.9	.9	.7

(b) Thiopropionic acid

7.5×10^{-6}	6.0	ZFV_o	43	37	24	18	12	9	6	4	3	1
		$F(V_o)$*	1.0	1.0	.8	.8	.6	.6	.6	.5	.4	.3

(c) Thiobutyric acid

2.5×10^{-6}	6.3	ZFV_o	31	43	38	27	20	16	11	7	5	2
		$F(V_o)$*	-	1.6	2.0	2.0	2.0	2.0	2.0	1.4	1.2	1.0

Table 38 (continued)

(d) Mercaptoacetic acid

Additive concentration (mole/l)	i_o (mA/cm^2)		Current density (mA/cm^2) 20	18	16	14	12	10	8	6	4	2
2.5×10^{-4}	4.0	ZFV_o	-	-	-	-	-	46	14	6.0	3.0	1.2
		$F(V_o)$*	-	-	-	-	-	3.0	1.1	0.5	0.3	0.15
1.0×10^{-4}	5.0	ZFV_o	-	-	-	-	234	39	17	7.0	3.0	1.0
		$F(V_o)$*	-	-	-	-	16	3.5	2.0	0.9	.45	0.2
5.0×10^{-5}	4.0	ZFV_o	-	-	-	-	-	440	42	13	5.0	2.0
		$F(V_o)$*	-	-	-	-	-	39	5.0	2.0	1.0	0.4

*$F(V_o) = ZFV_o \exp(-\eta ZF/RT)$

additive concentration the smaller is ZFV_o at a given current density. 3) Additive type: This is particularly clear in comparing thioacetic acid and mercaptoacetic acid. The former gave much smaller ZFV_o values at a given current density and additive concentration. At a current density <16 mA/cm^2 surface-diffusion is rate-controlling in the case of thioacetic acid, for mercaptoacetic acid lower current density was needed to overcome the surface-diffusion process ($i \sim 10$ mA/cm^2).

From the above points it can be concluded that ZFV_o, which represents the rate-determining step, also represents the depolarization behavior, i.e. any factor that increases the depolarization has the opposite effect on ZFV_o, and accordingly, on the rate-determining step.

Accordingly, from an understanding of the kinetics of copper deposition from acidified $CuSO_4$ containing thioacids or mercaptoacetic acid, the mechanism of depolarization can be predicted. This will be discussed in the next section.

It can be concluded from the results in Table 38 that the charge-transfer process cannot be the only rate-determining step, and surface-diffusion must play an important role in copper deposition from acidified $CuSO_4$ containing thioacids or mercaptoacetic acid as an additive. This conclusion is supported by the following facts: 1) the low steady-state overpotential obtained, 2) high exchange current density compared to the standard solution without additives and 3) the lack of applicability of the

Tafel-relation to the overpotential-current density curves. Similar results were obtained by Bockris (12) for copper deposition at low current density and also for copper deposition from standard solution on a copper electrode, the surface of which was prepared by quenching in helium. It has also been reported by Bockris (6,79,80) for Ag deposition that similar results were obtained, i.e. the inapplicability of the Tafel relation, low overpotential at the steady-state compared to that predicted by calculation for the charge-transfer process, and high exchange current density. The general explanation of this behavior was that surface diffusion of adions, from sites at which the ions are transferred across the double layer to or from those at which they are built into the lattice, is the likely rate-determining step. Since at a given current-density the rate-determining step changes from charge-transfer to surface-diffusion by a change in the way in which the cathode was prepared, Bockris (12) concluded that surface-diffusion would be shown on the type of cathode with fewer growth sites. The number of growth sites was found to be in the order of 10^9 cm^{-2}, which would be low enough to make surface-diffusion rate-determining.

The fact that there was no change in the type of electrode used in this work eliminates the possibility that the behavior of copper deposition from acidified $CuSO_4$ containing thioacids or mercaptoacetic acid might be due to the effect of the number of growth sites. It has been argued recently (14) for deposition of copper from copper

perchlorate on a copper single crystal, that the increase in the cuprous ion concentration in the diffusion layer and consequently the departure of the adion concentration from the equilibrium value could change the rate-determining step to diffusion-control. It should also be mentioned that an initial maximum was also obtained by Jenkins (14) for the cathodic and anodic galvanostatic transient and is in agreement with the results obtained here. This subject will be discussed in detail later. Similar conclusions were obtained by Ugo Bertocci (15) in which he indicated that whenever the Cu^{+} ion activity is larger than the equilibrium value, the process is said to be diffusion-controlled.

According to the above argument, it is possible to conclude for copper deposition from acidified $CuSO_4$ solution containing thioacids or mercaptoacetic acid, the following: 1) There is definite change in the mechanism of copper deposition, 2) It is most likely that surface-diffusion is the rate-determining step, and 3) The surface-diffusion mechanism cannot be explained by the number of dislocations or the number of growth sites, and therefore, 4) It is most likely that the change in the mechanism is due to the change in the cuprous ion concentration in the diffusion layer, consequently increasing the adion concentration. Therefore, the removal of the adions from the metal surface to the lattice site will be an important factor in controlling the electrodeposition. The probable causes of increased concentration of cuprous ions in the

electrode vicinity are discussed below.

Klotz, Czerlinski & Fiess (72) examined the copper complexes with thio-compounds (thiomalic and thioglycolic acids) and found that on adding copper (II) ion to the thiol solution the following reactions took place:

$$RSH + Cu(II) = \tfrac{1}{2}\ RSSR + Cu(I) + H^+ \qquad \text{-------(65)}$$

$$Cu(I) + RSH = RS - Cu(I) + H^+ \qquad \text{-------(66)}$$

so that the net result is

$$2RSH + Cu(II) = RS - Cu(I) + \tfrac{1}{2}RSSR + 2H^+ \qquad \text{-------(67)}$$

These authors found evidence for the above reaction by polarographic analysis. It was also found that β-mercaptopropionic acid did not form such a complex with copper (72). This could tie in with the fact that β-mercaptopropionic acid and similarly, 4-mercaptobutyric acid, did not cause depolarization in this work. The RS-Cu(I) complex was reported (72) to have a yellow color. Similar results have also been reported (81) when copper(II) is added to a solution of mercaptosuccinic acid. A transient blue-purple color was observed initially, and the solution developed a yellow color when the addition of copper(II) was completed. The yellow color indicated that copper(II) was reduced to copper(I) and the presence of the latter in solution was confirmed by reaction with neocuproine and subsequent extraction with chloroform (81) (see results

obtained in this work, page 149). Schinzel and Benoit (82) reported that mercaptoacids form Cu^{+} salts in water (yellow) and behave like respiratory pigments, absorbing oxygen with the formation of Cu^{++} salts (brown) which liberate oxygen at reduced pressure with regeneration of Cu^{+} salt. It is also reported (83) that thiourea undergoes the following reaction

$$2Cu^{2+} + 2C(NH_2)(NH_2)=S \rightarrow 2Cu^{+} + C(NH_2)(NH_2) - S - S - C(NH_2)(NH_2) + 2H^{+} \qquad \text{-------(68)}$$

Werner (84) studied the oxidizing action of selenous acid on organic sulfur compounds according to the following reaction

$$H_2SeO_3 + 4RSH = 2RSSR + Se + 3H_2O \qquad \text{-------(69)}$$

and reported that thioalcohols and thioacids needed extreme acidity to favor the oxidation. In diluted acid solution thioacids give a white ppt. which is a complex of the acid and H_2SeO_3. Another factor worth noting is that thioglycolic acid (mercaptoacetic acid) can be prepared from its disulfide by electroreduction in 2N H_2SO_4 solution with almost 100% efficiency (85,86).

In the light of the above discussion the results obtained in this work can be discussed as follows:

The Effect of the Sulfuric Acid on the Depolarization

As indicated previously, p.114, increasing the sulfuric acid concentration increased the depolarization

effect of the thioacids and mercaptoacetic acid (see Table 21). A typical plot of the total overpotential as a function of the sulfuric acid concentration is given in Fig. 34. It can be seen that the addition of acid caused an appreciable increase in the depolarization, but change from about 0.25 to 1.0 mole/l H_2SO_4 caused only a relatively small further increase. The effect of sulfuric acid on the depolarization ability of thioacids and mercaptoacetic acid, is most likely due to its influence on their reducing power. As mentioned previously for mercaptoacetic acid at a given concentration (see page 145), increasing the sulfuric acid concentration increased the intensity of the yellow component in the solution. This could indicate the effect of the sulfuric acid on the reducing power of the additive through its ability to reduce Cu^{++} to Cu^{+} (yellow) (72,81,82).

In the case of standard solution without additive, increasing the sulfuric acid caused an increase in the total overpotential (see Part I of Chapter III). For standard solution containing thioacid or mercaptoacetic acid, increasing the sulfuric acid concentration caused a decrease in the total overpotential. This could well indicate that the effect of the sulfuric acid is not likely due to some surface effect, but rather to chemical effect on the thioacids.

Werner (84) also mentioned that high acidity was needed to oxidize the thioacids. At 0.0M H_2SO_4, therefore, the reducing property of the thioacids is

Figure 34

Overpotential as a function of sulfuric acid concentration for thioacids

- ● 7.5×10^{-6} thiopropionic acid
- ⬢ 1.0×10^{-4} thioacetic acid
- ■ 5.0×10^{-5} thiobutyric acid

Fig. 34

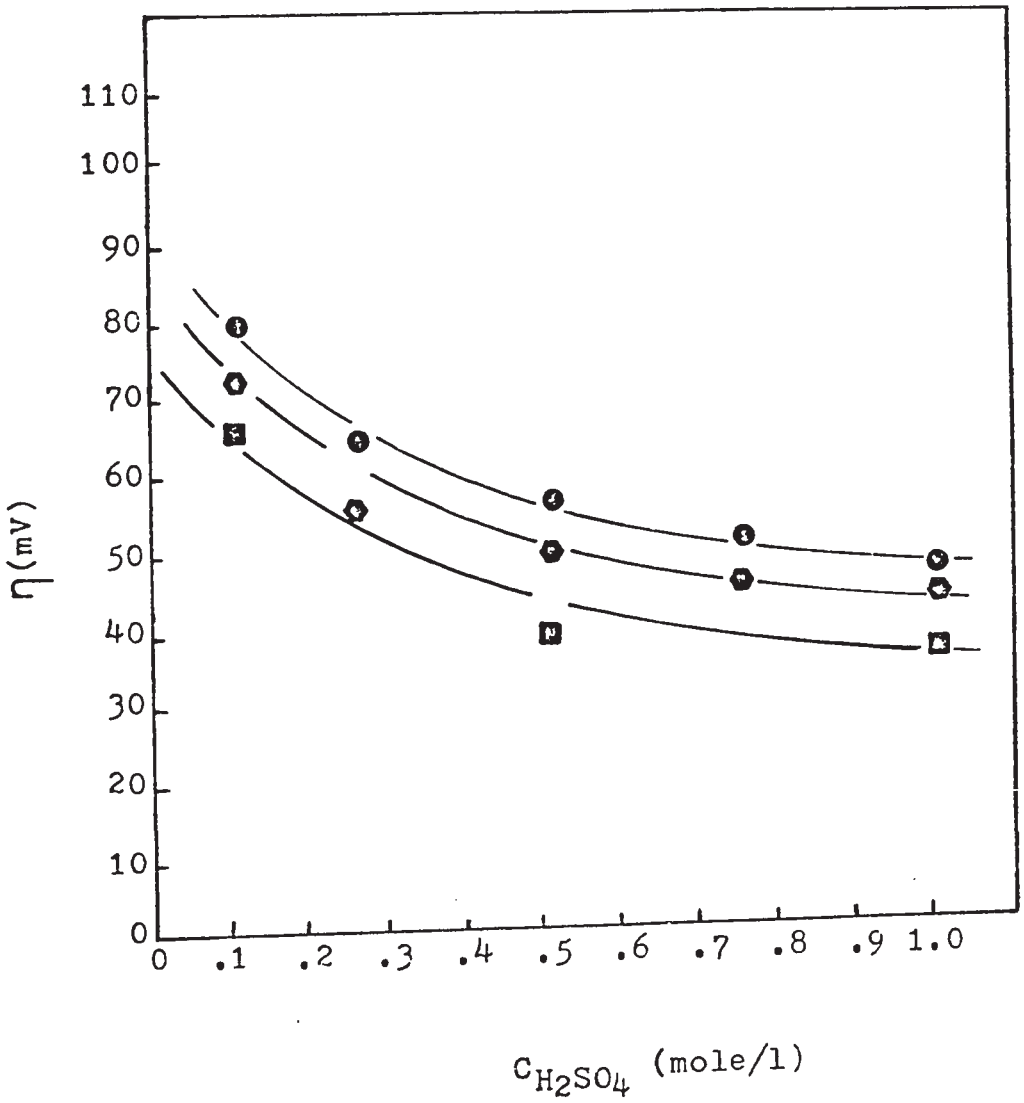
110
100
90
80
70
60
50
40
30
20
10
0
η (mV)
0
.1
.2
.3
.4
.5
.6
.7
.8
.9
1.0
$C_{H_2SO_4}$ (mole/l)

most likely zero or very small and the additives will act as normal polarizers. Increasing the acid concentration will increase the RS-Cu(I) complex or even the Cu(I) ion, equations (65) & (66), in the diffusion layer, and consequently, depolarization will take place. However, it seems that a minimum amount of acid is needed to induce reactions like (65) to (67), (compare 0.25 mole/l H_2SO_4). At acid concentrations lower than 0.25M, a mixed potential, partially polarization and partially depolarization, will be obtained (compared at 0.1 mole/l H_2SO_4).

The Effect of Additive Concentration on the Depolarization

As indicated on page 114, at a given sulfuric acid concentration, increasing the additive concentration slightly increased the depolarization effect. This behavior can be understood, bearing in mind the effect of the additive concentration on equations (65) & (66). However, increasing the sulfuric acid from 0.1 to 0.25 mole/l caused a great increase in the depolarization (e.g. 2.5×10^{-4} mole/l thioacetic). The overpotential dropped from 69 to 49 mV, while increasing the thioacetic concentration from 1.0×10^{-4} to 2.5×10^{-4}, i.e. 2.5 times, at 0.1 mole/l H_2SO_4, caused a drop in the overpotential of only 4 mV. Therefore, the effect of the additive concentration seems to be secondary in comparison to the effect of the sulfuric acid.

The Effect of Increasing the Hydrocarbon Chain on the Depolarization

Increasing the hydrocarbon portion of the molecule

of the thioacids caused a slight increase in the depolarization (page 117). This phenomenon can be connected with the polarization effect of these acids in neutral $CuSO_4$ solution. Increasing the hydrocarbon chain length caused an increase in the overpotential in neutral $CuSO_4$ solution, i.e. it increased the relative reactivity of additive toward the metal surface. Therefore, similar behavior should be expected in the case of depolarization. Since the longer the chain length of the molecule, the more stable the product RS-SR and consequently, reactions (65) & (66) are more favorable.

The Effect of Na_2SO_4 on the Depolarization Effect of the Thioacids

From the results obtained (page 143, see Table 31), it can be argued that the depolarization effect of the thioacids is independent of the ionic strength but that it is a function of the pH. A similar conclusion has been reached by Klotz, et al (72) who indicated that the addition of 0.2M KNO_3 to a solution containing RSH and Cu(II) produces no differences in behavior, but pH change produces the colored complex. This supports the fact that sulfuric acid is important for the depolarization mechanism.

At a given thioacid concentration, increasing the Na_2SO_4 concentration decreases the total overpotential up to about 1.0M Na_2SO_4, at which point the solution gave the same overpotential as a solution containing no additive. This result might arise because preferential adsorption of the positive sodium ions on the negative metal surface

replaces the additive. At high Na_2SO_4 concentration (1.0M) the additive will be ineffective, particulary because of the low additive concentration and low mobility of the sodium ions. The fact that the overpotential increment was not appreciably negative (see Table 31) indicates that there is no depolarization effect of the thioacids in the presence of Na_2SO_4.

From the results obtained one can contradict the argument given by Barnes (69) for the depolarization behavior of the thio-compounds (see page 165) in which it is assumed that these compounds replace hydrogen ions on the metal surface and on the account of their high polarizability (due to the presence of SH group), stimulate the copper deposition. If the thio-compounds do replace the hydrogen ions, they should be more strongly adsorbed on the surface, and consequently, they should cause an increase in the overpotential. Thiols, mercaptopropionic and mercaptobutyric acids, which also contain the -SH group, do not cause any depolarization. These facts suggest that the above argument by Barnes (69) is most likely erroneous.

Discussion of Qualitative Results

From the qualitative results, it can be argued that the addition of mercaptoacetic acid to $CuSO_4$, or to $CuSO_4$ containing Na_2SO_4, did not change the oxidation state of the copper ions, while its addition to acidified $CuSO_4$ caused a decrease in oxidation state.

It should be noted that the addition of thioacids to non-acidified $CuSO_4$ did not cause any change in color, however, its addition to the acidified $CuSO_4$ caused the development of a yellow color similar to the mercaptoacids. Therefore, it is most likely that mercaptoacetic acid forms a curpous complex with the copper ions in acidified $CuSO_4$. Accordingly, and from the last part of the qualitative results, page 146, it can be argued that the depolarization effect of a thioacid or of mercaptoacetic acid must be due to the cuprous complex formation.

Discussion of Polarographic Results

These results, page 146, support the previous argument that acidified solution is needed for the oxidation of the RSH, and consequently, for the reduction of copper II ions. The shift of the new cathodic wave(2) obtained (see Table 33), and its increase with increasing sulfuric acid concentration, could indicate the formation of cuprous complex. In the case of 0.01M $CuSO_4$, 0.0M H_2SO_4 and $1.0x10^{-4}$M thiobutyric acid, both waves(1) and (2) were obtained which could indicate that there is a slight possibility of the formation of cuprous complex.

As a further check for the proposed depolarization, a test was made for the presence of cuprous ion. The results indicated the presence of these ions when thioacids or mercaptoacetic acid were added to acidified $CuSO_4$ solution.

Microscopic Examination of Surfaces

The results of the microscopic examination (see page 151) of the electrodeposited surface indicated that there is no marked difference between the surface obtained by electrodeposition from standard solution with and without the additives. Therefore, it is possible to exclude the idea that depolarization might be due to an increase in the roughness of the surface with a consequent decrease in the true current density. Similar conclusions have been reached before (77).

The Depolarization Effect of Mercaptoacids

The relative effectiveness of mercaptoacetic acid in decreasing the total overpotential is slightly less than for the corresponding thioacids, i.e. thioacetic acid (see Tables 21 & 26). Comparing the effect of mercaptopropionic acid and mercaptobutyric acid to the corresponding thiopropionic and thiobutyric from the results obtained in Table 18 & 21, it can be seen that while the depolarization increased slightly from the thiopropionic to thiobutyric, mercaptopropionic and mercaptobutyric acids did not cause depolarization with any sulfuric acid concentration. Accordingly, it can be concluded that not only the presence of the -SH group is required to cause depolarization, but also a strong electron-withdrawing group close to it. This will explain the fact that mercaptoacetic showed less ability to depolarize than thioacetic since the -SH group is further away from the carboxyl group. For mercaptopropionic and

mercaptobutyric acids, the depolarizing effect of the -SH group will completely disappear and the additives will act as normal polarizers. Supporting evidence for this conclusion is found in work done by Klotz et al. (72) in which thiomalic acid gave a strongly colored complex with copper ions, thioglycolic gave a less strongly colored complex while β-mercaptopropionic acid did not form such a complex with copper. It has also been suggested by Fernando & Freiser (87) that β-mercaptopropionic acid is much more stable than thioglycolic acid, which is readily oxidized to dithioglycolic acid. In addition, Sukava et al. (17) have found that β-mercaptopropionic acid cause only an increase in the overpotential of copper electrodeposition, which agrees with this work.

From the above discussion the mechanism of the depolarization behavior of the thioacids and mercaptoacetic acid can be summarized as follows: 1) In non-acidified $CuSO_4$ solution these additives behave as normal polarizers, 2) In acidified $CuSC_4$ solution, the additives reduce the cupric ions to either cuprous ion or most likely cuprous complex from which discharge takes place. The fact that small amounts of additive can cause appreciable depolarization for long periods of electrolysis ($\sim$ 12 hours) could indicate that the cuprous complex is most likely preferentially adsorbed on the metal surface. On discharging the cuprous ion, the additive part of the complex will be free to enter the reaction again (43).

3) The presence of -SH group alone is insufficient to cause depolarization (thiols, mercaptopropionic, and mercapto-butyric acids). Accordingly, the assumption that depolarization might be due to the high polarizability of the -SH group and its stimulation of the discharge process can be excluded. 4) It is unlikely that depolarization is due to any increase in the true surface area. 5) Since the discharge process will take place from a cuprous ion or cuprous complex, a change in the mechanism of deposition can be expected.

From the above points the mechanism of copper deposition in the presence of depolarizer is most probably as follows:

$$Cu^{+} + e \longrightarrow Cu_{ad} \qquad \text{-------(70)}$$

$$Cu_{ad} \xrightarrow{\text{surface diffusion}} Cu_{latt.} \qquad \text{-------(71)}$$

Or

$$RS - Cu(I) + e \longrightarrow Cu_{ad} + RS^{-} \qquad \text{-------(72)}$$

$$Cu_{ad} \xrightarrow{\text{surface diffusion}} Cu_{latt.} \qquad (71)$$

Reactions (70) or (72) are known to be fast (10, 12). Therefore, it is most likely that reaction (71) is the rate-dtermining step, i.e. the rate of removal of the adions will be rate-controlling. This argument agrees with the results obtained from the kinetics of deposition considering the overpotential-current density relation in which surface-diffusion was concluded to be rate determining.

On the basis of the above mechanism, it can be predicted that if the current density increases above 20 mA/cm^2, a mixed mechanism will take place. Further increase in current density might cause a complete change in mechanism, i.e. when the current density is high enough to consume all the cuprous ions supplied by the additives, as soon as they arrive at the metal surface, the discharge process must also begin to take place from the cupric ions. Accordingly, a charge-transfer mechanism will become rate-controlling. This prediction is in agreement with the results obtained by Sukava et al (42) in which the addition of cystine to solutions containing mercaptoacetic acid caused an intermediate overpotential. Since the mercaptoacetic acid acts on the mechanism of deposition and the cystine acts on the surface of the metal by adsorption to increase the current density, an intermediate overpotential will be expected. Results obtained by Shrier & Smith (43) also agree with this prediction.

Discussion of the Initial Maximum Overpotential

Initial maximum overpotential, at the beginning of electrolysis, has been observed and reported by several authors (20,69,70,71,88,89) similar to the one reported in this work (see page 117 & Table 23). Vermilyea(89) had analyzed the long-time transient behavior of a metallic electrode subjected to a current pulse. The analysis was based on the spiral growth model and assumed that if there is partial surface-diffusion control of the rate of deposition, it follows that there is initially a large overpoten-

tial corresponding to a relatively large distance between steps; a decrease in the overpotential would then be observed over a period of time corresponding to the shortening of the distance between steps as the growth spiral winds up. This assumption has been supported experimentally (89,90) in copper deposition and also with zinc, which show a transient lasting for about 0.5 second. Transients were also observed by Essin, Antropov, and Levin (91,92) during deposition of copper from very pure copper sulfate solution. The initial overpotential was higher than the steady value, and the difference increased with increasing current density. These transients lasted for a few minutes at about 1 mA/cm^2. It was also noted by Vermilyea (89) that if the steady-state current was interrupted for about a second, the overpotential was unchanged upon reapplication of the current. After a minute, there was a transient smaller than the original, and about an hour was required to restore the initial conditions and produce the same high overpotential transient. Identical results were obtained with the initial overpotential in this work. Fig. 35 shows a replot of one of the curves for zinc deposition at a current density of 1 mA/cm^2, which shows transient lasting for about 0.05 seconds (90). Jenkin's (14) explanation of this phenomenon can be summarized as follows. The dependence of the overpotential on time can be understood if it is assumed that surface diffusion coefficients are much smaller than those for

tial corresponding to a relatively large distance between steps; a decrease in the overpotential would then be observed over a period of time corresponding to the shortening of the distance between steps as the growth spiral winds up. This assumption has been supported experimentally (89,90) in copper deposition and also with zinc, which show a transient lasting for about 0.5 second. Transients were also observed by Essin, Antropov, and Levin (91,92) during deposition of copper from very pure copper sulfate solution. The initial overpotential was higher than the steady value, and the difference increased with increasing current density. These transients lasted for a few minutes at about 1 mA/cm^2. It was also noted by Vermilyea (89) that if the steady-state current was interrupted for about a second, the overpotential was unchanged upon reapplication of the current. After a minute, there was a transient smaller than the original, and about an hour was required to restore the initial conditions and produce the same high overpotential transient. Identical results were obtained with the initial overpotential in this work. Fig. 35 shows a replot of one of the curves for zinc deposition at a current density of 1 mA/cm^2, which shows transient lasting for about 0.05 seconds (90). Jenkin's (14) explanation of this phenomenon can be summarized as follows. The dependence of the overpotential on time can be understood if it is assumed that surface diffusion coefficients are much smaller than those for

Figure 35

a) Voltage variation during deposition from 1M $ZnSO_4$ solution onto a single crystal of zinc at a current density of the order of 1 mA/cm^2.
This report was taken from reference (89).

b) Overpotential-time relation for Ag deposition

$$i = 500\ mA/cm^2$$

This figure was taken from the original reference(6).

Fig. 35

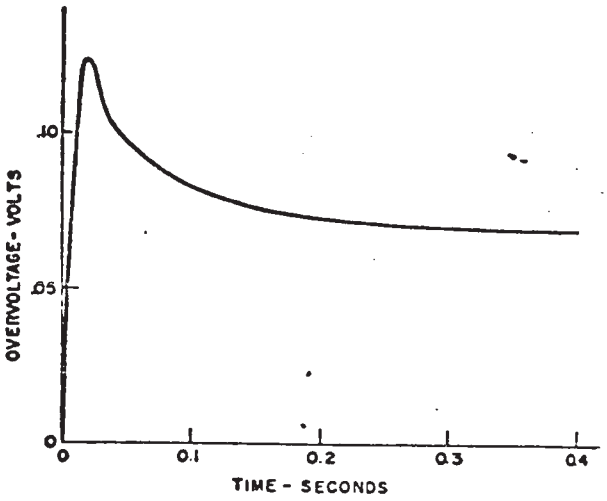
OVERVOLTAGE - VOLTS
.10
.05
0
0
0.1
0.2
0.3
0.4
TIME - SECONDS

a

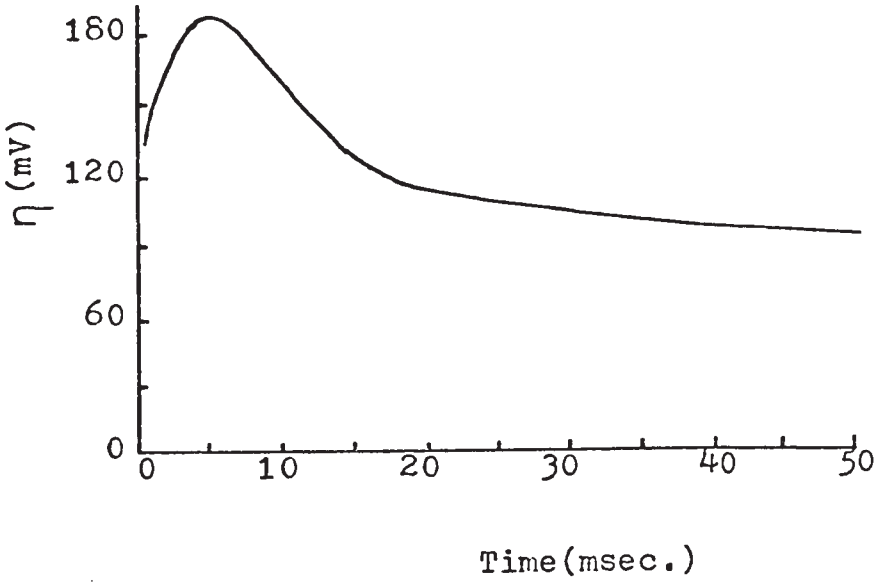
η (mV)
180
120
60
0
0
10
20
30
40
50
Time(msec.)

b

similar processes in solution, and if it is assumed that the exchange of adatoms at steps are hindered in some manner. On closing a circuit, the initial current is carried largely without reaction at the steps. As the surface concentration of adatoms changes rapidly from the equilibrium value, other necessary events occur such that the conditions required for steps to act as sources or sinks for adatoms are established. Therefore, reaction begins to occur at steps, and continued reaction produces gradual changes in surface adatom concentration toward the equilibrium value in efforts to establish the steady-state concentration. However, under the given experimental conditions, the net flux of adatoms at steps was assumed to be such that the theoretical steady-state surface adatom concentration was slow in being established, since most of the adatom flux at steps served largely to support the net reaction rather than to change the average surface concentration of the species (as will be seen later). It is also proposed that voltage-time relationships are influenced by events occurring at the metal-solution interface. Obviously such a mechanism assumes the occurrence of time-dependent phenomena.

Accordingly, it can be assumed that if the steady-state process is surface-diffusion controlled, an initial maximum should be observed on starting the electrolysis. Since an initial maximum was obtained with all additives that caused depolarization, then surface-diffusion is likely to be rate-determining. This agrees with the results ob-

tained previously (see pages 166, 183).

Discussion of the Factors Affecting the Initial Maxima

From the x-ray diffraction of the powder collected from the surface of the copper electrode after immersion in $CuSO_4$ electrolyte containing thioacids (see page 139), it was found that a non-stiochiometric copper sulfide was formed on the surface of the copper. The experimental results for the effect of H_2S (see page 141) and the immersion time-initial overpotential relation (see page 128) also indicate that the tarnishing of the copper surface, most likely due to formation of copper sulfide, is a contributing factor in the initial overpotential. The sulfurization of copper is well known, due to the high reactivity of copper to sulfur. The tarnishing process of copper has been studied by several authors (93,94,95). The effect of elementary sulfur dissolved in organic liquids (93) on copper results in a highly porous deposit appearing as black or grey spots of copper sulfide with a composition varying between $Cu_{1.66}S$ and $Cu_{1.88}S$. The sulfurization of copper has also been studied using different sulfur-containing organic compounds (thiourea, diphenylthiourea, diethyldisulfide and diethyltrisulfide) by Llopis, Gamboa & Arizmendi (94,95). The results obtained (94,95) indicate the formation of a non-stiochiometric sulfide with the approximate composition Cu_2S. Gorbunova & Suntiagina (96) have studied the effect of S-containing additives (thioacetic acid, thiourea, etc.) on the electrodeposition of Ni from $NiSO_4$ electrolyte,

and it was found that the sulfur content in the deposits increased with increasing solution acidity and increasing concentration of the additives. The sulfur content (96) was found to be due mainly to nickel sulfide.

The effect of sulfuric acid and additive concentration on the initial overpotential maximum obtained in this work for thioacids and mercaptoacetic acid agrees with the results obtained by Gorburnova & Sutiagina (96). The effect of additive concentration can be easily understood, since increasing this concentration will increase the rate of sulfurization, and consequently increase the initial maximum. The effect of sulfuric acid, which is not directly involved in the sulfurization, is most likely to enhance the reactivity of the additive (95). The effect of deoxygenation on the initial overpotential (see page 134) indicated that there was no significant effect if the electrode was immersed after stopping the nitrogen bubbling. However, if bubbling took place while the electrode was immersed in the solution, the initial overpotential increased. With this experimental fact and with the effect of immersion time on the inital overpotential, it is possible to argue that sulfurization of the copper surface is diffusion-controlled, i.e. the diffusion of the additive from the bulk of the solution to the metal surface is rate-determining. This is supported by the fact that plotting the initial overpotential as a function of $t^{\frac{1}{2}}$ as seen in Fig. 27 gave a linear relation, indicating that the rate of sulfurization is diffusion controlled

(30,97).

Discussion of the Initial Overpotential-Current Density Relation

From the results obtained (see page 125, Table 23 and Fig. 26), it can be argued that initially charge-transfer is the rate-determining step. It can also be argued that τ_{max} is a direct function of the rate of formation of fresh copper surface. The initial overpotential obtained in the presence of mercaptoacetic acid occurred for a short duration, $\tau_{max} < 20$ msec., compared to that obtained when thioacids were used, $\tau_{max} \sim 27$ sec. This can be attributed to a difference in reactivity of these additives and consequently, a difference in the amount of sulfurization. In the case of mercaptoacetic acid only very light tarnishing was obtained, therefore, only a short period of time was required to reach the steady-state value. For thioacids, a dark heavy tarnishing was obtained, and a longer time was needed to reach the stage where deposition takes place on fresh copper surface. This argument can also be supported by the observation that mercaptoacetic acid was less effective in causing depolarization relative to thioacetic acid, i.e. the former was less reactive (see Table 21 & 26).

General Discussion of the Initial Overpotential

From the experimental results and the preceding discussion, the following points may be noted: 1) On immersing the copper electrode in $CuSO_4$ solution containing thioacids or mercaptoacetic acid, a dark brown film was

formed on the surface of the copper. This has been identified as a non-stoichiometric form of copper sulfide. 2) On closing the circuit, copper deposition will commence, but due to the presence of Cu_2S on the copper surface, the exchange process involving the adatoms will be hindered (14). Due to the coverage of the surface by a sulfide film, high overpotentials will be obtained corresponding to high local current density. The adatom concentration at this instant will be much less than the equilibrium value, consequently, charge-transfer will be rate-controlling. The reaction produces gradual changes in the surface adatom concentration toward the equilibrium value as the sulfide film is covered or occluded in the newly deposited layer of copper. Simultaneously, the approach to equilibrium adatom concentration and the formation of a clean copper surface will change the rate-determining step from charge-transfer to surface diffusion. 3) The overpotential will gradually decrease to establish the steady-state value.

Since the sulfurization process is most probably diffusion controlled, that is, it is much slower than the arrival of copper ions to the surface, a fresh copper surface will be obtained after a short period of electrolysis. After the fresh surface is achieved, the steady-state process will normally take place. To support this argument, it may be noted that on interrupting the electrolysis for only a few minutes, no initial maximum overpotential was observed. A long cessation of current flow was required to

restore the conditions for the initial maximum overpotential. This is consistent with the argument that the initial overpotential was most probably due to sulfurization of the copper surface, and secondly, that sulfurization was probably diffusion controlled.

PART IV

Results & Discussion of Group III Addition Agents

1) Results:

This group includes the dihydroxy compounds, the diols. These compounds, similar to Group I additives, increase the steady-state overpotential during copper electrodeposition. An alternation similar to the dicarboxylic acids was observed in the effectiveness of the diols in increasing the steady-state overpotential. Steady-state overpotentials as a function of additive concentration are shown in Fig. 36. Generally, a higher concentration was needed to give any significant increase in the overpotential than that required with Group I compounds. The numerical values are given in Table 39. For a given diol, the overpotential increases with increasing concentration of the additive. Generally, diols with an odd number of carbon atoms are more effective than those with an even number in increasing the overpotential. This is easily seen by comparing 1,3 propanediol to 1,4 butanediol and 1,5 pentanediol to 1,6 hexanediol. However, the expected increase in overpotential on increasing the chain length from 1,3 propanediol to 1,5 pentanediol was not observed. Instead, 1,5 pentanediol was found to be less effective in increasing the overpotential than 1,3 propanediol. It should be reported that the 1,3 butanediol used in this study was a mixture of the d & l form, and gave a slightly higher overpotential increment than the 1,4 butanediol.

Figure 36

Overpotential increment as a function of additive concentration for diols ($\Delta\eta$ vs. log C)

○ 1,2 ethanediol

⊖ 1,3 propanediol

▲ 1,4 butanediol

■ 1,3 butanediol

● 1,5 pentanediol

△ 1,6 hexanediol

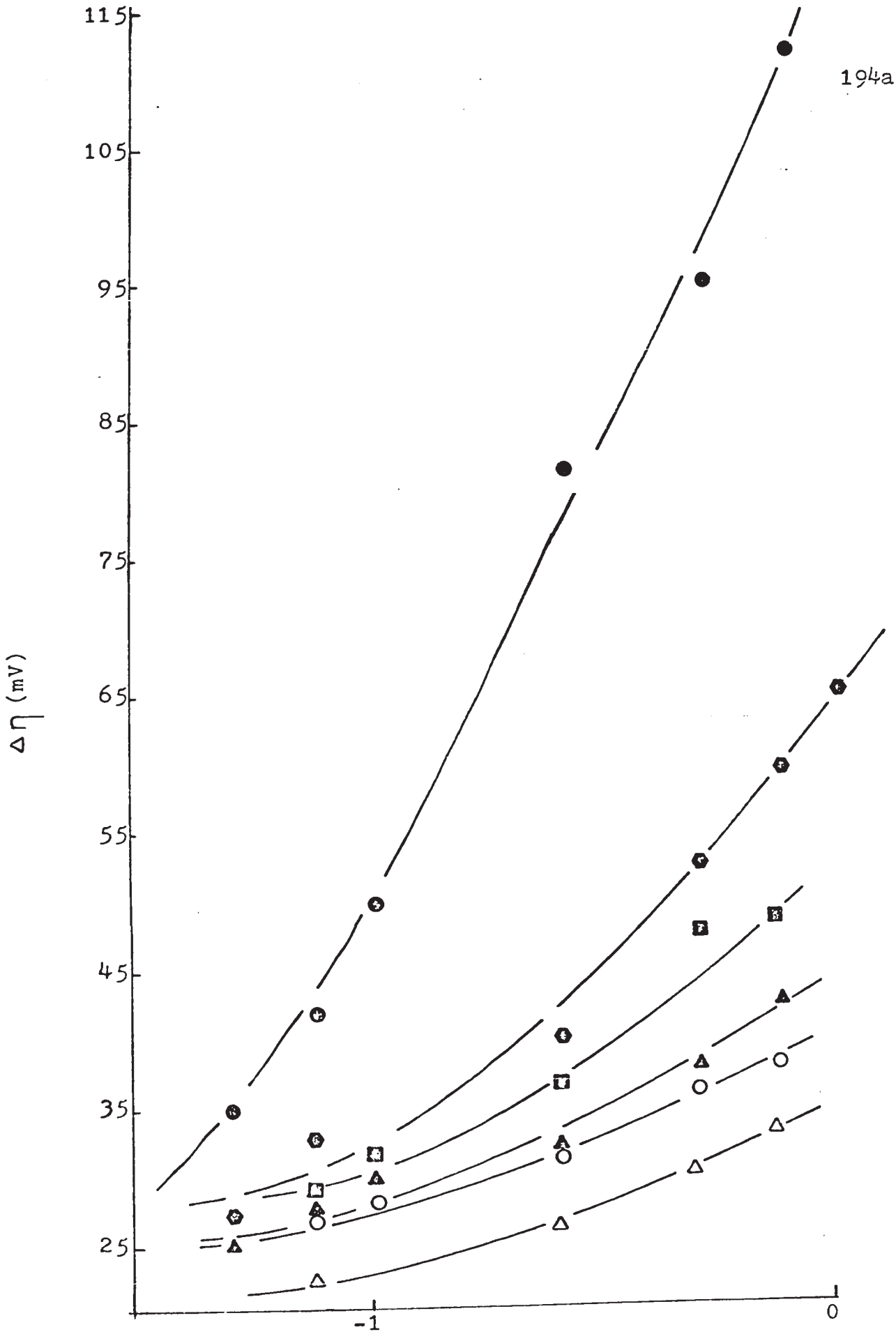

Fig. 36

Table 39

Overpotential as a function of additive concentration for copper deposition

Current density = 20 mA/cm^2

(a) 1,2 Ethanediol

Additive concentration (mole/l)	Overpotential Increment (mV)
5.0×10^{-2}	25
7.5×10^{-2}	27
1.0×10^{-1}	28
2.5×10^{-1}	31
5.0×10^{-1}	36
7.5×10^{-1}	38

(b) 1,3 Propanediol

Additive concentration (mole/l)	Overpotential Increment (mV)
5.0×10^{-2}	35
7.5×10^{-2}	42
1.0×10^{-1}	50
2.5×10^{-1}	83
5.0×10^{-1}	96
7.5×10^{-1}	113

(c) 1,4 Butanediol

Additive concentration (mole/l)	Overpotential Increment (mV)
5.0×10^{-2}	25
7.5×10^{-2}	28
1.0×10^{-1}	30
2.5×10^{-1}	32
5.0×10^{-1}	38
7.5×10^{-1}	43

Table 39 (continued)

(d) 1,5 Pentanediol

Additive concentration (mole/l)	Overpotential Increment (mV)
5.0×10^{-2}	27
7.5×10^{-2}	33
1.0×10^{-1}	40
2.5×10^{-1}	53
5.0×10^{-1}	60
7.5×10^{-1}	66

(e) 1,6 Hexanediol

Additive concentration (mole/l)	Overpotential Increment (mV)
5.0×10^{-2}	19
7.5×10^{-2}	22
1.0×10^{-1}	24
2.5×10^{-1}	26
5.0×10^{-1}	30
7.5×10^{-1}	37

(f) 1,3 Butanediol

Additive concentration (mole/l)	Overpotential Increment (mV)
5.0×10^{-2}	27
7.5×10^{-2}	29
1.0×10^{-1}	32.5
2.5×10^{-1}	37
5.0×10^{-1}	48
7.5×10^{-1}	49

?) Discussion:

As seen from the results (page 193), alternating behavior was observed with increasing chain length for the effect of these additives on the cathode overpotential. (It should be mentioned that 1,3 propanediol and 1,5 pentanediol have a distinct odor while 1,4 butanediol and 1,6 hexanediol do not, which is another indication that alternation in the physical properties of these compounds occurs).

A typical plot of the overpotential increment vs. concentration is shown in Fig. 37. The initial slopes $(\Delta\eta/C)_{C\to 0}$ were obtained for all the additives in this group and the ΔG_a^o values were calculated according to Equation (59)

$$(\Delta\eta/C)_{C\to 0} = \frac{2b}{55.5}\, e^{-(\Delta G_a^o)_{\theta=0}/RT} \qquad (59)$$

It should be noted that there was considerable difficulty in obtaining the inital slope with ethanediol, 1,4 butanediol, and 1,6 hexanediol, and the corresponding ΔG_a^o values are uncertain. The numerical values for the slopes and the apparent standard free energies of adsorption are given in Table 40.

The plot of $\mathrm{Log}(\Delta\eta/C)_{C\to 0}$ vs. x, the number of carbon atoms in diol molecules, is shown in Fig. 38. It is clear that an alternation behavior exists. Fig. 38 also indicates that the degree of alternation decreases with increasing number of carbon atoms. The same argument which

Figure 37

Overpotential increment as a function of additive concentration for 1,3 propanediol ($\Delta\eta$ vs. C)

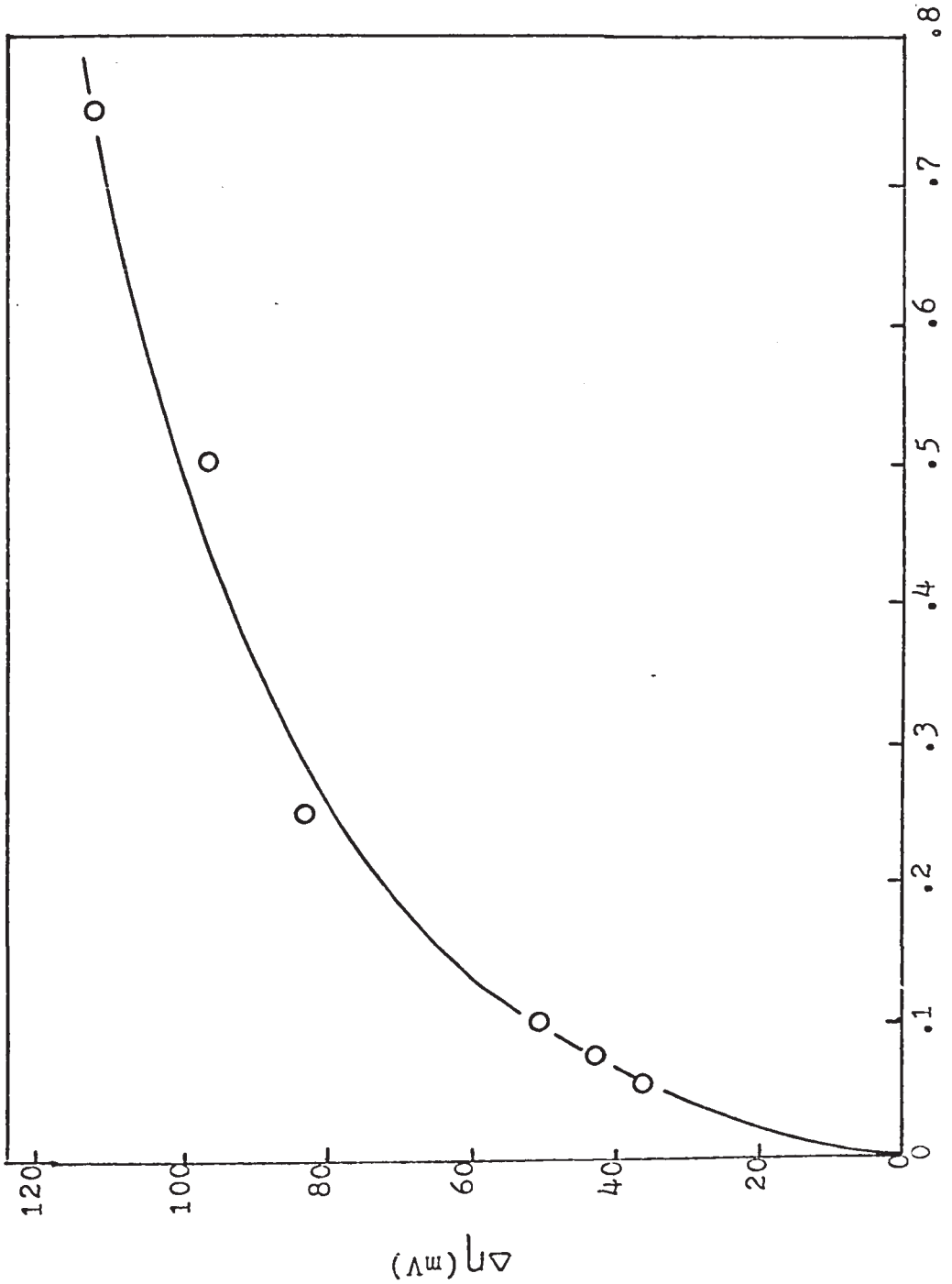

Fig. 37

Table 40

Initial slope $(\Delta\eta/C)_{C\to 0}$ and the standard free energy of adsorption for the diols

Additive	$\text{Log}(\Delta\eta/C)_{C\to 0}$	$(\Delta\eta/C)_{C\to 0}$	$-\Delta G_a^o$(Kcal/mole)
1,2 ethanediol	2.5250	$3.35\text{x}10^2$	3.10
1,4 butanediol	2.5855	$3.85\text{x}10^2$	3.20
1,6 hexanediol	2.6628	$4.60\text{x}10^2$	3.30
1,3 propanediol	2.9542	$9.00\text{x}10^2$	3.70
1,5 pentanediol	2.8262	$6.70\text{x}10^2$	3.53
1,3 butanediol	2.7260	$5.20\text{x}10^2$	3.38

Figure 38

Logarithm of the initial slope $(\Delta\eta/c)_{c\to 0}$ vs. number of methylene groups in the diol molecule

△ 1,3 butanediol

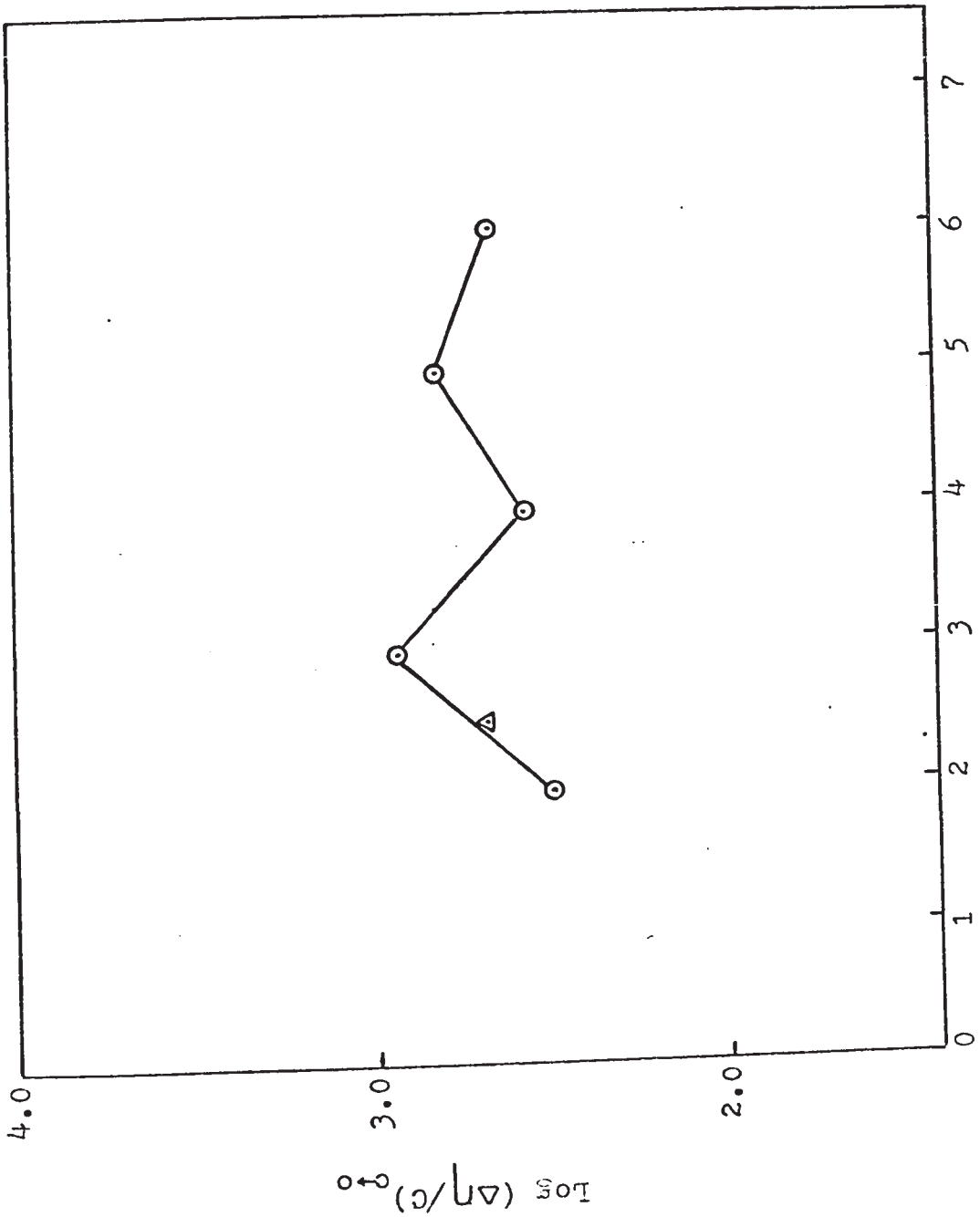

Fig. 38

applied for dicarboxylic acids with (ENCA) and (ONCA) can be used to explain the behavior of the diols. That is, diols with (ONCA) most likely form two-point attachments with the copper surface, and consequently a higher free energy of adsorption is expected, whereas diols with (ENCA) with the two hydroxyl group in trans-configuration can only adsorb with one functional group. The non-adsorbing group will most likely be solvated.

Considering 1,3 propanediol, the internuclear distance between the two hydroxyl groups is 2.49Å, which matches closely the shortest internuclear distance of the copper lattice. Therefore, strain-free two-point adsorption might be possible.

In the case of 1,5 pentanediol, the internuclear distance between the two hydroxyl groups is 4.9Å, which is different than the closest internuclear distance of the copper lattice, 5.1Å. (about 4Å). Due also to the high solvation power of the hydroxyl group, a total contribution from each part of the molecule to the adsorption free energy cannot be expected.

Considering the fact that the hydroxyl group can be more solvated than the carboxyl group, the behavior of the 1,5 pentanediol relative to the 1,3 propanediol can be understood.

1,3 butanediol was a mixture of the d- and l-forms, and accordingly, no definite conclusions can be drawn about the effect of structural differences. However, if it is

assumed that the 1,3 butanediol is a 50-50 mixture of the d & l configurations, its free energy of adsorption, and consequently its $\log(\Delta\eta/C)_{C\to 0}$ value, should be between that of the trans-1,2 ethanediol and the cis- 1,3 propanediol. This assumption agrees very well with the experimental results (see Fig. 38).

In the case of 1,2 ethanediol, 1,4 butanediol and 1,6 hexanediol, adsorption is likely to take place with one-point attachment, while the non-adsorbing hydroxyl group will be solvated.

The increase in the standard free energy of adsorption from 1,2 ethanediol to 1,6 hexanediol is very small. This could be attributed to the strong solvation power of the hydroxyl group.

The free energy of adsorption of the hydroxyl group could be predicted from the results obtained for 1,3 propanediol, in which each part of the molecule contributes to the free energy of adsorption. Assuming the average value of $\Delta G^{o}_{CH_2}$ is -760 cal/mole, the total contribution from the hydrocarbon part of the molecule is -2280 cal/mole. Accordingly, each hydroxyl group will contribute an average of -710 cal/mole to the free energy of adsorption (see Table 40). This result agrees with that obtained by Demaskin & Survilla (64) for the adsorption of aliphatic alcohols on mercury on the basis of differential capacitance measurements, $\Delta G^{o}_{OH} = -770$ cal/mole.

From the results of thioacids (page 155), thiols (page 159), and monocarboxylic acids (page 83), the following equation can be introduced:

$$\begin{array}{cccccccc} & -COSH & + & -OH & = & -COOH & + & -SH \\ \Delta G^{\circ}_{a} & = & -7.15 & + & ? & = & -1.57 & + & -6.37 \text{ Kcal/mole} \end{array}$$

-------(73)

Accordingly, ΔG°_{OH} can be calculated. The average value of ΔG°_{OH} was found to be -790 cal/mole and for $\Delta G^{\circ}_{C=O}$ -780 cal/mole. This results in satisfactory agreement with the value obtained for 1,3 propanediol.

From the value of ΔG°_{OH}, it can be predicted that adsorption of aliphatic monofunctional alcohols with the functional group toward the metal is not strongly favored, since its free energy of adsorption is approximately the same as that of the methylene group. Since the hydroxyl group is much more hydrophilic than the hydrocarbon part of molecule, adsorption with the hydrocarbon part of the molecule will be more likely. This is in complete agreement with the results obtained in experiments on the adsorption of aliphatic monofunctional alcohols on a copper electrode (97), and in turn, it supports the results obtained in this work.

From the results of thioacids (page 155), thiols (page 159), and monocarboxylic acids (page 83), the following equation can be introduced:

$$\begin{array}{cccccccc} & -COSH & + & -OH & = & -COOH & + & -SH \\ \Delta G_a^o = & -7.15 & + & ? & = & -1.57 & + & -6.37 \text{ Kcal/mole} \end{array}$$

-------(73)

Accordingly, ΔG_{OH}^o can be calculated. The average value of ΔG_{OH}^o was found to be -790 cal/mole and for $\Delta G_{C=O}^o$ = -780 cal/mole. This results in satisfactory agreement with the value obtained for 1,3 propanediol.

From the value of ΔG_{OH}^o, it can be predicted that adsorption of aliphatic monofunctional alcohols with the functional group toward the metal is not strongly favored, since its free energy of adsorption is approximately the same as that of the methylene group. Since the hydroxyl group is much more hydrophilic than the hydrocarbon part of molecule, adsorption with the hydrocarbon part of the molecule will be more likely. This is in complete agreement with the results obtained in experiments on the adsorption of aliphatic monofunctional alcohols on a copper electrode (97), and in turn, it supports the results obtained in this work.

PART V

Results & Discussion of Group IV Addition Agents

1) Results:

Similar to Group I and III, the compounds in Group IV caused an increase in the steady-state overpotential during electrodeposition of copper. The effectiveness of cyclohexanol was much less than that of cyclohexanecarboxylic acid. However, the unsaturated (i.e. aromatic) benzoic acid was much more effective than the corresponding saturated cyclohexanecarboxylic acid. 1,2 (cis) cyclohexanedicarboxylic acid is slightly more effective than the corresponding monofunctional compound, but less effective than 1,2 benzenedicarboxylic acid, phthalic acid. The latter in turn is more effective than the corresponding monofunctional benzoic acid. 1,3 benzenedicarboxylic acid, isophthalic acid, was also used as an additive, but due to solubility problems, only qualitative results were obtained. The above results are shown in Fig. 39 and numerical values are given in Table 41.

2) Discussion:

Benzoic, Phthalic & Isophthalic Acids

The relative effectiveness of these additives in increasing the cathode overpotential was found to be fairly high. The adsorption of aromatic compounds on a metal surface, particularly mercury, has been studied (24,25,53). In particular, the adsorption of aromatic amines on mercury has been studied in some detail by Conway & Barradas (25, 53) and by Bockris, et al. (24). Their results can be

Figure 39

Overpotential increment as a function of additive concentration ($\Delta\eta$ vs. log c)

- ● Phthalic acid
- ⬢ Benzoic acid
- ■ 1,2-cis-cyclohexanedicarboxylic acids
- ▲ Cyclohexanecarboxylic acid
- ⊙ Cyclohexanol
- ◐ Phenol

Figure 39

Overpotential increment as a function of additive concentration ($\Delta\eta$ vs. log c)

● Phthalic acid

● Benzoic acid

■ 1,2-cis-cyclohexanedicarboxylic acids

▲ Cyclohexanecarboxylic acid

⊙ Cyclohexanol

◐ Phenol

Fig. 39

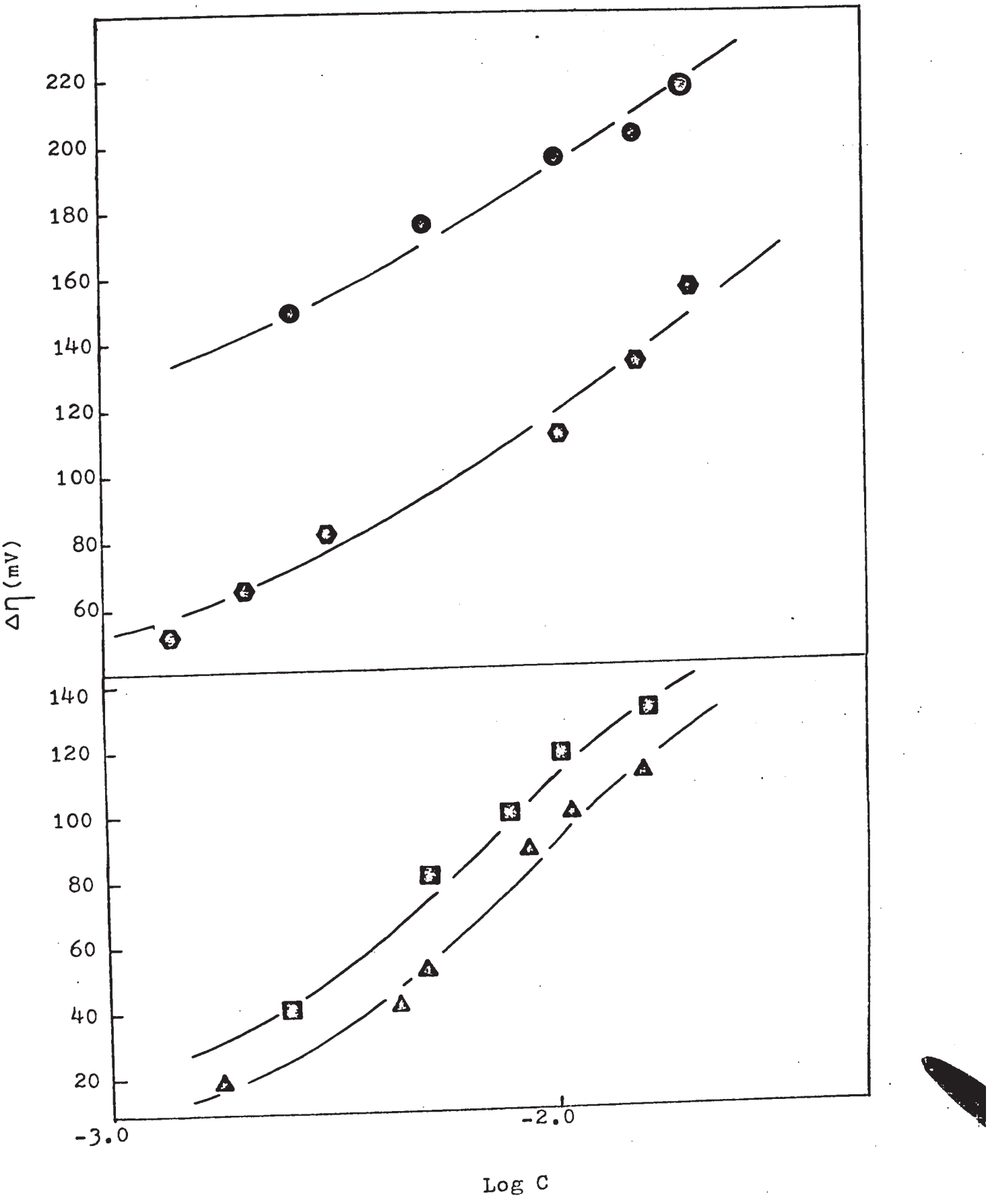
220
200
180
160
140
120
100
80
60
Δη (mV)
140
120
100
80
60
40
20
-3.0
-2.0
Log C

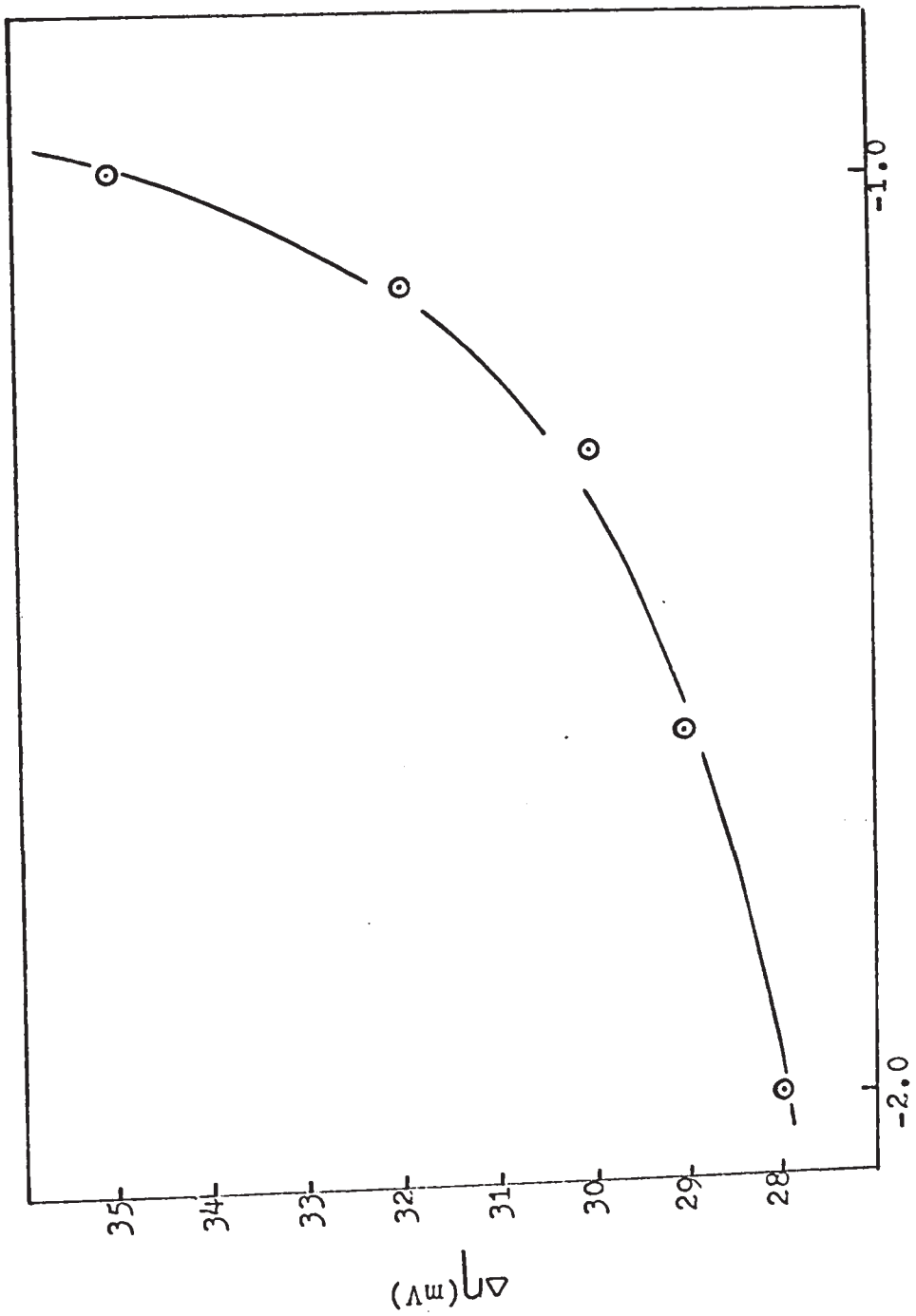

Fig. 39

Fig. 39

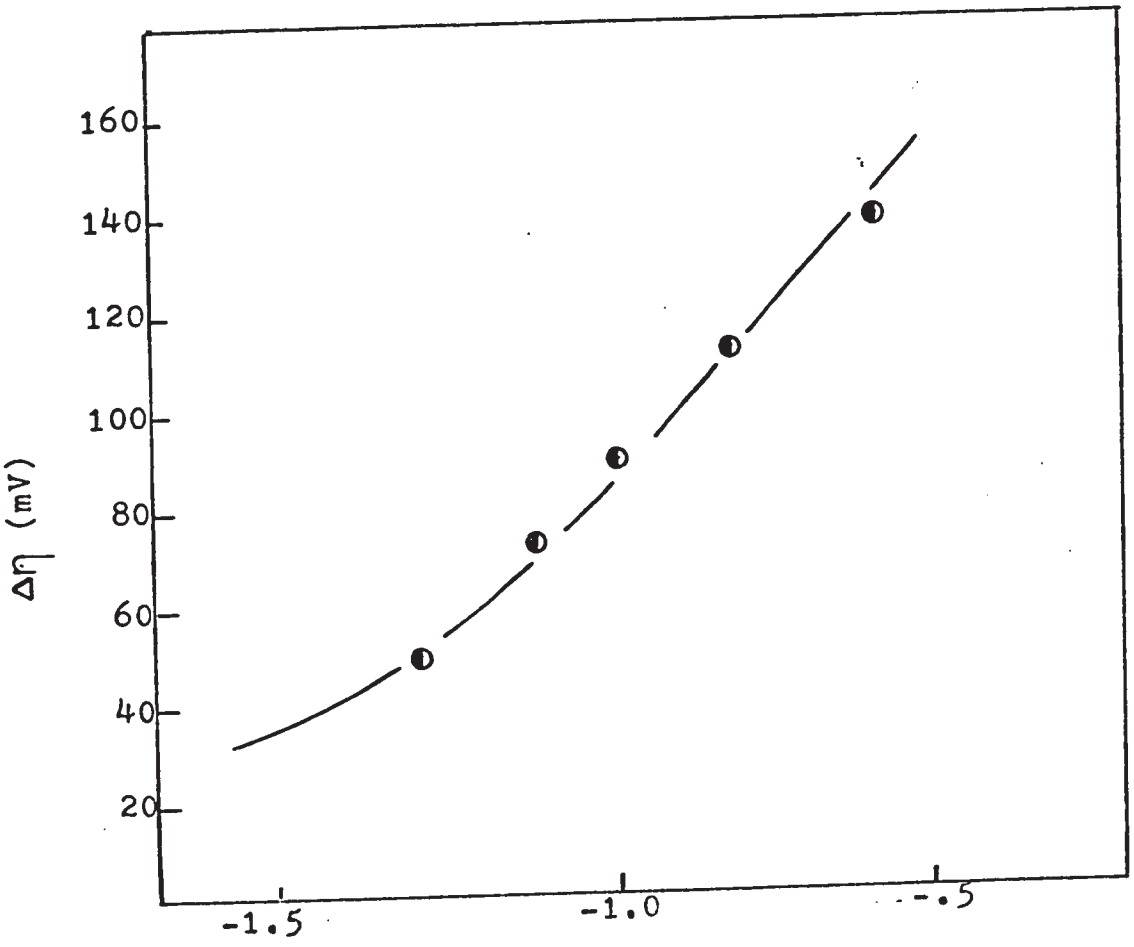

Table 41

Overpotential as a function of additive concentration for copper deposition

Current density = 20 mA/cm^2

(a) Cyclohexanol

Additive concentration (mole/l)	Overpotential Increment (mV)
1.0×10^{-2}	18
2.5×10^{-2}	29
5.0×10^{-2}	30
7.5×10^{-2}	32
1.0×10^{-1}	35

(b) Cyclohexanecarboxylic acid

Additive concentration (mole/l)	Overpotential Increment (mV)
1.8×10^{-3}	18
4.4×10^{-3}	40
5.2×10^{-3}	52
8.8×10^{-3}	88
1.07×10^{-2}	98
1.6×10^{-2}	110

(c) 1,2 - cis-cyclohexanedicarboxylic acid

Additive concentration (mole/l)	Overpotential Increment (mV)
2.5×10^{-3}	40
5.2×10^{-3}	82
8.0×10^{-3}	100
1.02×10^{-2}	117
1.60×10^{-2}	130

Table 41 (continued)

(d) Benzoic acid

Additive concentration (mole/l)	Overpotential Increment (mV)
7.0×10^{-4}	50
1.0×10^{-3}	64
5.0×10^{-3}	110
7.5×10^{-3}	132
1.0×10^{-2}	154

(e) Phthalic acid

Additive concentration (mole/l)	Overpotential Increment (mV)
1.3×10^{-3}	148
2.6×10^{-3}	172
5.1×10^{-3}	194
7.5×10^{-3}	200
1.0×10^{-2}	216

(f) Isophthalic acid (Qualitative)

Additive concentration (mole/l)	Overpotential Increment (mV)
2.5×10^{-5} (approx.)	23.5
3.7×10^{-5} "	28.0
5.0×10^{-5} "	30.0
1.2×10^{-4} "	35.0
2.5×10^{-4}	45.0

(g) Phenol

Additive concentration (mole/l)	Overpotential Increment (mV)
5.0×10^{-2}	50
7.5×10^{-2}	73
1.0×10^{-1}	90
1.5×10^{-1}	112
2.5×10^{-1}	140

summarized as follows: 1) Aromatic compounds, whose π-electron ring may interact with a metal surface in the anodic region of the coverage-voltage curve, are adsorbed as regular cations in the cathodic region. 2) The adsorption of aromatic compounds on the positive branch was principally determined by π-electron interaction and on the negative branch by Coulombic forces. 3) The π-electron interaction with the electrode surface can be neglected in the perpendicular configuration.

From the above argument, and since the copper cathode is negatively charged, it is most likely that benzoic acid and phthalic acid adsorb perpendicular to the copper surface with the functional group toward the metal. Accordingly, the apparent standard free energy of adsorption of benzoic and phthalic acids can be obtained by using Equation (72). Plotting $C/\theta(2-\theta)$ vs. C gave a straight line, the slope and the intercept of which were obtained from a least-square computer program to minimize graphical error. The results are shown in Table 42.

Table 42

The Adsorbability & Standard Free Energy of Adsorption of Aromatic Compounds

Additive	Slope	Intercept	K(1/mole)	$-\Delta G_a^o$(Kcal/mole)
Benzoic	.99	5.94×10^{-5}	4.22×10^{3}	7.4
Phthalic	.99	2.9×10^{-6}	8.51×10^{4}	9.2
Isophthalic*	-	-	1.4×10^{4}	8.1

*qualitative results

The internuclear distance between the two carboxyl groups in phthalic, isophthalic and terephthalic acids, is 2.6Å, 4.65Å and 5.4Å respectively, as obtained from Prentice-Hall molecular models. In comparing these values to the internuclear distances of the copper lattice, it can be seen that phthalic acid could most likely form two-point attachments, while isophthalic could not. This might explain the fact that phthalic acid has a higher ΔG_a^o than isophthalic acid. Accordingly, the ΔG_a^o value for terephthalic acid would be expected to be high and similar to phthalic acid, however, due to solubility problems, this compound was not used.

Since phthalic acid has the possiblity of two-point attachment, then contributions from each part of the molecule can be assumed. Therefore, by subtracting ΔG_a^o for benzoic acid from ΔG_a^o for phthalic acid, the value of ΔG^o_{COOH} can be obtained as follows:

	HOOC-Ph-COOH	-	Ph-COOH	=	-COOH
ΔG^o_{COOH}	= -9.15	-	-7.4	=	-1.75 Kcal/mole

-------(74)

This value for ΔG^o_{COOH} agrees satisfactorily with the value obtained from monocarboxylic acids where ΔG^o_{COOH} = -1.57 Kcal/mole, bearing in mind the electron-withdrawing effect of the -COOH group which can be expected to increase the value of ΔG^o_{COOH} slightly. If it is considered that ΔG^o_{COOH}

$=-1.57$ Kcal/mole and the mutual effect of the two carboxyl groups produces $\Delta G^{o}_{elec.} = -.18$ Kcal/mole, then the contribution of the phenyl part of the molecule to the free energy of adsorption can be calculated as follows:

For Benzoic acid:

$$\Delta G^{o}_{Benz.} = \Delta G^{o}_{COOH} + \Delta G^{o}_{Ph}$$

$$-7.4 \qquad -1.57$$

$$\therefore \Delta G^{o}_{Ph} = -5.83 \text{ Kcal/mole}$$

From the value of ΔG^{o}_{Ph}, the effect of the individual part of the phenyl group will be $\Delta G^{o}_{CH} = -5830/6$ $= -971$ cal/mole, which is definitely greater than $\Delta G^{o}_{CH_2}$. This result is expected because of the olefinic character of the phenyl group.

Cyclohexanecarboxylic & 1,2 Cis-Cyclohexanedicarboxylic Acids

In the same manner as for monocarboxylic acids, the values of ΔG^{o}_{a} were calculated from the initial slope of the overpotential increment vs. concentration curves (see Fig. 40). The results are given in Table 43.

Obviously, by subtracting ΔG^{o}_{a} for the monofunctional compounds from that of the difunctional compounds, ΔG^{o}_{COOH} can be obtained for the second carboxyl group. The value found, -0.27 Kcal/mole, is very small compared to what might be expected from the behavior of dicarboxylic aliphatic and aromatic compounds. This result can be attributed to the internuclear distance between the two carboxyl groups, and

Figure 40

Overpotential increment as a function of additive concentration ($\Delta\eta$ vs. c)

⊡ 1,2-cis-cyclohexanedicarboxylic acids

⬢ Phenol

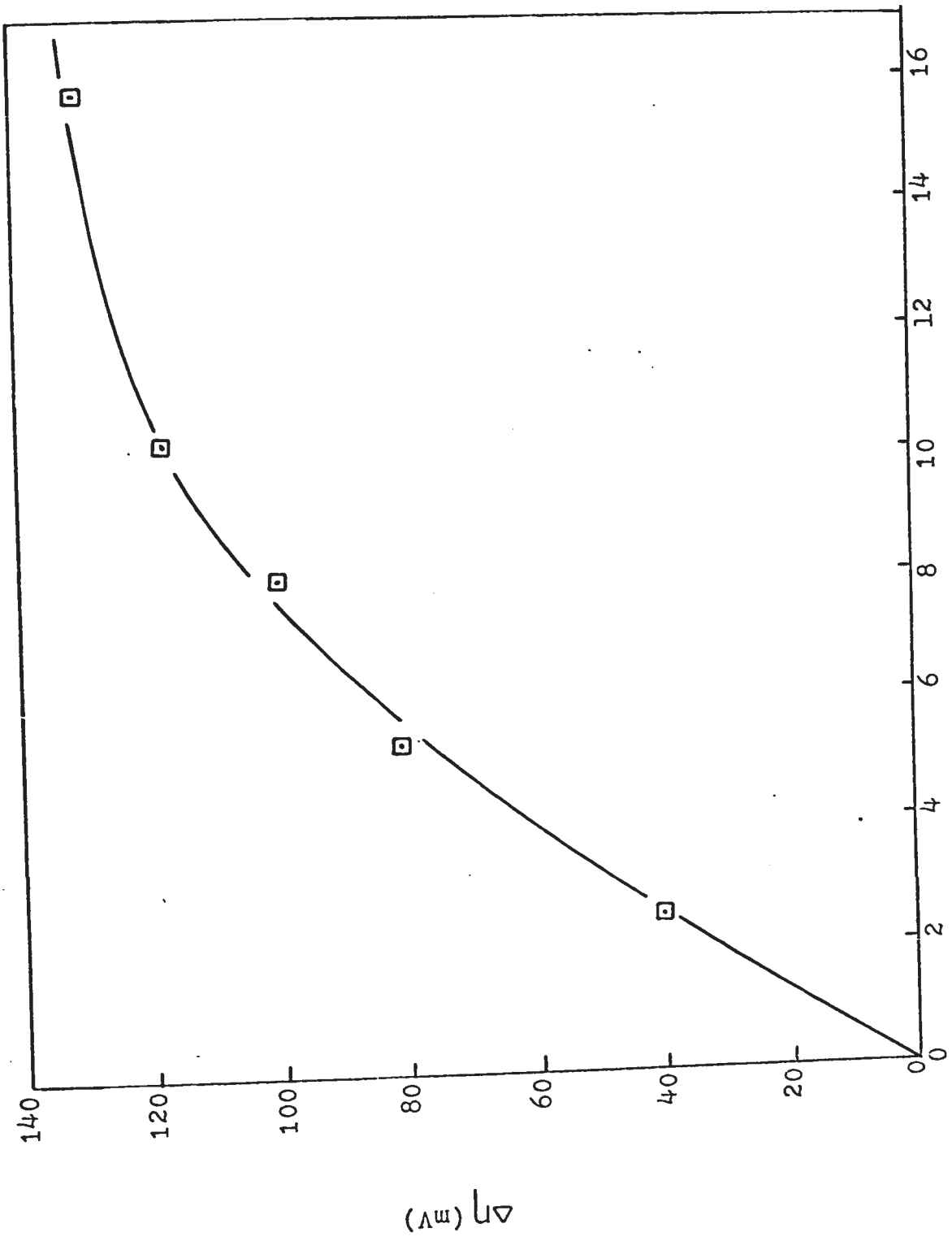

Fig. 40

Fig. 40

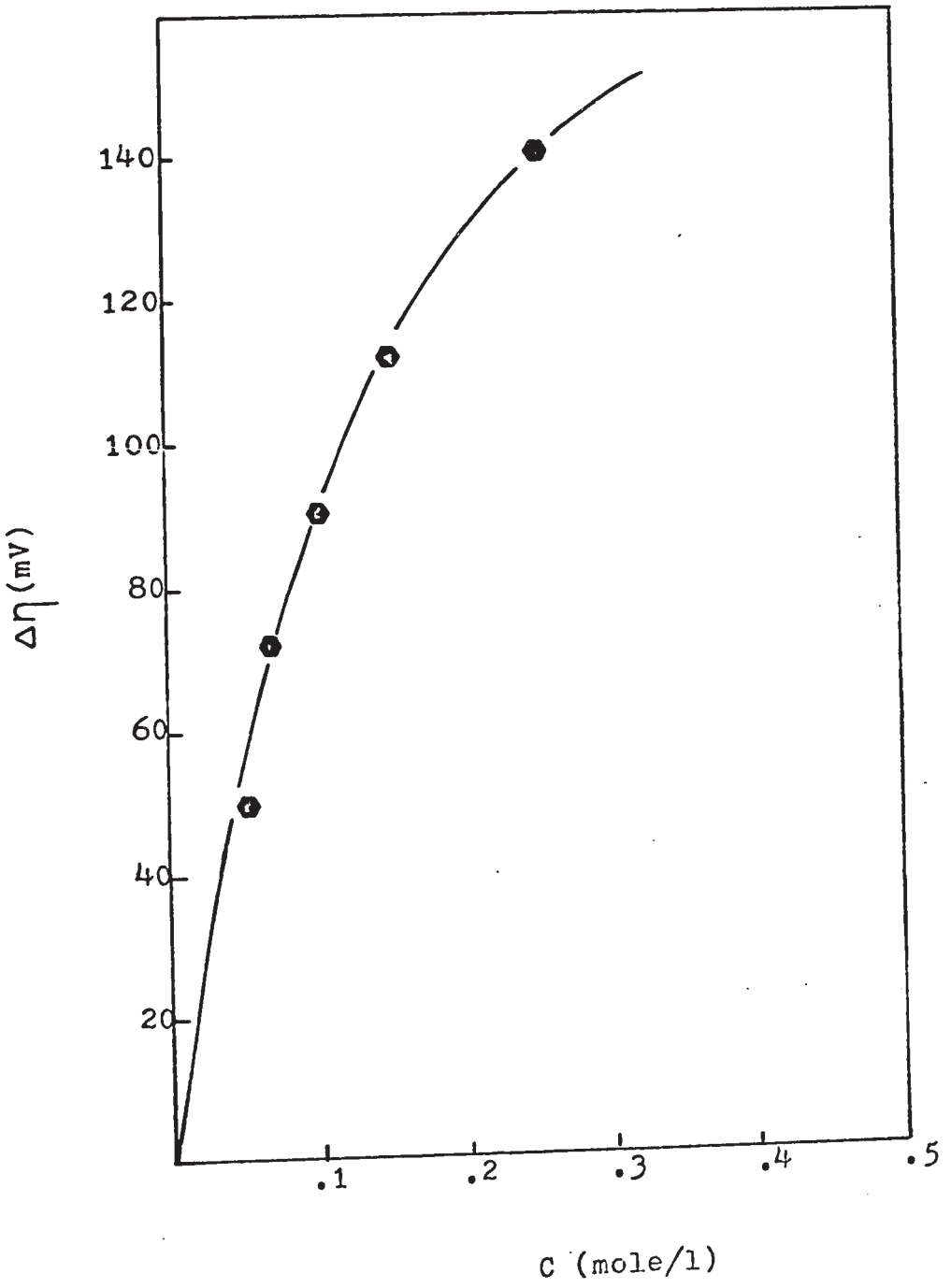

Table 43

Initial slope $(\Delta\eta/C)_{C\to 0}$ and the standard free energy of adsorption of cyclohexane compounds

Additive	Slope $(\Delta\eta/C)_{C\to 0}$	Log $(\Delta\eta/C)_{C\to 0}$	ΔG_a^o (Kcal/mole)
cyclohexane-carboxylic acid	11.6×10^3	4.06	-5.23
1,2 cis cyclohexane-dicarboxylic acid	17.8×10^3	4.25	-5.50

also to the non-planar configuration of the cyclohexane ring. Accordingly, adsorption with one carboxyl group is expected for the 1,2 cis cyclohexanedicarboxylic acid. For the cyclohexanecarboxylic acid, if the value of ΔG^{o}_{COOH} is considered to be that of the monocarboxylic acid, -1.57 Kcal/mole, then the free energy of adsorption of the cyclohexane ring can be calculated. It was found to be -3.66 Kcal/mole, giving the effect of each methylene group as $\Delta G^{o}_{CH_2}$ = -3660/6 =-610 cal/mole. Comparing this value to the average value of $\Delta G^{o}_{CH_2}$ = -760 cal/mole for the straight-chain aliphatic compounds, it is seen that cyclization of the aliphatic chain decreases the effect of each methylene group. Also, $\Delta G^{o}_{cyclohexane}$ is significantly less than ΔG^{o}_{Ph}, which is understandable, in view of the electron-withdrawing power and olefinic character of the phenyl ring.

The lateral interaction of compounds in Group IV was not investigated. However, it is likely that these compounds behave in a manner similar to the moncarboxylic acids.

Cyclohexanol and Phenol

Cyclohexanol showed very little effect on the cathode overpotential. This would not be expected on the basis of the expected high free-energy contribution from the cyclohexane part of the molecule, (see preceding section). Cyclohexanol is probably adsorbed with the functional group toward the solution, and the solvation of the hydroxyl group

probably accounts for its low adsorbability. This assumption is in agreement with the prediction on page 203.

Phenol caused a considerable increase in the overpotential of copper deposition. The free energy of adsorption of phenol was obtained from the initial slope of the overpotential increment vs. concentration curve, Fig. 40. The numerical results are given in Table 44.

Table 44

Initial Slope $(\Delta\eta/C)_{C\to 0}$ and standard free energy of adsorption for phenol

Additive	$(\Delta\eta/C)_{C\to 0}$	$\text{Log}(\Delta\eta/C)_{C\to 0}$	ΔG_a^o(Kcal/mole)
Phenol	1.52×10^3	3.1818	- 4.017

Comparing the effects of cyclohexanol and phenol, it can be seen that phenol is much more effective, as might be predicted from the behavior noted previously for the phenyl ring.

Considering the free energy of adsorption of phenol, -4.017 Kcal/mole, and that of the phenyl ring, $\Delta G_{Ph}^o = -5.38$ Kcal/mole, it is apparent that phenol cannot adsorb with the hydroxyl group toward the metal. Solvation of the hydroxyl group presumably gives rise to a desorption contribution to the phenol molecule. Again, this result agrees with the results obtained for cyclohexanol and the aliphatic alcohols.

CHAPTER IV

General Discussion and Summary

1) From the experimental results with monofunctional aliphatic additives (monocarboxylic acids, thioacids and thiols), it was found that each addition of a methylene group caused a constant increase in the total steady-state overpotential at a given additive concentration, and consequently in the standard free energy of adsorption. The latter was found to be -760 cal/mole per methylene group, characteristic of physical adsorption. Accordingly, a general formula for the standard free energy of adsorption, at zero coverage, can be given as

$$\Delta G^{o}_{a\ \theta=0} = \Delta G^{o}_{p} + x\ \Delta G^{o}_{CH_2}$$

where ΔG^{o}_{p} is the contribution to the standard free energy of adsorption of the functional group (-CCOH, - COSH and -SH), x the number of methylene groups in the additive molecule, and $\Delta G^{o}_{CH_2}$ the methylene group contribution to the free energy of adsorption.

It should be noted that results were obtained as early as 1917 by Langmuir (99), who reported that the addition of each methylene group to alcohols, esters, monobasic acids, ketones, aldehydes, and amides, increased the potential energy λ, required to transfer the organic compound from the bulk of the solution to the water-air interface, on the average by about-625 calories, as obtained from the effects of these organic compounds on the surface tension of

water.

It might be interesting and useful to study the effects of various additives on the surface tension of the standard solution and to compare these effects to the overpotential results.

2) The degree of effectiveness of the functional group of the monofunctional aliphatic compounds decreases in the order:

$$-COSH > -SH \gg -COOH > -\overset{O}{\overset{\|}{C}}- \simeq -CH$$

A similar order of effectiveness was obtained by Bockris & co-workers (48) for the effect of aliphatic organic compounds on the mercury-solution interface.

It should be noted that the acidity of the above functional groups decreases in the same order as their effectiveness in increasing the free energy of adsorption. Accordingly, there is possible correlation between the acidity of the additives and their effect on adsorption.

3) In the case of aliphatic and saturated cyclic compounds studied in acidified $CuSO_4$ electrolyte, the standard free energy of adsorption varied with coverage. This was attributed to the lateral interaction between the adsorbed molecules. The main contribution to the lateral interaction free energy was found to be due to dipole-dipole interaction.

4) For aliphatic difunctional compounds (dicarboxylic acids, mercaptoacids, and diols), there was a definite alternation in the ability to increase the overpotential, the effect of

each additional methylene group depending on whether the molecule contained an even or odd number of carbon atoms. Generally, the relative effectiveness in increasing the overpotential was considerably higher for additves with an odd number of carbon atoms than for those with an even number. This behavior was most pronounced in the case of dicarboxylic acids.

5) The aromatic additives (benzoic and phthalic acids, and phenol) increased the overpotential more than the analogous saturated cyclic compounds (cyclohexanecarboxylic, 1,2 cyclohexanedicarboxylic acids and cyclohexanol). Comparing the results of cyclohexanecarboxylic, heptanoic, and benzoic acids, each with a total of 7 carbon atoms, shows that their effectiveness decreased in the order: benzoic acid > heptanoic acid > cyclohexanecarboxylic acid.

Similarly, difunctional aromatic compounds caused higher overpotential increments than the corresponding saturated cyclic compounds.

It should be noted that 1,2 cyclohexanedicarboxylic acid with free energy of adsorption -5.50 Kcal/mole, gave the same or slightly higher effect than the corresponding aliphatic difunctional octanedioic acid, with free energy of adsorption equal to -5.42 Kcal/mole. While the effect of cyclization was found generally to decrease the contribution of the individual methylene groups, the presence of the two carboxyl groups very close together in cyclohexanedicarboxylic acid seems to compensate for the cyclization effect. It

water.

It might be interesting and useful to study the effects of various additives on the surface tension of the standard solution and to compare these effects to the overpotential results.

2) The degree of effectiveness of the functional group of the monofunctional aliphatic compounds decreases in the order:

$$-COSH > -SH \gg -CCOH > -\overset{O}{\overset{\|}{C}}- \simeq -CH$$

A similar order of effectiveness was obtained by Bockris & co-workers (48) for the effect of aliphatic organic compounds on the mercury-solution interface.

It should be noted that the acidity of the above functional groups decreases in the same order as their effectiveness in increasing the free energy of adsorption. Accordingly, there is possible correlation between the acidity of the additives and their effect on adsorption.

3) In the case of aliphatic and saturated cyclic compounds studied in acidified $CuSO_4$ electrolyte, the standard free energy of adsorption varied with coverage. This was attributed to the lateral interaction between the adsorbed molecules. The main contribution to the lateral interaction free energy was found to be due to dipole-dipole interaction.

4) For aliphatic difunctional compounds (dicarboxylic acids, mercaptoacids, and diols), there was a definite alternation in the ability to increase the overpotential, the effect of

each additional methylene group depending on whether the molecule contained an even or odd number of carbon atoms. Generally, the relative effectiveness in increasing the overpotential was considerably higher for additves with an odd number of carbon atoms than for those with an even number. This behavior was most pronounced in the case of dicarboxylic acids.

5) The aromatic additives (benzoic and phthalic acids, and phenol) increased the overpotential more than the analogous saturated cyclic compounds (cyclohexanecarboxylic, 1,2 cyclohexanedicarboxylic acids and cyclohexanol). Comparing the results of cyclohexanecarboxylic, heptanoic, and benzoic acids, each with a total of 7 carbon atoms, shows that their effectiveness decreased in the order: benzoic acid $>$ heptanoic acid $>$ cyclohexanecarboxylic acid.

Similarly, difunctional aromatic compounds caused higher overpotential increments than the corresponding saturated cyclic compounds.

It should be noted that 1,2 cyclohexanedicarboxylic acid with free energy of adsorption -5.50 Kcal/mole, gave the same or slightly higher effect than the corresponding aliphatic difunctional octanedioic acid, with free energy of adsorption equal to -5.42 Kcal/mole. While the effect of cyclization was found generally to decrease the contribution of the individual methylene groups, the presence of the two carboxyl groups very close together in cyclohexanedicarboxylic acid seems to compensate for the cyclization effect. It

should also be noted that since cyclohexanedicarboxylic acid and octanedioic acid have almost the same free energy of adsorption, it is likely that both adsorb in the same fashion, i.e. with one carboxyl group only. This will explain the results obtained, namely, that ΔG^{o}_{COOH} could not be obtained by subtracting ΔG^{o}_{a} of cyclohexanecarboxylic acid from ΔG^{o}_{a} of 1,2 cyclohexanedicarboxylic acid.

6) Thioacids and mercaptoacetic acid, in acidified $CuSO_4$ solution, caused a reduction in the total overpotential below the steady-state value obtained with no additives. The amount of depolarization caused by these additives was a function of the additive concentration and the acidity of the solution. It was also a function of the hydrocarbon chain length.

From the overpotential-current density relation for solutions containing these depolarizing additives, it was concluded that the rate-determining step is most likely surface-diffusion. High exchange current density, inapplicability of the Tafel-relation, and low overpotential support the proposed surface-diffusion rate-controlling mechanism. Therefore, in general, the presence of depolarizers means a change in the kinetics of copper deposition. From a study of the mechanism by which these additives changed the kinetics of deposition, it was found that thioacids and mercaptoacetic acid in acidified $CuSO_4$ solution reduced the cupric ions to a complexed cuprous form. The cuprous complexes, being the more easily discharged, caused an increase in the adatom

concentration, and consequently changed the rate-determining step from charge-transfer to surface-diffusion.

It was also shown that the presence of the -SH group is not in itself sufficient to cause depolarization, since mercaptopropionic and mercaptobutyric acids do not behave in this way. A study of the effects of α mercaptopropionic acid or α mercaptobutyric acid might be very useful.

7) The solutions which gave depolarization at steady-state always started with a maximum overpotential for a short period, after which the overpotential decreased to the steady-state value. This maximum overpotential increased with increasing additve and sulfuric acid concentrations, and also with increasing length of the hydrocarbon portion of the molecule. The initial maximum was attributed to the formation of a copper sulfide film on the cathode surface before electrolysis. The high overpotential persisted until the sulfide film was removed or occluded in the deposited copper and a fresh clean surface was formed.

REFERENCES

1. K.J. Vetter, Z. Physik. Chem., 194, 284 (1950).
2. K.J. Vetter, Z. Elektrochem., 56, 931 (1952).
3. W.J. Newby, Ph.D. Thesis, University of Western Ontario, 1966.
4. E.C. Potter, "Electrochemistry", Cleaver-Hume Press Ltd., London, 1961, Ch. 6.
5. M. Fleischmann, W.P. Thrisk and I. Tordesillas, Trans. Faraday Soc., 58, 1865 (1962).
6. W. Mehl and J. O'M. Bockris, Can. J. Chem., 37, 190 (1958).
7. J. Tafel, Z. Physik. Chem., 50, 641 (1905).
8. J. O'M. Bockris and G.A. Razumney, "Fundamental Aspects of Electrocrystallization", Plenum Press, New York, 1967.
9. B.E. Conway and J. O'M. Bockris, Electrochim. Acta, 3, 340 (1961).
10. E. Mattson and J.O'M. Bockris, Trans. Faraday Soc., 55, 1586 (1959).
11. B.E. Conway and J. O'M. Bockris, Amer. Electroplaters Soc., AES Research Project No 16, (1959).
12. J. O'M. Bockris and M. Enyo, Trans. Faraday Soc., 58, 1187 (1962).
13. J. O'M. Bockris and K. Hideaki, J. Electrochem. Soc., 109, 928 (1962).
14. L.H. Jenkins, J. Electrochem. Soc., 117, 630 (1970).
15. U. Bertocci, Electrochim. Acta, 11, 1261 (1966).
16. I. Frank, J. Phys. Chem. (USSR), 9, 392 (1945).
17. A.J. Sukava, H. Schneider, D.J. McKenney and A.T. McGregor, J. Electrochem. Soc., 112, 571 (1965).

18. H. Schneider and A. J. Sukava, J. Electrochem. Soc., 112, 568 (1965).

19. E.J. Duwell, J. Electrochem. Soc., 109, 1013 (1962).

20. S.S. Kruglikov, V.D. Gamburg and N.T. Kudryavtsev, Electrochim. Acta, 12, 1129 (1967).

21. I.A. Ammar, S. Darwish, M.W. Khalil, Electrochim. Acta, 12, 657 (1967).

22. R.S. Hansen and B.H. Clampett, J. Phys. Chem., 58, 908 (1954).

23. A.N. Frumkin and B.B. Damaskin, "Modern Aspects of Electrochemistry", Vol. 3, Butterworth, London, 1964, p. 149-223.

24. J. O'M. Bockris and B.E. Conway, "Modern Aspects of Electrochemistry", Vol. 3, Butterworth, London, 1964.

25. B.E. Conway and R.G. Barradas, Electrochim. Acta, 5, 319 (1961).

26. L.K. Partride, A.C. Tansley and A.S. Porter, Electrochim. Acta, 11, 517 (1966).

27. Ibid., 13, 2029 (1968).

28. A.N. Frumkin, Z. Phys. Chem., 116, 466 (1925).

29. Y. Nastuda and H. Tamura, Electrochim. Acta, 14, 427 (1969).

30. E. Gileadi, E.T. Rubin and J. O'M. Bockris, J. Phys. Chem., 69, 3335 (1965).

31. E. Gileadi, J. Electroanal. Chem., 11, 137 (1966).

32. J.J. Kipling, "Adsorption From Solutions of Non-Electrolyte", Academic Press, London, 1965, p. 126.

33. A.K.P. Chu, "Cathodic-Overpotential and Electrosorption Effects of Organic Additives", Ph.D. Thesis, University of Western Ontario (1968).

34. J. O'M. Bockris, D.A.L. Swinkels, J. Electrochem. Soc., 111, 736 (1964).

35. D.O. Hayward and B.M.T. Trapprell, "Chemisorption", Butterworth and Co. Ltd., London, 1964.

36. G.C. Bond, "Catalysts by Metals", Academic Press, Inc., New York, 1962.

37. E. Gileadi, "Electrosorption", Plenum Press, New York, 1967.

38. K.J. Vetter, "Electrochemical Kinetics", Academic Press, New York, 1967, p. 392-394.

39. E. Emmet Reid, "Organic Chemistry of Bivalent Sulfur", Chemical Publication Co., Inc., New York, 1962.

40. A.K.P. Chu and A.J. Sukava, J. Electrochem. Soc., 116, 1188 (1969).

41. A.J. Sukava and C.A. Winkler, Can. J. Chem., 33, 961 (1955).

42. O.R. Brown and H.R. Thirsk, Electrochim. Acta, 10, 383 (1965).

43. L.L. Shreir and J.W. Smith, J. Electrochem. Soc., 99, 64 (1952).

44. P. Ruetschi and P. Delahay, J. Chem. Phys., 23, 195 (1955).

45. H. Freundlich, Z. Physik. Chem., 57, 385 (1907).

46. R.S. Hansen and R.P. Craig, J. Phys. Chem., 58, 211 (1954).

47. L. Morrison and D.M. Miller, Can. J. Chem., 33, 330 (1955).

48. H.H. Wills, Nature, 127, 126 (1931).

49. E.A. Blomgren, J. O'M. Bockris and C. Jesch, J. Phys. Chem., 65, 2000 (1961).

50. M.A.V. Devanathan, Proc. Roy. Soc., London, 267, 257 (1962).

51. O.M. Dzhigit, A.V. Kiselev and K.G. Krasilnikov, Doklady Akad. Nauk S.S.S.R., 58, 413 (1947).

52. K.S. Markley, "Fatty Acids", Interscience Publishers Inc., New York, 1949.

53. "Handbook of Chemistry and Physics" Chemical Rubber Publishing Co., Cleveland, 1963.

54. B.E. Conway and R.G. Barradas, Electrochim. Acta, 5, 349 (1961).

55. E.A. Blomgren and J. O'M. Bockris, J. Phys. Chem., 63, 1475 (1959).

56. J. Traube, Lieb. Annalen, 265, 27 (1891).

57. A.F.H. Ward, Trans. Faraday Soc., 42, 399 (1946).

58. L. Pospisil and J. Kuta, Collection Czechoslov. Chem. Commun., 34, 3047 (1969).

59. H.A. Pohl, M.E. Hobbs and P.M. Gross, Ann. N.Y. Acad. Sci., 40, 389 (1940).

60. C.H. Townes and A.L. Schalow, "Microwave Spectroscopy", McGraw-Hill Book Company, Inc., New York, 1955.

61. A.L. McClellan, "Tables of Experimental Dipole Moments", W.H. Freeman & Co., London, 1963.

62. M.T. Rogers, J. Phys. Chem., 61, 1442 (1957).

63. J. O'M. Bockris, M.A.V. Devanathan and K. Matter, Proc. Roy. Soc., London, 274A, 55 (1962).

64. A.A. Maryatt and E.R. Smith, "Table of Dielectric Constants of Pure Liquids", National Bureau of Standards Circular

65. B.B. Damaskin, A.A. Survila, Elektrokhimiya, 3, 146 (1967).

66. R. Ya. Pullerits, U.V. Palm and V.E. Past, Elektrokhimiya, 5, 886 (1969).

67. R.S. Hansen, R.E. Minturn and D.A. Kickson, J. Phys. Chem., 61, 953 (1957).

68. D.A. Fairweather, Proc. Roy. Soc. Edinburgh, 45, 283 (1925).

69. S.C. Barnes, J. Electrochem. Soc., 111, 296 (1964).

70. L.L. Shreir and J.W. Smith, Trans. Faraday Soc., 49, 393 (1953).

71. A.J. Sukava and C.A. Winkler, Can. J. Chem., 34, 128 (1956).

72. I.M. Klotz, G.H. Czerlinski and H.A. Fiess, J. Am. Chem. Soc., 30, 2920 (1955).

73. G.H. Morrison and H. Freiser, "Solvant Extraction in Analytical Chemistry", John Wiley, New York, 1957.

74. S.C. Barnes, Electrochim. Acta, 5, 79 (1961).

75. Y.M. Porarov and L.V. Eroshkina, Elektrokhimiya, 5, 512 (1969).

76. D.R. Turner and G.R. Johnson, J. Electrochem. Soc., 109, 798 (1962).

77. H. Schneider, M.Sc. Thesis, University of Western Ontario, 1964.

78. Y.N. Lebedeva and M.Y. Popereka, Elektrokhimiya, 4, 79 (1968).

79. A.R. Despic and J. O'M. Bockris, J. Chem. Physics, 32, 389 (1960).

80. W. Mehl and J. O'M. Bockris, J. Chem. Physics, 27, 817 (1957).

81. G.E. Cheney, Q. Fernando and H. Freiser, J. Phys. Chem., 63, 2055 (1959).

82. T. Schinzel and G. Benoit, Bull. Soc. Chem. No. 5, 6, 501 (1939).

83. S.S. Kruglikov, Y.I. Sinyakov and N.T. Kudryavtsev, Elektrokhymia, 2, 100 (1966).

84. A.E.A. Werner, Sci. Proc. Roy. Dublin Soc., 22, 387 (1941).

85. E. Larsson, Svensk. Kem. Tid., 40, 149 (1928).

86. E. Larsson, Univ. Lund. Ber., 61B, 1439 (1928).

87. Q. Fernando and H. Freiser, J. Am. Chem. Soc., 80, 4928 (1958).

88. L.L. Wikstron and K. Nobe, J. Electrochem. Soc., 116, 525 (1969).

89. D.A. Vermilyea, J. Chem. Phys., 25, 1254 (1956).

90. V.A. Yuza and L. D. Kopyl, J. Phys. Chem., (U.S.S.R.), 14, 1047 (1941).

91. O.A. Essin, L. Antropov and A. Levin, Acta Physicochim. U.R.S.S., 6, 447 (1937).

92. Ibid., J. Phys. Chem. (U.S.S.R.), 9, 269 (1937).

93. J. Llopis, J.M. Gamboa, and L. Anizmendi, J. Electrochim. Acta, 4, 294 (1961).

94. J. Llopis, J.M. Gamboa, and L. Anizmendi, J. Electrochim. Acta, 3, 75 (1960).

95. J. Llopis, J.M. Gamboa, and L. Anizmendi, J. Electrochim. Acta, 3, 85 (1960).

96. K.M. Gorburnova and A.A. Sutiagina, Electrochim. Acta, 10, 367 (1965).

97. W. Heiland, E. Gileadi & J. O'M. Bockris, J. Phys. Chem., 70, 1207 (1966).

98. B. Sheltor, B.Sc. Research Project, University of Western Ontario, 1969.

99. I. Langmuir, J. Am. Soc., 39, 1883 (1917).

Appendix A

The current-overpotential relation for a one-step, single-electron transfer reaction is given by

$$i = i_o \left[e^{\beta F \eta / RT} - e^{-(1-\beta) F \eta / RT} \right]$$

where β, the symmetry factor, is the fraction of the overpotential assisting the ion-to-electrode transfer and $(1-\beta)$ is the fraction of the overpotential hindering the metal-to-solution reaction.

For a multi-step reaction, e.g. the case concerned in this work, the current-overpotential relation is given by

$$i = i_o \left[\exp(\gamma + r\beta) \frac{F\eta}{RT} - \exp-(\gamma + r - r\beta) \frac{F\eta}{RT} \right]$$

where γ is the number of the steps preceding the rate-determining step, and r is the number of electrons involved in the rate-determining step. Accordingly, for copper electrodeposition the cathodic reaction is

$$Cu^{++} + e \longrightarrow Cu^{+} \qquad \text{rds}$$

$$Cu^{+} + e \longrightarrow Cu \qquad \text{fast}$$

$\gamma = 0$ & $r = 1$, accordingly the cathodic current is given by

$$\vec{i} = i_o \exp \beta F \eta / RT$$

and for the anodic reaction

$$Cu \longrightarrow Cu^{+} + e \qquad \text{fast}$$

$$Cu^{+} \longrightarrow Cu^{++} + e \qquad \text{rds}$$

$\gamma = 1$ & $r = 1$, therefore, the anodic current is given by

$$\overleftarrow{i} = i_o \exp -(2-\beta) F \eta / RT$$